Deciphering molecular mechanism of induction of biotic stress tolerance by *Trichoderma* spp. in castor (*Ricinus communis* L.)

A thesis submitted to the University of Hyderabad for the award of

Doctor of Philosophy

In Plant Sciences

By

Doris Abhirupa Pradhan

(Reg. No. 13LPPH08)

Department of Plant Sciences

School of Life Sciences

University of Hyderabad

Hyderabad 500046

Telangana, India

February 2024

Department of Plant Sciences

School of Life Sciences

University of Hyderabad

DECLARATION

I, Doris Abhirupa Pradhan hereby declare that the work described in this thesis entitled "Deciphering molecular mechanism of induction of biotic stress tolerance by *Trichoderma* spp. in castor (*Ricinus communis* L.)" submitted by me under the supervision of Professor Ragiba Makandar, Department of Plant Sciences, is an original research work. I also declare that it has not been submitted previously in part or in full for any other degree or diploma to any other university or Institution. A report on plagiarism statistics from the university librarian is enclosed.

Date - 17.02.2024

Name - Doris Abhirupa Pradhan

Signature- Doris Abhirupa Pradhan

Reg. No. - 13LPPH08

Department of Plant Sciences
School of Life Sciences
University of Hyderabad

CERTIFICATE

This is to certify that the thesis entitled "Deciphering molecular mechanism of induction of biotic stress tolerance by *Trichoderma* spp. in castor (*Ricinus communis* L.)" submitted by Doris Abhirupa Pradhan bearing Reg. No. 13LPPH08 in partial fulfilment of the requirement for the award of Doctor of Philosophy in Plant Sciences in the Department of Plant Sciences, School of Life Sciences, University of Hyderabad is a record of bonafide work carried out by her under my supervision and guidance.

This thesis is free from plagiarism and has not been submitted previously in part or in full to this or any other University or Institution for the award of any degree or diploma.

Parts of the thesis have been published in the following journals:

- **Pradhan DA**, Bagagoni P, Makandar R. 2023. Biological Control. 184: 105280.
- **Pradhan DA**, Makandar R. 2023. Rhizosphere. 27: 100745.
- **Pradhan DA**, Bagagoni P, Slathia S, Prasad RD, Makandar R. 2023. Biocatalysis and Agricultural Biotechnology. 54:102945.

Further the student has passed the following courses towards the fulfilment of the coursework requirement for Ph.D.

S.No.	Course	Name	Credits	Pass/Fail
1	PL801	Seminar 1	1	Pass
2	PL802	Research ethics and management	2	Pass
3	PL803	Biostatistics	2	Pass
4	PL804	Analytical Techniques	3	Pass
5	PL805	Lab Work	4	Pass

19/02/2024

Supervisor
RAGIBA MAKANDAR Ph.D
Professor
Department of Plant Sciences
School of Life Sciences
University of Hyderabad
Hyderabad 500 046 India

Head of the Department
HEAD
Dept. of Plant Sciences
School of Life Sciences
University of Hyderabad
Hyderabad-500 046. INDIA

20/2/24

Dean of the School
डीन / Dean
जीव विज्ञान संकाय / School of Life Sciences
हैदराबाद विश्वविद्यालय / University of Hyderabad
हैदराबाद / Hyderabad-500 046.

James 1:17

"Every good thing comes from God"

Dedicated to Jesus Christ and my family

ACKNOWLEDGEMENTS

I take the opportunity to acknowledge the support and encouragement given by various people during the years of my doctoral research. I had the pleasure of being associated with them in achieving the goals of my research work. I wish to express my gratitude for them.

First, my sincere, humble indebtedness and whole-hearted sense of gratitude to my honourable supervisor **Prof. Ragiba Makandar**. I humbly express my deepest gratitude to her for the constant encouragement, inspiring guidance, and valuable suggestion, which helped me to complete the research work in time. I am grateful for the affection, guidance and support offered by her throughout the doctoral research work.

I wish to express my sincere thanks to my doctoral committee members. Prof. S. Rajagopal and Prof. Brahmananda for their motivation and critical suggestions during doctoral committee presentations towards my research work.

I am thankful to present and former Head of the Department of Plant Sciences, Prof. S. Rajagopal and Prof. G. Padmaja respectively for allowing me to use the facilities of the Department.

I sincerely express my gratitude to present and former deans, School of Life Sciences (SLS) Prof. Anand Kondapi, Prof. N. Shiva Kumar, Prof. S. Dayananda, Prof. KVA Ramaiah, Prof. M.N.V. Prasad, Prof. P Redanna, Prof. R.P. Sharma and Prof. A.S. Raghavendra respectively for allowing me to use the school facilities.

I am extremely thankful to all the faculty members and non-teaching staff of SLS for their help towards this endeavour.

I acknowledge DOR, Hyderabad for providing the castor seeds.

I thank Mr. Bipin Kumar at Nucleome Informatics for the service and help in transcriptome studies.

I am also thankful to UGC-NET for the financial support in form of fellowship as JRF and SRF.

I acknowledge the funding bodies DST, DBT, ICAR, UGC-SAP, DST-FIST, DST-PURSE, DST-CREBB and UPE for funding to the laboratory.

I thank all my lab mates Dr. Malathi, Dr. Jang, Dr. Sheetal, Ms. Massarat, Ms. Annapurna, Mr. Hanan, Ms Priyamvada, Ms. Prathyusha and Ms. Keerthi for all the support and help.

One needs sincere friends at all major junctures in life to bear the strain and fatigue cheerfully. My warmest thanks to all my dear friends Sheetal, Yugantak, Kowshik, Kavya, Pratik and others.

I feel honour to dedicate this work to my always supportive husband Leonard Jackson and beloved parents Daisy Pradhan and Shekhar Pradhan for their unconditional love, encouragement, and moral support to achieve my goal. Without them this would not have been possible.

Last but most importantly, I thank my Lord and Saviour Jesus Christ for his grace and blessings throughout my life.

Name - Doris Abhirupa Pradhan

Signature- Doris Abhirupa Pradhan

TABLE OF CONTENTS

Abbreviations

List of Tables

List of Figures

List of Supplementary Tables

List of Supplementary Figures

Chapter 1 Research purpose and Objectives

1.1 Introduction
1.2 Importance of castor beans
1.3 Worldwide production of castor
1.4 Castor oil derivatives
1.5 Diseases and pests that affect castor production
1.6 *Trichoderma* – The Biocontrol agent
1.7 *Trichoderma* growth and development
1.8 Microparasitic ability of *Trichoderma*
1.9 Root colonization of *Trichoderma*
1.10 Secondary metabolites
1.11 Induced resistance
1.12 Rationale for research study
1.13 Hypothesis and research purpose
1.14 Objectives of the study

Chapter 2 Characterization of *Trichoderma* strains for novel species-specific markers by multiplex PCR and antagonistic property against *Alternaria ricini* in castor (*Ricinus communis* L.)

2.1 Introduction
2.2 Materials and Methods
2.3 Results
2.4 Discussion

Chapter 3 Assessing rhizosphere *Trichoderma asperellum* strains for root colonizing and antagonistic competencies against *Fusarium* wilt through molecular and biochemical responses in castor

3.1 Introduction
3.2 Materials and Methods
3.3 Results
3.4 Discussion

Chapter 4 Delineating host responses induced by *Trichoderma* in castor through comparative transcriptome analysis by next generation sequencing

4.1 Introduction
4.2 Materials and Methods
4.3 Results
4.4 Discussion

Chapter 5 Summary and Conclusion

Chapter 6 Bibliography

Supplementary Tables
Supplementary Figures
Publications from the study
Plagiarism Report

ABBREVIATIONS

RA	Ricinoleic acid
%	Percent
°C	Degree Celsius
µL	Microlitre
µg	Microgram
µM	Micromolar
pmol	Picomoles
ng	Nanogram
mL	Millilitres
mM	Millimolar
nm	Nanometer
g	Grams
mg	Milligrams
v/v	Volume by volume
w/v	Weight by volume
Psi	Pound force per square inch
h	Hours
min	Minutes
s	Seconds
hpi	Hours post inoculation
dpi	Days post inoculation
rpm	Revolutions per minute
bp	Base pairs
BCA	Biological control agent
CFU	Colony forming unit
CTAB	Cetyltrimethyl ammonium bromide
EDTA	Ethylene diamine tetraacetic acid
PDA	Potato Dextrose Agar
CMC	Carboxymethyl cellulose
Depc	Diethyl pyrocarbonate
ITS	Internal transcribed spacer

SCAR	Sequence characterized amplified region
RAPD	Random amplified polymorphic DNA
cDNA	Complementary DNA
PCR	Polymerase chain reaction
qPCR	Quantitative polymerase chain reaction
RT-qPCR	Real Time-quantitative polymerase chain reaction
ANOVA.	Analysis of variance
SE	Standard error
DEG	Differentially expressed genes
ROS	Reactive oxygen species
NAD	Nicotinamide adenine dinucleotide
NADP	Nicotinamide adenine dinucleotide phosphate
JA	Jasmonic acid
SA	Salicylic acid

LIST OF TABLES

Table 1.1 Physical properties of castor.

Table 1.2 State wise area, production and yield of castor in India (Source- Solvent Extractor's Association of India).

Table 1.3 Classification of various castor oil derivatives that are used in the chemical industry.

Table 1.4 Classification of *Trichoderma*, the biological control agent.

Table 2.1 Morphological characteristics of six fungal strains cultured on potato dextrose agar (PDA) medium.

Table 2.2 BLAST-search results of ITS and D1-D2 sequences of *Trichoderma* strains amplified using ITS-1F/ITS-4R primers and NL-1/NL-4 primers respectively.

Table 2.3 Grouping of monomorphic RAPD markers. The monomorphic markers were demarcated based on presence (+) or absence (-) of bands.

Table 2.4 Grouping of ploymorphic RAPD markers.

Table 2.5 RAPD-based genetic similarity among the six strains of *Trichoderma* analysed in a pairwise manner.

Table 2.6 Primer sequence information of SCAR primers designed for developing species-specific markers.

Table 2.7 Percentage fungal pathogen growth inhibition by antagonistic effect of *Trichoderma* strains.

Table 2.8 Disease scoring of *Trichoderma*-treated castor genotypes through detached leaf assays for antibiosis against the leaf spot causing fungal pathogen, *Alternaria ricini* using 0–5 scale. The scale 0: immune/ highly resistant, (+): resistant, (++): moderately resistant, (+++): moderately susceptible, (++++): susceptible and (+++++): highly susceptible.

Table 3.1 The effect of biopriming with *Trichoderma* strains on seed germination and radicle growth of castor genotypes at 4 dpi.

Table 3.2 Percentage *Fusarium* pathogen growth inhibition by the antagonistic effect of *Trichoderma* strains. Statistical significance levels for treatments with each of the *Trichoderma* isolates. Mean ± SE with different letters indicate significance level at $P<0.05$, according to Tukey test.

Table 4.1 Composition of the Hoagland solution (with modifications) used to grow castor plants hydroponically. (*Ricinus communis* L.).

Table 4.2 The list of primers and internal controls used for Real Time-quantitative polymerase chain reaction (RT-qPCR).

Table 4.3 Transcriptome analysis for read counts from *Ricinus communis* –*Trichoderma* interaction.

Table 4.4 Read mapping distribution in castor (*Ricinus communis* L.) in response to *Trichoderma*.

Table 4.5 List of gene transcripts downregulated in the roots of castor DCS-107 in response to *T. asperellum* 7316 at 48hpi.

Table 4.6 List of gene transcripts upregulated in the roots of castor DCS-107 in response to *T. asperellum* 7316 at 48hpi.

LIST OF FIGURES

Figure 1.1 Global and state wise (India) percentages of production of castor (Department of Science and Technology, TIFAC).

Figure 1.2 Graphical representation of year wise castor production from 2011-2021 as given by Solvent Extractor's Association of India.

Figure 2.1 Leaf spot infected leaves of castor (*Ricinus communis* L.) were used to isolate *Alternaria ricini*. (a) Isolation of *A. ricini* spores from the leaf spot of castor (b) Spores of *Alternaria* visualized by light microscopy at 40X. (C) Single spored culture of *A. ricini* grown in the sporulation (S) medium at 25 °C as visualized seven days post culturing.

Figure 2.2 Monitoring the mycelia growth of six fungal strains grown on potato dextrose agar (PDA) medium at 25 °C as visualized seven days post culturing. (a) N13, (b) 7316, (c) TV5, (d) TV2B16 (e) TV3 and (f) TS4.

Figure 2.3 Comparison of morphological states of six fungal strains using phase-contrast microscopy. (a) N13, (b) 7316, (c) TV5, (d) TV2B16, (e) TV3 and (f) TS4. Scale Bar: 20 μm.

Figure 2.4 Gel image showing (a) ITS region based PCR amplification of *Trichoderma* strains. (b) Gel image showing D1-D2 region-based amplification of *Trichoderma* strains. Lanes 1-8: *Trichoderma strains* - *T. asperellum* N13 (L-1), *T. asperellum* 7316 (L-2), *T. asperellum* TV5 (L-3), *T. asperellum* TV2B16 (L-4), *T.* asperellum Ta05 (L-5), *T. harzianu*m TV3 (L-6), *T. harzianum* TS4 (L- 7) and *T. harzianum* Th03 (L-8). M: 100 bp DNA ladder.

Figure 2.5 Phylogenetic tree of *Trichoderma* strains based on ITS. Ex-type strains of *Trichoderma* species are marked by an asterisk.

Figure 2.6 Phylogenetic tree of *Trichoderma* strains based on D1-D2. Ex-type strains of *Trichoderma* species are marked by an asterisk.

Figure 2.7 Phylogenetic tree of *Trichoderma* strains based on ITS sequences of 20 strains. Ex-type strains of *Trichoderma* species are marked by an asterisk.

Figure 2.8 Phylogenetic tree of *Trichoderma* strains based on D1-D2 sequences of 20 strains. Ex-type strains of *Trichoderma* species are marked by an asterisk.

Figure 2.9 Phylogenetic tree (radial view) of six strains of *Trichoderma* spp. along with 100 other reported *Trichoderma* ITS sequences.

Figure 2.10 *Trichoderma*-species specific PCR amplification. (a) T2AF/T2AR amplified *T. asperellum*-specific polymorphic band in N13, 7316, TV5, TV2B16 and Ta05 (L-1 to L-5) at 507 bp but absent in TV3, TS4 and Th03 (L-6 to L-8). (b) TH1F/TH1R amplified *T. harzianum*-specific polymorphic band in TV3, TS4 and Th03 at 824 bp (L-6 to L-8) but absent in N13, 7316, TV5, TV2B16 and Ta05 (L-1 to L-5). (c) Multiplex PCR confirmed the results. The *Trichoderma strains*: *T asperellum* N13 (L-1), *T. asperellum* 7316 (L-2), *T. asperellum* TV5 (L-3), *T. asperellum* TV2B16 (L-4), *T. asperellum* Ta05 (L-5), *T. harzianum* TV3 (L-6), *T. harzianum* TS4 (L- 7), *T. harzianum* (L-8). L-9 is non-template control. M: DNA 100 bp ladder.

Figure 2.11 *Trichoderma*-species specific PCR amplification. (a) 2F2/2R2 SCAR marker amplified *T. harzianum*-specific polymorphic band in TV3, TS4 and Th03 (L-6 to L-8) at 278 bp but absent in N13, 7316, TV5, TV2B16 and Ta05 (L-1 to L-5). (b) 2F2/2R3 also generated a polymorphic band in TV3, TS4 and Th03 at 448 bp (L-6 to L-8) but absent in N13, 7316, TV5 TV2B16 and Ta05 (L-1 to L-5). (c) Multiplex PCR confirmed the results. The *Trichoderma* strains: *T. asperellum* N13 (L-1), *T. asperellum* 7316 (L-2), *T. asperellum* TV5 (L-3), *T. asperellum* TV2B16 (L-4), *T. asperellum* Ta05 (L-5), *T. harzianum* TV3 (L-6), *T. harzianum* TS4 (L- 7), *T. harzianum* (L-8). L-9 is non-template control. M: DNA 100 bp ladder.

Figure 2.12 Genetic relatedness among the six *Trichoderma* fungal strains based on RAPD analysis, where 1: *Trichoderma asperellum* N13; 2: *Trichoderma asperellum* 7316; 3: *Trichoderma asperellum* TV5; 4: *Trichoderma asperellum* TV2B16; 5: *Trichoderma harzianum* TV3 and 6: *Trichoderma harzianum* TS4.

Figure 2.13 Gel images showing the PCR amplification of the polymorphic RAPD markers which were developed into SCAR markers following DNA sequencing. (a) OPZ-06_{950} marker showed a polymorphic band with uniform amplification for N13, 7316, TV5 and TV2B16 at 950 bp (red arrow) but absent in TV3 and TS4. (b) OPK-10_{1400} marker showed a polymorphic band with uniform amplification for TV3 and TS4 at 1400 bp (red arrow) but absent in N13, 7316, TV5 and TV2B16. The lanes 1 to 6 represent the *Trichoderma* strains: *T. asperellum* N13 (L-1), *T. asperellum* 7316 (L-2), *T. asperellum* TV5 (L-3), *T. asperellum* TV2B16 (L-4), *T. harzianum* TV3 (L-5), T. *harzianum* TS4 (L- 6). M: DNA 100bp ladder.

Figure 2.14 Developing a new set of *Trichoderma* species-specific SCAR markers. (a) T1/T2 showed a specific band with uniform amplification at 467 bp in N13, 7316, TV5, TV2B16 and Ta05 but absent in the strains TV3, TS4 Th03, IC13 and IC14. (b) T3/T4 showed a band with uniform amplification at 436 bp in TV3, TS4 and Th03 but absent in N13, 7316, TV5, TV2B16 Ta05 and IC13 and IC14. (c) Multiplex PCR amplification of the SCAR markers T1/T2 and T3/T4 simultaneously confirmed the results. T1/T2 and T3/T4 amplified the 467 bp (L-1 to L-5) and 436 bp (L-6 to L-8) bands respectively. The lanes representing the *Trichoderma* strains are: *T asperellum* N13 (L-1), *T. asperellum* 7316 (L-2), *T. asperellum* TV5 (L-3), T. *asperellum* TV2B16 (L-4), *T. asperellum* Ta05 (L-5), *T. harzianum* TV3 (L-6), *T. harzianum* TS4 (L- 7), *T. harzianum* Th03 (L-8), *T. longibrachiatum* IC13 (L-9), *T. virens* IC14 (L-10). L-11 is non-template control. M: DNA 100 bp ladder.

Figure 2.15 Confrontation plate assays with dual cultures grown with *A. ricini* and *T. asperellum* strains at 7 dpi. Plates growing only *T. asperellum* 7316, N13, TV5 and TV2B16 (a, b, c, d) and *A. ricini* (e) served as controls. Test plates included *Alternaria* grown with *T. asperellum* 7316 (f), *Alternaria* grown with *T. asperellum* N13 (g), *Alternaria* grown with *T. asperellum* TV5 (h) and *Alternaria* grown with *T. asperellum* TV2B16 (i)

Figure 2.16 Effect of *Trichoderma* treatment on *Alternaria* leaf spot in castor by detached leaf assays. Two castor genotypes; (A) DCS-107 and (B) 48-1 treated individually with each of the four strains of *T. asperellum*; 7316, N13, TV5, and TV2B16 were compared to untreated samples at 3 and 7 dpi. The *Alternaria* leaf spot spread

was monitored at 3 dpi (a, c, e, g, i, k, m, o, q, s) and 7dpi (b, d, f, h, j, l, n, p, r, t) respectively.

Figure 3.1 Colony forming unit (CFU) counts of bulk soil of *Trichoderma* treated roots of DCS-107 and 48-1 respectively at 12, 24, 36 and 48 days post inoculation (dpi). *T. asperellum* 7316 treated DCS-107 (a), *T. asperellum* 7316 treated 48-1 (b), *T. asperellum* N13 treated DCS-107 (c), *T. asperellum* N13 treated 48-1 (d), *T. asperellum* TV5 treated DCS-107 (e), *T. asperellum* TV5 treated 48-1 (f), *T. asperellum* TV2B16 treated DCS-107 (g), and *T. asperellum* TV2B16 treated 48-1 (h). Statistical difference between treatments displayed at Tukey <0.05. Vertical bars represent Mean ± standard error (SE).

Figure 3.2 Colony forming unit (CFU) counts of rhizosphere soil of *Trichoderma* treated roots of DCS-107 and 48-1 respectively at 12, 24, 36 and 48 dpi. *T. asperellum* 7316 treated DCS-107 (a), *T. asperellum* 7316 treated 48-1 (b), *T. asperellum* N13 treated DCS-107 (c), *T. asperellum* N13 treated 48-1 (d), *T. asperellum* TV5 treated DCS-107 (e), *T. asperellum* TV5 treated 48-1 (f), *T. asperellum* TV2B16 treated DCS-107 (g), and *T. asperellum* TV2B16 treated 48-1 (h). Statistical difference between treatments displayed at Tukey <0.05. Vertical bars represent Mean ± standard error (SE).

Figure 3.3 The graphical representation of percentage germination of seeds of castor genotypes, DCS-107 and 48-1 recorded 4 days-post treatment with *Trichoderma* strains: 731-6, N13, TV5 and TV2B16. Vertical bars represent Mean ± standard deviation (SE). Untreated: Mock (water)-treated seed samples.

Figure 3.4 Effect of bio-priming with *T. asperellum* strains on the radicle length of castor seedlings of two genotypes; DCS-107 (a) and 48-1 (b) respectively. Graphical representation of the radicle length of DCS-107 and 48-1 seeds of castor treated with *T. asperellum* strains: 7316, N13, TV5 and TV2B16 4 days post treatment (c). Untreated: Control seeds treated with CMC solution alone, T: *Trichoderma*-treated seeds. Statistical difference between the treatments displayed at Tukey <0.05. Vertical bars represent Mean ± standard deviation (SE).

Figure 3.5 Effect of *Trichoderma* treatment on plant growth of castor plants of DCS-107 genotype. The roots (a), leaves (b) and shoot (c) of two-week-old plants treated with *T. asperellum* strains; 7316, N13, TV5 and TV2B16. Graphical representation of length of the stem (d) measured in millimeters (mm), fresh weight (e) and dry weight (f) measured in grams (g) of castor plants. Untreated: Castor plants mock-treated with CMC solution alone, T: *Trichoderma* treated plants. Statistical difference between the treatments displayed at Tukey <0.05. Vertical bars represent Mean ± standard error (SE).

Figure 3.6 Confrontation plate assays with dual cultures grown with *Fusarium oxysporum ricini* along with *Trichoderma asperellum* strains at 7 dpi. Plates growing only *T. asperellum* 7316 (a), N13 (b), TV5 (c) and TV2B16 (d) or *Fusarium* (e) alone served as controls. Test plates included *Fusarium* grown with *T. asperellum* 7316 (f), *Fusarium* grown with *T. asperellum* N13 (g), *Fusarium* grown with *T. asperellum* TV5 (h), *Fusarium* grown with *T. asperellum* TV2B16 (i). Graphical

representation of percentage inhibition of *F. oxysporum* growth upon treatment with *Trichoderma asperellum* strains at 4 and 7 dpi (j). Statistical difference between the treatments displayed at Tukey <0.05. Vertical bars represent Mean ± standard deviation (SE). Petri plates growing *Trichoderma* and pathogen discs alone served as controls.

Figure 3.7 Effect of *Trichoderma* treatment on plant growth in castor (*Ricinus communis L.*). *Fusarium* wilt incidence monitored on aerial and underground parts of the DCS-107 castor plants treated with *T. asperellum* strains at 7 dpi (a). Plant growth and tolerance to *Fusarium* wilt monitored in DCS-107 plants treated with *Trichoderma* strains at 21 dpi (b).

Figure 3.8 Effect of *Trichoderma* treatment on Fusarium wilt disease in castor. Percentage Fusarium wilt incidence recorded in the roots of DCS-107 plants treated with *T. asperellum strains*: 7316, N13, TV5 and TV2B16 at 21 dpi. The data was normalized against the control/untreated samples for all treatments. Statistical difference between the treatments displayed at Tukey <0.05. Vertical bars represent Mean ± standard error (SE).

Figure 3.9 Relative expression of defence response genes in roots of *Trichoderma* treated DCS-108 and 48-1 genotypes of castor. Relative levels of mRNA transcript accumulation of 13 genes in *T. asperellum* 7316-treated (a) and *T. asperellum* N13-treated (b) roots of castor at 48 hpi. Actin gene expression was used as control to normalize the expression of the defence genes, using the $2^{-\Delta\Delta CT}$ method. The graphs show the mean expression levels ± standard deviation (SD). The alphabets denote the level of significance of each gene amongst the two genotypes of castor. a: p<0.0; b: p<0.05.

Figure 3.10 Relative expression of defence response genes in leaves of *Trichoderma* treated DCS-108 and 48-1 genotypes of castor. Relative levels of mRNA transcript accumulation of 13 genes in *T. asperellum* 7316-treated (a) and *T. asperellum* N13-treated (b) leaves of castor at 48 hpi. Actin gene expression was used as control to normalize the expression of the defence genes, using the $2^{-\Delta\Delta CT}$ method. The graphs show the mean expression levels ± standard deviation (SD). The alphabets denote the level of significance of each gene amongst the two genotypes of castor. a: p<0.0; b: p<0.05.

Figure 3.11 Effect of *Trichoderma asperellum* 7316 on the accumulation of antioxidative enzymes CAT (a), SOD (b) and GPX (c) and, total phenol content (TPC) (d) either individually or in the combination with *Fusarium* in castor at 3 dpi. Histograms shown by different letters indicating statistical significance level between treatments displayed at Tukey <0.05. Vertical bars represent Mean ± standard deviation (SE).

Figure 4.1 Colonization of DCS 107 roots by *Trichoderma asperellum* 7316 observed through light microscopy. A visual representation of fungal growth in trypan blue stained DCS roots inoculated with *T. asperellum* 7316 at 48 hours post inoculation (hpi); (a) mycelial spread on the root surface, (b) penetration into the roots and (c) enlargement of hyphal tips into vesicles was observed. Arrows indicate *Trichoderma* colonization in root samples. Scale bar 20 μm.

Figure 4.2 Heat map identification of differentially expressed genes across control and *Trichoderma* treated roots of castor at 48hpi. The overall results of hierchial cluster analysis was computed using the log2(FC) value. The colour scale indicates the relative expression levels of all genes in the obtained data. Red colour represents relative increase in abundance, yellow colour represents relative decrease.

Figure 4.3 Venn diagrams representing the DEGs involved in different gene ontology components detected in *Trichoderma* treated roots of castor DCS-107 at 48hpi. The classification includes three GO categories - cellular component (CC), Biological process (BP) and Molecular function (MF).

Figure 4.4 Gene enrichment analysis of plant DEGs in DCS-107 by GO term classification – Cellular components: a – Downregulated, b - Upregulated.

Figure 4.5 Gene enrichment analysis of plant DEGs in 7316 treated roots of castor DCS-107 by GO term classification – Molecular functions.

Figure 4.6 Gene enrichment analysis of plant DEGs in 7316 treated roots of castor DCS-107 by GO term classification – Biological process (Upregulated genes).

Figure 4.7 Gene enrichment analysis of plant DEGs in 7316 treated roots of castor DCS-107 by GO term classification – Biological process (Downregulated genes).

Figure 4.8 Validation of plant DEGs by quantitative Real Time-Polymerase Chain Reaction (RT-qPCR). The relative level of mRNA transcript accumulation of 9 stress and defense-related genes at 12, 24 and 48 hpi in 7316 treated castor DCS-107 roots. Confirmation of (a) upregulated and (b) downregulated plant DEGs using plant Actin as an internal control and non-template DNA control (NTC) is detected in the study. Statistical difference between the time-points is displayed at Tukey $p \leq 0.05$. Vertical bars represent ±SE of the mean values. Statistical significance levels indicated by case letters: a-c.

LIST OF SUPPLEMENTARY TABLES

Table S1 The GenBank accession numbers of submitted ITS and D1-D2 sequences amplified using ITS-1F/ITS-4R primers and NL-1/NL-4 primers respectively.

Table S2 List of RAPD primers used for PCR-based DNA amplification in *Trichoderma* strains.

Table S3 Analysis of percentage polymorphism obtained with RAPD markers in six *Trichoderma* strains.

Table S4 The list of genes and their primer information used for RT-qPCR.

LIST OF SUPPLEMENTARY FIGURES

Figure S1 The schematic diagram of the ITS and D1-D2 regions amplified using universal primers.

Figure S2 Fungal cultures of *Trichoderma asperellum* strains grown on Potato Dextrose Agar (PDA) and *Fusarium oxysporum ricini* grown on CMC medium 7 days - post plating. *Trichoderma asperellum* 7316 (a), *Trichoderma asperellum* N13 (b), *Trichoderma asperellum* TV5 (c), *Trichoderma asperellum* TV2B16 (d) and *F. oxysporum ricini* (e).

Figure S3 Bulk and rhizosphere soil collection from castor roots. Loosely adhering bulk soil that falls off from the root on shaking vigorously (a) and rhizosphere soil that tightly clings to the root surface (b).

Chapter 1

Research Purpose and objectives of study

1.1 Introduction

Castor bean (*Ricinus communis* L.) is considered as one of the most important oil seed crop. It belongs to the genus *Ricinus* and family Euphorbiaceae. Castor plant requires an optimum temperature between 20 °C – 25 °C to grow. Generally it requires well drained sandy and clay loam textured soil to grow to an ideal height of approximately 2-3 metres. Though it is widespread throughout the tropical regions, castor growth is also found abundantly in south-eastern Mediterranean region, Africa and India. Castor bean is reported to tolerate annual precipitation of 2.0 to 42.9 dm, annual temperature of 7.0 to 27.8 °C and pH of 4.5 to 8.3 (Duke, 1983).

Alongside China and Brazil, India is also one of the significant producers and exporters of castor. However, recent data has bought to light that there has been a substantial dip in the percentage of production of castor from India which has obviously affected the economy of the country. Biotic factors like pests and diseases has been the prime factor behind the fall in production of castor. *Alternaria* (Holliday, 1980) and *Fusarium* (Patel and Pathak, 2011) causing leaf spots and wilting respectively cause considerable damage to the crop.

1.2 Importance of castor beans

The major constituent of castor oil is Ricinoleic acid (RA) which constitutes of 90% of the total composition, followed by linoleic acid (4%), oleic, acid (3%), stearic acid (1%) and other linolenic fatty acids. In comparison to other oils, castor oil has a higher oxidative stability and shelf life due to the presence of a hydroxyl functional group that prevents the formation of peroxides. This enables the oil to perform various chemical reactions like dehydration, esterification, halogenation, sulfation and alkoxylation. It is a triglyceride of RA that is whitish in color. It has a faint odour and a viscosity of 889.3 centistokes (**Table 1.1)**. Castor oil has an extensive industrial application.

Castor oil is used majorly in the chemical industry like paints, lubricants, inks and coatings due to the presence of high content of RA.

Table 1.1 Physical properties of castor oil.

Physical Property	**Units**	**Value**	**Physical Property**	**Value**
Density	g/mL	0.959	Hydroxyl Value	162-165
Specific heat	kJ/kg/K	0.089	Saponification Value	177-188
Pour point	(°C)	2.7	Refractive index	1.480
Viscosity	centistoke**s**	889.3	Acetyl Value	143-150
Thermal conductivity	W/m^0C	4.727	Iodine Value	82-90
Flash point	(°C)	145	Unsaponifiable	0.3-0.7%

Castor oil also has numerous application in the pharmaceutical industry. However, before being used in the above industry, the oil is always processed to remove a component called ricin from the oil. Ricin is a allergenic (2S albumin) protein that acts as a strong plant toxin. It is present in the endosperm of the castor seed. It behaves as a type 2 ribosome-inactivating protein that inhibits protein synthesis that ultimately causes cell death.. Hence, castor oil is always processed to remove ricin before being used in any applications.

1.3 Worldwide production of castor

The three main castor-growing nations—India, China, and Brazil account for up to 90% of the world's production. India itself produces 85% of total world production of castor (**Figure 1.1**). making her the leading exporter of castor. Countries like United States, UK, Netherland, European Union, Korea, Belgium, France, Thailand, Japan, Italy, Brazil are the major importers of castor (Patel et al., 2016). The main states in India that cultivate castor are Gujarat, Andhra Pradesh, and Rajasthan; Gujarat accounts for more than 73.02% of the nation's total production, followed by Rajasthan, Telangana, Odisha, and Andhra Pradesh. (**Figure 1.1**). **Table 1.2** provides us with a clear picture of the area and yield of castor seeds produced by state in India. Gujarat produces 2239 kg/ha of castor, while Rajasthan follows with 1591 kg/ha.

Seed output increased between 2001 and 2014 as a result of growing demand for castor oil use in various industries and global export. The Solvent Extractor's Association of India, however, estimates that production in India decreased by 21.4% in 2018–19 compared to 2017–18 (**Figure 1.2**). The production and cultivation of castor are influenced by a number of factors. The slow pace at which seeds germinate, the scarcity of water, weeds, pests, illnesses, and different forms of abiotic stress are some of the factors that hinder the growth of castor.

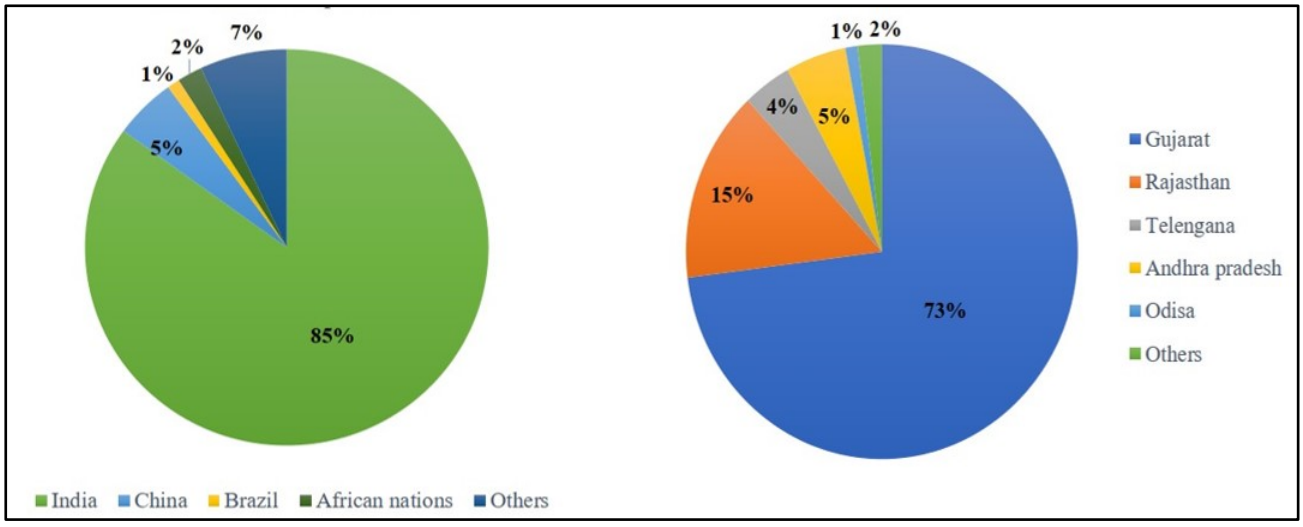


Figure 1.1 Percentages of castor produced worldwide and in each Indian state (Department of Science and Technology, TIFAC).

Table 1.2 India's state-by-state castor seed output and yield data (Source – Solvent Extractor's Association of India).

District	Estimated Area * Under Crop ('000 ha.)			Estimated Production * ('000 tonnes)			Estimated Yield * (Kg / ha.)		
	2021-22	2020-21	2019-20	2021-22	2020-21	2019-20	2021-22	2020-21	2019-20
Gujarat	652	638	741	1547	1494	1659	2371	2342	2239
Rajasthan	120	126	154	203	224	245	1690	1780	1591
A.P. & Telangana	23	38	57	35	56	33	1500	1454	579
Other State #	16	24	21	10	15	24	650	630	600
Total	811	826	973	1795	1789	1962	2228	2166	2016

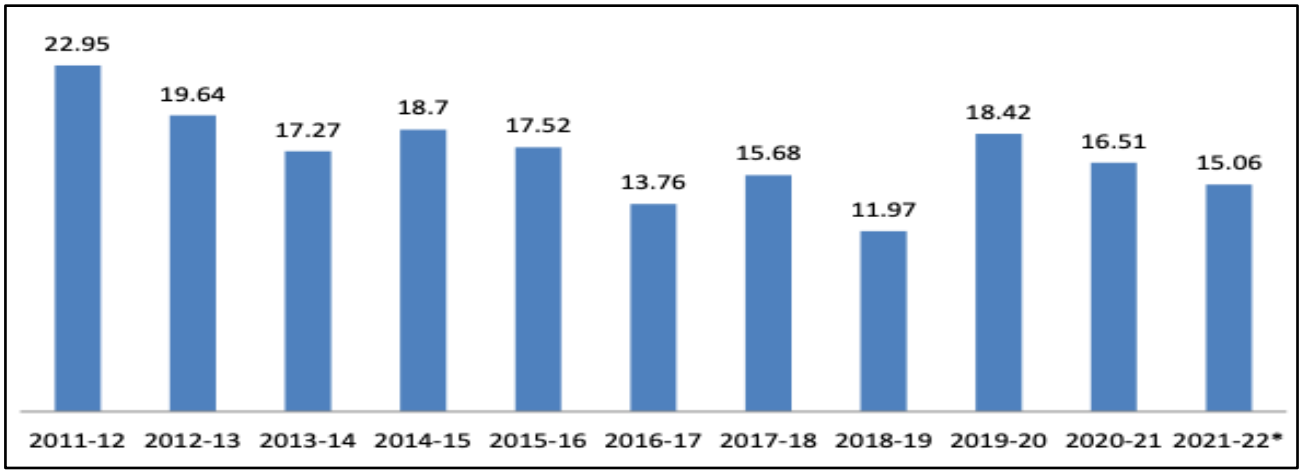


Figure 1.2 A visual depiction of the production of castor beans per year from 2011 to 2022. * Third Advance estimates, Directorate of Economics and Statistics (DES).

1.4 Castor oil derivatives

The chemical industry employs castor oil and its derivatives (**Table 1.3**) for a variety of purposes. They are environmentally friendly and biodegradable because they are made of renewable resources.

Table 1.3 Categorization of diverse castor oil derivatives utilised in the chemical sector (Source – Solvent Extractor's Association of India).

Classification of castor oil derivatives	
Main grades Commercial, FSG, BSS, First Pressed Degummed Grade Castor Oil, Refined Castor Oil, Extra Pale Grade, Castor Oil, Pharmaceutical Grade, Blown Castor Oil, Urethane Grade, Pale Pressed Grade	**Generation I derivatives** Dehydrated Castor Oil, Ethoxylated Castor Oil, Hydrogenated Castor Oil, 12-Hydroxy Stearic Acid (12-H.S.A.), Sulfonated Castor Oil – Turkey Red Oil
Generation II derivatives Sebacic Acid, Heptaldehyde, Undecylenic Acid, Polyols, Ricinoleic Acid, Other Dimer Acids , Undecylenic Aldehydes, 2-Heptanol, 2-Octanol	**Generation III derivatives** Zinc Ricinoleate, Zinc Undecylenate, Methyl 12-HSA, Methyl Ricinoleate, Methyl Undecylenate, Calcium Undecylenate, Others

1.5 Diseases and pests that affect castor production

The decline in castor production is due to numerous biotic and abiotic reasons. several illnesses and pests that cause castor plant extinction are among the several causes of the decline in castor production. In India, the following insect pests are known to affect castor: tobacco caterpillar (*Spodoptera litura*), red hairy caterpillar (*Amsacta* spp.), semilooper (*Achaea janata*), castor shoot borer (*Conogethes punctiferalis*), capsule borer (*Dichocrosis punctiferalis*), and leaf miner (*Liriomyza trifolii*) (Basappa, 2007; Anjani et al., 2010). According to Severino et al., 2012 the main pests in Brazil are the mites *Tetranychus urticae* and *Tetranychus ludeni*, as well as the armyworm (*Spodoptera frugiperda*), *A. janata*, black cutworm (*Agrotis ipsilon*), and stink bug (*Nezara viridula*). Castor plants in Colombia have been observed to be affected by the cotton lace bug (*Corythucha gossypii*) (Varón et al., 2010). An increase in seed production of 28% was achieved by castor farmers in Andhra Pradesh, India, by using an Integrated Pest Management programme that included pesticides, crop rotation, insect traps, and neem extract (Basappa, 2007). It was discovered that cultivars of castor with purple leaves and high anthocyanin

content may withstand leaf miner damage. It has been demonstrated that applying a layer of epicuticular wax (blooming) to castor leaves lessens infestation and defoliation brought on by *A. janata* and *S. litura* (Sarma et al., 2006). Grey mould (*Botryotinia ricini*), vascular wilt (*Fusarium oxysporum* f.sp. ricini), charcoal rot (*Macrophomina phaseolina*), leaf spots (*Alternaria ricini*), *Cercospora ricinella*, and *Xanthomonas axonopodis* pv. *ricini* are the main diseases that impede the growth of castor. *A. ricini* is one of these that does the most harm because it is a seedborne fungus that may also cause pod rot and seedling blight, which can result in a 70% reduction in seed yield (Holliday, 1980).

In recent research, genotypes of castor that are resistant to a variety of castor illnesses have been developed. This necessitates a thorough investigation into the inheritance of disease resistance, as well as the fundamental interactions between the pathogen and the host and the environment that are required for the development of illness in castor (Soares, 2012).

1.6 *Trichoderma*- The Biocontrol agent

In the agro-industry, *Trichoderma*, a member of the Ascomycetes genus, is regarded as one of the most successful biocontrol agents. **Table 1.4** describes the *Trichoderma* classification system. *Trichoderma*, which multiplies quickly in practically all climates, is crucial for improving environmental health. This fungus is not only a common component of the soil's microflora, but it also grows well on plant wastes, soil organic matter, bark, and other materials. *Trichoderma* is thought to play a biocontrol function because of its capacity to interact with soil pathogens, resulting in the development of antibiotics, cell wall-degrading enzymes, mycoparasitism, antibiosis, rhizosphere alteration, and competition for soil resources. (Singh et al., 2018; Mukhopadhyay et al., 2020). It can colonise plant roots and create resistance in them to fight infections, which is how it is classified as an opportunistic avirulent plant symbiont in addition to its direct contact with soil pathogens. Apart from mitigating plant diseases, these fungi exhibit a broader spectrum of activities, such as enabling plants to withstand abiotic stressors like salt and water deficiency (Zhang et al., 2022; Oljira et al., 2020), enhancing nutrient uptake and utilisation (Nunzio et al., 2018), promoting plant growth and development, and removing pollutants from the environment (Harman and Lynch, 2004). Nevertheless, *Trichoderma*'s industrial success stems from its ability to target soil pathogens directly, including bacteria, viruses, fungi, and some nematodes. As a result, more than 60% of approved biopesticides are *Trichoderma*-based formulations (Verma et al., 2007).

Table 1.4 Classification of *Trichoderma*, the biological control agent.

Scientific Classification	
Kingdom	Fungi
Phylum	Ascomycota
Class	Sordariomycetes
Subclass	Hypocreomycetidae
Order	Hypocreales
Family	Hypocreaceae
Genus	*Trichoderma*

1.7 *Trichoderma* growth and development

Trichoderma asperellum, Trichoderma harzianum, Trichoderma atroviride, Trichoderma virens, Trichoderma reesei, and many other significant species are included in the *Trichoderma* strain. In addition to growing on organic matter and bark, *Trichoderma* is isolated from the rhizosphere. Following the testing of 200 novel *Trichoderma* species in China, phylogenetic analysis placed 16 of them in the *Viride* clade. Out of them, seven were wood-occupying species: *T. albofulvopsis, T. densum, T. laevisporum, T. sinokoningii, T. sparsum, T. sphaerosporum, and T. subviride* (Qin and Zhuang, 2016). The growth and development pattern of *Trichoderma* and the factors impacting it have been better understood thanks to existing research. According to research on photoinduced mycelial growth and sporulation of, conidiation is triggered by blue/UV-A light, which is most effective at wavelengths of 320, 380, 440, and 480 nm. Longer wavelengths were less effective, and the response is primarily mediated by BLR-1 and BLR-2 (Flores et al., 2004; Gressel et al., 1968; Kumagai et al., 1969). According to Ramirez et al. (2002), there is evidence linking the G-protein α-subunit with GTPase activity to conidiation. A mutation in the tga1 gene that codes for this subunit prevents *Trichoderma atroviride* IMI 206040 from sporulating. Similar to this, *Trichoderma reesei*'s growth in the dark was greatly inhibited by the deletion of GNA I, one of the G-α subunit's regulatory targets (Siebel et al., 2009). *Trichoderma reesei* contains two Ras subfamily GTPases, TrRas1 and TrRas2, which are essential for fungal morphogenesis and proliferation. Although the effect of TrRas1 was more prominent than TrRas2, null mutation of the previously stated proteins results in total impaired protein and negatively affects fungal growth and morphology (Zhang et al., 2012). In *Trichoderma reseei*, the orthologue of *Aspergillus nidulans*' VELVET A, *VEL1*, has been demonstrated to be essential for both reproduction and structural integrity. Deletion of the

orthologue resulted in swollen, deformed hypha that displayed over branching, with total loss of conidiation and sexual reproduction (Aghcheh et al., 2014).

Trichoderma's ability to reproduce is also impacted by numerous abiotic variables. Temperature is arguably the most important factor influencing its growth out of all of them. According to available data, most *Trichoderma* spp. grow best at temperatures between 25 and 30 °C (Klein and Eveleigh, 1998), with 25 °C being the ideal range for *T. atroviride* LU132 conidiation, which decreased at both low (20 °C) and high (30 °C) temperatures. According to Darayaei et al. (2016), two peaks in conidium production were observed at 20 days and 40-50 days, respectively, during a 25-day and 50-day incubation cycle. This finding supports the earlier finding by Steyaert et al. (2010b) that conidiation is induced by nutrient deprivation. The study also demonstrated that conidiation was significantly reduced in carbon and nitrogen rich media, while conidiation was triggered by carbon/nitrogen deficiency. Nevertheless, despite the fact that *Trichoderma atroviride* LU132 conidiation happened best at 25 °C and at various incubation times, conidia generated at the high incubation temperature, 30 °C, followed by 25 °C and 20 °C, germination was fastest when they were created at these temperatures. Additionally, the composition of the media plays a significant role in the proliferation and sporulation of fungi. Water agar has historically been the least successful proliferating solid medium for *Trichoderma*, while potato dextrose agar (PDA) has always been the best (Jahan et al., 2018; Maurya et al., 2017). After five days of incubation at the ideal temperature of 28 °C and pH 6, Sabouraud Malt Yeast extract Agar (SYMA) medium, however, revealed to be the best for *Trichoderma viride* after testing on a variety of media. The colony diameter of SYMA medium was 3.2 cm. (Mishra et al., 2015). According to Rajput et al., 2014, *Trichoderma harzianum* grows well on sorghum and millet grains, and the fungus is also influenced by carbon and nitrogen supplies during its growth and sporulation.

1.8 Mycoparasitic ability of *Trichoderma*

The ability of *Trichoderma* to mycoparasitize its victim is a major factor in how effective it is as a BCA. A repertoire of enzymes is needed for the entire behavioural process, which includes sensing the prey, moving towards it, recognising it, forming structures resembling haustorias for attachment, coiling, and releasing enzymes that break down cell walls, and finally lysing the prey. Twenty new isolates of *Trichoderma* were recently recovered from Keralan soils; of these, twelve exhibited a strong antagonistic effect against a number of important plant pathogens, including *Rhizoctonia solani*, *Pythium aphanidermatum*, *Phytophthora capsici*, *Fusarium oxysporum, Sclerotium rolfsii, and Ganoderma lucidum* (Hima and Beena, 2016). Small chemicals

that the pathogen secretes—possibly oligopeptides—that are produced by *Trichoderma'*s proteases prior to contact with its prey allow it to "smell" the presence of the pathogen. Furthermore, it has been suggested that G-protein coupled receptors (GPCR) recognise these peptides and then activate a signalling cascade that in turn induces the expression of genes encoding for enzymes needed for cell wall degradation and secondary metabolite biosynthesis (Kubicek et al., 2011; Seild et al., 2009).

In *Trichoderma atroviride*, the GPCR genes gpr1 and tga3 were silenced in order to confirm the likelihood, and neither mutant showed mycotrophy. Zeilinger et al. (2005); Omann et al. (2008). On the other hand, growth inhibition of the host fungus was clearly observed, even though gene deletion of *tga1*, coding for the α subunit of GPCR, resulted in reduced expression of chitinase and antimicrobial metabolites, as well as a complete loss of microparasitic overgrowth of *Trichoderma atroviride* over pathogenic fungus in dual culture experiments. This might be caused by antifungal compounds that *Trichoderma* secretes into the growth media, which would suggest that tga1 has different functions (Reithner et al., 2005). *Trichoderma* moves chemotactically in the direction of its prey after detecting its presence. Mycoparasitism, in which the mycoparasite grows alongside its prey and coils to form infection structures like appresoria/papillae, requires physical contact between prey and *Trichoderma*. The attachment of prey to the mycoparasite is primarily dependent on the recognition of lectins from the fungal prey (Lu et al., 2004; Inbar and Chet, 1996).

According to studies that have been reported, hydrophobins stimulate the creation of appresoria and aid in the identification and adhesion of mycoparasites to their host surface. (Linder and others, 2005; Dubet and others, 2014). A recent study revealed that tvhydii1, a member of the Class II hydrophobin family, may be involved in both mycoparasitism and plant root colonisation. In accordance with the hypothesis, overexpressed and knockout strains of the gene were created and tested for their antagonistic and root colonisation competence. The overexpressed strains demonstrated strikingly opposite results from the knockout strains, which demonstrated less ability to antagonise *R. solani* and less colonisation of tomato roots (Guzman et al., 2017). Enzymes that *Trichoderma* constitutively expresses start the process of breaking down cell walls when infections are recognised and coiling. Hydrolytic enzymes, such as chitinases, β-(1,6), β-(1,3) glucanases, and proteases, mediate the breakdown of cell walls (Djonocic et al., 2006; Geremia et al., 1993; Sanz et al., 2005; Lima et al., 1997). Compared to its natural type, *Trichoderma* has a greater capacity for mycoparasitise due to overexpression of the genes *ech42, cht42*, and *Tvbgn3* expressing the same (Djonocic et al., 2006; Kowsari et al., 2014; Baek et al., 1999). When *T. harzianum* was cocultured with *R. solani* cell wall fragments

that were generated by digesting the cell wall with pure endochitinase 42 (CHIT42, encoded by *ech42*) from *T. harzianum*, Zeilinger et al., 1999 demonstrated that expression of *ech42* was high. Constitutive production of chitinase produces host plant cell wall fragments containing GlcNAc, which sets off *Trichoderma*'s antifungal defence mechanism.

In a genetically engineered experiment, *ech42* was disrupted in *Trichoderma harzianum* P1, preventing the formation of the 42KD endochitinase CHIT42. However, the biocontrol activity of a few stable transformants against *Rhizoctonia solani* and *Botrytis cinerea* revealed varying results. Although the *ech42* defective strain's capacity to parasitize *B. cinerea* was reduced by 40% in vivo, it did not completely lose this ability, suggesting that other mechanisms may be involved in biocontrol. Fascinatingly, when the same mutant was tested against *R. solani*, the results were remarkably different, with the *ech42*-deficient strains demonstrating greater antagonistic potential in vivo than the wild type strain. These findings clearly suggest that a host's influence on the production of hydrolytic enzymes or the activation of alternative pathways, as well as the participation of multiple additional enzymes in mycoparasitism, are present (Woo et al., 1999). Evidence points to the potential participation of α-1,2-mannosidases in mycoparasitism in addition to chitinase and glucanase. The expression of this gene was found to be slightly elevated in *T. harzianum* compared to control in experiments where the mycelium of the fungus was transferred to media containing cell wall components of three pathogenic fungus, namely *Sclerotinia sclerotiorum*, *Fusarium solani*, and *Fusarium oxysporum*. These experiments were followed by RT-qPCR and confrontation dual culture between *T. harzianum* and three fungal pathogens. The highest expression was observed with *F. oxysporum* (58-fold). These findings show that *Trichoderma*'s production of enzymes that break down cell walls causes molecules in F*usarium*'s cell wall to break down, which in turn causes α-1,2-mannosidases to be induced (Paulo et al., 2015). Recently, the use of MALDI MSI has shown several metabolites during the interaction between *Trichoderma* and *R. solani*; among them, some have been recognised as known peptaibols based on their m/z ratio (Holzlechner et al., 2016).

1.9 Root colonization of *Trichoderma*

Plant damage from different phytopathogens is causing an increasing amount of output loss, hence there is a growing need for disease management measures. In lieu of herbicides and insecticides, BCAs and other plant growth-promoting rhizobacteria (PGPR) are a great environmentally friendly option. One of the best biocontrol agents that not only fights plant diseases but also speeds up the growth and development of the plant is *Trichoderma* spp. Plants

colonised by *Trichoderma* roots have a changed gene expression profile, which modifies how the plants react to different biotic and abiotic stimuli. Numerous plant species have previously shown enhanced plant health and growth in addition to disease resistance throughout time.. Plant elicitors of defensive response include Sm1 and Ep1, which have been identified and characterised in *T. virens* and *T. atroviride*, respectively. Exogenous administration of Sm1 has demonstrated resistance to infection by *Colletotrichum* sp. in cotton and other plant diseases. (Salas Marina et al. (2015); Djonovic et al. (2006); Seidl et al. (2006)).

Recently, a paralog of the same *sm2* was found in *T. virens*, and deletion mutants showed much reduced vigour of plant protection in addition to severely defective colonisation of maize roots. (Crutcher and colleagues, 2015; Gaderer and colleagues, 2015). Simultaneously, *Ep1* was subjected to additional investigation, leading to the hypothesis that it functions not only as a defense-inducing agent but also assists *Trichoderma* in perceiving their own and other environments by potentially interacting with their cell walls, shielding them from enzymatic degradation, hyphal coiling, and upregulating mycoparasitic genes that code for multiple lytic enzymes. *Ep1*'s secretion peptide signal revealed that it had a direct role in interacting with various hosts. The absence of *Ep1* caused the plant to perceive *Trichoderma* as a pathogen, which supports the role of *Ep1* as a cell protection agent. This is confirmed by the upregulation of many defensive response genes in beans inoculated with *T. harzianum Ep1* knockout mutants as compared to wild type (Gomes et al., 2015). *Trichoderma* can distinguish between a fungal prey and a plant host and react accordingly. In their 2007 study, Rosado et al. demonstrated the role of the cell wall protein quid 74 in *Trichoderma* self-defense. They found that while both overexpressed and disrupted mutants displayed the same biomass yield, overexpressed mutants exhibited greater resistance to lytic enzymes and improved adhesion to binding surfaces. However, there was an increase in the length and number of secondary roots in overexpressing mutants compared to the knockouts, which led to an increase in the overall biomass due to enhanced nutrient uptake and utilisation. In contrast, disrupting and overexpressing the same in *T. harzianum* CECT did not alter the cucumber root colonisation pattern or capacity (Samolski et al., 2012).

1.10 Secondary metabolites

Numerous data indicate that secondary metabolites play a part in *Trichoderma*'s protective function. Alkanes, aldehydes, and terpenes with antagonistic qualities were among the compounds released by a high salt-tolerant species of *Trichoderma koningiopsis* YIM PH30002, according to GC-MS analysis of the culture media (Chen et al., 2016). Non-ribosomal peptide

synthetases (NRPS) are responsible for the synthesis of a wide range of secondary metabolites, including peptaibols, cyclopeptides, pseudopeptides, siderophores, antibiotics, phytotoxins, and terpenoids. *T. virens'* capacity to synthesise pal was harmed by inactivating mutants of a polyketide synthase (PKS)/NRPS hybrid enzyme, suggesting a function for the corresponding metabolite in induced systemic resistance (Mukherjee et al., 2012).

Trichoderma secretes 80–85% of the peptabiols, as reported in the Peptaibiotics Database (PDB) (Neumann et al., 2015). Peptabiols are short peptides that have been shown to have antibacterial properties (Rahimi et al., 2017), elicit cytotoxic effects, and stimulate the immune system and defence mechanisms in plants. They are being proposed as antibiotic substitutes (Duclohier et al., 2007). Trichokonin VI, which causes apoptosis in plant fungal pathogens, is one of the trichokonins secreted by *Trichoderma pseudokoningii* SMF2 that have demonstrated antimicrobial activities. Trichokonin VI also induces resistance against TMV infection in tobacco by increasing the production of ROS and several defence genes, including pal and pod (Chen et al., 2012; Luo et al., 2010). In comparison to the wild type, a genetic mutation in tex1 that results in the absence of an 18-residue peptabiol led to a reduced level of induced resistance against *Pseudomonas syringae* pv. l*achryman*s and restricted antibacterial activity in cucumbers. Increased resistance against the pathogens can result from the synthetic application of TvBI and TvBII peptabiols (Viterbo et al., 2007). One of the most thoroughly researched peptaibols is alamenthicin, which when extracted from *T. viride* was applied to lima beans and caused a reaction mediated by jasmonic acid (JA) and salicylic acid (SA) (Engelberth et al., 2001). In *Trichoderma*, a wide variety of these peptaibols have been found and described (Wiest et al., 2002; Daniel et al., 2007; Djonovic et al., 2006). Recent research has demonstrated that the harzianolide extracted from *T. harzianum* not only functions as a strong promoter of plant development but also triggers the expression of multiple genes involved in the defence response, ultimately resulting in effective biocontrol of *Sclerotinia sclerotiorum* in tomato plants (Cai et al., 2013).

In order to phytoextract iron from its surroundings and prevent other microorganisms from accessing it, *Trichoderma* secretes siderophores, ion-chelating compounds/metabolites that also cause competitive antagonism (Anke et al., 1991; Lehner et al., 2013; Segarra et al., 2010; Srinivasan et al., 1995; Chakraborty et al., 2008). Cucumber plants exhibiting siderophore-producing *Trichoderma asperellum* Q1 demonstrated growth-promoting capabilities under abiotic conditions of salt stress. Due to its affinity for Fe3+ bingeing and plant uptake, harzianic acid, a siderophore, has recently demonstrated to be a potent plant growth promoter when fed with tomato seeds. These findings suggest that siderophores have a role in

enhancing plant nutrition (Vinale et al., 2013; Qi et al., 2013). *F*or the manufacture of its isoprene unit, hydroxy-methylglutaryl-CoA reductase (HMGR) is necessary for a variety of distinct terpenoids that have been found in *Trichoderma*. *Rhizoctonia solani* and *Fusarium oxysporum* were less susceptible to the antifungal effects of hmgR mutants of *Trichoderma harzianum* with reduced enzyme activity (Cardoza et al., 2007). Research has shown that *T. gamsii*, when applied to wheat plants, can both alleviate *Fusarium* leaf blight and reduce the production of trichothecene deoxynivalenol (DON) by *Fusarium* species. Trichothecenes are another group of toxic secondary metabolites that are primarily secreted by *Fusarium* (Sarrocco et al., 2013). Trichodermin, a toxic trichothecene, requires the enzyme trichodiene synthase, which is represented by the *tri5* gene. *Trichoderma brevicompactum* overexpressing mutants produced higher amounts of trichodermin, and the agar diffusion assay demonstrated that trichodermin exhibited antifungal activity against a variety of plant pathogens with a vigour greater than that of conventional antibiotics such as hygromycin (Tijerino et al., 2011). Terpene synthase is also necessary for the production of Harzianum A (HA), another trichothecene produced by *Trichoderma arundinaceum.* In contrast to wild type strains, the loss of function of the *tri5* and *tri4* genes, which both result in loss of HA synthesis, not only caused a dramatic loss of antagonistic activity against *Botrytis cinerea* and *Rhizoctonia solani,* but also prevented tomato plants from mounting a defence response against *Botrytis* through the use of SA or JA. Malmoerca et al., 2013 and Malmierca et al., 2015 conducted a study wherein they observed that the overexpression of *tri5* in *T.harzianum* CECT 2413 led to the manufacture of a trichodiene, which in turn increased the expression of defensive response genes associated to SA in tomatoes. Thus, all of these studies suggest that terpenoids may play a part in interactions between *Trichoderma* and plants. It has been shown that *Trichoderma virens* contains novel terpenoids and other terpene-containing substances that can inhibit DNA polymerases. Although the function of *Vir4*, which codes for a terpene cyclase in *Trichoderma virens*, is yet unknown, it is in charge of the production of several volatile terpene chemicals. In 2003, viridepyronone—an antifungal chemical derived from *Trichoderma viride*—was first reported to exhibit antagonistic activity against fungi that cause infections in the body. (Crutcher et al., 2013; Yamaguchi et al., 2010; Evidente et al., 2003). Furthermore, plants that have been colonised by *Trichoderma* also produce terpenoids. Desoxyhemigossypol and hemigossypol buildup in cotton roots colonised by *Trichoderma virens* was demonstrated by Howell et al., 2000, and this significantly inhibited the growth of *R. solani*. Many other studies have demonstrated the role of terpenoids in the defence response triggered by *Trichoderma* 6-pentyl pyrone, a lactone that is derived from linoleic acid and is also known as an oxylipin. In addition

to breaking down the toxin fusaric acid, which is secreted by *Fusarium moniliforme*, 6-PP, which was isolated from *Trichoderma* and applied as a foliar spray and stem treatment, enhanced plant height and leaf area, decreased the severity of *Botrytis* infection in tomato plants, and increased *PR* gene expression in plants that were treated. Furthermore, 6-PP and harzianic acid significantly changed the composition of the metabolome in tomato leaves. (Mazzei et al., 2016; El-Hasan et al., 2007; Vallare et al., 2008). *Trichoderma* also produces a different class of metabolites known as polyketides (Baker et al., 2012); nevertheless, there isn't any concrete proof of their involvement in promoting plant growth. Nevertheless, there is a clear indication from gene deletion studies about its participation in the green coloration of fungus, the formation and stability of the conidial call wall, as well as *T. reesei*'s antagonistic character against other pathogenic fungi (Atanasova et al., 2013).

1.11 Induced Resistance

Trichoderma has demonstrated its beneficial effects on a wide variety of plants for many years, including against some of the most destructive plant infections, such as pests like *Leucinodes orbonalis*, which is responsible for brinjal infestations (Ghosh et al., 2016, Redda et al., 2018). *Trichoderma* treatment has led to a notable increase in biomass and yield in pea, rice, and tomato. It has also helped to prevent *Meloidogyne javanica* wilt and root rot caused by *Verticillium dahlia*, *Fusarium oxysporum* f.*sp. lycopersici*, and *F. solani* in tomato and chickpea. (Ahmad et al., 2016; Yan et al., 2021; Idris et al., 2014; Singh et al., 2016; Doni et al., 2016; Doni et al., 2017). *T. asperellum ZJSX5003* and *T. gamsii 6085,* respectively, effectively inhibited the growth of *Fusarium graminearum* on maize and rice, with 6085 lowering the formation of the mycotoxin trichothecene deoxynivalenol (DON) by 92%. *T. gamsii* 6085 expressed every chitinase both before and after coming into touch with the pathogen, according to the qPCR data. (Matarese et al.,2012; Li et al., 2016). Three *Trichoderma* isolates, TCN-8, TCN-11, and TCN-12, significantly inhibited the growth of *Fusarium moniliformae*, which causes sugarcane wilt (Gawade et al., 2012). When tested with rice, *Trichoderma viride* T14 was shown to produce the maximum amount of IAA, demonstrating both the crop's strong growth promotion activity and antagonistic ability. (Kale and others, 2016). Recently, metabolite profiling of *Trichoderma cremeum* liquid culture revealed the existence of cremenolide, a new antifungal molecule with growth-promoting and antifungal effects. (Vinale et al., 2016). It has been demonstrated that *Magnaporthe grisea* and *Bipolaris oryzae*, two of the main rice pathogens, are significantly inhibited by *Trichoderma viride* and *Trichoderma harzianum Rifai*. *Heminthosporium oryzae, Pyricularia oryzae, Sarcocalsdium oryzae,* and *Rhizoctonia solani* (Ramalingam et al., 2013;

Saldana et al., 2016). When applied as a talc-based formulation, *Trichoderma rifai* has been demonstrated to be effective against fungal infections in tomato plants and to promote overall fruit development and yield (Satish et al., 2016). Additionally, it triggers an antioxidant defence response in wheat and groundnuts to combat the oxidative burst brought on by *Fusarium oxysporum* and *Aspergillus niger*, respectively. (Subhalaxmi et al., 2017; Gajera et al., 2016). The mycelial extracts of *T. harzianum* and *T. viride* revealed a variety of volatile and non-volatile chemicals, as well as HPLC-purified compounds, that exhibited the highest growth retardation of *C. falcatum*, the sugarcane red rot pathogen (Suresh and Nelson, 2016).

In vivo and in vitro treatment of potato late blight, a disease caused by *Phytophthora infestans*, has been alleviated by strains of *T. harzianum*. In addition, (Buysens et al., 2016; Yao et al., 2016) rice treated by *Trichoderma* showed distinct expression of the genes encoding dehydrin and aquaporins, which led to drought tolerance in genotypes of maize and rice. (Zhang et al., 2016; Pandet et al., 2016; Guler et al., 2016). Many plant pathogenic fungi were significantly suppressed in their growth by *T. harzianum* ST5 and PBT 23 (Kamaruzzaman et al., 2016; Saxena et al., 2014). In Arabidopsis plants treated with *T. harzianum* T34, where *PR-1*, *WRKY* transcription factor, and glutathione transferase—which are typically activated by SA—were downregulated, microarray analysis revealed the role of JA and SA mediated defensive response. According to Moran-Diez et al., 2012, there was a downregulation of several defence genes activated by JA, such as β-amylase, chalcone synthase, and chlorophyllase 1. This suggests that both JA and SA responses were inhibited, maybe in an effort to start a symbiotic relationship with *Trichoderma.* In conjugation with the plant growth-promoting *Bacillus* sp. WG4, *Trichoderma harzianum* PBT23 also demonstrated strong mycoparasitic and antibiotic effects against major destructive pathogens such as *S. sclerotiorum*, *R. solani*, S*. rolfsii*, *F. oxysporum f.sp. cice*ri, and *B. cineria* (Sabalpara et al., 2009; Jimtha et al., 2016). Under the attack of the leaf pathogen *Colletotrichum capsici*, *T. harzianum* (BHUF4) and *T. asperellum* (T16A) treatment in chilli showed enhanced growth response along with elevated levels of phenolic content and PAL activity in leaves of *Trichoderma*-foliar sprayed plants. This indicates the protective role of *Trichoderma* regardless of its application (Saxena et al., 2016). *Trichoderma* biopriming and seed treatment have increased germination rates and growth in several plants, including wheat (Behzad et al., 2016).

1.12 Rationale for research study

Since India is one of the main exporters of castor oil, the development and manufacturing of castor oil has significant economic benefits for the nation. Reports, however, indicate that a

significant reduction in castor output may result from plant mortality from a variety of illnesses. Because of the importance of castor plants and their derivatives, it is necessary to be able to boost this output while reducing the number of castor plant losses. Testing *Trichoderma*'s potential to prevent diseases that cause castor loss makes sense, since it has already been shown to be a very effective biological control agent, protecting a variety of plants against a range of phytopathogens by boosting their growth and stimulating their immune response.

Though *Trichoderma*'s promise as a BCA has already been demonstrated, further research is still needed to fully comprehend the underlying molecular pathways. Therefore, a better understanding of the process causing resistance will let the fungus be used to treat castor plants more extensively and effectively.

1.13 Hypothesis and research purpose

Trichoderma is thought to increase the output of castor plants and be able to withstand two of the major castor diseases, *Alternaria* and *Fusarium*. In order to verify the theory, research is done to determine which strain of *Trichoderma* is the most promising by looking at a variety of factors. The study aims to determine important defence chemicals involved in inducing systemic resistance in castor and comprehend the molecular mechanism behind it, in addition to discovering a strong strain of *Trichoderma*. Thus, the following goals were created, tested, and the results are presented objectively in different chapters in order to complete the aforementioned research study.

1.14 Objectives of the study

1. **Characterization of *Trichoderma* strains for novel species-specific markers by multiplex PCR and antagonistic property against *Alternaria ricini* in castor (*Ricinus communis* L.)**
2. **Assessing rhizosphere *Trichoderma asperellum* strains for root colonizing and antagonistic competencies against Fusarium wilt through molecular and biochemical responses in castor.**
3. **Delineating host responses induced by *Trichoderma* in castor through comparative transcriptome analysis by next generation sequencing.**

Chapter 2

Characterization of *Trichoderma* strains for novel species-specific markers by multiplex PCR and antagonistic property against *Alternaria ricini* in castor (*Ricinus communis* L.)

2.1 INTRODUCTION

In agriculture, Biological control agents (BCAs) refer to microorganisms or modified organisms that can reduce the incidence of diseases in plants caused by various pathogens. The direct interaction between soil microorganisms and the rhizosphere of plant plays a vital role in modulating plant growth, the yield, nutrient absorption and also energy conversion in soil (De et al., 2015). Fungi are an essential component of any ecosystem whereby they can either act as potential BCAs or cause mild and severe plant diseases. The fungal members of the genus, *Trichoderma* have been identified as efficient BCAs that are able to minimize the occurrence of diseases in plants.

Trichoderma fungi are yellowish green to green spored, soil-borne microorganisms that are classified as opportunistic and avirulent plant symbionts dwelling majorly in plant-root ecosystems (Harman et al., 2004). *Trichoderma* helps plants in various different ways. Previous studies have demonstrated the ability of *Trichoderma* to promote growth and development by colonizing the roots of plants (Guzman-Guzman et al., 2018). Application of *Trichoderma harzianum* strain, T-22 induced systemic resistance in tomato against cucumber mosaic virus (Vitti et al., 2016). Similarly, biopriming with *Trichoderma asperellum* showed direct improvement in plant growth in a large variety of vegetable crops like cucumber, tomato, brinjal, chilli, guar, and okra (Singh et al., 2016). It has also been demonstrated that seed treatment with *Trichoderma* spp. has been able to activate defence responses against pathogens, along with an increase in the seed yield and overall production in wheat crops (Xue et al., 2017).

Trichoderma strains isolated from the rhizosphere may vary in their ability to perform the functions of a BCA. Considering the positive effect of *Trichoderma* on overall plant growth and protection, it essentiates the need for more number of beneficials strains to be identified and characterised. Identification of *Trichoderma* strains are done through morphology-based screening for genus level identification along with molecular data for accuracy. Therefore, it necessitates the screening of *Trichoderma* strains to assess their genetic variability based on both morphological and molecular differences. In order to do so, it is mandate to have precise molecular methods that can reveal reliable phylogenetic information. For decades, assessing molecular differences between strains through PCR-based amplification and sequencing of the internal transcribed spacer (ITS) region (White et al., 1990) and D1-D2 region of nuclear ribosomal DNA (Kwiatkowski et al., 2012) have been regularly used to conduct phylogenetic studies. The demarcation of ITS as the official DNA barcode marker is considered as a notable

progress and has helped the scientific community immensely. For instance in 2011, a multinational consortium of mycologists nominated the ITS region as the official fungal barcode, which was later approved by the Consortium for the Barcode of Life and Schoch et al., 2012 showed that ITS region has the highest probability for the correct identification of the largest array of fungi. It serves as the most clearly defined barcode gap between inter and intra specific variation among fungal strains. However, over the years there has been some debate on the performance of ITS and D1-D2 as the sole and most suitable fungal barcoding marker specially for genera like *Aspergillus, Cladosporium, Fusarium, Penicillium, and Trichoderma* that have a very narrow or no barcode gap in their ITS region. Therefore, this limitation led research to include other gene loci as well to identify and characterise fungal species. Liu et al., 1999 proved the suitability of using the *rpb2* (nuclear gene) that encodes the second largest largest subunit of the RNA polymerase II to provide good resolution to the identification of Ascomycota. Additionally, a study was conducted by a group of mycologists with >1500 species of Dikarya (Ascomycota and Basidiomycota) for different markers (Stielow et al., 2015) and they concluded that translation elongation factor 1-alpha (*TEF1*) can be used additionally as an efficient secondary barcode marker that would definitely enhance the resolution to ITS and D1-D2 based fungal identification. Zheng et al., 2021 isolated 208 isolates of *Trichoderma* out of which 23 new species of *Trichoderma* was identified using *TEF1* and *rpb2* as the molecular markers. Thus, compiling the inputs from other genetic loci data that include *TEF1* and *rpb2* sequences have been suggested for accurate phylogenetic analysis (Chaverri et al., 2015; Dou et al., 2018; Cai et al., 2021).

Random amplified polymorphic DNA (RAPD) markers are a set of molecular marker comprising of DNA fragments obtained by PCR of the genomic DNA by short synthetic arbitrary primers. Identification of microorganisms using RAPD is an inexpensive yet powerful typing method for many fungal and bacterial species. Several studies have confirmed the same (Bautista-Muñoz et al., 2003). Caligiorne et al., 1999 used RAPD method to test genetic variation among 13 different strains of chromoblastomycosis and phaeohyphomycosis etiologic agent fungi. The research concluded that such a genotypical data can provide sufficient information for the scientific community to use the unweighted pair-group method to cluster the strains in accordance to their respective species. Thus, it can be safely said that RAPD markers could be used as an easy and robust tool for the characterization of several microbial species. In our context, investigating for DNA-based polymorphism among the *Trichoderma* strains would not only reveal nucleotide level variability (Sagar et al., 2011) but also enable to develop markers for the detection of *Trichoderma* in samples. SCAR markers are DNA fragments amplified by

PCR using specific 15-30 bp primers that are designed from sequenced nucleotide sequences that are procured from cloned RAPD fragments. Yang et al., 2018 developed a 797 bp marker specific to *Ps. citricarpa* via the RAPD technique which was used to design a primer Pc-SFP/Pc-SRP that identified *Ps. citricarpa* with a single and distinct band of 389 bp but did not amplify DNA from other tested fungal species. Similar work was done in Korea by Lee et al., 2013 for the rapid and accurate detection of *Phytophthora katsurae*, the causative agent of chestnut ink disease. The SCAR markers are highly specific and reproducible, and are used mainly in gene mapping studies and marker assisted selection.

Therefore the work behind the first objective of the research study is aimed at identifying and characterising a set of isolated fungal strains as *Trichoderma* and detect interspecies variation among the strains under study. In order to achieve the above goal, both morphological and molecular screening of all the isolated fungal strains was carried out by multiplex PCR using different fungal barcode markers like ITS, D1-D2, TEF1 and rpb2. Further, confirmation of the results obtained in the above PCR reactions was done by the additional use of previously identified species-specific SCAR markers. Additionally, RAPD markers were also used to analyse genetic variation among the isolated fungal strains. The study also included the synthesis of a new set of SCAR markers to detect *Trichoderma* strains. Knowing the mycoparasitic antimicrobial characteristic of *Trichoderma* strains, experiments were done against *Alternaria ricini* that causes the leaf spot disease of castor through confrontation plate and detached leaf assays. This enabled the detection of potential strain(s) of *Trichoderma* to utilize them as a BCA for disease control.

2.2 MATERIALS AND METHODS

2.2.1 Fungal isolation, maintenance and multiplication

Six fungal strains- N13, 7316, TV5, TV2B16, TV3 and TS4 were procured from the Indian Institute of Oilseeds Research (IIOR), Hyderabad. They were isolated from the rhizospheric soil of castor growing region in Telangana, India. Single-spored cultures were grown at 25 °C on Potato Dextrose Agar (PDA) for 7 days. Two strains of *Trichoderma*; *Trichoderma asperellum* Ta05 (JN104485, JN104500) and *Trichoderma harzianum* Th03 (JN039047, JN0390101) were obtained from Indian type Culture Collection (ITCC) (Devi et al., 2012) and included in all experiments as controls. *Alternaria ricini,* a fungal pathogen, that causes leaf spot disease was isolated from lesions on leaves of castor that was grown in greenhouse conditions at the University of Hyderabad (UoH) (**Figure 2.1**). The diseased leaves were surface sterilized with 0.5% sodium hypochlorite solution for 2 min followed by washing three times with sterile distilled water. The mycelial growth from the pathogen infected leaves was streaked with a sterile loop on PDA plates and incubated at 25 °C. A pure culture was prepared by isolating a single spore from a single colony and plated on PDA medium. The spores were confirmed by examining under a light microscope (Leica model; make: Olympus-IX81) at 40X. In order to achieve effective sporulation, *A. ricini* was cultured in a sporulation (S) medium that was prepared by dissolving 20 g sucrose and 30 g $CaCO_3$ per litre of distilled water. The media was autoclaved at 121 °C at 15 psi for 15 min before inoculation.

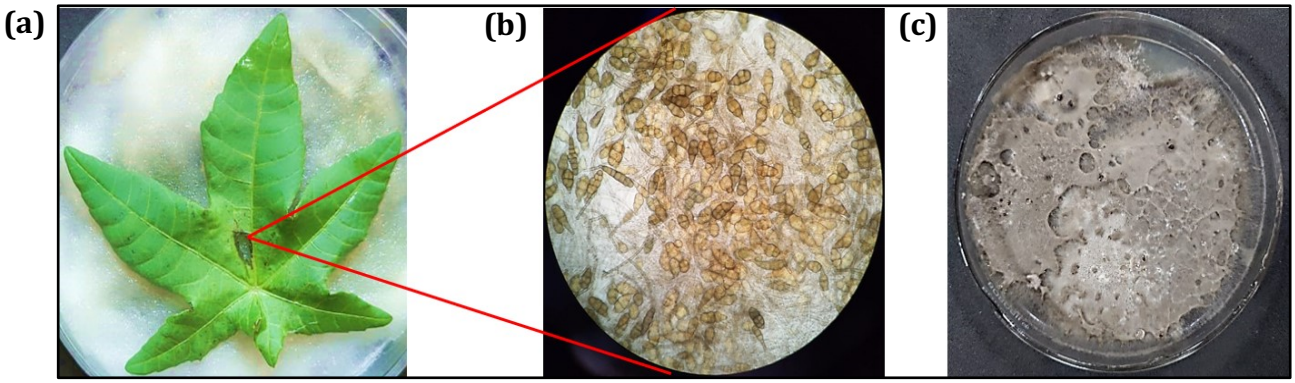


Figure 2.1 Leaf spot infected leaves of castor (*Ricinus communis* L.) were used to isolate *Alternaria ricini*. (a) Isolation of *A. ricini* spores from the leaf spot of castor. (b) Spores of *Alternaria* visualized by light microscopy at 40X. (c) Single spored culture of *A. ricini* grown in the sporulation (S) medium at 25 °C as visualized seven days post culturing.

2.2.2 Microscopic examination of fungal strains

A specimen of each of the fungal strains grown on PDA medium was transferred to sterilized glass slides using a sterilized inoculation loop and examined under the scanning confocal

microscope (M/s Carl Zeiss make; Model no- LSM 880). Monitoring of mycelial growth rate, colony appearance, and structural features including phialides and spores as described previously (Bissett 1984, 1991a, 1991b, 1991c) was carried out for phenotypic evaluation of the strains.

2.2.3 Fungal DNA Extraction

Genomic DNA was extracted individually from the six fungal strains under study by adopting the method given by Jaisani and Pandey (2017) with modifications. Fungal mycelia was ground to a fine powder using liquid nitrogen in a mortar. CTAB buffer was added and the mixture was incubated for 15 min at room temperature with occasional mixing. Post incubation, the mixture was centrifuged at 12,500 rpm for 10 min and supernatant transferred to a sterile 1.5 ml Eppendorf tube. An equal volume of phenol:chloroform:isoamyl alcohol (25:24:1) was added to the supernatant and gently mixed. The emulsion was again centrifuged at 12,500 rpm for 15 min. An equal volume of isopropanol was added to the upper aqueous layer. The mix DNA was incubated at −20 °C for 1h followed by centrifugation at 12,500 rpm for 15 min for genomic DNA precipitation. The precipitated DNA was washed with 70% ethanol by centrifuging at 12,500 rpm for 5 min. The DNA pellet was air-dried at room temperature for 15 mins and re-suspended in 1X Tris-EDTA (TE) buffer. The amount of DNA was quantified using Nano drop Spectrophotometer (Hitachi-Hi Tech Co. Ltd.) at 260 nm absorbance and checked on 0.8% agarose gel electrophoresis as well.

2.2.4 PCR amplification, gel elution and sequencing

PCR was carried out in 25 µL reaction volumes containing 9 µL of PCR grade water, 2 µL each of forward and reverse primers (10 pmol), 3 µl of 1:10 (20 ng) diluted genomic DNA and 9 µL of Emerald Master-mix (Emerald GT PCR MM - 2X premix; Takara brand). The PCR amplification of the ITS region was carried with the primer pair, 1F (5'-TCCGTAGGTGAACCTTGCGG-3´) and 4R (5´-TCCTCCGCTTATTGATATGC-3´) (White et al., 1990; Chakraborty et al., 2010). The PCR amplification of D1-D2 region was carried using NL-1 (5'-GCATATCAATAAGCGGAGGAAAAG-3') and NL-4 (5'-GGTCCGTGTTTCAAGACGG-3') (Kwiatkowski et al., 2012) primers. The schematic diagram of the ITS and D1-D2 regions amplified using universal primers is presented in **Supplementary Figure S1**. The cycling conditions for ITS amplification was standardized as initial denaturation step at 95 °C for 5 min followed by 30 cycles with denaturation at 95 °C for 30 s, annealing at 55 °C for 45 s and extension at 72 °C for 30 s, followed with a final extension of 10 min at 72 °C and storage at 4

°C. The PCR conditions for D1-D2 region amplification were set at an initial denaturation step at 95 °C for 2 min, followed by 30 cycles with denaturation at 94 °C for 15 s, annealing at 55 °C for 30 s, extension at 68 °C for 2 min followed by a final extension of 5 min at 68 °C and storage at 4 °C. The PCR products were subjected to electrophoresis for 40 min on a 1.2% (w/v) agarose gel (HiMedia Laboratories Pvt. Ltd.) that was stained with ethidium bromide (HiMedia Laboratories Pvt. Ltd.) and observed under UV trans-illuminator. The resulting amplicons were eluted from the agarose gel using Nucleospin Gel (Macherey-Nagel brand) and PCR Clean-up kit (Takara brand) according to the manufacturer's instructions and confirmed through a re-run on a 1.2% agarose gel. The amplified PCR products were sequenced and submitted to GenBank (**Supplementary Table S1**).

2.2.5 *In-silico* and phylogenetic analysis of ITS and D1-D2 sequences

In order to conduct a homology-based search between the ITS and D1-D2 DNA sequences of the six fungal strains under study against previously reported *Trichoderma*, BLASTn tool and multiple sequence alignment tool Clustal Omega (EMBL-EBI) was used. The ITS and D1-D2 sequence information of other reported *Trichoderma* strains were obtained from National Center for Biotechnology Information (NCBI) public domain. They were compared with the ITS and D1-D2 sequence information of the six fungal strains. The phylogenetic tree was constructed based on the neighbour-joining method using sequences amplified with ITS-1F/ITS-4R and NL-1/NL-4 primers. Phylogenetic analyses were performed by MEGA10 (Molecular Evolutionary Genetics Analysis) program (Tamura et al., 2011). A parsimony analysis was conducted using a heuristic search, with a starting tree obtained via stepwise addition, with random addition of sequences with 1000 replicates.

2.2.6 PCR for *Trichoderma* identification

In order to confirm that the fungal strains under study belong to the genus *Trichoderma*, the primer pair, T2AF (5'-CTCTGCCGTTGACTGTGAACG-3') and T2AR (5'-CGATAGTGGGGTTGCCGTCAA-3') which is specific to *T. asperellum* (Devi et al., 2017) was used to amplify translation elongation factor1 (*TEF1*). The PCR reaction mix consisted of 10 pmol of primer concentration**.** The reaction cycle was optimised at an initial denaturation step at 94 °C for 1 min followed by 30 cycles of 45 s at 94 °C, 45 s at 62 °C, and 1 min at 72 °C, followed by a final extension step for 10 min at 72 °Cand final storage at 4 °C. Similarly, the primer pair Th1F (5'-TTGCATGGGTTCGCTAAAGG-3') and Th1R (5'-TCTTGTCAGCATCATGGCCGT-3') which is specific to *T. harzianum* (Devi et al., 2017) was used to amplify the second largest subunit of

RNA polymerase II (*rpb2*). The PCR reaction is as follows: an initial denaturation step at 94 ^{0}C for 2 min followed by 35 cycles of 30 s at 94 °C, 30 s at 57.30 °C, and 1 min at 72 °C, followed by a final extension step for 10 min at 72 °C and storage at 4 °C. Multiplex PCR was carried using both sets of primers simultaneously in the same PCR for all the strains of *Trichoderma.* The PCR products were resolved on a 1.2% agarose gel containing ethidium bromide.

2.2.7 PCR for *Trichoderma* specific SCAR markers

The SCAR primer sets; 2F2/2R2 and 2F2/2R3 (Perez et al., 2014) specific to *T. harzianum* were used. PCR conditions were set up as previously described. The thermal cycler conditions were set with an initial denaturation step at 94 °C for 3 min, followed by 30 cycles with denaturation at 94 °C for 1 min, annealing at 62 °C for 1 min, extension at 72 °C for 1 min and a final extension of 7 min at 72 °C and storage at 4 °C. Multiplex PCR was carried using both sets of primers simultaneously in the same PCR for all the strains of *Trichoderma.* The PCR products were resolved on a 1.2% agarose gel containing ethidium bromide.

2.2.8 Random amplified polymorphic DNA (RAPD) profiling and data analysis

Random decamer primers obtained from Operon Technologies Inc., USA (synthesized by using M/s Bioserve Biotechnologies (I) Pvt. Ltd) were (**Supplementary Table S2**) were used to evaluate genetic diversity within the fungal strains. A 20 µL reaction mixture was used for each primer that contained 100 ng of genomic DNA, 10 µL of Emerald master-mix (Emerald GT PCR MM - 2X premix; Takara brand), and 2.5 µL of the primer (5 pmol). The PCR parameters were as follows: initial denaturation at 94 °C for 5 min followed by 40 cycles: denaturation at 94 °C for 1 min, annealing at 36 °C for 1 min, extension at 72 °C for 2 min, with a final extension at 72 °C for 7 min and storage at 4 °C. In order to assess the consistency of the DNA band profiles each reaction was repeated twice. The PCR products were electrophoresed on a 1.2% agarose gel containing Ethidium bromide. Based on the presence or absence of bands, the PCR products from the gels were scored as '1' and '0' respectively. Only the prominent and reproducible bands were taken into account for statistical analysis. The significance of polymorphism detected between the strains was tested by the DARwin program (version 6.0.18) and phylogenetic trees were drawn to analyze the relatedness among the fungal strains and with other reported *Trichoderma* strains as described previously. The correlation coefficients were calculated for the mean values of the size of amplicons.

2.2.9 Developing new SCAR markers

In order to synthesize novel SCAR markers, the polymorphic DNA bands generated by RAPD primers; OPZ-06 and OPK-10 were selected. The amplicons were excised from the gel and purified by Nucleospin Gel (Macherey-Nagel brand) and PCR Clean-up kit (Takara brand) according to manufacturer's instructions. On sequencing the excised amplicons, Clustal Omega (EMBL-EBI) was used to align the sequences respectively. Primers were designed using the Primer3 software from conserved regions of *T. asperellum* and *T. harzianum* strains. Two SCAR primer pairs were designed. Primers T1 and T2 was designed as forward and reverse primer pairs for *T. asperellum* while T3 and T4 was designed as forward and reverse primers for identification of *T. harzianum* respectively. The PCR parameters comprised of an initial denaturation at 94 °C for 5 min followed by 40 cycles with denaturation at 94 °C for 1 min, annealing temperature gradient from 40 to 64 °C for 1 min, extension at 72 °C for 2 min, with a final extension at 72 °C for 7 min and storage at 4 °C. Multiplex PCR was performed using the two primer sets simultaneously in the same PCR for all the strains. *Trichoderma* strains; *T. asperellum* Ta05 and *T. harzianum* Th03 along with *T. longibrachiatum* and *T. virens* were used as controls to validate the specificity of the designed SCAR primers.

2.2.10 Dual culture assays

Antagonistic capability of *Trichoderma* isolates against *A. ricini,* the causative agent for leaf spot disease in castor was carried out using dual culture method. Petri plates containing approximately 15 mL of PDA (supplemented with CaCO3 0.03%). was inoculated with mycelial discs of size 5 mm in diameter that was taken from the actively growing end of seven-day-old *Trichoderma* cultures. Opposite to it, similar fungal discs of *Alternaria* was placed. Both the fungal discs were placed at equal distance from the periphery. Owing to the slow growth of *Alternaria*, each of the *Trichoderma* strains was placed at the opposite periphery 48 hours post inoculation (hpi) with *Alternaria* discs. The plates were incubated at 25 °C for 7 days. Radial growth of the fungal pathogen and *Trichoderma* was measured from 4 to 7 days post inoculation (dpi). The experiment was repeated three times with ten replications each and mean values were computed. The PDA plates cultured with *Trichoderma* and *Alternaria* discs only served as negative controls. The percentage inhibition was calculated as given below:

% Inhibition (Δ) = {(D1 – D2) / D1} X 100; wherein D1 is colony diameter in the control and D2 is colony diameter in the treated sample.

2.2.11 Detached leaf assays for antibiosis

Healthy leaves from four-week-old castor plants of the two genotypes; DCS 107 and 48-1 was collected. Before treatment, the leaves were surface sterilized. Leaves were washed with 70% ethanol followed by 1% sodium hypochlorite solution for 2 min. The leaves were then thoroughly rinsed with autoclaved double distilled water to remove any traces of sodium hypochlorite from the leaves. Rinsing was done three times separately. Sterilized leaves were then dried on autoclaved blotting paper. A conidial suspension of 1 x 10^6 spores/ml was prepared for all four strains of *Trichoderma.* The adaxial surface of each leaf segment was sprayed with 1mL of the spore suspension of each strain of *Trichoderma*. Leaves of control plants were sprayed with autoclaved sterile double distilled water. The *Trichoderma* inoculated and control leaves were stored in a laboratory incubator on moist cotton to avoid leaf drying and incubated for 24 h at 25 °C. After 24 h, the agar plugs of 5 mm diameter taken from growing margins of *Alternaria* were placed in the centre of the adaxial surface of each leaf segment. The experimental set up was incubated at 25 °C. Incubation period (IP) ie., the number of days from inoculation to the appearance of visible symptoms, monitored by daily observation was 3 days. The experiments were repeated three times with five independent replications. *Alternaria* disease incidence was monitored at 3 dpi and 7 dpi. Visual rating was given to each inoculated leaf based on disease symptom like lesion size and intensity of discoloration of leaves (in comparison to control leaves). The ratings ranged from 0-5 and are as follows:

i) 0 - no symptoms, immune to pathogen with no lesions or chlorosis (–)
ii) 1 - high resistance with a few lesions covering less than 10% of the leaf surface (+)
iii) 2 - moderately resistant covering 1–25% of the leaf surface with lesions (++)
iv) 3 - susceptible to pathogen with 26–50% of the leaf surface covered with lesions (+++)
v) 4 - highly susceptible showing 51–75% of the leaf surface infected (++++)
vi) 5 - above 76% infected, complete coverage with lesions (+++++)

2.3 RESULTS

2.3.1 Microscopic analysis of fungal strains for morphological characterization

The characteristics of the different fungal strains ware studies under the microscope and compared amongst each other. The fungal strains growing on PDA culture for five days post was analysed for their growth pattern. All four strains - N13, 7316, TV5 and TV2B16 formed a characteristic green-coloured mycelia and spores. The remaining two strains - TV3 and TS4 developed a whitish-yellow to yellowish-green colour.

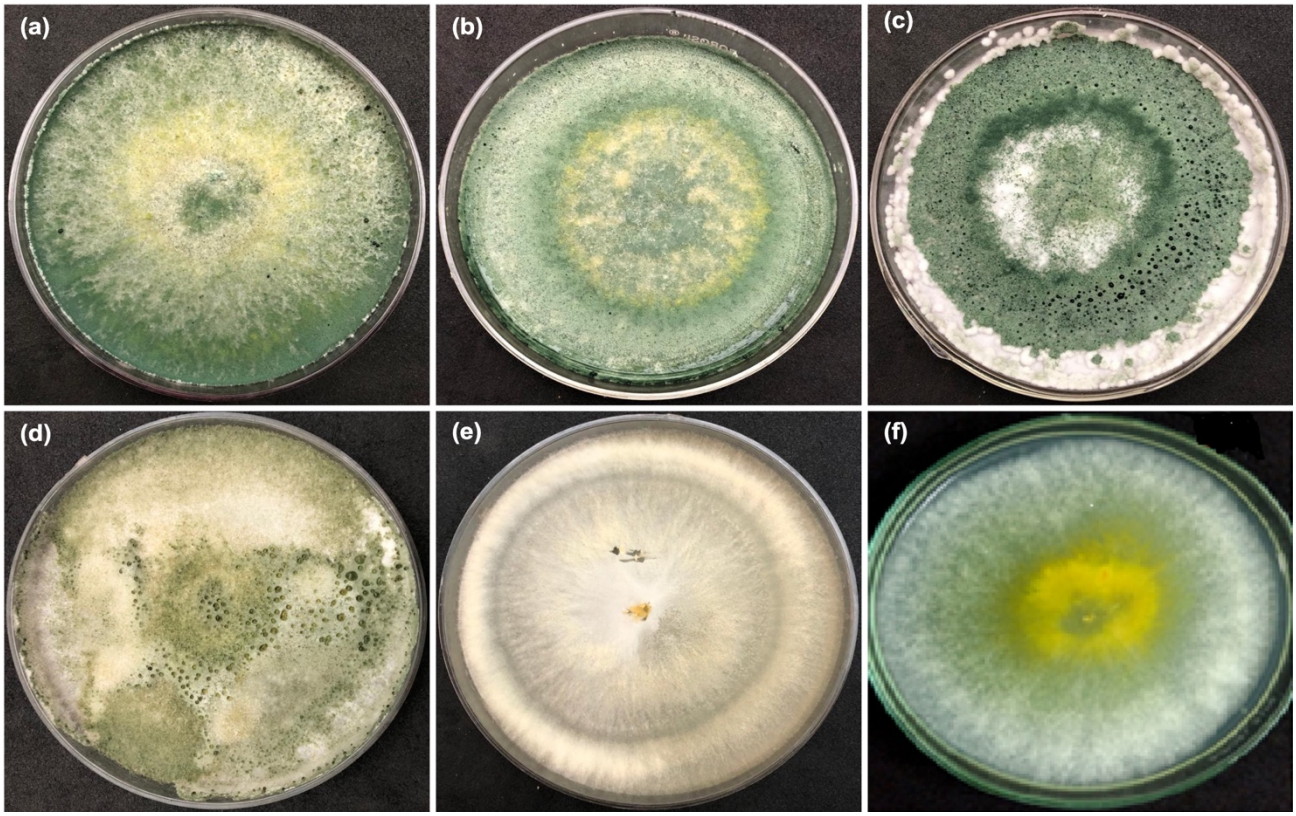


Figure 2.2 Monitoring the mycelia growth of six fungal strains grown on potato dextrose agar (PDA) medium at 25 °C as visualized seven days post culturing. (a) N13, (b) 7316, (c) TV5, (d) TV2B16 (e) TV3 (f) TS4.

This served as the first evidence indicating that the strains could belong to genus *Trichoderma* but maybe falling in two distinct groups (**Table 2.1**). Further, conidiation pattern of all the strains was also studied which showed visible variation (**Figure 2.2**). *Trichoderma* strains, N13, 7316 and TV5 yielded effusing concentric ring-like sporulation pattern. TV2B16 showed no ring formation but produced loose tufts of conidia. The strain, TS4 appeared to be fluffy and cottony while TV3 showed a radial growth pattern. The branching pattern showed striking difference among the strains. The conidiophores of the four strains; N13, 7316, TV5 and TV2B16 showed profuse alternating branching with lateral branches.

Table 2.1 Morphological characteristics of six fungal strains cultured on potato dextrose agar (PDA) medium.

Fungal strain	**Mycelium colour**	**Conidiation**	**Conidiophore**	**Conidia shape**	**Conidial colour**
N13	Pale white	Concentric zones	Moderately branched	Globose to obovoid	Dark green
7316	Snowy white	Effuse in concentric rings	Highly branched	Globose to sub-globose	Green
TV5	White	Effuse in concentric rings	Moderately branched	Globose to obovoid	Dark green
TV2B16	White	Lose tufts with no ring formation	Branched	Sub-globose to obovoid	Green
TV3	Watery white	Loose tufts in concentric rings	No branching	Globose to sub-globose	Yellow
TS4	White	Lose tufts in concentric zones	No branching	Globose to sub-globose	Whitish yellow

However, N13, 7316 and TV5 showed predominant branching of the main axis into phialides that formed penicillate heads at the tip of the branches, TV2B16 produced secondary branches with very less phialides. On the contrary, branching was absent in *Trichoderma* strains - TS4 and TV3. In addition, variation in the conidiation pattern was also detected among the *Trichoderma* strains. The strains N13, 7316, TV5 and TV2B16 sporulated profusely compared to TV3 and TS4 which produced very scarce number of spores which corresponds with the branching pattern observed in these strains by phase-contrast microscopy. Therefore, phenotyping of the *Trichoderma* strains revealed variation in mycelial morphology, branching of conidiophores, sporulation pattern and shape of conidia. The above results showed that TV3 and TS4 are morphologically different, thus distinguishing them from the remaining four *Trichoderma* strains; N13, 7316, TV5 and TV2B16 (**Figure 2.3**).

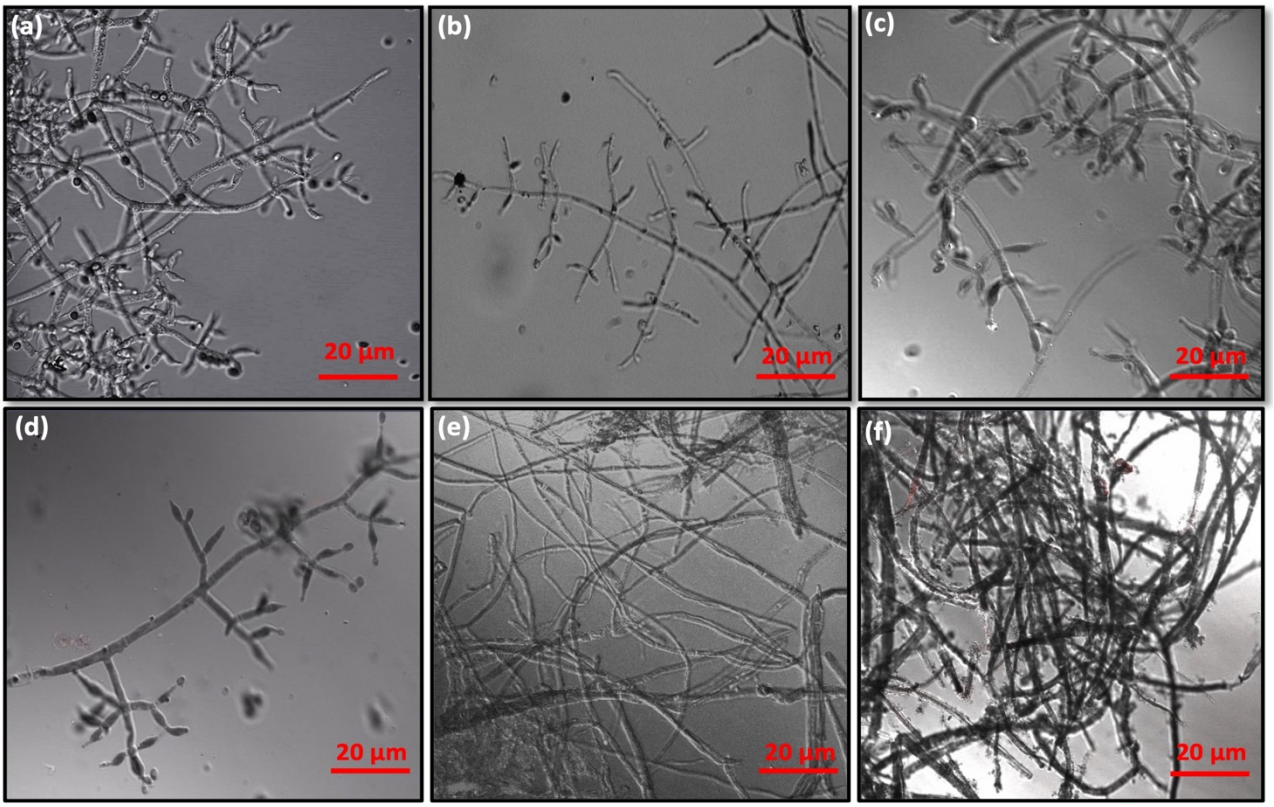


Figure 2.3 Comparison of morphological states of six fungal strains using phase-contrast microscopy. (a) N13, (b) 7316, (c) TV5, (d) TV2B16 (e) TV3 (f) TS4. Scale Bar: 20 µm.

2.3.2 Molecular characterization of fungal strains based on PCR amplification of their ITS and D1-D2 region

PCR amplification of the ITS and D1-D2 regions of all the six strains; N13, 7316, TV5, TV2B16, TV3 TS4 was done along with two control *Trichoderma* strains; *T. asperellum* Ta05 and *T. harzianum* Th03. Amplicons of size ranging between 500–600 bp were generated for all the strains. (**Figure 2.4**). The ITS and D1-D2 sequences obtained for the six fungal strains were subjected to a Blast search individually. All the obtained sequences showed significant sequence similarity with the two *Trichoderma* species - *T. asperellum and T. harzianum* respectively (**Table 2.2**). The highest similarity was seen between the ITS and D1-D2 sequences of the two strains - N13 and 7316 (MH356723.1 and MH236427.1 respectively) and *Trichoderma.* The ITS sequences of N13 and 7316 showed identical sequence similarity of 99.83% to *T. asperellum,* QT21984 (KY209917.1) and their D1-D2 sequences (MK411202.1) and MK411201.1) showed 99.82% and 99.65% similarity respectively with *T. asperellum,* CBS125571 (MH877858.1). Similarly, the ITS sequences of the two strains - TV5 (MK411216.1) and TV2B16 (MH393229.1) also showed >99 percent similarity to *T. asperellum*. The above results suggest first level confirmation that these strains were related to *T. asperellum*. On the

contrary, ITS and D1-D2 sequences of the two strains, TV3 and TS4 showed >99 percent similarity to *T. harzianum* strain, CBS 130681 (MH877292.1) indicating them as *T. harzianum* strains.

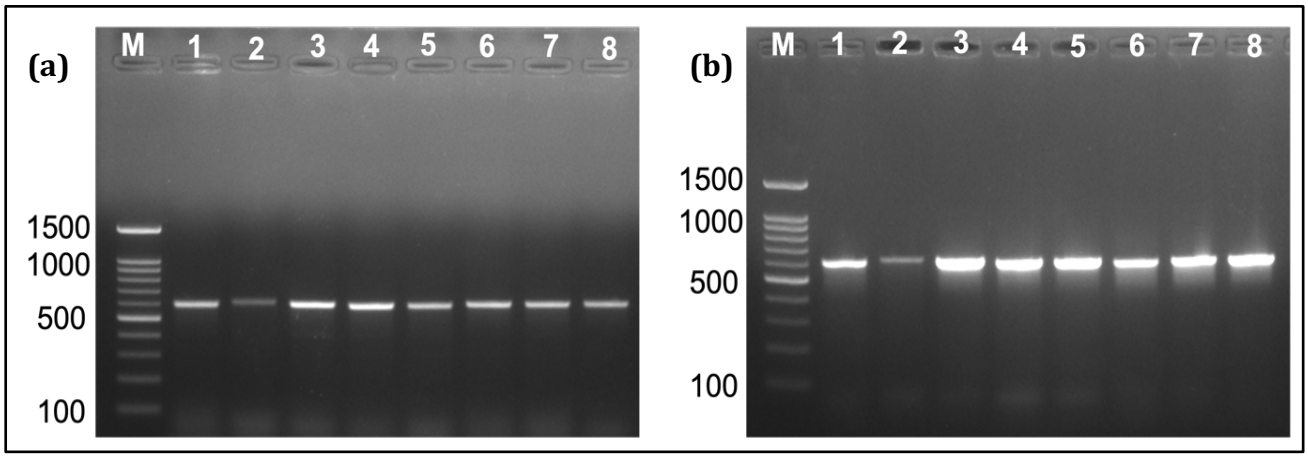


Figure 2.4 (a) Gel image showing ITS region based PCR amplification of *Trichoderma* strains, (b) gel image showing D1-D2 region-based amplification of *Trichoderma* strains. Lanes 1-8: *Trichoderma* strains-*T asperellum* N13 (L-1), *T. asperellum* 7316 (L-2), *T. asperellum* TV5 (L-3), *T. asperellum* TV2B16 (L-4), *T. asperellum* Ta05 (L-5), *T. harzianum* TV3 (L-6), *T. harzianum* TS4 (L- 7) and *T. harzianum* Th03 (L-8). M: 100 bp DNA ladder.

In order to assess the phylogenetic relationship among the six *Trichoderma* strains, a tree was constructed based on the neighbour-joining method using sequences amplified with ITS-1F/ITS-4R and NL-1/NL-4 primers. Two control strains; *T. asperellum* Ta05 and *T. harzianum* Th03 along with other recently reported strains of *T. asperellum* and *T. harzianum* (Zheng at al., 2021) were also included into the phylogenetic tree. Distant strains; *Trichoderma longibrachiatum* and *Trichoderma virens* were also added in the analysis to give a clear demarcation of strains. The fungal member, *Mycospharella etlingerae* strain, CBS 129062 (JF770452.1), a necrotroph was included as an out-group. The phylogenetic tree constructed using ITS sequences showed that the six strains clearly grouped into two clusters: cluster A and cluster B. (**Figure 2.5**). The two strains TV3 and TS4 along with. Th03 fell into the cluster A. Cluster B included the four strains- 7316, N13, TV5 and TV2B16 along with the control strain Ta05. Likewise, the D1-D2 sequences of the six fungal strains also cluttered into two major clusters: cluster C and cluster D (**Figure 2.6**). Cluster D included the four strains N13, 7316, TV5 and TV2B16 along with the control strain Ta05. Cluster E comprised of the two strains TV3and TS4 along with the control strain Th03.

Table 2.2 BLAST-search results of ITS and D1-D2 sequences of *Trichoderma* strains amplified using ITS-1F/ITS-4R primers and NL-1/NL-4 primers respectively.

Trichoderma strains	BLAST-search results of ITS sequences					BLAST-search results of D1-D2 sequences					
	Score values	Query cover %	E value	Similarity (%)	Accession No. of highest similarity strain	Score values	Query cover %	E value	Similarity (%)	Accession No. of highest similarity strain	Species
N13	1112	98	0	99.83	KY209917.1 (*T. asperellum* QT21984)	1038	97	0	99.82	MH877858.1 (*T. asperellum* CBS125571)	*Trichoderma asperellum*
7316	1112	98	0	99.83	KY209917.1 (*T. asperellum* QT21984)	1035	97	0	99.65	MH877858.1 (*T. asperellum* CBS125571)	*Trichoderma asperellum*
TV5	1101	98	0	99.51	KM268676.1 (*T. asperellum* DWG3)	1027	97	0	99.47	MH877858.1 (*T. asperellum* CBS125571)	*Trichoderma asperellum*
TV2B16	1094	98	0	99.34	MK691700.1 (*T. asperellum* T16)	1029	71	0	99.30	MH478122.1 (*T. asperellum* ERR11-12)	*Trichoderma asperellum*
TV3	1114	98	0	99.04	KY225678.1 (*T. harzianum* QT22144)	1031	97	0	99.65	MH877292.1 (*T. harzianum* CBS130681)	*Trichoderma harzianum*
TS4	1116	97	0	99.35	KY225678.1 (*T. harzianum* QT22144)	1037	98	0	99.65	MH877292.1 (*T. harzianum* CBS130681)	*Trichoderma harzianum*

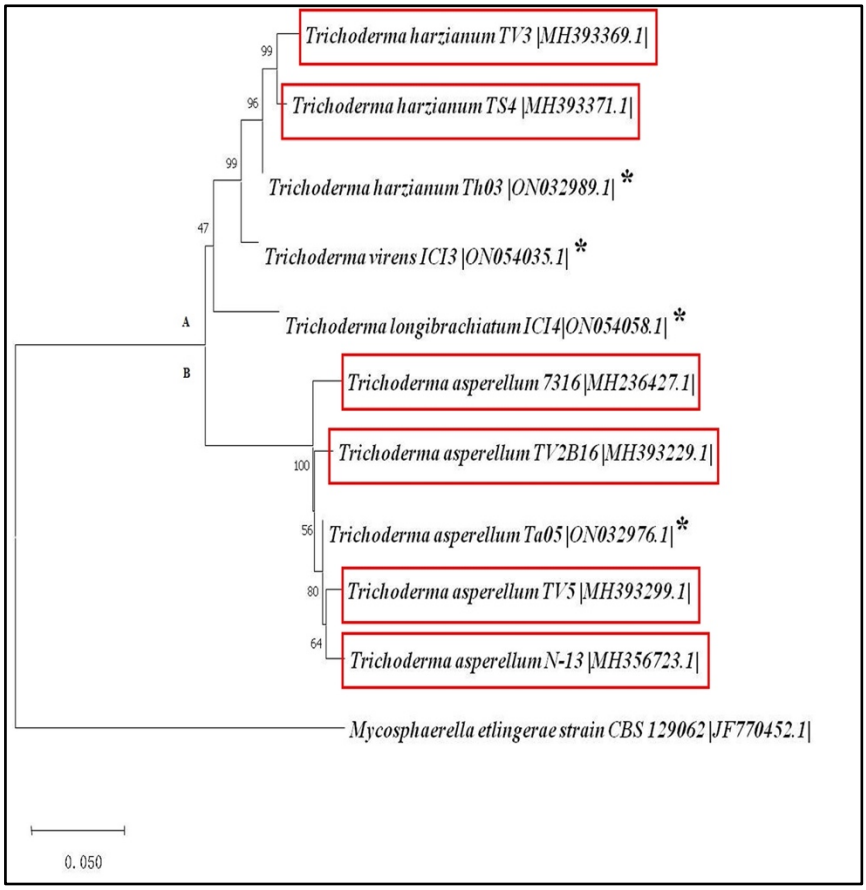


Figure 2.5 Phylogenetic tree of *Trichoderma* strains based on ITS sequences. Ex-type strains of *Trichoderma* species are marked by an asterisk.

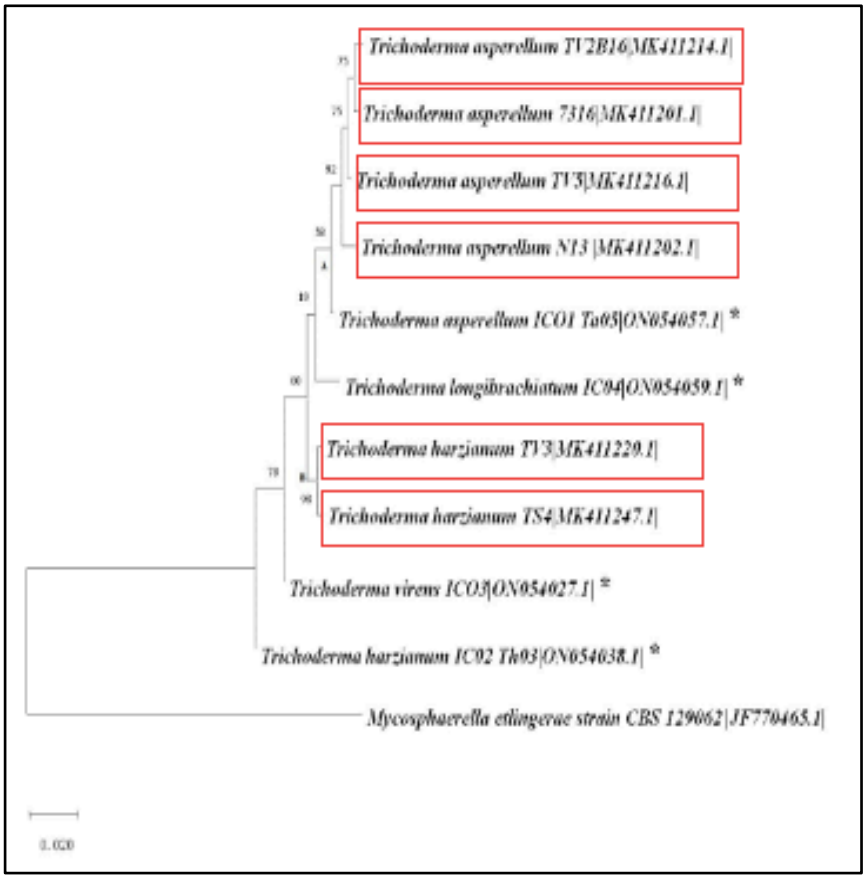


Figure 2.6 Phylogenetic tree of *Trichoderma* strains based on D1-D2 sequences. Ex-type strains of *Trichoderma* species are marked by an asterisk.

Now, to further validate the relatedness among the strains, dendrograms were drawn using complementary ITS (**Figure 2.7**) and D1-D2 (**Figure 2.8**) sequences of these six strains with 20 previously established and reported *Trichoderma* strains having both their ITS and D1- D2 sequences submitted in NCBI. A significant level of genetic similarity was observed among the *Trichoderma* strains confirming them as two distinct groups. The above results confirm that the cluster comprising of 7316, N13, TV5, and TV2B16 strains showed significant relatedness to *T. asperellum*, while TV3 and TS4 strains that formed a distinct separate group was genetically similar to *T. harzianum.* Thus, on comparison between the two phylogenetic trees, a clear demarcation was observed. Four of the strains, N13, 7316, TV5, and TV2B16 along with the reference strain Ta05 clubbed into a single cluster, while the remaining two strains, TV3 and TS4 along with the reference strain Th03 grouped into a separate cluster.

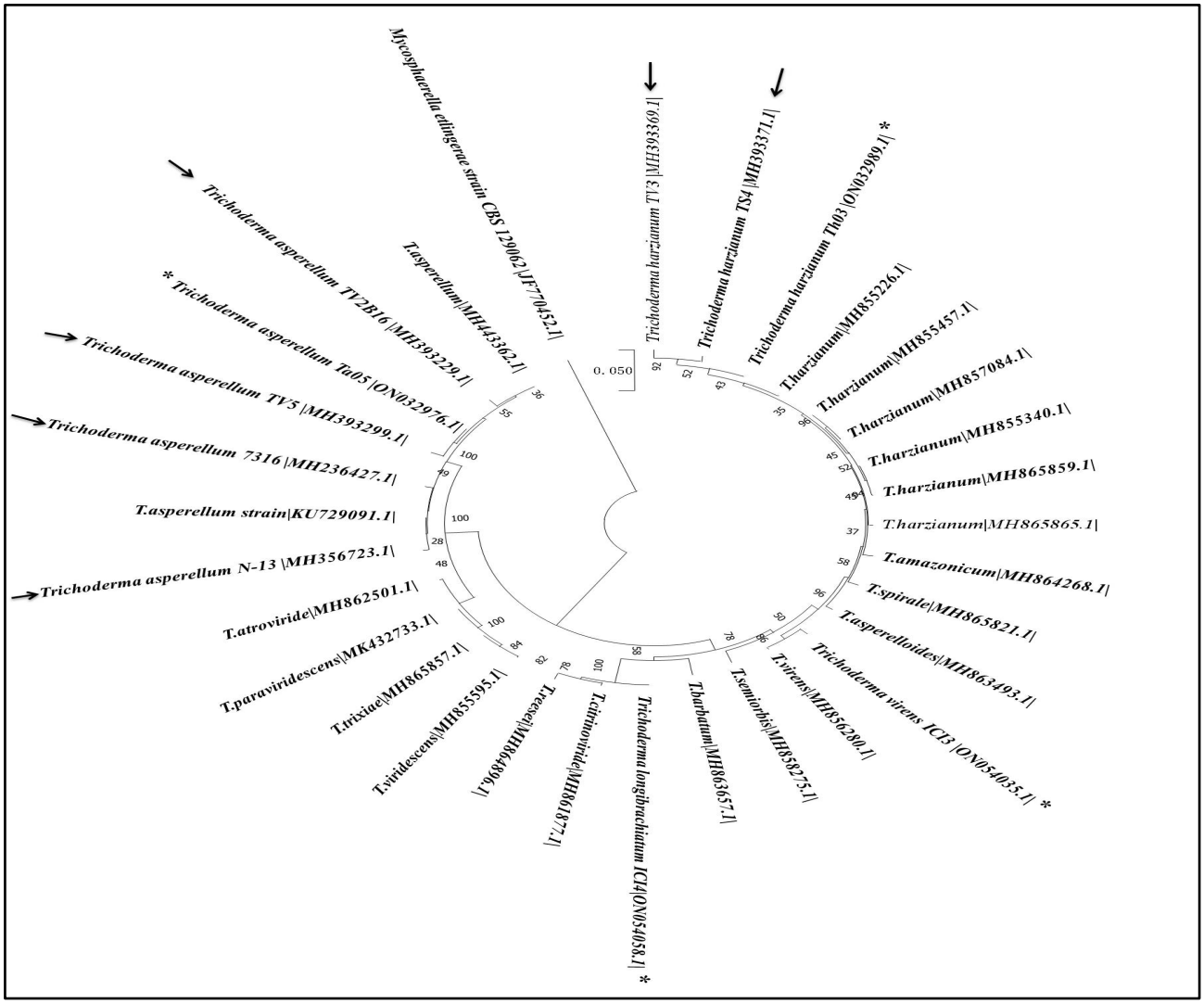


Figure 2.7 Phylogenetic tree of *Trichoderma* strains based on ITS sequences of 20 strains. Ex-type strains of *Trichoderma* species are marked by an asterisk.

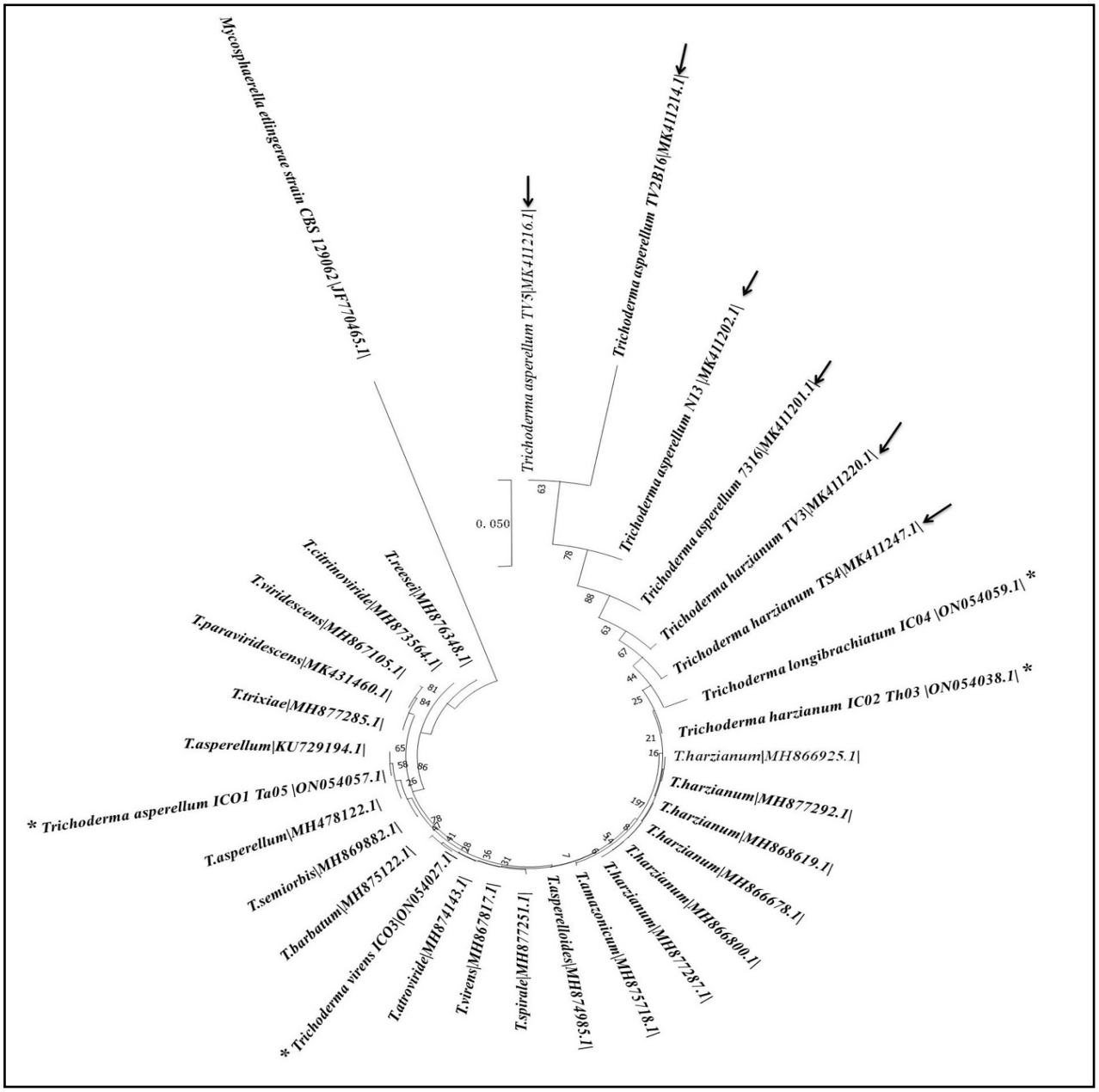


Figure 2.8 Phylogenetic tree of *Trichoderma* strains based on D1-D2 sequences of 20 strains. Ex-type strains of *Trichoderma* species are marked by an asterisk.

Further, the ITS sequence of these six strains was also compared with 100 reported *Trichoderma* sequences. Out of these 100 strains, 36 strains belonged to *T. asperellum*, 49 strains belonged to *T. harzianum*, along with strains of other distant *Trichoderma* species (**Figure 2.9**). The clustering pattern was consistent with the previous dendograms. Thus with all the above mentioned results, it was be concluded that strains N13, 7316, TV5 and TV2B16 showed a significant level of relatedness with *T. asperellum* while the strains TV3 and TS4 which formed a separate cluster showed great genetic similarity with *T. harzianum*.

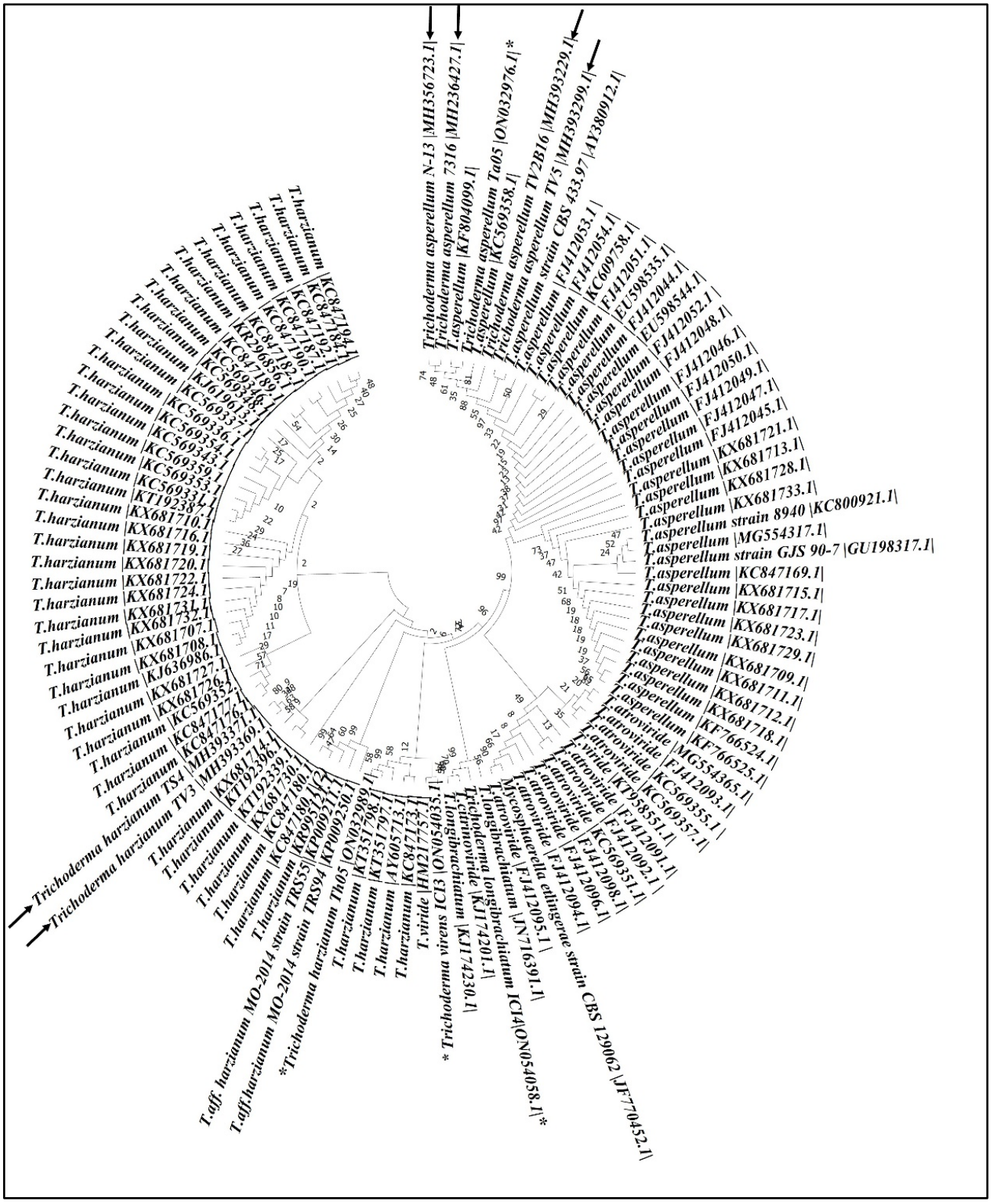


Figure 2.9 Phylogenetic tree (radial view) of six strains of *Trichoderma* spp. along with 100 other reported *Trichoderma* ITS sequences.

2.3.3 Confirmation of *Trichoderma* spp. based on PCR based amplification of *TEF* and *rpb2* genes

Post noticing the phylogenetic closeness of the six fungal strains to *T. asperellum* and *T. harzianum*, a PCR analysis was done to confirm the results. T2AF/T2AR and TH1F/TH1R are two *Trichoderma* species-specific primer pairs that is reported to be specific to *T. asperellum and T. harzianum* respectively. T2AF/T2AR primer amplifies the translation elongation factor 1 (*TEF1) gene*, and TH1F/TH1R primer pair amplifies the second largest subunit of RNA polymerase II (*rpb2) gene respectively.* PCR with T2AF/T2AR produced a unique amplicon of size 507 bp for 7316, N13, TV5, TV2B16 and Ta05 strains. However the band was absent in TV3, TS4 and Th03. (**Figure 2.10a**).

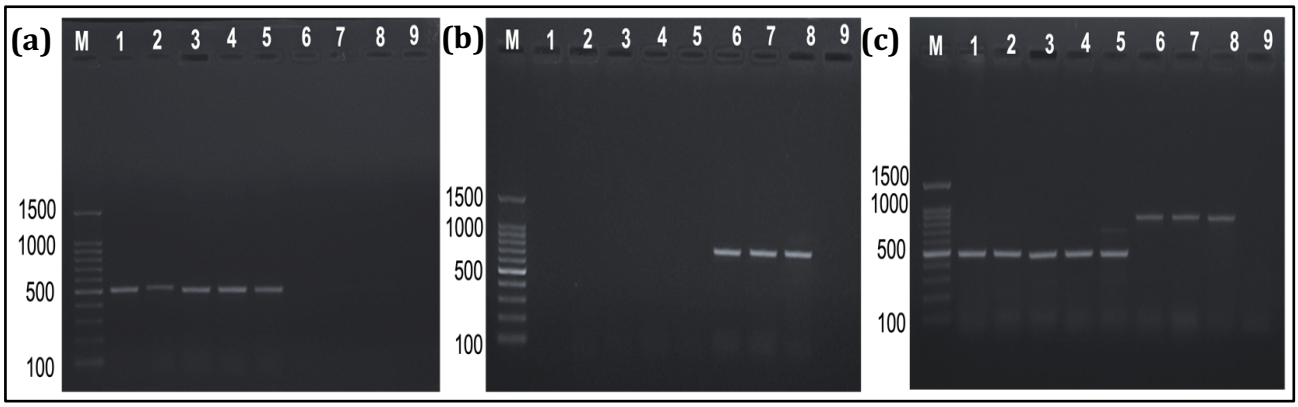


Figure 2.10 *Trichoderma*-species specific PCR amplification. (a) T2AF/T2AR amplified *T. asperellum*-specific polymorphic band in N13, 7316, TV5, TV2B16 and Ta05 (L-1 to L-5) at 507 bp but absent in TV3, TS4 and Th03 (L-6 to L-8). (b) TH1F/TH1R amplified *T. harzianum*-specific polymorphic band in TV3, TS4 and Th03 at 824 bp (L-6 to L-8) but absent in N13, 7316, TV5, TV2B16 and Ta05 (L-1 to L-5). (c) Multiplex PCR confirmed the results. The *Trichoderma* strains: *T asperellum* N13 (L-1), *T. asperellum* 7316 (L-2), *T. asperellum* TV5 (L-3), *T. asperellum* TV2B16 (L-4), *T. asperellum* Ta05 (L-5), *T. harzianum* TV3 (L-6), *T. harzianum* TS4 (L- 7), T. *harzianum* (L-8). L-9 is non-template control. M: DNA 100 bp ladder.

Similarly, PCR amplification of the *rpb2* gene with TH1F/TH1R primer pair produced a 824 bp amplicon that was observed in TV3, TS4 and Th03 strains (**Figure 2.10b**) only, while the band was absent in the strains 7316, N13, TV5, TV2B16 and Ta05. Multiplex PCR was done using both the primer sets T2AF/T2AR and Th1F/Th1R simultaneously in a single reaction mix to validate the specificity and accuracy of the obtained PCR results (**Figure 2.10c**). For all, PCR with non-template DNA was included as the negative control. The results were consistent with the above findings. Hence, it was confirmed that N13, 7316, TV5 and TV2B16 belonged to the

genus *Trichoderma asperellum* whereas TV3 and TS4 belonged to the genus *Trichoderma harzianum* respectively.

2.3.4 Validation of *Trichoderma spp*. based on PCR based amplification of SCAR markers

Further, to confirm the detected *Trichoderma* species, the SCAR markers specific to *T. harzianum* were tested by employing the two sets of primers; 2F2/2R2 and 2F2/2R3 in the screening of the strains under study. The 2F2/2R2 and 2F2/2R3 primer sets amplified 278 bp and 448 bp DNA fragments respectively in the strains, TV3, TS4 and Th03 while no amplification was observed in the strains: N13, 7316, TV5, TV2B16 and Ta05 (**Figure 2.11**). Multiplex PCR using 2F2/2R2 and 2F2/2R3 together also displayed a similar amplification pattern thereby confirming the findings that TV3 and TS4 were strains of *T. harzianum* (**Figure 2.11**). PCR using the non-template DNA served as negative control.

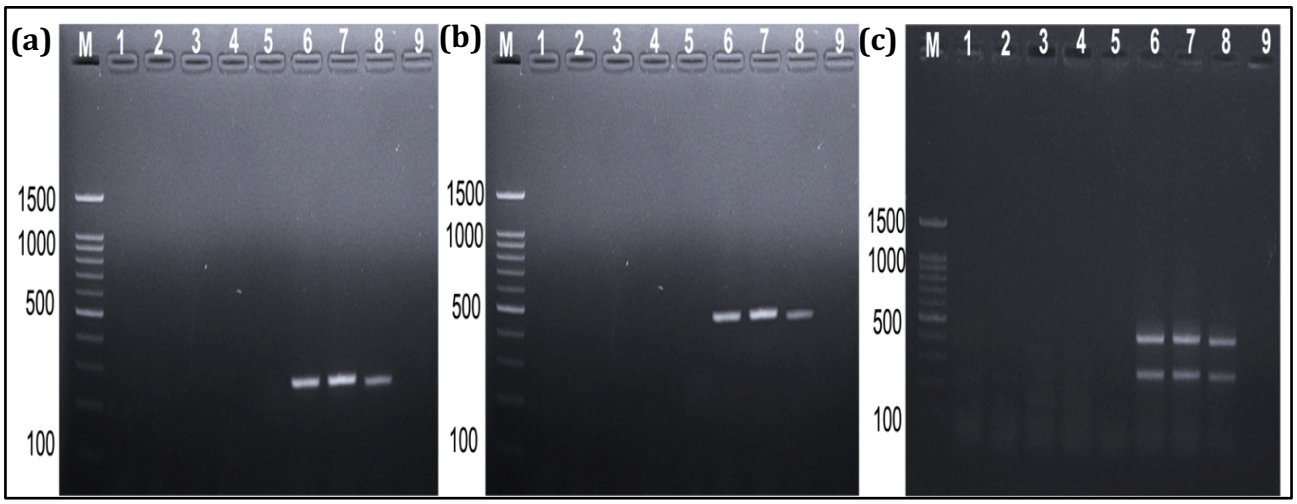


Figure 2.11 *Trichoderma*-species specific PCR amplification. (a) 2F2/2R2 SCAR marker amplified *T. harzianum*-specific polymorphic band in TV3, TS4 and Th03 (L-6 to L-8) at 278 bp but absent in N13, 7316, TV5, TV2B16 and Ta05 (L-1 to L-5). (b) 2F2/2R3 also generated a polymorphic band with in TV3, TS4 and Th03 at 448 bp (L-6 to L-8) but absent in N13, 7316, TV5 TV2B16 and Ta05 (L-1 to L-5). (c) Multiplex PCR confirmed the results. The *Trichoderma* strains: *T asperellum* N13 (L-1), *T. asperellum* 7316 (L-2), *T. asperellum* TV5 (L-3), *T. asperellum* TV2B16 (L-4), *T. asperellum* Ta05 (L-5), *T. Harzianum* TV3 (L-6), *T. harzianum* TS4 (L- 7), T. *harzianum* (L-8). L-9 is non-template control. M: DNA 100 bp ladder.

2.3.5 RAPD profiling and statistical analysis

Genotyping of the six strains of *Trichoderma* was carried using 185 Random RAPD markers to analyse the variability among the *Trichoderma* strains. A distinct genetic make-up of the fungal

strains was evident based on the polymorphic DNA markers. Out of a total of 185 primers, 136 primers showed reproducible polymorphic bands, wherein each primer showed 1–46 amplified bands. The approximate range of band size was 150–1500 bp, and 70.66% of the bands were polymorphic (**Supplementary Table S3**). The remaining markers were all monomorphic either amplifying similar DNA bands or no band altogether in all the strains. The detected putative monomorphic and polymorphic markers are listed in (**Table 2.3 and Table 2.4**). Among the monomorphic markers, 44 RAPD markers showed no amplification, while the remaining 5 markers showed uniform amplification generating a similar band size in all six *Trichoderma* strains. Relationships among the strains were evaluated by cluster analysis of the data based on the coefficients of the similarity matrix (**Table 2.5**).

Table 2.3 Grouping of monomorphic RAPD markers. The monomorphic markers were demarcated based on presence (+) or absence (-) of bands.

Monomorphic markers									
(+)	**(-)**								
OPE-10	OPA-03	OPB-11	OPD-09	OPE-13	OPJ-14	OPK-13	OPM-15	OPZ-08	OPZ-15
OPL-02	OPA-08	OPB-12	OPD-14	OPE-14	OPJ-15	OPK-18	OPM-16	OPZ-09	OPZ-16
OPM-11	OPA-09	OPB-15	OPD-17	OPE-16	OPK-05	OPL-09	OPM-17	OPZ-11	OPZ-17
OPN-1	OPA-15	OPC-03	OPD-19	OPE-17	OPK-06	OPM-03	OPM-18	OPZ-12	OPZ-18
OPX-20	OPB-10	OPD-01	OPE-01	OPJ-08	OPK-09	OPM-07	OPX-17	OPZ-13	OPAJ-04

Table 2.4 Grouping of polymorphic RAPD markers.

Polymorphic markers									
OPA-05	OPC-11	OPD-16	OPE-15	OPK-05	OPK-20	OPL-16	OPM-14	OPY-06	OPY-19
OPA-13	OPD-02	OPD-18	OPE-18	OPK-06	OPL-01	OPL-18	OPM-19	OPY-07	OPY-20
OPA-17	OPD-03	OPD-20	OPE-19	OPK-07	OPL-03	OPL-19	OPM-20	OPY-08	OPZ-01
OPA-19	OPD-04	OPE-04	OPJ-01	OPK-08	OPL-04	OPL-20	OPX-11	OPY-09	OPZ-02
OPA-20	OPD-05	OPE-05	OPJ-04	OPK-09	OPL-05	OPM-01	OPX-15	OPY-10	OPZ-03
OPB 14	OPD-06	OPE-06	OPJ-05	OPK-10	OPL-06	OPM-02	OPX-16	OPY-11	OPZ-04
OPC-01	OPD-07	OPE-07	OPJ-06	OPK-11	OPL-07	OPM-05	OPX-18	OPY-12	OPZ-05
OPC-02	OPD-08	OPE-08	OPJ-07	OPK-12	OPL-10	OPM-06	OPX-19	OPY-13	OPZ-06
OPC-04	OPD-10	OPE-09	OPJ-09	OPK-14	OPL-11	OPM-08	OPY-01	OPY-14	OPZ-07
OPC-07	OPD-11	OPE-11	OPJ-10	OPK-15	OPL-12	OPM-09	OPY-02	OPY-15	OPZ-10
OPC-08	OPD-12	OPE-12	OPJ-11	OPK-16	OPL-13	OPM-10	OPY-03	OPY-16	OPZ-19
OPC-09	OPD-13	OPE-13	OPJ-12	OPK-17	OPL-14	OPM-12	OPY-04	OPY-17	OPZ-20
OPC-10	OPD-15	OPE-14	OPJ-13	OPK-19	OPL-15	OPM-13	OPY-05	OPY-18	

Table 2.5 RAPD-based genetic similarity among the six strains of *Trichoderma* analysed in a pairwise manner.

	N13	**7316**	**TV5**	**TV2B16**	**TV3**	**TS4**
N13	1.00					
7316	0.88	1.00				
TV5	0.81	0.85	1.00			
TV2B16	0.92	0.91	0.82	1.00		
TV3	0.22	0.23	0.25	0.22	1.00	
TS4	0.22	0.23	0.25	0.22	0.98	1.00

Maximum genetic similarity was obtained between *T. harzianum* TV3 *and T. harzianum* TS4 (0.98) followed by *T. asperellum* N13 and *T. asperellum* TV2B16 (0.92). Minimum genetic similarity was observed between N13 and TV3 and, N13 and TS4 with a coefficient value of 0.22 each. Further, to understand the genetic relatedness among the six strains of *Trichoderma,* a dendrogram constructed using RAPD marker data revealed that the strains were segregated into two major clusters. Cluster I consisting of the strains N13, 7316, TV5, and TV2B16 was distantly placed from cluster II which consisted of TV3 and TS4 and the findings were in accordance with the ITS and D1-D2 region-based phylogenetic profiling (**Figure 2.12**).

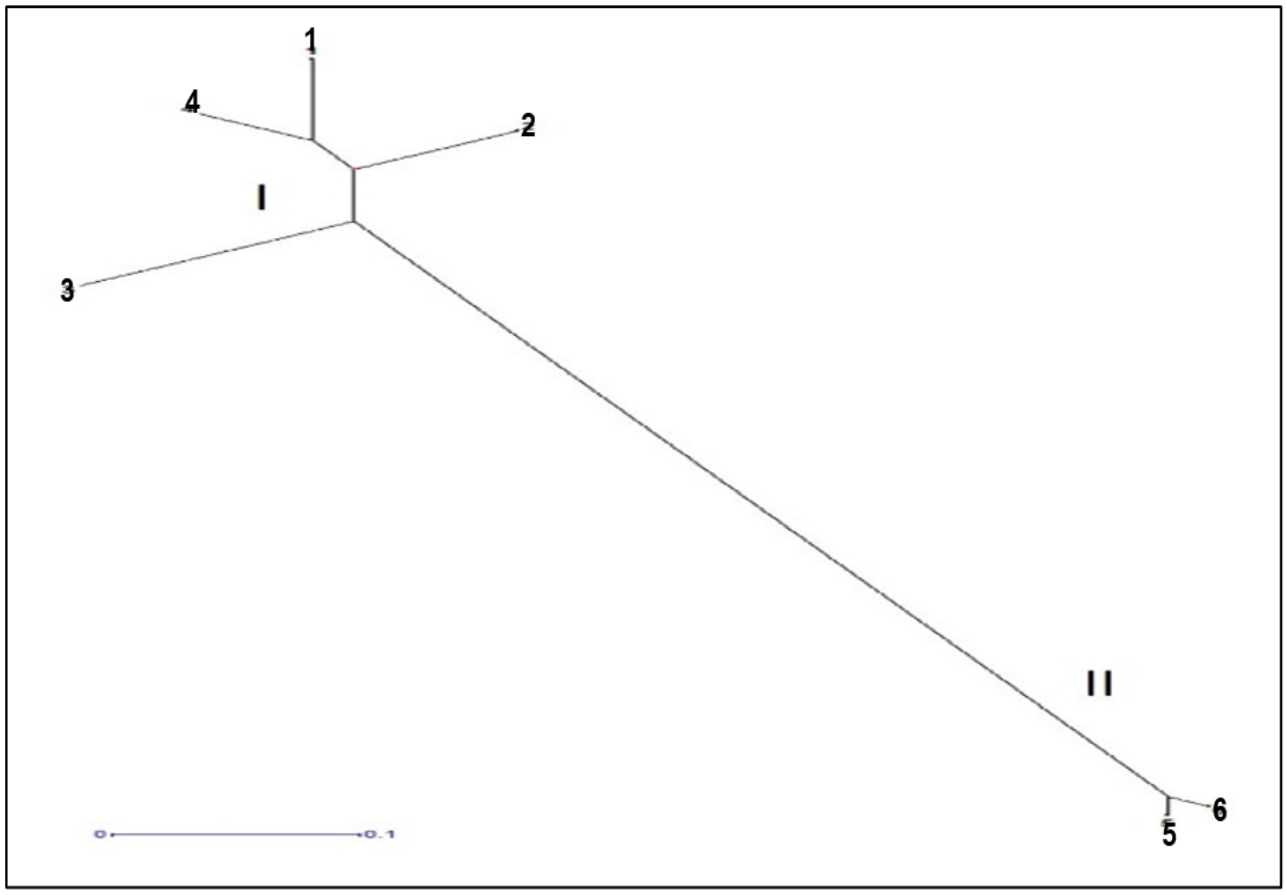


Figure 2.12 Genetic relatedness among the six *Trichoderma* fungal strains based on RAPD analysis, where 1: *Trichoderma asperellum* N13; 2: *Trichoderma asperellum* 7316; 3: *Trichoderma asperellum* TV5; 4: *Trichoderma asperellum* TV2B16; 5: *Trichoderma harzianum* TV3 and 6: *Trichoderma harzianum* TS4.

Among the RAPD amplified sequences, OPZ-06 and OPK-10 were selected to develop into SCAR markers owing to their reproducibility and distinct polymorphism between the six strains of *Trichoderma*. The marker, OPZ-06 showed a uniform amplification for N13, 7316, TV5 and TV2B16 with a monomorphic band of size at 950 bp while no amplification was observed for TV3 and TS4 (**Figure 2.13a**). On the contrary, OPK-10 showed a prominent band at 1400 bp for TV3 and TS4 with no amplification for N13, 7316, TV5 and TV2B16 respectively (**Figure 2.13b**).

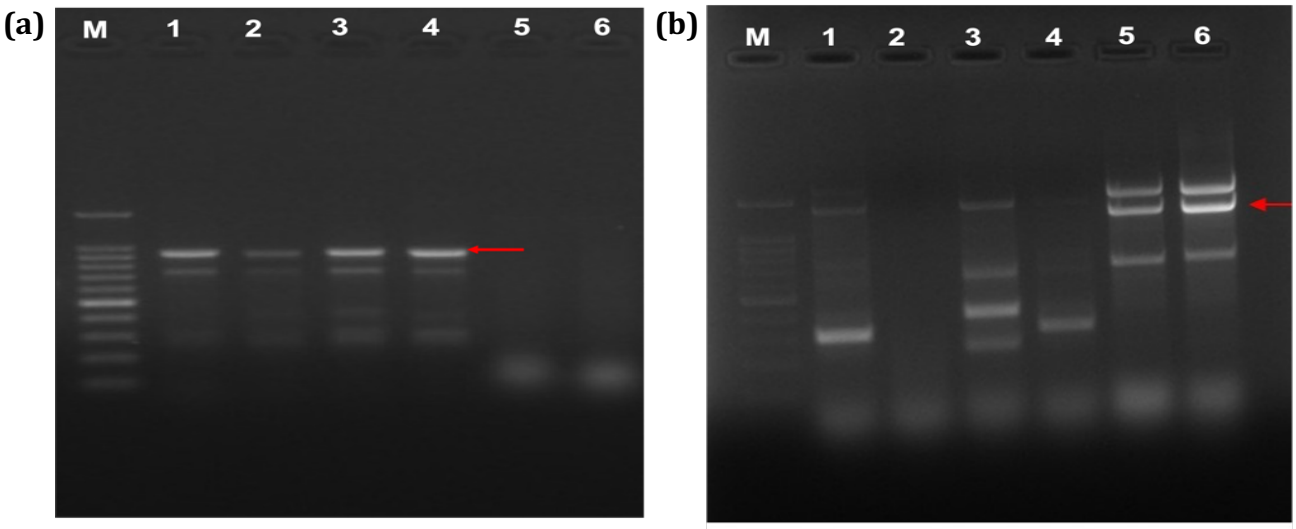


Figure 2.13 Gel images showing the PCR amplification of the polymorphic RAPD markers which were developed into SCAR markers following DNA sequencing. (a) OPZ-06_{950} marker showed a polymorphic band with uniform amplification for N13, 7316, TV5 and TV2B16 at 950 bp (red arrow) but absent in TV3 and TS4. (b) OPK-10_{1400} marker showed a polymorphic band with uniform amplification for TV3 and TS4 at 1400 bp (red arrow) but absent in N13, 7316, TV5 and TV2B16. The lanes 1 to 6 represent the *Trichoderma* strains: *T asperellum* N13 (L-1), *T. asperellum* 7316 (L-2), *T. asperellum* TV5 (L-3), *T. asperellum* TV2B16 (L-4), *T. harzianum* TV3 (L-5), *T. harzianum* TS4 (L- 6). M: DNA 100bp ladder.

The PCR amplicons generated by the RAPD markers, OPZ-06_{950} and OPK-10_{1400} were sequenced. The nucleotide sequences from the four strains related to *T. asperellum* amplified by the OPZ-06_{950} marker were aligned using the Clustal Omega program to test the nucleotide similarity among the strains. Likewise, the sequences amplified by OPK-10_{1400} marker from TV3 and TS4 strains were also aligned and significant level of similarity was observed in their nucleotide sequences (data not shown).

2.3.6. Developing SCAR markers specific to *T. asperellum* and *T. harzianum*

Two sets of forward and reverse primers (T1/T2 and T3/T4) designed for identification of *T. asperellum* and *T. harzianum* strains were synthesized from the deciphered nucleotide sequences. They were evaluated using a gradient of annealing temperatures ranging from 40 and 64 ˚C. The details of the species-specific primers along with their sequence information are given in **Table 2.6.**

Table 2.6 Primer sequence information of SCAR primers designed for developing species-specific markers.

SCAR Primer	Forward / Reverse	Primer specific to the species	Sequence (5'→3')	GC (%)	T_m (°C)
T1	Forward	*T. asperellum*	CTATTGAACTCTGGACTGCTT	42.86	56
T2	Reverse	*T. asperellum*	CAATCTCAGAAGACTGGCGAGCG	56.52	64
T3	Forward	*T. harzanium*	CATAGACATTGCTGCTAATATTGG	37.50	52
T4	Reverse	*T. harzanium*	AACAAAACAAAAGATGAGACGAAAG	32.00	51

The primer pair, T1/T2 showed a specific band of size 467 bp with uniform amplification in N13, 7316, TV5, TV2B16 and Ta05 strains which were absent in TV3, TS4 Th03 *T. longibrachiatum* and *T. virens* (**Figure 2.14a**). Similarly, the primer pair T3/T4 amplified a unique 436 bp DNA band in TV3, TS4 and Th03 strains only while no amplification was observed in N13, 7316, TV5, TV2B16, Ta05, *T. longibrachiatum* and *T. virens* (**Figure 2.14b**). The annealing temperature was fixed at 55°C to overcome non-specific amplification. Multiplex PCR with T1/T2 and T3/T4 primers generated a similar amplification pattern confirming the specificity of the SCAR markers to detect *T. asperellum* and *T. harzianumm* strains only (**Figure 2.14c**).

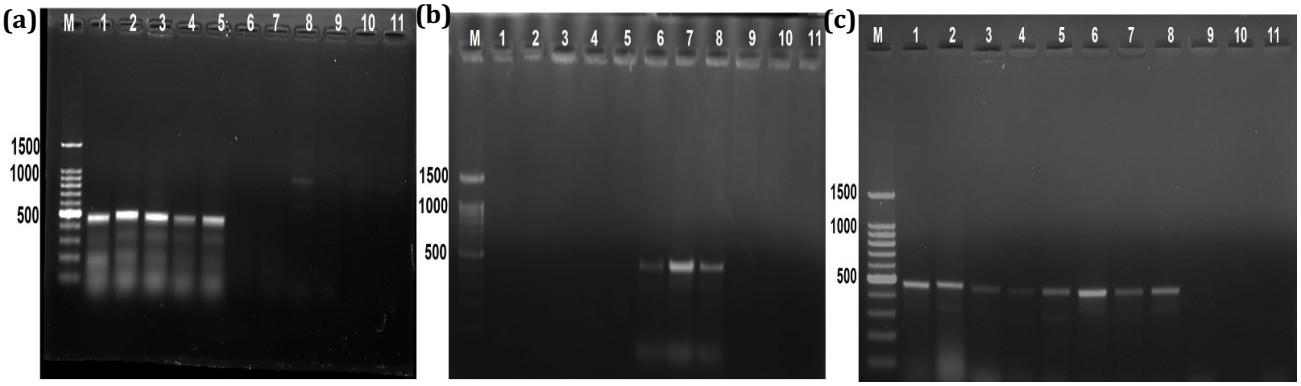


Figure 2.14 Developing a new set of *Trichoderma* species-specific SCAR markers. (a) T1/T2 showed a specific band with uniform amplification at 467 bp in N13, 7316, TV5, TV2B16 and Ta05 but absent in the strains TV3, TS4 Th03, IC13 and IC14. (b) T3/T4 showed a band with uniform amplification at 436 bp in TV3, TS4 and Th03 but absent in N13, 7316, TV5, TV2B16 Ta05 and IC13 and IC14. (c) Multiplex PCR amplification of the SCAR markers T1/T2 and T3/T4 simultaneously confirmed the results. T1/T2 and T3/T4 amplified the 467 bp (L-1 to L-5) and

436 bp (L-6 to L-8) bands respectively. The lanes representing the *Trichoderma* strains are: *T asperellum* N13 (L-1). *T. asperellum* 7316 (L-2). *T. asperellum* TV5 (L-3). *T. asperellum* TV2B16 (L-4). *T. asperellum* Ta05 (L-5), *T. harzianum* TV3 (L-6), *T. harzianum* TS4 (L- 7), T*. harzianum* Th03 (L-8), *T. longibrachiatum* IC13 (L-9), *T. virens* IC14 (L-10). L-11 is non-template control. M: DNA 100 bp ladder.

2.3.7. Antagonistic effect of *Trichoderma* on *Alternaria* through dual culturing

To study, the antagonistic property of *Trichoderma* against *A. ricini,* the *Trichoderma* strains N13, 7316, TV5, and TV2B16 were selected for confrontation plate assays. *Trichoderma harzianum* strains TV3 and TS4 were not included in this study due to its extremely low sporulation ability. The dual cultures were grown with the fungal pathogen, *A. ricini* along with each of the *T. asperellum* strains placed at equidistance from one another. Petri plates were monitored for the extent of mycelial spread. Petri plates growing *Trichoderma* and *Alternaria* alone were included as controls. All the strains grew to at least two-third of the medium surface thus showing the broad antifungal activity of *Trichoderma* (**Figure 2.15**). Percentage growth inhibition of *A. ricini* due to the antagonistic effect of *Trichoderma* strains was estimated based on the delta values of inhibition (Δ inhibition) as shown in **Table 2.7**. N13 and TV5 strains showed the highest percentage of inhibition of 59.54% and 59.48% respectively, followed by TV2B16 which showed an inhibition of 58%.

2.3.8. Effect of *Trichoderma* on *Alternaria ricini*-challenged castor leaves

To monitor the effect of *Trichoderma* treatment on *Alternaria* leaf spot disease, detached leaf assay was carried on two castor genotypes, DCS 107 and 48-1 which were tolerant and susceptible to the *Alternaria* leaf spot respectively. Leaves pre-treated with each of the *Trichoderma* strains (N13, 7316, TV5 and TV2B16) in isolation for 24 h where challenged by the fungal pathogen, *A. ricini*. Disease scoring of *Alternaria* leaf spot incidence on *Trichoderma* treated and control castor genotypes was assessed visually by monitoring at 3 dpi and 7 dpi using a 0–5 scale. The leaves of DCS-107 and 48-1 pre- treated with the *Trichoderma* strain, 7316 before challenging with *Alternaria* showed a resistant reaction (+) compared to the controls for most of the strains except the strain, TV2B16.

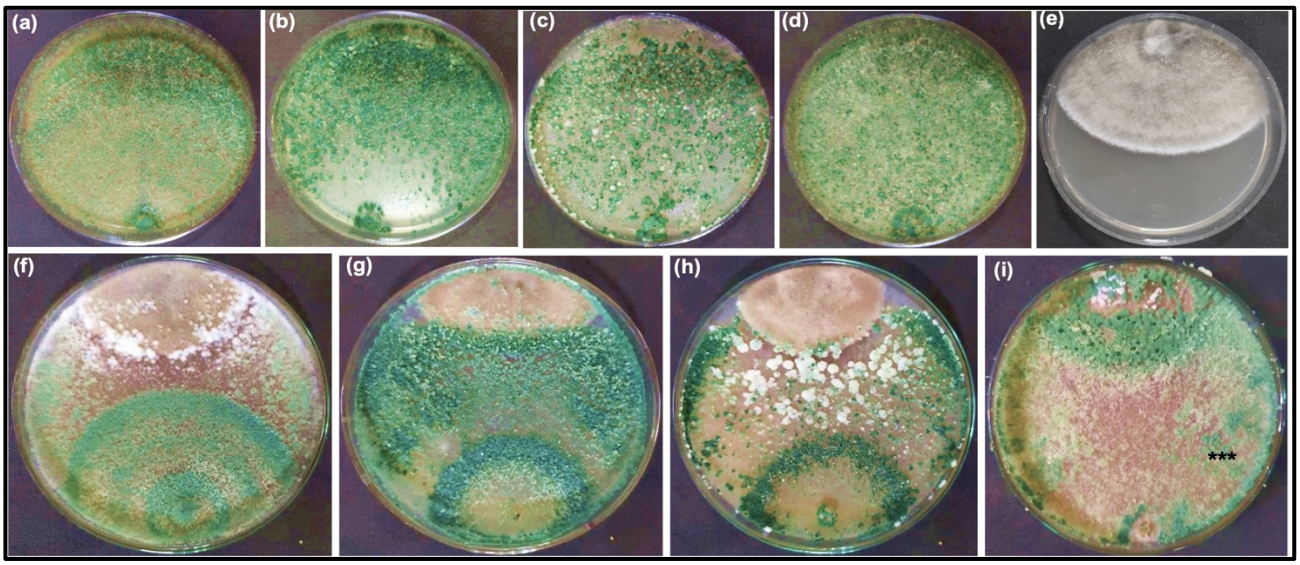


Figure 2.15 Confrontation plate assays with dual cultures grown with *A. ricini* and *T. asperellum* strains at 7 dpi. Plates growing only *T. asperellum* 7316, N13, TV5 and TV2B16 (a, b, c, d) and *A. ricini* (e) served as controls. Test plates included *Alternaria* grown with *T. asperellum* 7316 (f), *Alternaria* grown with *T. asperellum* N13 (g)**,** *Alternaria* grown with *T. asperellum* TV5 (h) and *Alternaria* grown with *T. asperellum* TV2B16 (i)

Table 2.7 Percentage fungal pathogen growth inhibition by antagonistic effect of *Trichoderma* strains.

***Trichoderma asperellum* strains**	**Percentage inhibition of pathogen growth (%)**	
	4 dpi	**7 dpi**
N13	28.56	59.54
7316	24.27	54.23
TV5	27.65	59.48
TV2B16	25.18	58.00

The leaves of both the castor genotypes, DCS-107 and 48-1 pre-treated with TV2B16 showed high level of disease severity (+++++) similar to the untreated controls at 7 dpi (**Table 2.8**). The typical disease phenotyping for leaf spot/ lesion size with pathogen-induced necrosis of leaf tissues carried to monitor the *Alternaria* pathogen spread in response to *Trichoderma* revealed variation among the strains. The leaves from the control plants which were pre-treated with sterile water alone, upon challenging with *Alternaria* pathogen showed a significant level of necrosis of the tissues at 7 dpi (**Figure 2.16**). While priming with N13 strain showed a resistant reaction in DCS-107, the castor genotype 48-1 showed moderately resistant and

moderately susceptible disease reaction at 3 and 7 dpi respectively. The *T. asperellum* strain, 7316 exhibited a high level of antibiosis in both the castor genotypes at 3 and 7 dpi compared to to the remaining strains thereby suggesting its potential application as a BCA ensued by N13 strain.

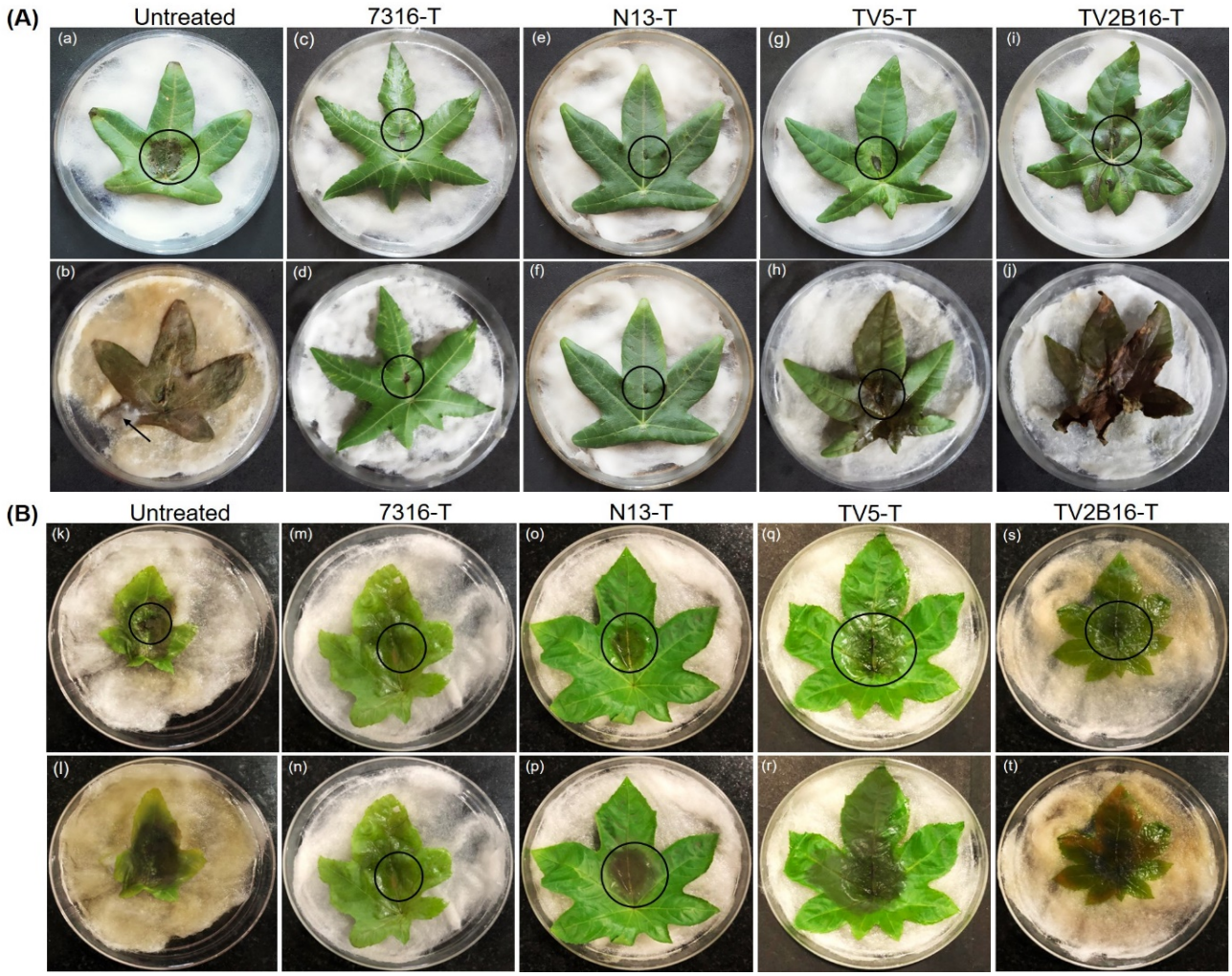


Figure 2.16 Effect of *Trichoderma* treatment on Alternaria leaf spot in castor by detached leaf assays. Two castor genotypes; (A) DCS-107 and (B) 48-1 treated individually with each of the four strains of *T. asperellum;* 7316, N13, TV5, and TV2B16 were compared to untreated samples at 3 and 7 dpi. The *Alternaria* leaf spot spread was monitored at 3 dpi (a, c, e, g, i, k, m, o, q, s) and 7dpi (b, d, f, h, j, l, n, p, r, t) respectively.

Table 2.8 Disease scoring of *Trichoderma*-treated castor genotypes through detached leaf assays for antibiosis against the leaf spot causing fungal pathogen, *Alternaria ricini* using 0–5 scale. The scale 0: immune/highly resistant, (+): resistant, (++): moderately resistant, (+++): moderately susceptible, (++++): susceptible and (+++++): highly susceptible.

***Trichoderma* strains**	**Disease severity index (0-5 scale)***			
	DCS-107		**48-1**	
	3dpi	**7dpi**	**3dpi**	**7dpi**
***Trichoderma asperellum* N13**	1(+)	1(+)	2(++)	3(+++)
***Trichoderma asperellum* 7316**	1(+)	1(+)	1 (+)	1(+)
***Trichoderma asperellum* TV5**	1(+)	3(+++)	2 (++)	4(++++)
***Trichoderma asperellum* TV2B16**	2 (++)	5 (+++++)	2 (++)	5 (+++++)
Untreated (Control)	3 (+++)	5 (+++++)	3 (+++)	5 (+++++)

2.4 DISCUSSION

The traditional methods employed for identifying fungal members had been carried mostly through phenotyping for morphological traits which included colony formation, mycelial growth rate, sporulation, and other microscopic features like branching pattern, phialides, and spore morphology (Bissett 1984, 1991a, 1991b, 1991c). In the present study, evaluation of the six strains of *Trichoderma*: 7316, TV2B16, N13, TV5, TV3, and TS4 for the above morphological traits demonstrated distinctness among the strains. Though morphological traits of fungi are considered for characterizing fungi in general, however, the accuracy can be obtained by a combination of both morphological and molecular analyses of fungal strains (Chaverri et al., 2015; Devi et al., 2017; Alsohaili and Hasan, 2018). The nucleotide sequence-based detection and species-specific marker assays were employed to accurately identify species within the genus, *Trichoderma* (Gupta et al., 2010). Furthermore, the recent advances in DNA sequencing and analytical techniques have revolutionized the fungal systematics for their identification with precision (Devi et al., 2017) and ribosomal DNA (rDNA) gene analysis has been used extensively as a reference for the identification of fungal isolates at a molecular level (Tamura et al., 2011). The ITS and D1-D2 regions of rDNA are considered as fungal barcode markers and have been used in studying intraspecific fungal diversity (Kullnig-Gradinger, 2002; Schoch et al., 2012). Similarly, in the present study, the ITS and D1-D2 regions of the *Trichoderma* strains were analyzed systematically through PCR, sequencing, followed by phylogenetic analysis of the nucleotide sequences in relation to other reported *Trichoderma* strains.

Our findings from *in silico*-based BLAST search analysis as well as nucleotide diversity comparison analysis of ITS and D1-D2 sequences of the six strains with other reported *Trichoderma* species in a concatenated dendrogram also revealed that the four strains: 7316, TV2B16, N13, and TV5 grouped into one cluster related to *T. asperellum* while the remaining two strains, TV3 and TS4 were placed in a separate cluster closely related to *T. harzianum* confirming the fungal strains as belonging to two different species.

The two genes; translation elongation factor1 (*TEF1*) and the second-largest subunit of RNA polymerase II (*rpb2*) are reported to serve as markers for detection of *Trichoderma asperellum* and *Trichoderma harzianum* strains respectively since they have highly conserved regions which allow unique and accurate amplification in *T. asperellum* and *T. harzianum* strains (Barrera et al., 2021; Chaverri et al., 2021). This enables an accurate detection and differentiation between the two species of *Trichoderma* (Chakraborty et al., 2010; Devi et al., 2017; Samuels et al., 2002; Vetrovsky et al., 2015). To confirm the results from the ITS and D1-

D2 region-based grouping of the strains, PCR was performed using species-specific markers. The findings revealed that the four strains, N13, 7316, TV5, TV2B16 along with Ta05 which served as a control could amplify a DNA band (507 bp) unique to *T. asperellum* using T2AF/T2AR primers while TV3 and TS4 along with the control strain Th03 amplified a DNA band (824 bp) with the primer TH1F/TH1R from unique to *T. harzianum*. Confirmation of the findings by simultaneous multiplex PCR using both T2AF/T2AR and TH1F/TH1R primer sets further reinforced that N13, 7316, TV5, and TV2B16 belonged to *Trichoderma asperellum,* whereas TV3 and TS4 belonged to *Trichoderma harzianum* respectively.

According to Perez et al., 2014, the primer sets 2F2/2R2 and 2F2/2R3 reportedly amplified a 278 bp and 448 bp sequence with high specificity to recognize the species *T. harzianum.* To confirm the accuracy of the *Trichoderma* species detection, the reported SCAR marker primer sets; 2F2/2R2 and 2F2/2R3 were tested and similar results were obtained for TV3, TS4 and Th03 which showed a prominent band each of size 278 bp and 448 bp with the primer pairs 2F2/2R2 and 2F2/2R3 respectively, thus confirming them as strains of *T. harzianum*.

Previous findings have demonstrated the applicability of RAPD markers to detect molecular variation among the *Trichoderma* strains (Perez et al., 2014; Gupta et al., 2010; Pandya et al., 2017). Likewise, studies were carried to assess genetic diversity among seventeen strains of *Trichoderma* using RAPD using 20 primers of the OPM series, which led to classifying the strains into two major groups (Gopal et al., 2008). In our study, characterization of the fungal strains with 185 random primers showed genetic variation among the strains. The polymorphic banding patterns detected in the study were indicative of molecular differences among the *Trichoderma* strains. The RAPD marker, OPY-02 showed the highest number of bands that ranged between 250 bp to 1200 bp.

Further, the statistical validation of the findings resulting from a pairwise comparison of correlation of coefficient values of the RAPD profiling data revealed that the strains, TV3 and TS4 were closely related to each other (0.98). Further, TV3 and TS4 fungal strains comprised one cluster far apart from the remaining four strains, N13, 7316, TV5, and TV2B16 suggesting distant relatedness between those strains. These results were in accordance with the findings revealed from the dendrograms obtained through ITS and D1-D2 sequences and RAPD sequences. Similarly, earlier studies conducted to test five random RAPD primers on 10 isolates of *Trichoderma* isolated from tomato rhizosphere also revealed intra and inter-specific variability among the isolates (Chandulal et al., 2016). Moreover, RAPD based profiling was reported to generate an identification pattern to detect *Trichoderma* isolates (Pandya et al.,

2017). The present study revealed also revealed the genetic diversity among the *Trichoderma* strains isolated from the rhizosphere soil adhering to the roots of the castor plant.

To convert RAPD assay into a more robust and accurate mode of strain characterization, the highly specific and reliable SCAR markers were generated using conserved sequences of *T. harzianum* and *T. asperellum*. The primer pair T1/T2 amplified a 467bp sequence exclusively in N13, 7316, TV5 and TV2B16 along with the control, Ta05 confirming its specificity to *T. asperellum* while the primer pair: T3/T4 amplified a 436 bp sequence in TV3 and TS4 along with the control, Th03 confirming its specificity to *T. harzianum*.

To validate the uniqueness and specificity of the new set of SCAR markers, the control strains of *Trichoderma* - *T. asperellum* Ta05 and *T.harzianum* Th03 which were identified and confirmed by Devi et al., 2012 using T2AF/T2AR primers (*TEF* sequence) were included. This finding reinstated that the synthesized SCAR primers T1/T2 and T3/T4 are highly specific to *T. asperellum* and *T. harzianum* respectively and can be utilized as standard markers in species identification. The findings from the present study led to the identification of the *Trichoderma* strains both at morphological and molecular levels along with the development of a set of SCAR markers for the detection of *T. asperellum* and *T. harzianum* specific-strains in samples.

The reduced lesion size observed in response to the resistant reaction to *Alternaria* fungus was correlating with the findings of the confrontation plate assay carried with dual cultures to test fungal pathogen inhibition by *Trichoderma* via in vitro culture studies. The mycoparasitic ability of *Trichoderma* to inhibit and confine the growth of *Alternaria* might be resulting from the sequential expression of antimicrobial proteins which include chitinases, glucanases and proteases (Sharma et al., 2011; Mora et al., 2001). In agreement with other reported findings (Begum et al., 2021; Nwankiti et al., 2018; Yassin et al., 2021), the findings from the present study also demonstrated that *Trichoderma* impeded the growth of *A. ricini* in castor.

Chapter 3

Assessing rhizosphere *Trichoderma asperellum* strains for root colonizing and antagonistic competencies against Fusarium wilt through molecular and biochemical responses in castor

3.1 INTRODUCTION

Because of the high oil content (50%) and utilitarian value in the farming, industrial and pharmaceutical sectors, castor (*Ricinus communis* L.) is considered as one of the most important non-edible oilseed crops. However, castor oil production represents only a mere 0.15% of the total vegetable oil content produced annually worldwide (Severino et al., 2012; Morris et al., 2012). The yield potential of castor has been very low and the growing regions worldwide are restricted to only the marginal lands. Various biotic and abiotic factors contribute towards the low yield of castor. The major reason behind the drop in castor production is damage caused to the crop by various diseases and pests. Therefore, it necessitates investigating other alternative measures to increase the productivity of castor plants. Among the biotic factors, the major diseases that affect castor growth are gray mold (*Botryotinia ricini* or *Amphobotrys ricini*), vascular wilt (*Fusarium oxysporum* f.sp. *ricini*), charcoal rot (*Macrophomina phaseolina*), leaf spots caused by the fungus *Alternaria ricini* and *Cercospora ricinella* and the bacteria *Xanthomonas axonopodis* pv. *Ricini*. Among these, *A. ricini* causes severe damage because it is a seedborne fungus that can also cause seedling blight and pod rot with loss of seed production ranging to 70% (Holliday, 1980).

The usage of BCA is a promising approach to elevate crop yield and minimize loss of productivity due to plant diseases. The advantage of BCA over any chemical or synthetic fungicides/pesticides includes lesser side effects, their efficacy against fungicide-resistant pathogens and environment friendly nature. *Trichoderma* are fast growing and non-virulent symbiotic species. Over decades, *Trichoderma* has been researched on and are considered as one of the most efficient BCAs in agriculture, that also help in promoting plant growth (Hermosa et al., 2012). *Trichoderma* has been explored extensively as commercial biocontrol agents because of its potential to minimize pathogen infection in plants under various soil conditions.

Previous studies to examine different *Trichoderma* strains highlighted potential strain/s of *Trichoderma* to function as promising BCAs when they were tested against a range of pathogenic fungi (Grondona et al., 1997; Elad, 2000; Qualhato et al., 2013). The key mechanisms employed by *Trichoderma* in direct interaction with pathogens include, antibiosis, competition and mycoparasitism (Elad, 2000; Karuppiah et al., 2019). In 2022, Modrzewska et al., showed that *Trichoderma* acts not only as a BCA but also as a biosimulator against *Fusarium* in the production of cereal crops. There are other various benefits that *Trichoderma* possesses that aids in plant overall growth like modification of the rhizosphere, better nutrient absorption

of plant roots, enhanced tolerance to biotic and abiotic stress, promotion of various of plant's morphological traits like elongated root and shoot length, branches, leaves and lateral root formation and root hair numbers. Liu et al., 2020 demonstrated the spike in production of pepper caused by the application of *Trichoderma guizhouense* NJAU4742. Similar findings were seen in cucumber yield caused by the root application of *Trichoderma* (Meng et al., 2019).

The above stated evidences and details provided, the rationale for the present study. Usage of *Trichoderma* is considered as a safe alternative to the usage of synthetic pesticide that is detrimental for the environment and consumer health. In our study, it is hypothesized that the *Trichoderma* may exhibit the characteristics as a BCA when interacting with castor. Therefore, in the present work, various strains of *Trichoderma asperellum* that were detected from castor growing regions of Telangana, India were isolated and tested for their castor root colonizing ability along with mycoparasitic/antibiosis against fungal pathogens. The third chapter in this study focussed on the identification of effective strain(s) of *Trichoderma* that could be employed for conferring antibiosis/resistance against the root wilt-causing fungal pathogen, *Fusarium oxysporum ricini* and promoting castor growth through molecular and biochemical approaches and the findings are presented.

3.2 MATERIALS AND METHODS

3.2.1 Plant and fungal material

Seeds of the two castor (*Ricinus communis* L.) genotypes: DCS-107 and 48-1, the fungal strains of *Trichoderma asperellum*: 7316 (MH236427.1, MK411201.1), N13 (MH356723.1, MK411202.1), TV5 (MH393299.1, MK411216.1) and TV2B16 (MH393229.1, MK411214.1) and, *Fusarium oxysporum ricini* used for the study as shown in **Supplementary Figure S2** were obtained from Indian Institute of Oilseeds Research (IIOR), Hyderabad in Telangana, India. The *T. asperellum* strains were isolated from the soil, whereas *F. oxysporum ricini* was isolated from the leaves of the castor plants grown in the field located at IIOR, Hyderabad at 17.3231 °N longitude and 78.4096 °E latitude with an altitude of 528.3 meters above the sea level.

3.2.2 Fungal inoculum preparation

Single-spored cultures were prepared by growing on Potato Dextrose Agar (PDA) as previously described (Devi et al., 2017). The medium was autoclaved at 121 °C and 15 psi for 15 min and plated before inoculation. The fungal cultures were incubated at 24±2 °C and spores were harvested from 7 day-old cultures with a fine camel hair brush by rinsing with sterile water containing 0.02% (v/v) Tween 20 as a surfactant to disperse the spores in the solution. For effective sporulation, *F. oxysporum ricini* was cultured on carboxymethylcellulose (CMC) medium. The CMC medium was prepared by dissolving 1.5 g low viscosity CMC, 1 g yeast extract, 1 g KH_2PO_4, 1 g NH_4NO_3, and 0.5 g $MgSO_4.7H_2O$ in a litre of distilled water. The chemical reagents were obtained from Hi-Media, India.

3.2.3 Soil sampling for rhizosphere and bulk soil

The seeds of DCS-107 and 48-1 castor genotypes were surface sterilized for 5 min with 1.5% sodium hypochlorite solution prepared in autoclaved water and thoroughly rinsed three times with sterile distilled water. The seeds were sown in twice autoclaved potting soil and grown until two leaf growth-stage in a plant growth chamber maintained at 28 °C and 14/10 day/night respectively under a PAR of 500 W m^{-2} with 55% relative humidity. The roots of the castor plants were treated with each of the four strains of *T. asperellum*: N-13, 7316, TV5 and TV2B16 in isolation at different concentrations (3 x 10^4, 6 x10^4 and 9 x 10^4 spores/mL) by dipping the root system in falcon tubes containing the three different spore suspensions for 24 h and transplanted to pots containing un-autoclaved field soil. The mock (water)-treated plants of the same age, grown under similar plant growth conditions and transplanted in the same field soil

served as controls. The rhizosphere and bulk soil samples were collected from *Trichoderma*-treated castor genotypes at 12, 24, 36, and 48 dpi.

The soil adhering to the roots was shaken vigorously until 80% of the loosely adhering soil fell off from the roots. The soil sample was collected and is referred to as bulk soil (**Supplementary Figure S3a**) while the soil that remains attached to the root is considered as rhizosphere soil as shown in **Supplementary Figure S3b**. Serial dilutions were prepared from the stock solution of bulk and rhizosphere soil samples by adding 1 g of each of the soil samples to 10 mL of autoclaved distilled water. A 100 µL of the solution per treatment was plated on Luria Bertani HiVeg media (LB) and the plates were incubated at 37 °C overnight. The colony-forming units (CFU) was counted 24 hours post plating from 15 replicates for each of the treatments carried with three different spore concentrations at four different time points. The experiments were repeated three times to check for consistency of the results.

3.2.4 Biopriming with *Trichoderma* and seed germination assay

The surface-sterilized castor seeds were inoculated for 2 h at 28 °C with each of the four strains of *Trichoderma* in isolation. The spore concentration of 1x 10^6 spores/ml prepared in 1.5% CMC was used. Castor seeds treated with CMC alone served as control. The *Trichoderma*-treated seeds were placed in Petri plates on moist sterile filter paper in the growth chamber at 28 °C. The germinated seed count and radicle length were recorded for the *Trichoderma*-treated and control seedlings 4 days-post treatment. The experiment was repeated three times independently, each having fifteen replicates for each of the treatments tested in the study.

3.2.5 *Trichoderma*-treated plant assays through pot trial

The surface sterilized seeds of DCS-107 and 48-1 castor genotypes were treated with the *Trichoderma* strains as described above. Both treated and control seeds were sown in twice-autoclaved potting soil and the plants were grown in a plant growth chamber maintained at 28 °C and 14/10 day/night respectively with 25% relative humidity. The two-week-old plants were analysed for the traits like the length of root and shoot, leaf size, fresh and dry weight of the plants. Fresh weight was measured immediately after sampling. To compute the dry weight, plants were oven-dried at 40 °C for 48 h before measuring the biomass of plants. The experiment was repeated three times independently, each having fifteen replicates for each of the treatments tested in the study.

3.2.6 Plate confrontation Assay

Mycelia discs of size 5 mm diameter from the actively growing end of 7 day-old *F. oxysporum* fungal culture was placed juxtaposed to a 5 mm diameter discs of *Trichoderma* cultures on Petri plates containing PDA (supplemented with calcium carbonate). The mycelia discs were placed at 1cm distance from the edge of the Petri plate. Each of the *Trichoderma* strains was placed at the opposite periphery 48 hpi with *Fusarium* discs owing to the slow growth of the fungi. The PDA plates cultured with *Trichoderma* and *Fusarium* mycelia discs alone served as negative controls. The inoculated plates were incubated at 28 °C for 7 days. Radial growth of the fungal pathogen, *F. oxysporum* and the *Trichoderma* strain was measured from fourth day till 7 dpi. The experiment was repeated three times independently, each comprising of ten replicates for each of the pathogen antagonism treatment and the mean values were computed. The percentage inhibition of radial growth (PIRG) was calculated using the formula developed by Skidmore and Dickinson (1976) and Rahman and associates (2011) as given below:

PIRG = $\{(R_1 - R_2)/ R_1\}$ X 100, whereas R_1 is Colony diameter in the control and R_2 is Colony diameter in treated.

3.2.7 Efficacy of *Trichoderma* treatment on *Fusarium* wilt

The roots of two-weeks-old castor plants of DCS-107 and 48-1 genotypes were treated with each of the *T. asperellum strains*: N13, 7316, TV5 and TV2B16 in isolation with a conidial suspension of 1 x 10^6 spores/ mL for 24 h. The *Trichoderma*-treated plants were transferred to Falcon tubes containing the conidial suspension of 1 x 10^6 spores/ml of *F. oxysporum*. Another set of plants of the same age, grown under similar growth conditions were treated with *F. oxysporum* spore suspension alone. The mock (water-treated) treated plants served as controls. The disease incidence was monitored at 7 and 21 dpi. The experiment was replicated three times independently with fifteen replicates for each of the strains of *Trichoderma* tested. Percentage wilt incidence was calculated at 21 dpi.

3.2.8 RNA isolation and cDNA synthesis

Total RNA was isolated from the roots and leaves of castor genotypes, DCS107 and 48-1 treated with the *T. asperellum* strains: 7316 and N13 respectively along with their controls at 48 hours post inoculation (hpi). 500 mg of root sample was ground to a fine powder in liquid nitrogen using a mortar and pestle. The powdered sample was transferred into 2 ml microcentrifuge tubes treated with 0.1% (v/v) diethylpyrocarbonate (DEPC). 1 ml of the pre-heated (65 °C) Extraction buffer-I comprising of 2% cetyltrimethyl ammonium bromide (CTAB) (w/v), 2%

polyvinylpolypyrrolidone (PVPP) (w/v), 100 mM Tris(hydroxymethyl)aminomethane hydrochloride (Tris–HCl; pH 8.0), 25 mM ethylenediaminetetraacetic acid (EDTA) and 2 M sodium chloride (NaCl) was added and mixed thoroughly by vortexing. To the contents of the tube, Beta-mercaptoethanol (2% final concentration) was added and incubated at 65 °C for 30 min, with occasionally mixing. 1 ml of chloroform:isoamyl alcohol (24:1/v:v) was added, mixed by brief vortexing and centrifuged at 13,000 rpm for 10 min at room temperature. The supernatant was transferred to fresh microcentrifuge tubes containing 1 ml of the Extraction buffer-II, comprising of phenol saturated Tris buffer of pH 6.7 (Sigma, USA) to which sodium dodecyl sulfate (SDS 0.1%; w/v), sodium acetate (NaOAc 0.32 M; w/v) and EDTA (0.01 M). A 200 µL of chloroform was added to the contents of the tubes, vortexed for a few seconds and, incubated for 15 min at room temperature. The samples were centrifuged at 13,000 rpm for 10 min at 4 °C. The upper aqueous phase was transferred into fresh tubes containing 0.6 volume of chilled isopropanol and stored at –20 °C overnight. The samples were centrifuged at 13,000 rpm for 10 min at 4 ^{0}C. The supernatant was drained and the RNA pellet was washed with 70% ethanol followed by air drying and finally dissolved in 25 µL of DEPC treated autoclaved water and stored at –80 °C. The cDNA was synthesized from the total RNA using the cDNA synthesis kit (Takara, Shiga, Japan) according to the manufacturer's instructions.

3.2.9 Real Time-quantitative PCR (RT-qPCR)

Primers used for RT-qPCR were designed by Oligo Analyzer 3.1 bioinformatics tool amplifying short fragments of 150–300 bp. Primers designed for 13 genes related to different defence response pathways and an internal control are listed in **Supplementary Table S4**. Actin gene expression was monitored which served as a reference control. The PCR conditions used were set at an initial denaturation of 95 °C for 3 min followed by 95 °C for 15 s, an annealing temperature specific to the gene for 30 s, 72 °C for 20 s followed by 40 cycles of 95 °C for 15 s followed by 60 °C for 15 s. The RT-qPCR reaction was performed using Applied Biosystems 7500 Real time PCR Systems. Experiment was repeated twice independently. Relative fold change gene expression was normalised against the reference control using the formula $2^{-\Delta\Delta CT}$.

3.2.10 Sampling of roots for biochemical and antioxidant activity assay

The treatments comprised of *Trichoderma*-treated alone (only T), *Fusarium*-treated alone (only F) and co-culturing with *Trichoderma* and *Fusarium* pathogen (T+F). 0.5 g of treated and untreated castor root samples at 3 dpi were frozen in liquid nitrogen to stop metabolism and

then homogenized with 2 mL of extraction buffer that consists of 50 mM phosphate buffer (pH 7) containing 1 mM EDTA and 2% w/v PVP (polyvinyl pyrrolidone) at 4 °C. The sample was then centrifuged at 13000 rpm for 20 min at 4 °C. The supernatant (enzyme extract) was used for assay of catalase (CAT), glutathione peroxidase (GPX) and superoxide dismutase (SOD). Propagation, inoculation, and sampling of plants were done independently with minimum of five replicates (plants) being evaluated for each experiment.

3.2.11 Catalase (CAT) activity assay

Catalase activity was measured following the method as described previously (Aebi, 1984). To 50 µL of enzyme extract, 2.9 mL of 50 mM phosphate buffer and 50 µL of 30 mM H_2O_2 was mixed rapidly at room temperature by adding H_2O_2 at the end of the reaction. The change in absorbance value was recorded at 240 nm at an interval of 30 s for 3 min. The CAT activity was assayed by measuring the initial rate of H_2O_2 disappearance at 240 nm, using an extinction coefficient of 40 $mM^{-1}cm^{-1}$ and expressed as Enzyme Unit (EU) mg^{-1} fresh weight.

3.2.12 Glutathione peroxidase (GPX) activity assay

GPX activity was assayed as described previously by Chance and Maehly (1955). To 50 µL enzyme extract 2.75 mL of 50 mM phosphate buffer (pH 7.0), 100 µL of 30 mM guaiacol and 40 mM H_2O_2 was added. The change in absorbance value was recorded at 470 nm at an interval of 30 sec for 3 min. GPX activity was determined following the formation of tetraguaiacol by measuring the absorbance at 470 nm and using an extinction coefficient of 26.6 $mM^{-1}cm^{-1}$. One unit (U) of peroxidase activity was represented by the amount of enzyme catalyzing the oxidation of l mol of guaiacol in 1 min and the enzyme activity was expressed as Enzyme unit (EU) mg^{-1} fresh weight.

3.2.13 Superoxide dismutase (SOD) activity assay

SOD activity was measured as described previously by Beyer and Fridovich (1987). To 50 µL enzyme extract, 1.5 mL of 50 mM phosphate buffer (pH 7.0), 0.3 mL of 100 µM ethylenediaminetetraacetic acid disodium salt (EDTA-Na2), 0.3 mL of 130 mM L-methionine, 0.3 mL of 750 µM nitro blue tetrazolium (NBT), 0.25 mL deionized water was added. Reaction was started by adding 0.3 mL of 20 µM riboflavin. Samples were incubated under a light source having two tungsten incandescent light bulbs having luminance of 8072.93 lux for 15 min. At

the same time, a control without the enzyme extract was also prepared. Increase in absorbance due to the formation of formazan was measured at 560 nm using spectrophotometer.

3.2.14 Total Phenol estimation

Total phenol content was extracted from 0.5 g of root tissue was homogenized in liquid nitrogen and extracted in 50% methanol at 80 °C for 90 min and centrifuged at 4000 rpm at 4 °C for 15 min. Saponification of the pellet was done by adding 0.5 N NaOH for 24 h at room temperature to remove the bound phenol and further neutralized with 0.5 ml (2 N) HCl after 24 h. The samples were centrifuged at 12000 rpm at 4 °C for 15 min. Further Folin-Ciocalteu's (FC) assay was performed by adding 100 µL of extracted supernatant diluted with water to make up volume of 1 mL and mixed with 0.5 mL 2 N FC reagent and 2.5 mL of 20% Na_2CO_3. The absorbance was measured at 725 nm. TPC was calculated by using gallic acid standard calibration curve. The result is expressed as mg gallic acid per mg fresh weight.

3.2.15 Statistical analysis

The data obtained is computed as the mean ± standard error of the mean. The data were statistically analysed by using one-way analysis of variance (ANOVA) and multiple mean comparisons were performed using Tukey's test at the $p \leq 0.05$ significance level. Differences at $p \leq 0.05$ were considered to be significant. In the figures, different letters above the bars indicate significant differences between the control and treatment groups at the $p \leq 0.05$ level according to Tukey's test.

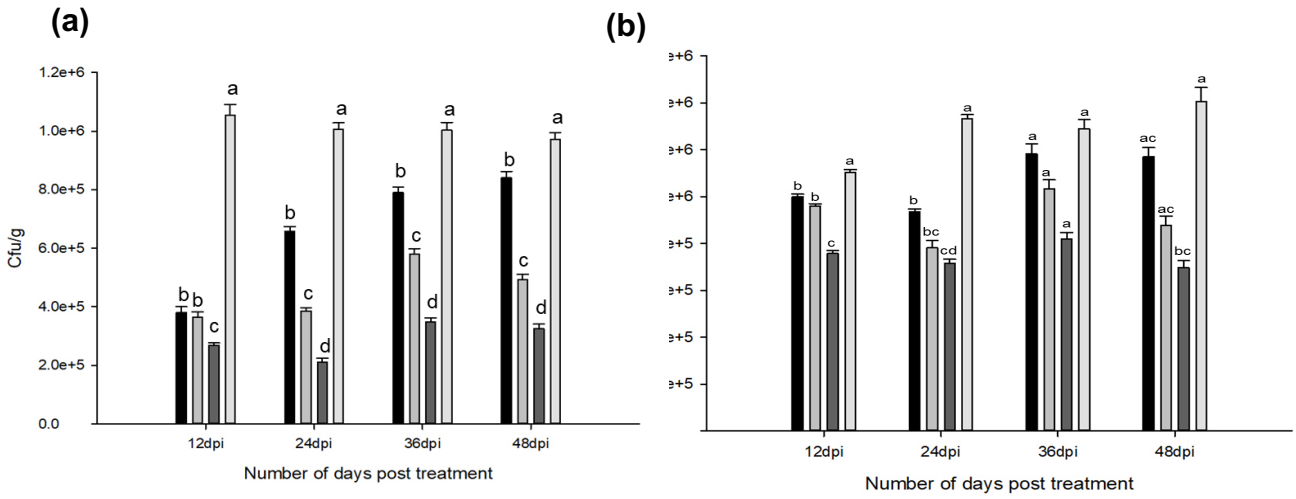
3.3. RESULTS

3.3.1 Monitoring the growth of *Trichoderma* and *Fusarium* fungal strains

The fungal cultures of four strains of *T. asperellum* (7316, N13, TV5 and TV2B16) and *F. oxysporum ricini* grown in isolation produced profuse mycelial growth and sporulation as shown in **Supplementary Figure S2**. The characteristic olive-green coloured spores of the *Trichoderma* fungal strains were visible at 7 days-post plating. Further, predominant mycelial proliferation and sporulation of *F. oxysporum* fungus was observed in CMC medium.

3.3.2 Bulk and Rhizosphere soil assays to assess the effect of *Trichoderma*

Compared to the controls, a significant decline was observed in CFU count in *Trichoderma*-treated bulk (**Figure 3.1**) and rhizosphere (**Figure 3.2**) soil samples for all the *Trichoderma asperellum* strains demonstrating their competence ability to restrict the growth of other microorganisms. However, these *Trichoderma* strains exhibited varying levels of competence in both bulk and rhizosphere soil samples with an effective competence activity mostly observed at a concentration of 9 x 10^4 spores/ml at 36 and 48 dpi. The bulk soil analysed from castor genotypes, DCS-107 (**Figure 3.1a**) and 48-1 (**Figure 3.1b**) treated with *Trichoderma asperellum* strain 7316 at a concentration of 9 x 10^4 spores/ml was found to be effective for DCS-107 compared to 48-1 genotype at an early point of 12 dpi suggesting that the differential response to *Trichoderma* might be resulting from the nature of the host genotypes (**Figure 3.1**). Likewise, the CFU count from the bulk soil sample treated with *T. asperellum* strain N13 was found to be effective at a concentration of 9 x 10^4 at a later time point (36 dpi) for both the genotypes while the CFU count significantly reduced at 24 dpi when treated with TV5 strain in



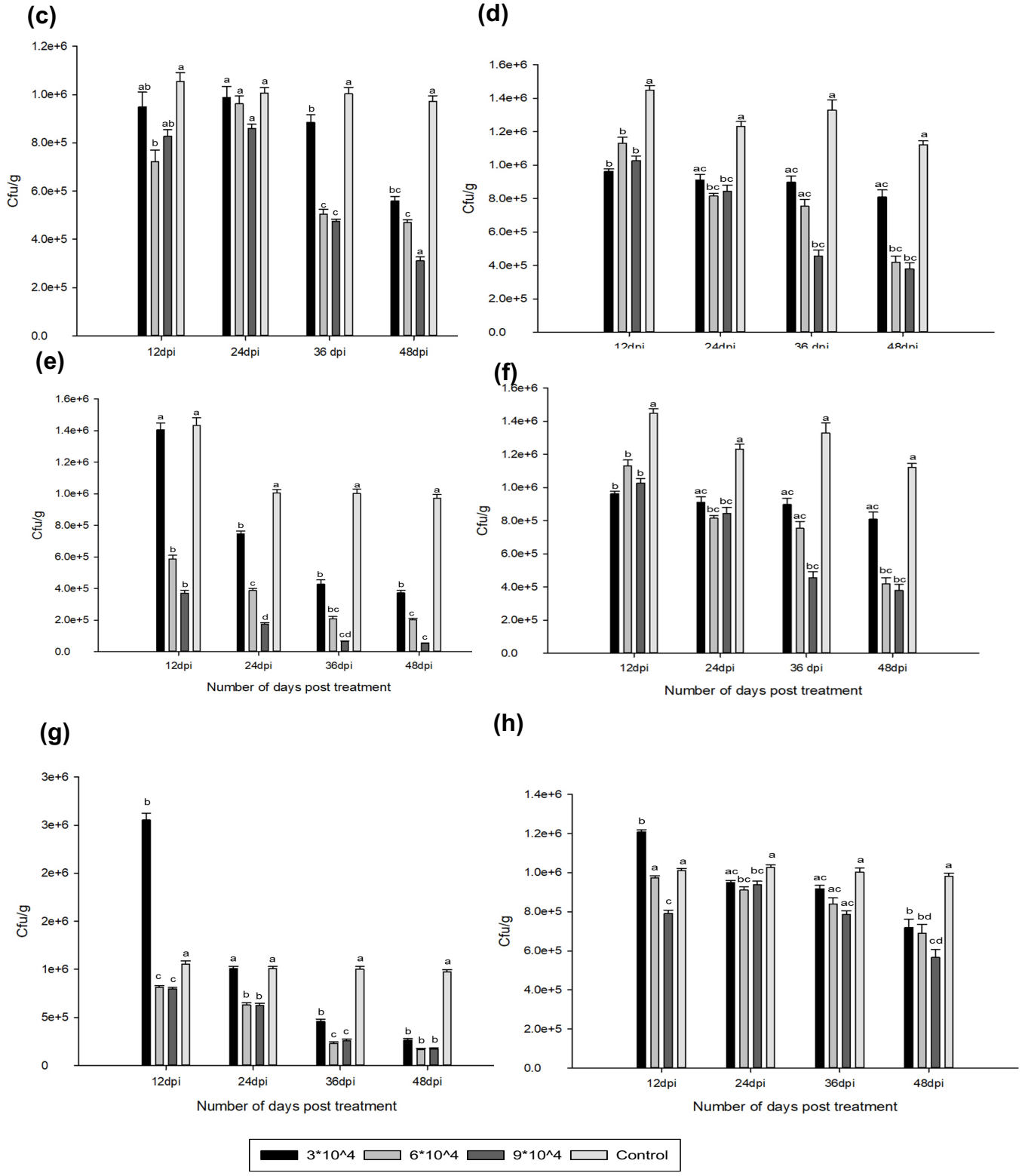
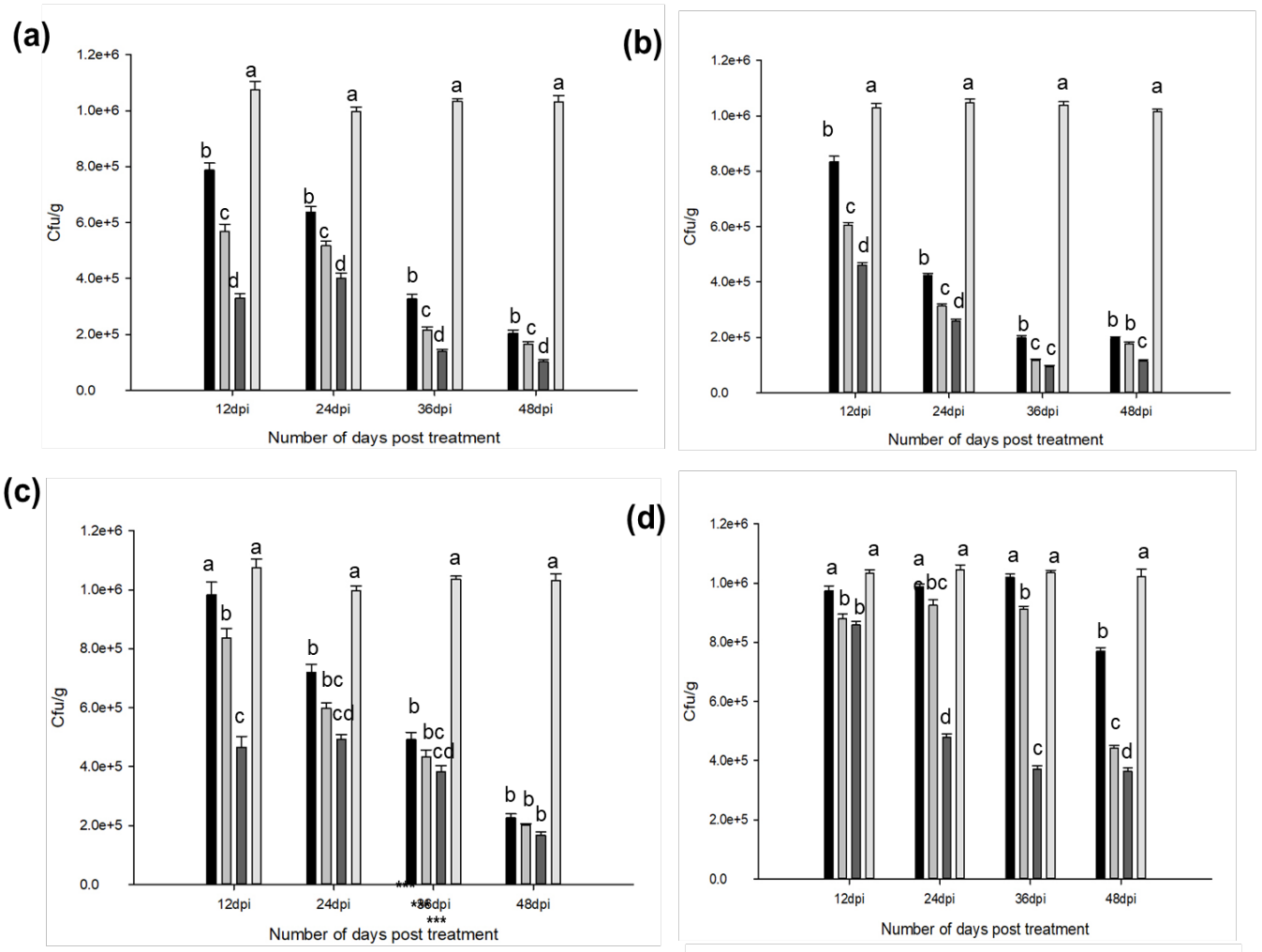


Figure 3.1 Colony forming unit (CFU) counts of bulk soil of *Trichoderma* treated roots of DCS-107 and 48-1 respectively at 12, 24, 36 and 48-days post inoculation (dpi). *T. asperellum* 7316 treated DCS-107 (a), *T. asperellum* 7316 treated 48-1 (b), *T. asperellum* N13 treated DCS-107 (c), *T. asperellum* N13 treated 48-1 (d), *T. asperellum* TV5 treated DCS-107 (e), *T. asperellum* TV5 treated 48-1 (f), *T. asperellum* TV2B16 treated DCS-107 (g), and *T. asperellum* TV2B16 treated 48-1 (h). Statistical difference between treatments displayed at Tukey <0.05. Vertical bars represent Mean ± standard error (SE).

both the genotypes demonstrating its competing ability with other *Trichoderma* strains (**Figure 3.1c-f**). Contrary to the above strains, bulk soil analysis for TV2B16 showed non-significant responses in the DCS-107 genotype (**Figure 3.1g**) while 48-1 genotype (**Figure 3.1h**) exhibited a significant reduction in the CFU count indicating variation in the response of the hosts to the treatment with *Trichoderma* strains.

A significant decrease in CFU count at all concentrations was observed in the rhizosphere soil collected from castor roots treated with the *Trichoderma* strain 7316 in 48-1 genotype compared to DCS 107, while the strain, N13 was more effective in DCS-107 compared to 48-1 suggesting variation among the strains for their rhizosphere competing ability (**Figure 3.2a-d**). The strain, TV5 (**Figure 3.2e-f**) was found to be more effective especially at the concentration of 6 x10^4 spores/ml at 36 dpi for both DCS-107 and 48-1 genotypes.



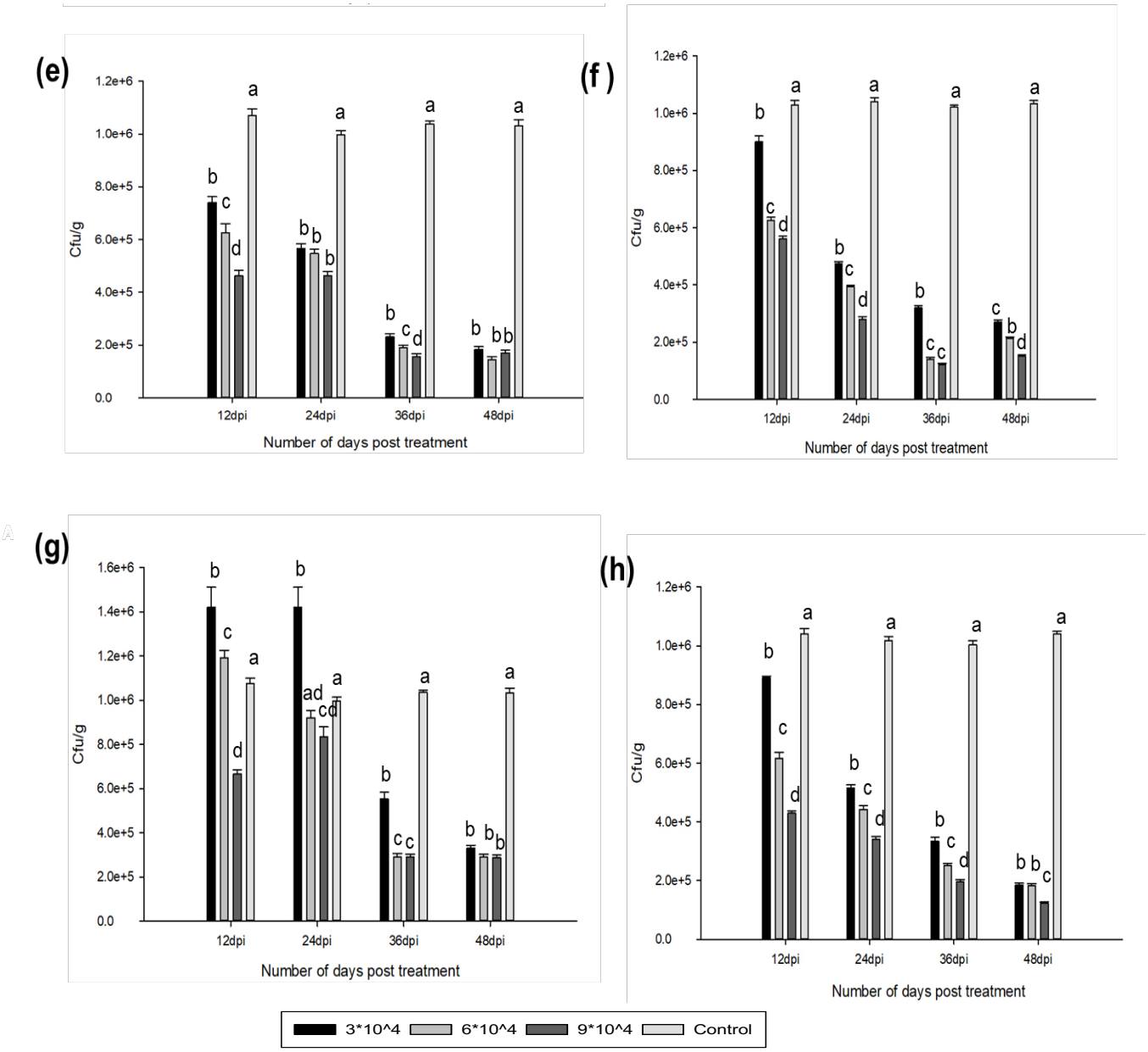


Figure 3.2 Colony forming unit (CFU) counts of rhizosphere soil of *Trichoderma* treated roots of DCS-107 and 48-1 respectively at 12, 24, 36 and 48 dpi. *T. asperellum* 7316 treated DCS-107 (a), *T. asperellum* 7316 treated 48-1 (b), *T. asperellum* N13 treated DCS-107 (c), *T. asperellum* N13 treated 48-1 (d), *T. asperellum* TV5 treated DCS-107 (e), *T. asperellum* TV5 treated 48-1 (f), *T. asperellum* TV2B16 treated DCS-107 (g), and *T. asperellum* TV2B16 treated 48-1 (h). Statistical difference between treatments displayed at Tukey <0.05. Vertical bars represent Mean ± standard error (SE).

indicating its potential as the strain with high rhizosphere competing ability. The CFU count in rhizosphere soil treated with TV2B16 reduced significantly in 48-1 compared to DCS-107 suggesting variation in host responses to TV2B16 (**Figure 3.2g-h**).

3.3.3 Effect of bio-priming with *T. asperellum* strains on seed germination and plant growth

To study the effect of *Trichoderma* treatment on castor plants, the percentage seed germination and radicle growth were monitored at 4 dpi for DCS-107 and 48-1 genotypes which were treated with *Trichoderma* strains individually with a concentration of 1 x 10^6 spores/ml (**Table 3.1**). The seeds treated with CMC solution alone served as controls. The highest percentage of germination was observed for *T. asperellum* strain, 7316 treated seeds showing a 23% and 33% spike in the germination of DCS-107 and 48-1 genotypes respectively compared to their controls. Treatment with TV2B16 showed a similar spike in the germination percentage of DCS-107 seeds, but no significant increase in 48-1. Though treatment with *Trichoderma* strains N13 and TV5 increased the germination rate, the effect was less compared to 7316 (**Figure 3.3**).

Table 3.1 The effect of biopriming with *Trichoderma* strains on seed germination and radicle growth of castor genotypes at 4 dpi.

Biopriming with *Trichoderma*	**Percent seed germination (%)**		**Radicle length (mm)**	
	DCS-107	**48-1**	**DCS-107**	**48-1**
***Trichoderma asperellum* N13**	85±3.19^{c}	46.67±2.72^{a}	49.77±1.53^{c}	22.09±0.56^{c}
***Trichoderma asperellum* 7316**	96.67±1.93^{b}	71.67±3.19^{b}	69.56±1.44^{b}	25.82±0.62^{b}
***Trichoderma asperellum* TV5**	81.67±3.19^{acd}	41.67±4.519^{a}	39.8±1.18^{a}	16.76±0.41^{a}
***Trichoderma asperellum* TV2B16**	91.67±1.67^{bcd}	40±2.72^{a}	41.77±1.72^{a}	18.83±0.35^{d}
Untreated (Control)	73.33±2.72^{a}	38.33±3.19^{a}	40.13±1.32^{a}	15.45±0.59^{a}

The effect of biopriming on the radicle length of DCS-107 and 48-1 seeds of castor 4 days-post treatment with the four strains is shown in **Figure 3.4**. The radicle length of seedlings treated with 7316 showed an increase of 73% in DCS-107 and 67% in 48-1 compared to the controls of DCS-107 and 48-1 genotypes respectively. Likewise, an increase of 24% and 43% radicle growth in DCS-107 and 48-1 respectively was observed when treated with N13. While TV5 did not show any significant effect on radicle growth, TV2B16 displayed a 22% higher radicle length for 48-1 treated seeds compared to control as shown in **Table 3.1**.

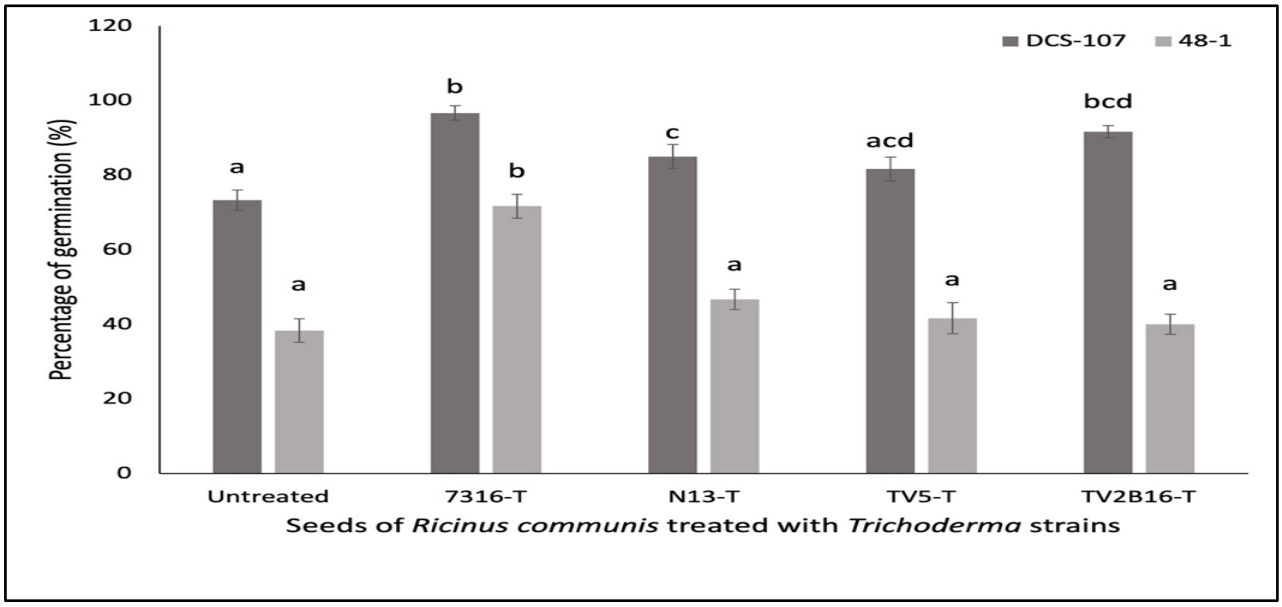


Figure 3.3. Graphical representation of percentage germination of seeds of castor genotypes, DCS-107 and 48-1 recorded 4 days-post treatment with *Trichoderma* strains: 7316, N13, TV5 and TV2B16. Vertical bars represent Mean ± standard deviation (SE). Untreated: Mock (water)-treated seed samples.

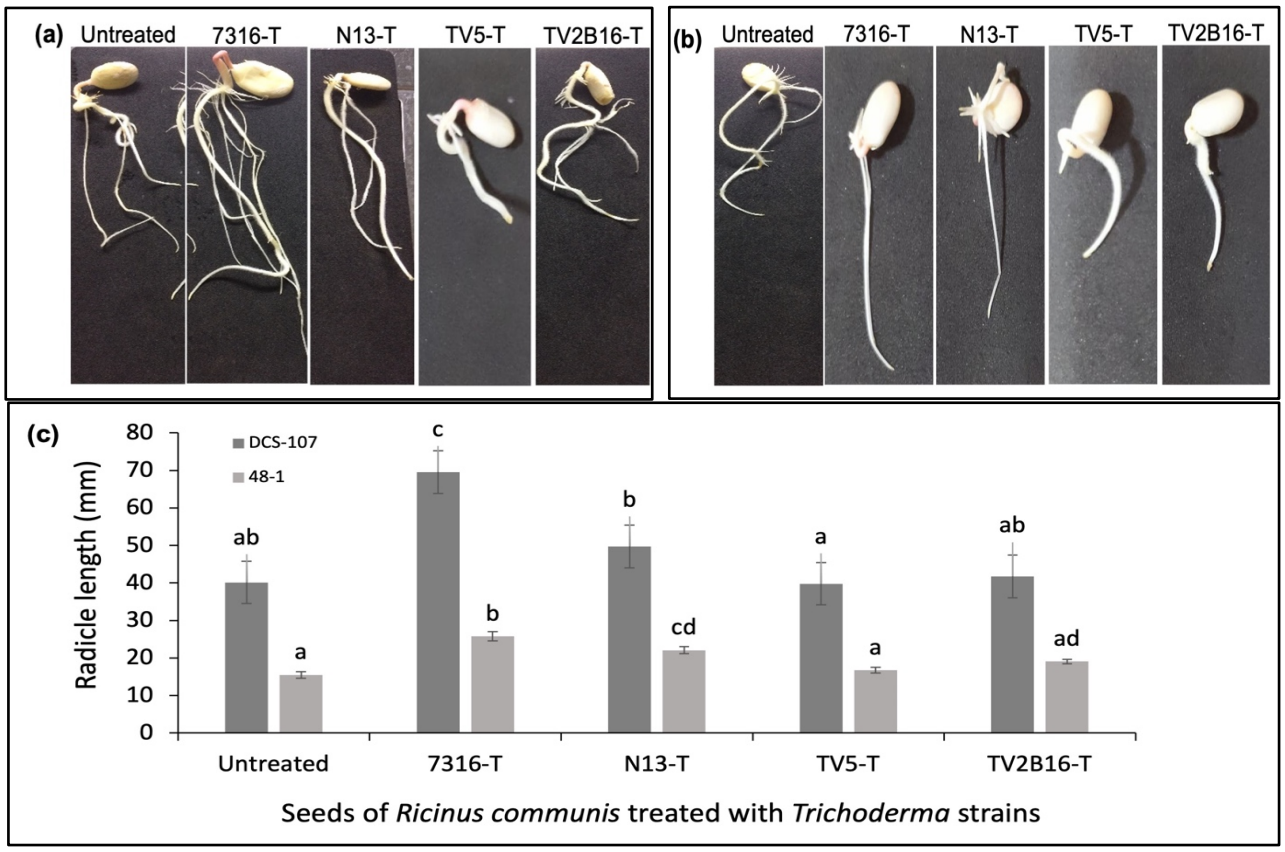


Figure 3.4. Effect of bio-priming with *T. asperellum* strains on the radicle length of castor seedlings of two genotypes: DCS-107 (a) and 48-1 (b) respectively. Graphical representation of the radicle length of DCS-107 and 48-1 seeds of castor treated with *T. asperellum* strains: 7316,

N13, TV5 and TV2B16 4 days-post treatment (c). Untreated: Control seeds treated with CMC solution alone; T: *Trichoderma*-treated seeds. Statistical difference between the treatments displayed at Tukey <0.05. Vertical bars represent Mean ± standard deviation (SE).

3.3.4 Effect of biopriming seeds with *Trichoderma* on the growth of castor

A remarkable feature exhibited by the roots of *Trichoderma* treated DCS-107 genotype was luxuriant roots with higher number of secondary root formation (**Figure 3.5**). The seeds of 48-1 genotype were also bio-primed with all four strains of *Trichoderma*, however, their mortality rate ranged between 75% and 80% within the first two weeks of biopriming thereby indicating the sensitivity of seeds of 48-1 to biopriming. Since the effect of biopriming of the seeds with *Trichoderma* strains was predominant on the castor genotype, DCS-107, these plants were

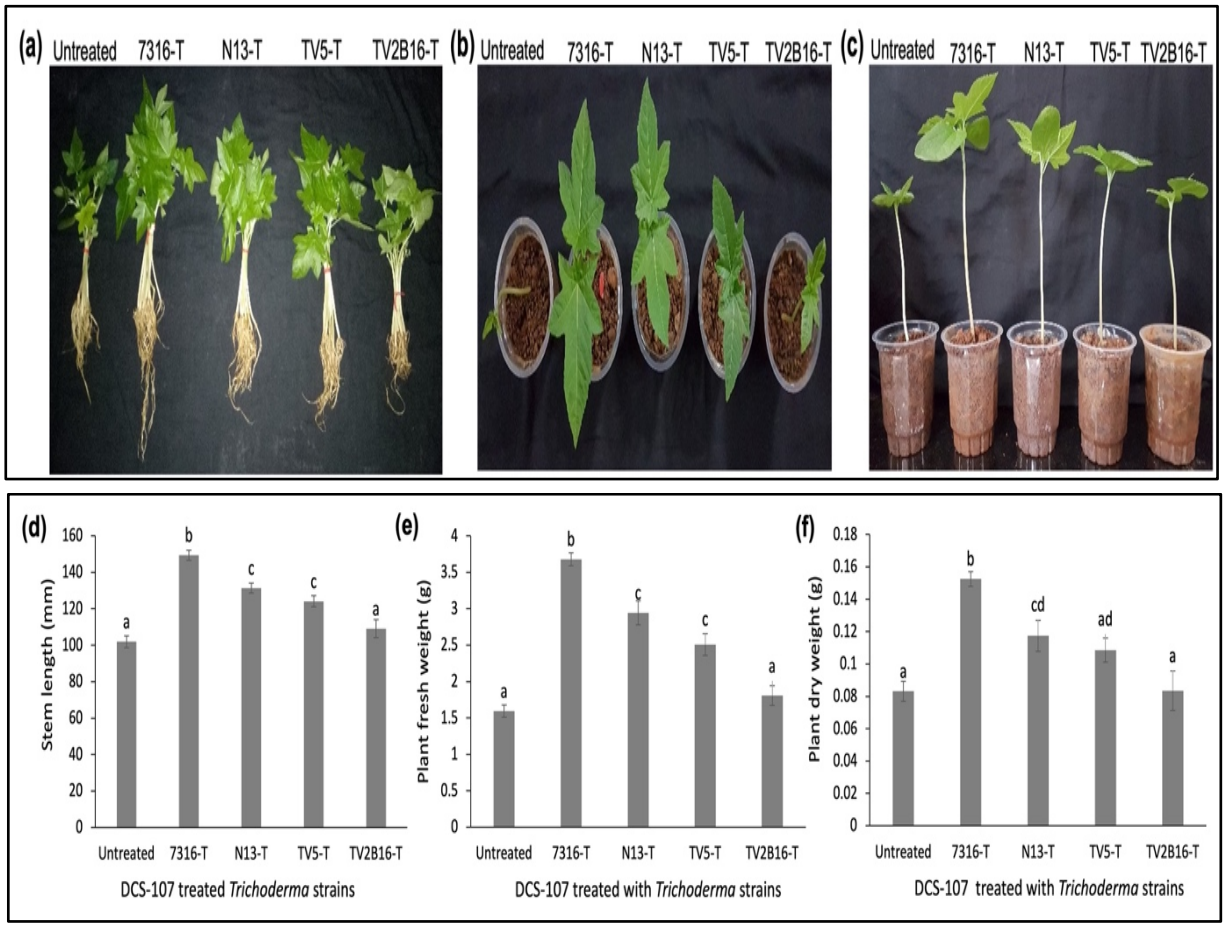


Figure 3.5. Effect of *Trichoderma* treatment on plant growth of castor plants of DCS-107 genotype. The roots (a), leaves (b) and shoot (c) of two-week-old plants treated with *T. asperellum* strains; 7316, N13, TV5 and TV2B16. Graphical representation of length of the stem (d) measured in millimeters (mm), fresh weight (e) and dry weight (f) measured in grams (g) of castor plants. Untreated: Castor plants mock-treated with CMC solution alone: T:

Trichoderma-treated plants. Statistical difference between the treatments displayed at Tukey <0.05. Vertical bars represent Mean ± standard error (SE).

further analysed for other growth parameters. Significant differences in the growth of roots (**Figure 3.5a**), leaves (**Figure 3.5b**), and shoot (**Figure 3.5c**) was observed in DCS-107 in response to all the *Trichoderma* strains. A significant increase in plant growth demonstrated by an increase in shoot length by 46.5, 28.9, and 23% in 7316, N13, and TV5 treated DCS-107 respectively was noted when compared to untreated controls. Similarly, bio-priming led to enhanced plant fresh weight and dry weight in DCS-107. The total biomass calculated for *Trichoderma*-treated plants showed a 131, 85 and 60% increase in fresh weight and 84, 41, 31 % increase in dry weight in 7316, N13 and TV5 treated DCS-107 respectively when compared to untreated controls. TV2B16 treatment showed a marginal 13% increase in fresh weight for DCS-107 (**Figure 3.5d-f**).

3.3.5 Antagonistic effect of *Trichoderma* on *Fusarium* through dual-fungal cultures

To study, the antagonistic properties of *Trichoderma* against *F. oxysporum ricini,* the fungal strains were tested through confrontation plate assays. The dual cultures grown with *F. oxysporum* along with each of the four strains of *T. asperellum,* kept at equidistance from one another in Petri plates were monitored for the extent of mycelia spread.

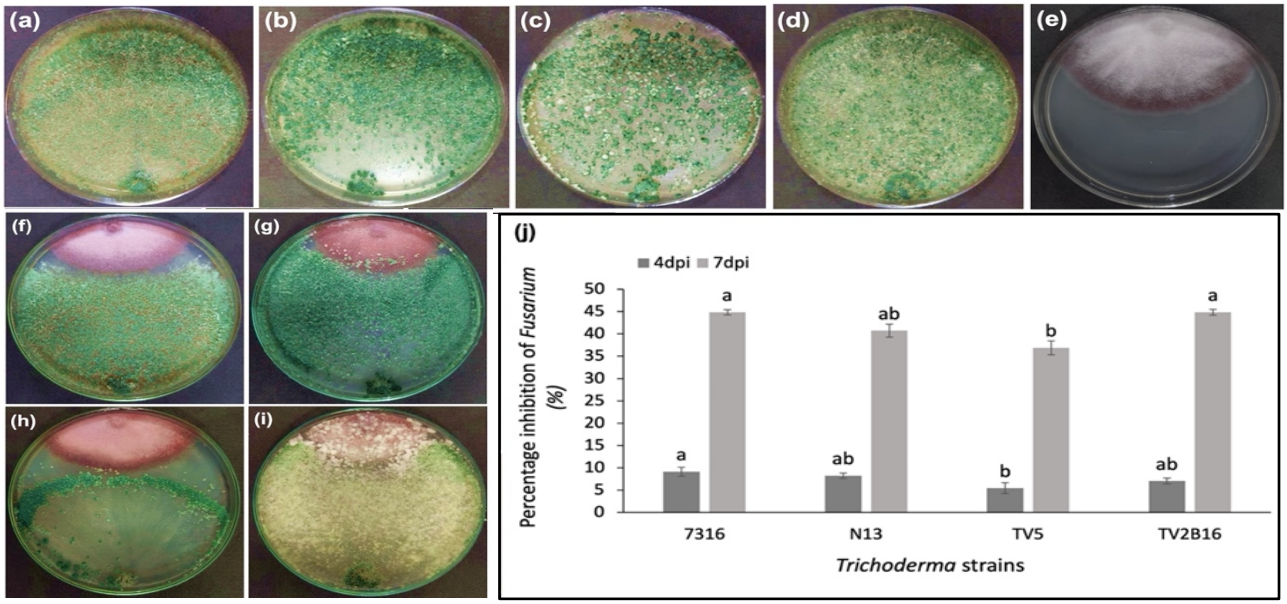


Figure 3.6. Confrontation plate assays with dual cultures grown with *Fusarium oxysporum ricini* along with *Trichoderma asperellum* strains at 7 dpi. Plates growing only *T. asperellum* 7316 (a), N13 (b), TV5 (c) and TV2B16 (d) or *Fusarium* (e) alone served as controls. Test plates included *Fusarium* grown with *T. asperellum* 7316 (f), *Fusarium* grown with *T. asperellum* N13

(g), *Fusarium* grown with *T. asperellum* TV5 (h), *Fusarium* grown with *T. asperellum* TV2B16 (i). Graphical representation of percentage inhibition of *F. oxysporum* growth upon treatment with *Trichoderma asperellum* strains at 4 and 7 dpi (j). Statistical difference between the treatments displayed at Tukey <0.05. Vertical bars represent Mean ± standard deviation (SE). Petri plates growing *Trichoderma* and pathogen discs alone served as controls.

All the strains overgrew at least two-third of the medium surface thus showing a pronounced antifungal activity of *Trichoderma* (**Figure 3.6**). TV2B16 showed profuse growth-inhibiting *Fusarium* fungal growth on 7 dpi while a clear zone of inhibition was observed for 7316 against *F. oxysporum*.

Table 3.2. Percentage *Fusarium* pathogen growth inhibition by the antagonistic effect of *Trichoderma* strains. [a,b] Statistical significance levels for treatments with each of the *Trichoderma* isolates. Mean ± SE with different letters indicate significance level at P<0.05, according to Tukey test.

***Trichoderma* isolates**	**Percentage inhibition of *Fusarium* growth (%)**	
	4 dpi	**7 dpi**
***Trichoderma aperellum* N13**	9.13±0.49[a]	40.69±0.98[ab]
***Trichoderma asperellum* 7316**	9.761±0.77[a]	44.82±0.43[a]
***Trichoderma asperellum* TV5**	5.9±0.95[a]	36.83±1.08[b]
***Trichoderma asperellum* TV2B16**	7.51±0.5[a]	44.81±0.48[a]

Percentage fungal pathogen growth inhibition caused by the antagonistic effect of *Trichoderma* strains was estimated based on the delta values of inhibition (Δ inhibition) as shown in **Table 3.2**. The strains 7316 and TV2B16 showed a higher degree of antibiosis against *F. oxysporum* with 9.38 and 7.5% pathogen growth inhibition respectively on the fourth day and 44.8 and 40.7 % inhibition by both the strains on the seventh day of plating (**Table 3.2**).

3.3.6 Effect of *Trichoderma* on castor challenged with *Fusarium oxysporum*

To test the effect of *Trichoderma* treatment on the root wilt disease caused by *F. oxysporum, Trichoderma* treated roots of DCS-107 and 48-1 were co-stressed with the fungal pathogen, *F. oxysporum.* Wilt disease symptoms along with plant growth were monitored at 7 and 21 dpi

respectively (**Figure 3.7**). The set of plants that were treated with *Fusarium* pathogen alone showed yellowing of roots and wilting at 7dpi (**Figure 3.7a**), followed by complete death of the plant by 21 dpi (**Figure 3.7b**). The *T. asperellum* strains; 7316 and N13- treated plants showed no major wilting at 7dpi, even though N13 showed yellow discoloration of the roots. Whereas both TV5 and TV2B16 treated plants showed slight drooping of leaves along with yellowed roots at 7dpi.

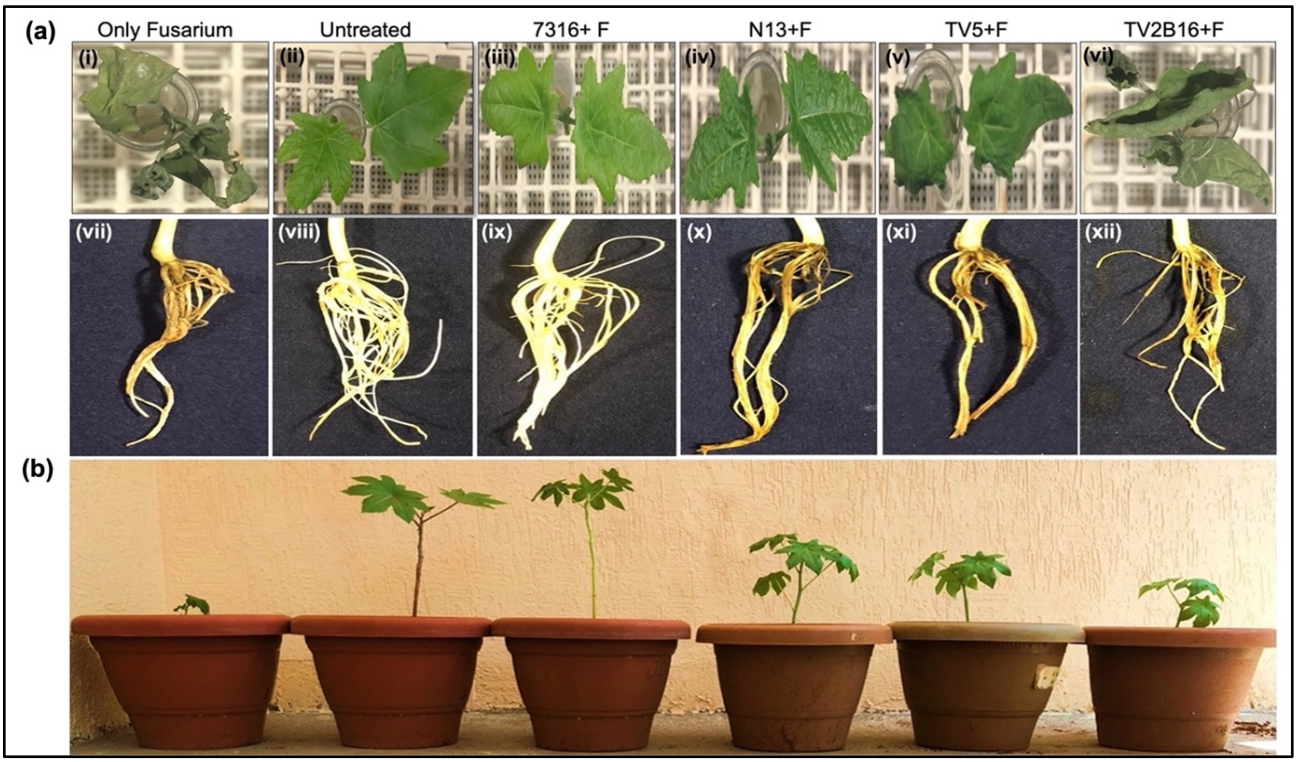


Figure 3.7 Effect of *Trichoderma* treatment on plant growth in castor (*Ricinus communis L.*). Fusarium wilt incidence monitored on aerial and underground parts of the DCS-107 castor plants treated with *T. asperellum* strains at 7 dpi (a). Plant growth and tolerance to *Fusarium* wilt monitored in DCS-107 plants treated with *Trichoderma* strains at 21 dpi (b).

At 21 days, it was evident that 7316 showed elevated level of biocontrol compared to all the other strains used in the experiment with the lowest percentage of wilt incidence, which is 24% (**Figure 3.8**). This is consistent with the results obtained in dual culture experiment where 7316 showed maximum antibiosis.

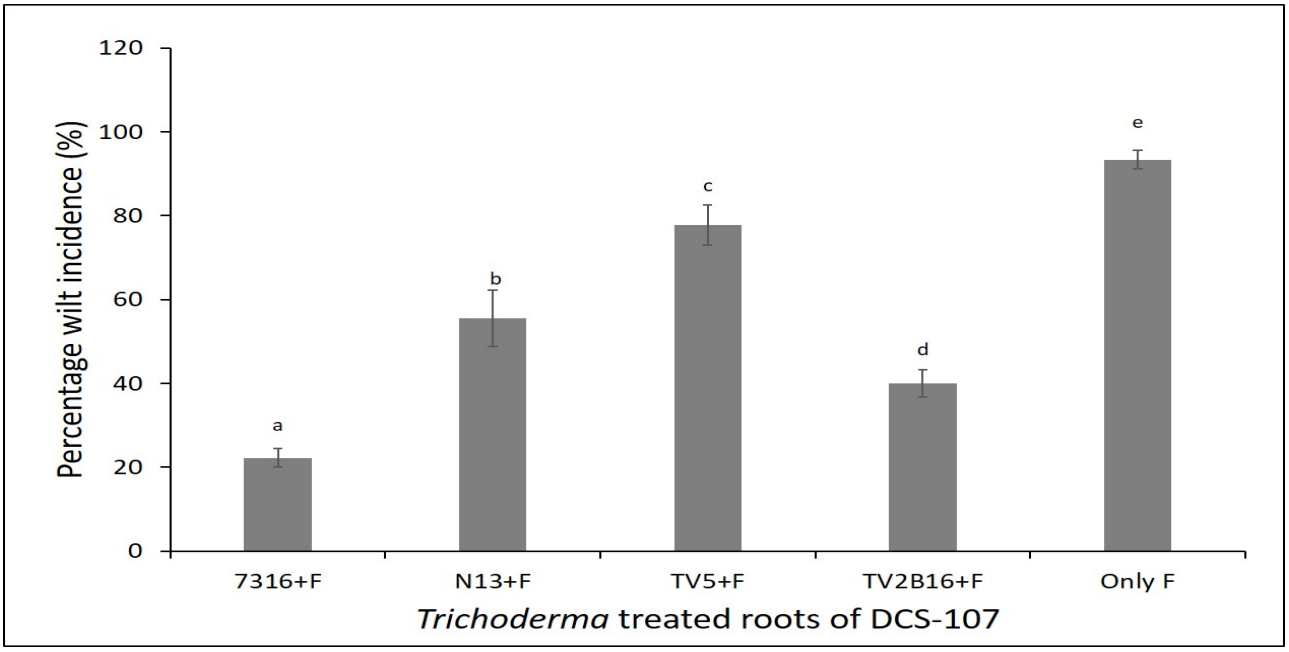


Figure 3.8 Effect of *Trichoderma* treatment on *Fusarium* wilt disease in castor. Percentage *Fusarium* wilt incidence recorded in the roots of DCS-107 plants treated with *T. asperellum* strains: 7316, N13, TV5 and TV2B16 at 21 dpi. The data was normalized against the control/untreated samples for all treatments. Statistical difference between the treatments displayed at Tukey <0.05. Vertical bars represent Mean ± standard error (SE).

Though TV5 showed relatively higher wilt disease incidence when compared to TV2B16, the level of disease incidence was significantly lower than that of the control plants. Moreover, the three strains; N13, TV5, and TV2B16 displayed a moderate level of resistance to *Fusarium* when compared to the pathogen-challenged plants. The castor genotype, 48-1 on the other hand did not withstand biopriming with *Trichoderma*, thus indicating the sensitivity of seeds of 48-1 to biopriming (data not shown).

3.3.7 RT-qPCR for host response to *Trichoderma* treatment

To test host responses to *Trichoderma* treatment, the relative expression of 13 putative defence response genes comprising of Phenylalanine lyase (*PAL*), Pathogenesis Related Protein1 (*PR1*), Pathogenesis Related Protein2 (*PR2*), Pathogenesis Related Protein5 (*PR5*), 12-oxophytodienoate reductase (*OPR*), Responsive to Desiccation29 (*RD29*), Calreticulin (*CRT*), Glutaredoxin (*GRX*), Chalcone synthase (*CHS*), MYB (myeloblastosis) family of transcription factor (*MYB75*), UDP-glucose:flavonoid 3-o-glucosyltransferase (*UF3GT*), Lipoxegenase (*LOX*) and S-Adenosyl-L-methionine (*SAM*) genes were monitored in *Trichoderma*-treated DCS-107 and 48-1 plants with two strains, 7316 and N13 individually compared to the controls (mock-treated with water). Relative expression of defence response genes showed significant

variation not only between the two strains of *Trichoderma*, but also between the two genotypes of castor (**Figure 3.9**). 7316 treated roots of castor showed a down-regulation of majority of the defence response genes in both 48-1 and DCS-107. The *PR2* transcripts were up-regulated 3 fold-change in 7316 treated DCS-107 roots while its expression was down-regulated in N13. Though *OPR* was up-regulated in both 48-1 and DCS-107, a 4 fold-change up-regulation was observed in DCS-107 compared to 48-1. *LOX* and *SAM* showed prominent up-regulation only in DCS-107. Conversely, treatment with N13 showed up-regulation of all the twelve defence response genes in DCS-107 roots whereas all genes except GRX were down-regulated in 48-1 roots.

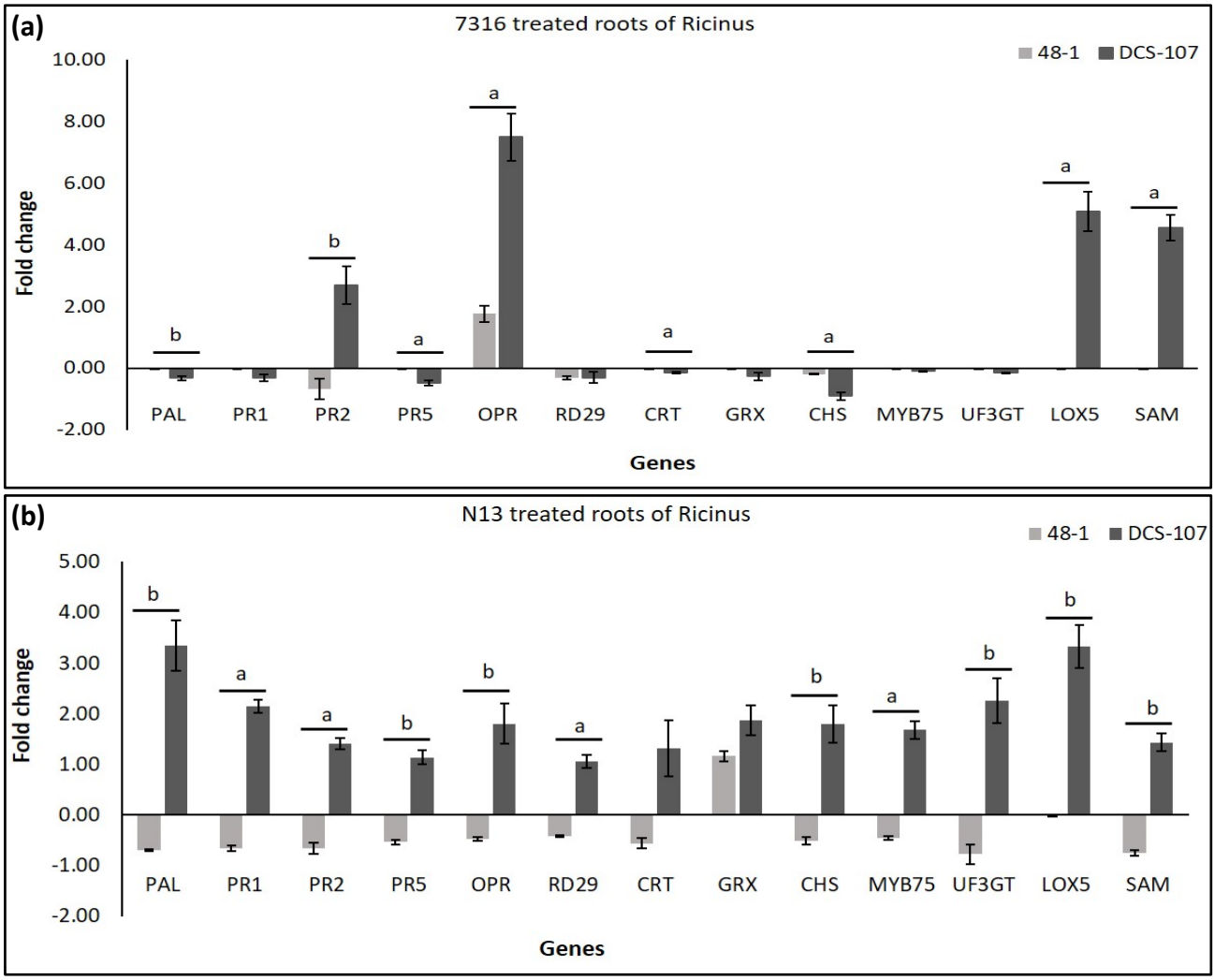


Figure 3.9 Relative expression of defence response genes in roots of *Trichoderma* treated DCS-108 and 48-1 genotypes of castor. Relative levels of mRNA transcript accumulation of 13 genes in *T. asperellum* 7316-treated (a) and *T. asperellum* N13-treated (b) roots of castor at 48 hpi. Actin gene expression was used as control to normalize the expression of the defence genes, using the $2^{-\Delta\Delta CT}$ method. The graphs show the mean expression levels ± standard deviation

(SD). The alphabets denote the level of significance of each gene amongst the two genotypes of castor. a: p<0.0; b: p<0.05.

Interestingly, leaves of 7316 treated plants (root treatment) showed an enhanced expression of major defence related genes like *PAL*, *PR1*, *PR5*, *RD29*, *CRT*, and *GRX* in both the genotypes of castor (**Figure 3.10**).

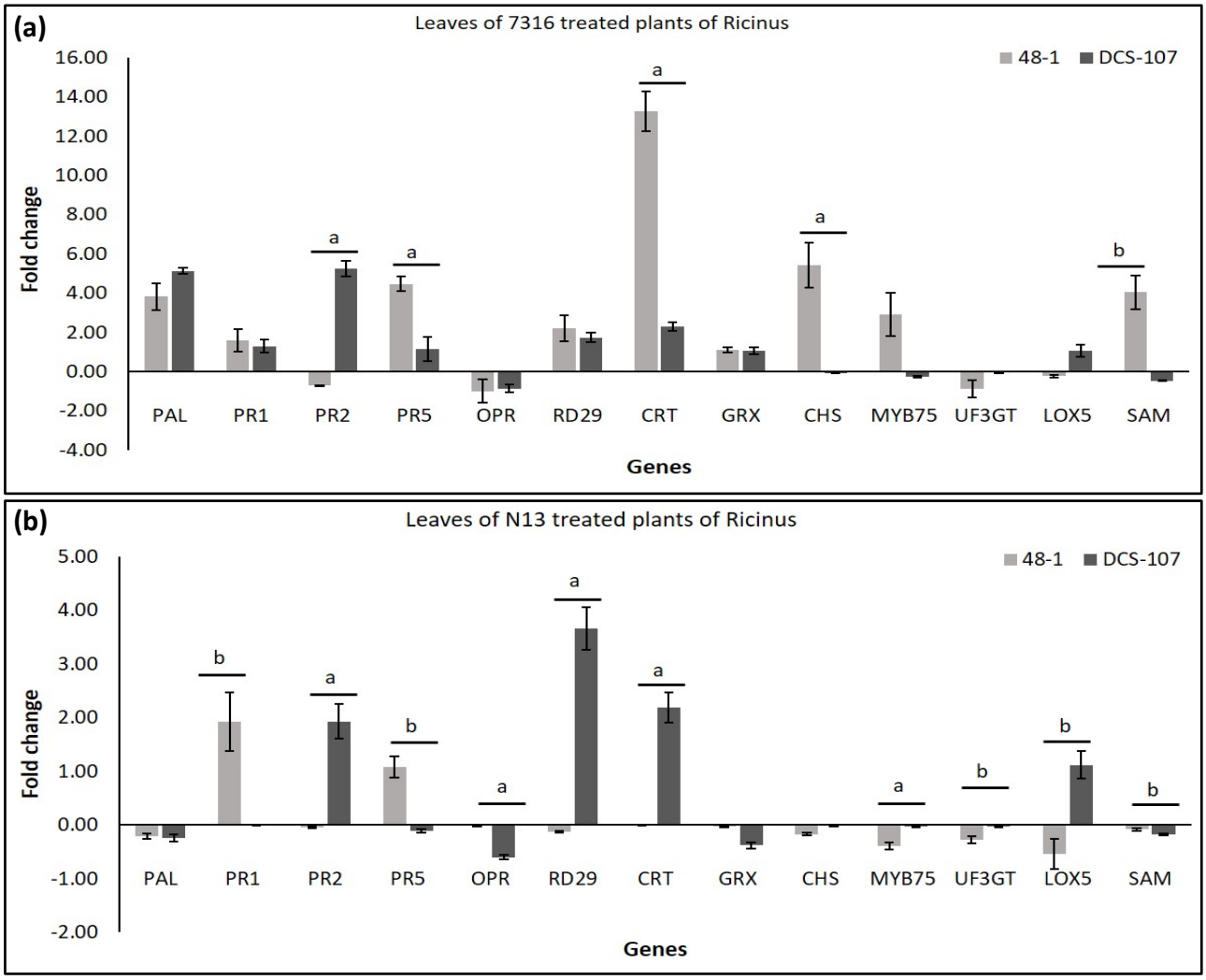


Figure 3.10 Relative expression of defence response genes in leaves of *Trichoderma* treated DCS-108 and 48-1 genotypes of castor. Relative levels of mRNA transcript accumulation of 13 genes in *T. asperellum* 7316-treated (a) and *T. asperellum* N13-treated (b) leaves of castor at 48 hpi. Actin gene expression was used as control to normalize the expression of the defence genes, using the $2^{-\Delta\Delta CT}$ method. The graphs show the mean expression levels ± standard deviation (SD). The alphabets denote the level of significance of each gene amongst the two genotypes of castor. a: p<0.0; b: p<0.05.

The genes *PR2*, *CHS*, *MYB75*, *UF3GT*, *LOX5* and *SAM* were differentially regulated in the two genotypes while *OPR* remains downregulated in both. Notably, leaves of N13 (root treatment)

treated plants showed a downregulation of most genes in 48-1 except *PR1*. The genes *PR2*, *RD29*, *CRT* and *LOX5* were upregulated in DCS-107 leaves whereas PAL, *OPR*, *GRX* and *SAM* were downregulated suggesting fine-tuning of the activation of different network pathways of defence genes. Together these data indicate that *Trichoderma* strains 7316 and N13 activate both localized and induced systemic resistance in the roots and leaves of castor respectively that shows substantial variation across the two genotypes of castor.

3.3.8 Biochemical analysis to evaluate host responses to *Trichoderma* treatment

To monitor the biochemical responses of *Trichoderma* against *Fusarium* wilt causing pathogen, *Fusarium oxysporum,* the DCS-107 plants were inoculated in isolation with three different treatments: *Trichoderma* alone, *Fusarium* alone and co-culturing with *Trichoderma* and *Fusarium* pathogen. Of the two strains used for testing the host response to *Trichoderma* treatment, it was noticed that for 7316, majority of the defence response genes were downregulated. Further, 7316 has shown better growth promoting and antibiosis ability suggesting it's recognition by the host as not only non-threatening but also beneficial for plant growth.

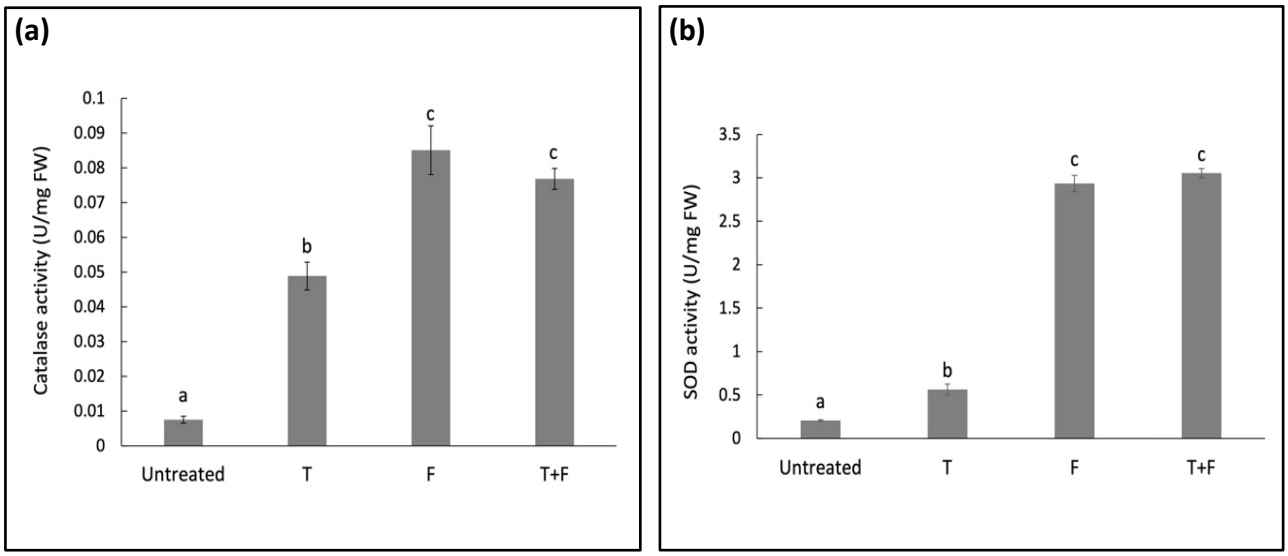
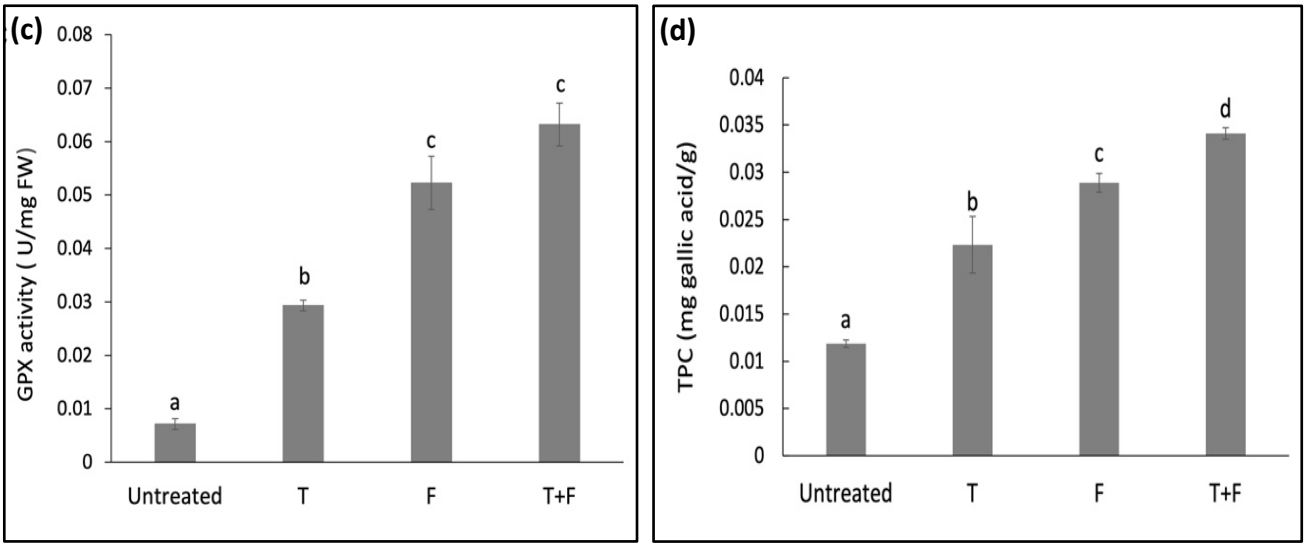


Figure 3.11 Effect of *Trichoderma asperellum* 7316 on the accumulation of antioxidative enzymes CAT (a), SOD (b) and GPX (c) and, total phenol content (TPC) (d) either individually or in the combination with Fusarium in castor at 3 dpi. Histograms shown by different letters indicating statistical significance level between treatments displayed at Tukey <0.05. Vertical bars represent Mean ± standard deviation (SE).



Hence our results narrowed down to 7316 which was chosen to carry forward further biochemical studies. The castor genotype, 48-1 on the other hand did not withstand biopriming with *Trichoderma*, thus indicating the sensitivity of seeds of 48-1 to biopriming. In *Trichoderma*-treated roots of DCS-107 plants, SOD and CAT levels were enhanced, though the upregulation of SOD is lesser compared to CAT (**Figure 3.11a-b**). SOD level was even higher in case of co-stressed plants. CAT activity was observed to be elevated in *Fusarium*-infected plants as well as *Trichoderma*-inoculated and co-stressed samples compared to healthy controls which might be due to accumulation of excess H_2O_2 during pathogen infection.

GPX also plays an important role in the fine regulation of ROS levels in the cell through the activation and deactivation of H_2O_2. Just like SOD, GPX level was seen to be the highest in the case of co-stressed plants (**Figure 3.11c**). Total phenol content (TPC) in *Trichoderma*-treated tissues was significantly higher (**Figure 3.11d**) than that in untreated castor plants, though the highest expression was seen in co-stressed samples. Synthesis of high amount of phenols by 7316, compared to the controls, suggests their role in inducing resistance against Fusarium wilt in castor.

3.4. DISCUSSION

Trichoderma strains being promising BCA have demonstrated both root colonizing and biocontrol properties. In our study, the effectiveness of four strains of *Trichoderma asperellum* were tested against *Fusarium* that causes wilting in castor along with their effect on growth and development on two genotypes of castor - DCS-107 and 48-1.

Xue et al., 2017 demonstrated seed treatment is one of the most effective methods to confer resistance against biotic and abiotic stresses and also to increase crop yield (Singh et al., 2016). The research findings in this chapter showed that the four strains of *T. asperellum* used in the study varied in their biocontrol, rhizosphere competency and plant growth-promoting properties. The success of biocontrol agents depends on their ability to efficiently proliferate and colonize in the rhizosphere (Lo et al., 1996). The ability of *Trichoderma* to colonize roots efficiently and show noteworthy rhizosphere competence has been measured by the reduction of CFU in both rhizosphere and bulk soil in both genotypes of castor. All the strains have shown efficient competence, however two strains 7316 and TV5 showed significant competitive ability when compared to the others. N13 showed enhanced activity in the rhizosphere space post 36 days. This could be due to a considerable amount of time required by N13 to establish and proliferate in the rhizosphere compared to other strains.

Further, variation among the two genotypes has had been noticed when treated with the same *Trichoderma* strain which indicates that there could be an involvement of any gene products or secondary metabolites that are being produced by the host genotypes which is affecting the colonization and rhizosphere competence ability (Saravanakumar et al., 2016; Li et al., 2016; Kumar and Ashraf, 2017) of the four different strains of *Trichoderma*. The significant reduction of CFU count by *Trichoderma* might be due to its high propensity to mobilize soil nutrients at a rapid rate divesting the uptake of nutrients, resulting in the limitation and starvation of other competing microorganisms (Benitez et al., 2004). It also directs towards an effectual colonization of the fungal strains on the roots of castor and its proliferation in bulk and rhizosphere soil samples. Modification of environmental pH of the rhizosphere and ability to survive in a wide range of pH conditions (Benítez et al., 2004; Sharma and Gothalwala, 2017) could also contribute to a decline of the CFU count in the rhizosphere of the plants. Along with competitive nutrient uptake, *Trichoderma* appears to even alter the surrounding pH that could result in impeding the pathogens to secrete pathogenicity factors and thereby reducing their virulence in the host genotype (Saravanakumar et al., 2016; Li et al., 2016; Kumar and Ashraf, 2017).

The results obtained from dual culture experiments conducted with all strains of *Trichoderma* was in agreement with the previous studies. *Trichoderma* releases a wide range of secondary metabolites that are antifungal and antibacterial in nature which include epipolythiodioxopiperazines, peptaibols, pyrones, pyridones, butenolides, azaphilones, koninginins, lactones, steroids, anthraquinones and trichothecenes that inhibits the growth of various phytopathogens (Khan et al., 2020a,b; Schuster and Schmoll, 2010). All the fungal strains in our study were able to impede the growth of *F. oxysporum.* Out of the four strains, 7316 and TV2B16 showed better inhibition. TV2B16 which showed high proliferation, was able to rapidly overgrow on *Fusarium* pathogen. A clear zone of inhibition was observed between 7316 and *Fusarium* which might be caused by diffusible metabolites secreted by *Trichoderma.* All the above observations indicated the antibiosis effect of *Trichoderma.* In continuation, challenging of *Trichoderma*-primed roots of castor with *F. oxysporum* highlighted the protective influence of *Trichoderma* on root wilt caused by the pathogen, thus confirming the role of *Trichoderma* in combating biotic stress. Both the antagonistic and invitro greenhouse studies showed that 7316 is the most effective stain in controlling *Fusarium* pathogen.

In addition to the antagonistic property of *Trichoderma*, one of its major roles lies in plant growth promotion and development. The effect of *Trichoderma* on growth and development of various economically important agricultural crops has already been reported and proven (Singh et al., 2016; Xue et al., 2017). In our present study, seeds of castor were bioprimed with the *Trichoderma* strains. When comparing the growth promotion, 7316 showed greatest seed germination percentage of compared to the control samples similar to the findings by Hajieghrari and associates (2010) followed by overall plant growth. Overall, three strains in this study 7316, N13 and TV5 showed varying levels of antagonism, rhizosphere competence and growth promotional response in castor genotype. The strains could be thus utilized either singly or in combination to enhance castor production and yield.

Global reprogramming of gene transcription in plants caused by *Trichoderma* spp. (Brotman et al., 2013) has been a topic of extreme importance. Taking the advantage of *Trichoderma*, being opportunistic plant symbionts, a comparative gene transcript analysis carried to understand the response of castor to two selected *Trichoderma* strains (7316 and N13). The reason behind selecting 7316 and N13 were that both the strains demonstrated effective rhizosphere competence, showed enhanced mycoparasitism and resistance to *Fusarium* and demonstrated greater plant growth and development than the other two strains. Our studies revealed that 7316 and N13 showed a remarkable variation in the pattern of genetic reprogramming in castor. The transcription level of 13 different putative defense response

genes were tested and compared between *Trichoderma* treated and control roots and corresponding leaves of both the genotypes of castor. In DCS-107 treated with N13 strain showed up-regulated *PAL*, OPR and *LOX5* activity compared to 48-1 suggesting the activation of defence pathways were genotype dependent. 7316 treated plants of both the genotypes of castor showed down-regulated *PAL* activity. Phenylalanine ammonia lyase (*PAL*) is the first enzyme in the phenylpropanoid biosynthesis pathway which is involved in the biosynthesis of lignin, phenols and even salicylic acid (Kim and Hwang, 2014). However there was an up-regulation in *OPR.* The gene 12-oxo-phytodienoic acid reductase (*OPR*) is important in the jasmonic acid (JA) biosynthesis pathway (Scalschi et al., 2015) and thus plays a vital role in plant defence. Upregulation in OPR indicates the priming of JA related defence response by 7316. *LOX5* up-regulated in DCS-107 alone. *LOX5* plays an important role in defence response and lateral root development (Park et al., 2010; Caldelari et al., 2010).

Overexpression of *PAL* in pepper leads to enhanced production of *PR1*. *PR1* plays a vital role in the SA dependent SAR response. *PR1* is a part of Pathogenesis-related (*PR*) proteins which are a specific set of proteins that are induced on pathogen attack and play a very vital role in the defence response of plants (Jain and Khurana, 2018). This is in agreement with our study where N13 treated roots of DCS-107 showed upregulated *PAL* and *PR1* activity. This is consistent with findings of Shoresh and associates (2005) where *T. asperellum* T203 modulated the expression of major genes involved in the JA pathway. At the same time a downregulation in *PAL* activity indicated that 7316 could have repressed the SA dependent SAR response response in DCS-107. Other PR genes like *PR2* and *PR5* were upregulated in N13 treated DCS-107 roots whereas in 48-1 all of the genes were downregulated. *PR2* (β-1,3 glucanase) is involved in increased lignin content and callose deposition which provides the first line of defence response to pathogen entry. 7316 treated roots of DCS-107 showed a 3 fold-change upregulation of *PR2* gene. From the above observation, it can be concluded that different genotypes of castor can show varied response to different strains of *Trichoderma*, in our case 7315 and N13.

We know *Trichoderma* is the most efficient BCA. For *Trichoderma* to be able to establish itself as a plant-beneficial agent, it must be able to coexist as a symbiont in the roots. For such a successful plant and fungal association to take place, the fungus must be able to evade the innate immunity of the plant for which down-regulation of most of the defence response genes is a must. Accumulation of ROS and oxidative burst are among such mechanisms that fall under the fisr line of defence in plants. GRX is an antioxidant that is involved in the cellular response to oxidative stress. Enhanced GRX activity in N13 treated roots compared to 7316 indicates a

higher oxidative burst compared to 7316. From the above observation, it can be said that compared to N13, colonization of 7316 results in modulating several defence genes to enable better colonization of the fungi in the host. Brotman and associates (2013) showed similar observations in *Trichoderma* treated roots of *Arabidopsis thaliana* along with a range of other host plants (Morán-Diez et al., 2021).

Though *Trichoderma* is sensed by the plant as a "safe" organism and is also able to evade the innate immune system of the plant for effective colonization, one of its most vital contribution is its ability to prime the internal defence response of the plant. This helps the plant react to any subsequent pathogen attack (Gupta and Bar, 2020) before substantial damage. Previously we showed that 7316 was the most efficient strain out of the strains under study to combat the *Fusarium* infection in castor. This could be due to the elevation of *OPR* gene shows that triggers the JA-mediated signalling in the leaves of both the genotypes of castor that lead to better growth compared to the others.

Interestingly, the results obtained in the leaves were contrastingly different from the roots, where majority of the defence response genes under study, like *PAL*, *PR1*, *PR2*, *PR5*, *RD29*, *CRT*, *GRX* and *LOX5* were upregulated in leaves of DCS-107, whereas only 4 genes - *PR1*, *RD29*, *CRT* and *LOX5* were upregulated in N13 treated DCS-107. In the leaves of the 48-1 genotype of castor there was more upregulation of genes by 7316 compared to N13. Our results were similar to what was seen in the leaves of grapevine on the root colonization by *Trichoderma atroviride* (Stempien et al., 2020). It can be concluded that root colonization of 7316 led to elevated levels of defense response genes in the leaves which are an indicative of elevated SA-mediated defence response. Such a pattern leads to "priming" the plant from any subsequent pathogen infiltration.

During a pathogen infiltration, though an oxidative burst production of superoxide (O_2^-) and hydrogen peroxide (H_2O_2) is one of the earliest defence responses, overproduction of ROS is highly toxic that leads to irreversible oxidative damage to cells. Shoresh et al., 2010 had shown that *Trichoderma* is able to protect plants against such damage by reducing ROS level. In our current study, biochemical analysis was done whose results were in agreement with the above findings. SOD, CAT and GPX are major ROS scavenging and antioxidant enzymes reported in plants that are elicited in response to biotic stress. Though, SOD catalyses the dismutation of O_2^- which helps in reducing O_2^- content, it leads to the production of H_2O_2, whereas CAT enzyme catalyses H_2O_2 breakdown into water and oxygen in an energy-efficient manner. GPX also plays an important role in the fine regulation of ROS levels in the cell through the activation and deactivation of H_2O_2. SOD, GPX level was seen to be the highest in the case of co-stressed plants.

The enhanced levels of antioxidative enzymes (SOD, CAT and GPX) in co-stressed castor plants compared to plants infected with *F. oxysporum*, suggested that *Trichoderma* protects castor from the damage of oxidative stress.

Total phenol content (TPC) was significantly higher in *Trichoderma*-treated tissues compared to untreated castor plants, though the highest expression was seen in co-stressed samples. Such increase in phenolic content in plants is responsible for the deposition of lignin that acts as a physical barrier to pathogen entry. It also regulates molecules that are directly related to defence response (Keswani et al., 2017). Our results are in agreement with the findings reported by Bigirimana and associates (1997) and Singh and associates (2014) wherein inoculation of *Trichoderma* either alone or in consortium with other microbes caused enhanced phenolic accumulation. Synthesis of high amount of phenols by 7316, compared to the controls, suggests their role in inducing resistance against *Fusarium* wilt which might have elicited the production of sensing molecules in castor during disease resistance against wilt. Further, an in-depth study of the *Trichoderma* strains to synergize the effect of all toxic metabolites and hydrolytic enzymes may lead to formulating a complex strain that would enhance the antagonistic potential of *Trichoderma* as a BCA.

Chapter 4

Delineating host responses induced by *Trichoderma* in castor through comparative transcriptome analysis by next generation sequencing

4.1 INTRODUCTION

Owing to the property of *Trichoderma* spp. to exhibit efficient mycoparasitism against various pathogens (Rajani et al., 2021), it has been recognized as a key biocontrol. The mycoparasitism of *Trichoderma* is due to the ability to secrete various hydrolytic enzymes, secondary metabolites, ABC transporter membrane pumps. Also it is capable of modification and competition for nutrients (Qualhato et al., 2013). Besides the parasitic nature of *Trichoderma*, many rhizosphere competent strains of *Trichoderma* are able to interact and colonize the roots of plants leading to the formation of a symbiotic association that leads to overall plant growth promotion and yield (Benitez et al., 2004). In addition to enhanced plant growth and development, *Trichoderma* colonization in plant roots has been demonstrated to induce both local and induced systemic resistance (ISR) responses in a vast variety of agricultural crops like pepper, tomato, pea, tobacco and sorghum (Liu et al., 2020; Singh et al., 2016; Li et al., 2015; Saber et al., 2017). Identifying the key defense response molecules and understanding the mechanism employed by *Trichoderma* to modulate the plant's defense response to ensure a long-lasting beneficial association with the host plant is of prime importance.

Lately, transcriptomic analyses have been extensively studied to understand host-microbe interactions and to identify key signaling molecules. Though, previous studies revealed that ISR gets activated by *Trichoderma* treatment in crop plants as well as model plants like *Arabidopsis thaliana* and tomato (Alfano et al., 2007; Tucci et al., 2011; Mathys et al., 2012; Martinez-Medina et al., 2013), recent studies have indicated that partial suppression of SA-dependent responses in plants is necessary to form a symbiotic association between mycorrhiza and the host (Nishad et al., 2020).

India contributes about 85% of the global production of castor. However over the last couple of years there has been a drop in the overall production of castor due to various biotic and abiotic factors. The rapid growth in population and the crop losses caused by emerging plant pathogens are major hindrances that require immediate action to ensure crop security in the coming years. Also, eco-friendly, non-hazardous practices for crop production are being promoted to achieve sustainability. *Trichoderma* has displayed such promising results for many agricultural crops. From an applicative perspective, sufficient evidence of a strong mutualistic relation between host and microorganism is necessary, before any biocontrol organism can be introduced to a crop. Hence, a better understanding of what really happens during *Trichoderma*'s interaction with the host, will definitely open new ways to exploit the potential of *Trichoderma* for better performance in agriculture.

We hypothesized that similar molecular mechanism might be involved for colonization of *Trichoderma* in castor. To delineate the changes induced by *Trichoderma* colonization in the roots of castor, transcriptome study was carried by treating the roots of the castor genotype, DCS-107 grown in controlled conditions with *Trichoderma asperellum* strain, 7316 compared to the mock-treated control castor plants and the research findings are presented.

4.2 MATERIALS AND METHODS

4.2.1 Plant material and growth conditions

Seeds of castor genotype, DCS-107 were obtained from Indian Institute of Oilseeds Research (IIOR), Hyderabad, India. Surface sterilized seeds were germinated on sterile filter paper for 4 days. The germinated seedlings were grown hydroponically in autoclaved Hoagland solution (**Table 4.1**) for 14 days in a plant growth chamber maintained at 28 ˚C and 14/10 day/night respectively under a PAR of 500 W m^{-2} with 55% relative humidity (RH).

Table 4.1 Composition of the Hoagland solution (with modifications) used to grow castor plants hydroponically. (*Ricinus communis* L.).

Compounds		**Concentration of stock solutions (mM)**	**Volume of stock solution (mL) used to prepare a litre (L) of the working solution**
Macronutrients	KNO_3	1000	6
	$Ca(NO_3)_2 \cdot 4H_2O$	1000	4
	KH_2PO_4	1000	2
	$MgSO_4 \cdot 7H_2O$	1000	1
Micronutrients	KCL	25	2
	H3BO3	12.5	
	$MnSO_4.H_2O$	1.0	
	$ZnSO_4 \cdot 7H_2O$	1.0	
	$CuSO_4.5H_2O$	0.25	
	MoO	0.25	
	FeNaEDTA	64	1

4.2.2 Culturing *Trichoderma* and plant inoculation

Trichoderma asperellum 7316 (MH236427.1, MK411201.1) isolated from arable soils of Telangana region of India was obtained from IIOR, Hyderabad, India. Purified culture of *Trichoderma* streaked from a single spore was maintained on Potato Dextrose Agar (PDA) at 24±2 °C. The media was autoclaved at 121 °C and 15 psi for 15 min before inoculation.

Trichoderma spores were harvested from 7-day old culture by rinsing with sterile water containing 0.02% (v/v) Tween 20 to disperse the spores in the solution. *Trichoderma* inoculum was added to the 14-day-old plant cultures grown in Hoagland's liquid plant growth medium under aseptic conditions following three washes to remove traces of Tween 20. The hydroponic cultures were adjusted to a final concentration of 10^5 germinated spores per ml. Castor plants treated with sterile distilled water alone served as controls. Three biological replicates for each of the treatment were collected at 48 hpi and the root samples were quick-frozen in liquid nitrogen for RNA isolation.

4.2.3 Microscopic examination of *Trichoderma* root colonization

To monitor the growth and colonization of *Trichoderma*, roots of *Trichoderma*-treated castor plants harvested at 48 hpi were stained with trypan blue in lactic acid. Root samples were cleared in 5% potassium hydroxide (KOH), stained in 0.1% trypan blue and stored at room temperature. The root samples were cut longitudinally into one cm-long fragments. The samples were mounted on a clean glass slides containing 20 µL of autoclaved 70% glycerol, covered with a cover slip and observed under the light microscope (Make: Olympus U-Cmad3).

4.2.4 Gene expression profiling using RNA-Seq

4.2.4.1. RNA Isolation

Total RNA was isolated from control and *Trichoderma*-treated castor roots at 12, 24 and 48 hpi. The solutions and buffers were prepared in water pre-treated with 0.1% (v/v) diethylpyrocarbonate (DEPC) overnight and autoclaved at 121 °C at 15 psi for 15 min. 500 mg of root sample was ground to a fine powder in liquid nitrogen using a pestle and mortar. The powdered sample was transferred into 2 mL microcentrifuge tubes containing 1 mL of the Extraction buffer I which was pre-heated at 65 °C. Extraction buffer I comprised of 2% cetyltrimethylammonium bromide (CTAB) (w/v), 2% polyvinylpolypyrrolidone (PVPP) (w/v), 100 mM *tris*(hydroxymethyl)aminomethane (Tris–HCl; pH 8.0), 25 mM ethylenediamine tetra-acetic acid (EDTA; pH, 8.0) and 2 M sodium chloride (NaCl) that were mixed and autoclaved. Beta-mercaptoethanol (2% final concentration) was added just before use. The samples were briefly mixed and incubated at 65 °C for 30 min. 1 mL of chloroform:isoamyl alcohol (24; v:v) was added and the samples were gently mixed and centrifuged at 13,000 rpm for 10 min at room temperature. The supernatant from the tubes was transferred to fresh micro centrifuge tubes. 1 mL of Extraction buffer II comprising of phenol saturated with Tris buffer with pH of 6.7 ± 0.2 (Sigma, USA), sodium dodecyl sulphate (SDS; 0.1% w/v), sodium acetate (NaOAc; 0.32

M) and EDTA (0.01 M. pH 8.0) was added to the above supernatant and vortexed briefly. 200 µL of chloroform was added to the tube, vortexed for a few seconds, and incubated for 15 min at room temperature. The samples were centrifuged at 13,000 rpm for 10 min at 4 °C. The upper aqueous phase was transferred into fresh tubes containing. 0.6 volume of isopropanol and mixed gently and the samples were stored at –80 °C for 15 min. The samples were centrifuged at 13,000 rpm for 10 min at 4 °C. The supernatant was decanted and the RNA pellet was washed with 70% ethanol followed by air drying and suspending in 25 µL of DEPC treated autoclaved water and stored at –80 °C.

4.2.4.2. RNA-Seq library construction

Total RNA of the samples was quantified by Agilent 2100 Bioanalyzer (Agilent Technologies, Palo Alto, CA, USA), NanoDrop (Thermo Fisher Scientific Inc.) and resolution on 1% agarose gel. 1 µg total RNA with RIN value above 7 was used for following library preparation. Next generation sequencing library preparations were constructed using RNA of the castor root samples collected at 48 hpi according to the manufacturer's protocol (NEBNext® UltraTM RNA Library Prep Kit for Illumina®). Total RNA was treated with Oligo (dT) beads (Magnetic mRNA Isolation Kit from NEB, Hyderabad, India) for mRNA enrichment and Ribo-Zero kit (TruSeq Stranded Total RNA with Ribo-Zero Plant from Illumina, San Diego, USA) to remove rRNA from the samples. The double strand cDNA library was prepared through size selection and PCR enrichment. Quality control was evaluated by Qubit 3.0, Agilent 2100 system and Q-PCR and sequenced on Illumina HiSeq 2500 using SBS kit V4 at Nucleome Informatics Ltd., Hyderabad, India.

4.2.5 Read Mapping and data analysis

Raw sequence reads in the FASTQ format were processed to remove Illumina adaptor sequences by Trimmomatic program (Bolger et al., 2014). After filtering approximately 21–25 million paired-reads were retained. The reads were mapped with HISAT2 Once the reads were aligned to the reference genome, the tool feature counts was used to get the total number of reads that were aligned to the reference genes. EdgeR software (Robinson et al., 2010) was used to detect differential expression between the samples. The assembled genes with log fold-change 2 and >2 and the p-adj value lesser than 0.05 were considered to be significant. The enriched genes were then checked for GO enrichments using KOBAS 3.0 (Xie et al., 2011). The differentially expressed genes (DEGs) were detected by pairwise comparison of mRNA transcript abundance levels between *Trichoderma*-treated and control castor roots.

4.2.6 RT-qPCR to confirm putative genes

For validation of gene expression by RT-qPCR, first strand cDNA was synthesized using 2 µg/ µL total RNA per each of the *Trichoderma*-treated and control samples collected at 12, 24 and 48 hpi using cDNA synthesis kit (Takara, Shiga, Japan). Primers were designed by Oligo Analyzer 3.1 bioinformatics tool amplifying short fragments of 100–250 bp. Primers were designed for 9 stress and defense related genes and 2 internal controls; Elongation Factor β1 (*EFB1*) and Actin (*ACT*)) as listed in Table 4.2. The RT-qPCR reaction was performed on 96-well PCR plate on Eppendorf gradient with gene specific primers. The 10 µL reaction mix contained 5.2 µL of 1X SYBR mix, 0.5 µL of 0.25 µM of each primer, 1 µL of 1:20 diluted cDNA and 2.8 µL of water to make up the volume. The cycling conditions used were initial denaturation of 95 °C for 3 min followed by 95 °C for 15 sec, specific annealing temperature for the specific gene for 30 sec, 72 °C for 20 sec followed by 40 cycles of 95 °C for 15 sec, 60 °C for 15 sec. The expression of relative fold change was calculated by 2^-ΔΔCt at (Livak and Schmittgen, 2001).

Table 4.2 The list of primers and internal controls used for quantitative Real Time Polymerase Chain Reaction (RT-qPCR).

S. No.	Gene Name	Primer Sequences (5'to 3')	Amplicon size (bp)
1	Peroxidase 12 (*PER12*)	F: TGAAGCACAAAGCAGACCAC R: ATCGCATCCCATAACAAAGC	181
2	Serine/threonine-protein kinase (*FLS2*)	F: AGAAAAGGCGTCCTTCCCTG R: GTGCTCTGCTAGTGGCTTCAC	179
3	Pathogenesis related protein 5 (*PR5*)	F: ATGCTGCTGTGTTTTCAATC R: GCTTGGATATTGACCGAGTA	133
4	Endoglucanase (*ENDO*)	F: TTTGCCAGTCACAACTACAGGGACG R: GAACACCCTGATAGCCCTCCTGACCA	350
5	Wound induced protein 2 (*WIN2*)	F: CCTAATAACCTATGTTGTAGCCAG R: AGTATTTGTCACCCTCAAGCACT	350
6	WRKY Transcription factor (*WRKY71*)	F: CAAGATGGAGTCTCTACAAGATGA R: ATTGGATTCATACACCTCATAGCAT	172
7	Disease resistance protein (*RPV1*)	F: ATTGAAGAGTCCAAAATCTCAGT R: CCACCCATTCCCCATATTCCAACA	498
8	Zinc finger protein (*ZAT5*)	F: GAAGAAGAGGATATGGCGAAT R: AATGAAAGTGTAGTGTTCGTAT	320
9	Disease resistance protein (*RPS2*)	F: TTGTTAGATGATGTTTGGGAAG R: TCCATTCTTCCTCAGTCTCTTTATT	327
10	Elongation Factor 1B (*EFB1*)	F: GAAAAAGTTGGAGGAGGCAG R: AGGGAGTCCACAGAAACAAG	144
11	Actin (*ACT*)	F: GAGAGGTTCCGGTGCCCAGA R: GGGATGCGAGGATGGATCCTC	450

Statistical analysis was carried using SigmaPlot 11.0 and RT-qPCR was plotted to compare gene expression using student t-test at 12, 24 and 48 hpi. Statistical difference between the time-points displayed at Tukey $p \leq 0.05$. Vertical bars represent ±SE of the mean values.

4.3 RESULTS

4.3.1. Colonization by *Trichoderma* in castor roots

Trichoderma-treated roots of castor were monitored by light microscopy to visualize the colonization of the fungus in the root tissue. Longitudinal sections of root samples taken from *Trichoderma*-treated roots of castor showed both external and internal growth of *Trichoderma*. Trypan blue-stained roots of castor at 48 hpi showed predominant growth of the mycelium and vesicle formation in the root tissue.

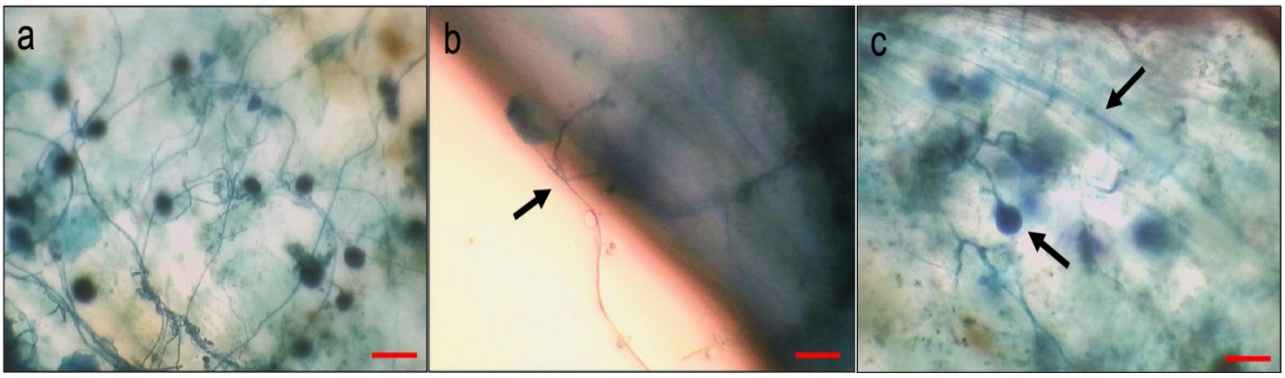


Figure 4.1 Colonization of DCS 107 roots by *Trichoderma asperellum* 7316 observed through light microscopy. A visual representation of fungal growth in trypan-blue stained DCS roots inoculated with *T. asperellum* 7316 at 48 hpi: (a) mycelial spread on the root surface, (b) penetration into the roots and (c) enlargement of hyphal tips into vesicles was observed. Arrows indicate *Trichoderma* colonization in root samples. Scale bar 20 μm.

The microscopic images confirmed complete attachment of the fungal hyphae to the surface of castor (**Figure 4.1**). Along with mycelial spread on the roots surface (**Figure 4.1a**) and penetration into the roots (**Figure 4.1b**), enlargement of hyphal tips into vesicles (**Figure 4.1c**) was observed at 48 hpi indicating intracellular colonization of *Trichoderma*.

4.3.2. Genome-wide mRNA abundance levels in *Trichoderma*-treated castor

To delineate the changes in castor gene expression induced by *Trichoderma* colonization, the transcriptome profiles of castor roots grown in hydroponic cultures treated with and without *Trichoderma* were compared. The differentially expressed genes (DEGs) were detected by pairwise comparison of mRNA transcript abundance levels between *Trichoderma*-treated and control castor roots. The total raw sequences generated by RNA sequencing from both control and *Trichoderma*-treated root samples were estimated to be 21–25 million reads (**Table 4.3**).

Table 4.3 Transcriptome analysis for read counts from *Ricinus communis* –*Trichoderma* interaction.

Sample	Raw reads	Clean reads
Control	25284924.0	24488556.0
Treated	21740846.0	21027788.0
Total	47046770.0	45516344.0

The reads were filtered using stringent parameters and the read map distribution generated by computational analysis is listed in **Table 4.4**. Following the alignment of the sequence reads to the reference genome, the tool feature counts was used to get the total number of reads that were aligned to the reference genes.

Table 4.4 Read mapping distribution in castor (*Ricinus communis* L.) in response to *Trichoderma.*

Sample	PE mapped discordantly uniquely	PE mapped uniquely	PE one mate mapped uniquely	PE neither mate aligned	PE multi-mapped	PE one mate multi-mapped	Overall Mapping %
Control	13 (0.00%)	928 (0.00%)	5429 (0.01%)	24487614 (100.00%)	1 (0.00%)	3767 (0.02%)	0.03%
Treated	23259 (0.11%)	1323041 (6.29%)	836986 (2.13%)	19677721 (93.58%)	3767 (0.02%)	5495 (0.01%)	8.42%

The transcriptome obtained from *Trichoderma*-treated castor plants has been deposited at Gene Expression Omnibus (GEO) GSE198090. A total of 20,696 plant transcripts were detected in the roots of *Trichoderma*-treated castor at 48 hpi. Of these gene transcripts, 1508 differentially expressed genes (DEGs) were detected using DEGSeq software. 474 of these DEGs were found to be upregulated while 1034 DEGs were downregulated with a significant level of expression at $P<0.05$ in *Trichoderma*-treated castor roots. A hierarchical clustering of the DEGs of castor plants was performed as shown in **Figure 4.2**. Gene ontology (GO) analysis is presented as Venn diagrams showing three GO categories; cellular component (CC), biological process (BP) and molecular function (MF) as shown in **Figure 4.3.**

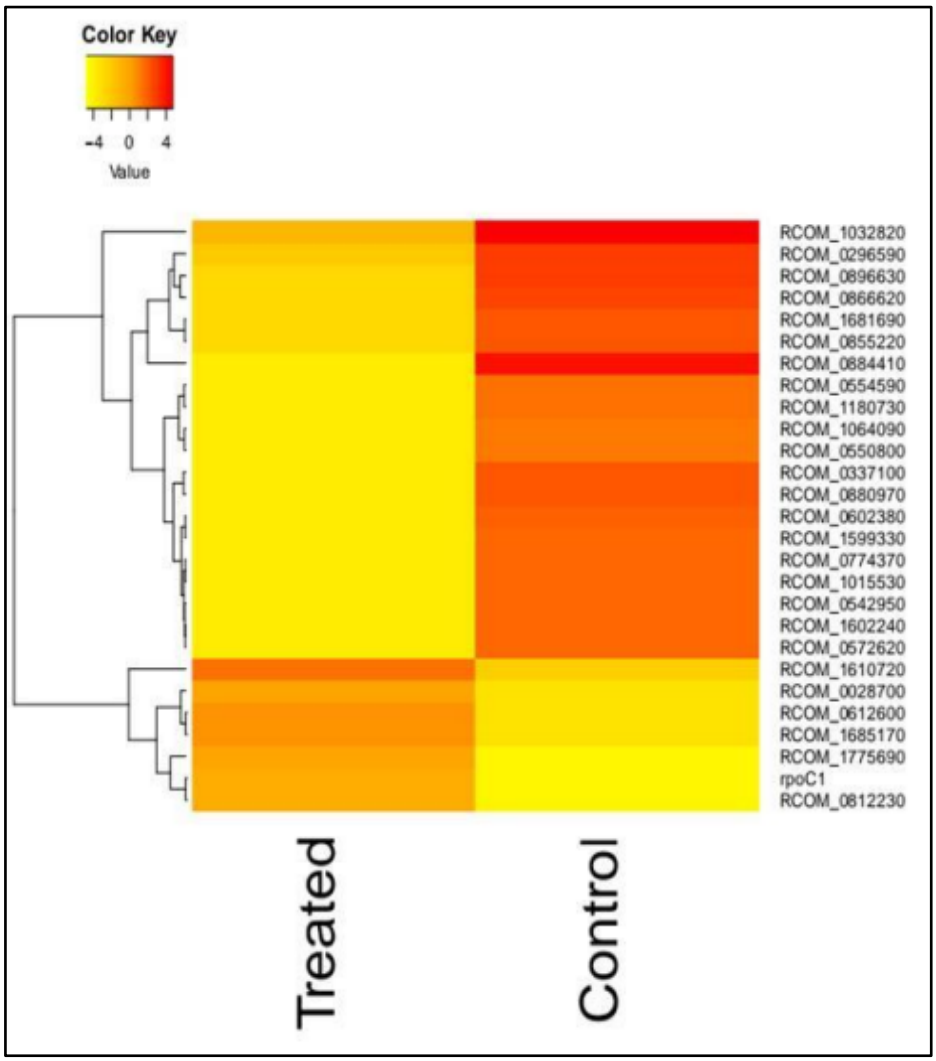


Figure 4.2 Heat map identification of differentially expressed genes across control and *Trichoderma* treated roots of castor at 48hpi. The overall results of hierchial cluster analysis was computed using the log2(FC) value. The colour scale indicates the relative expression levels of all genes in the obtained data. Red colour represents relative increase in abundance, yellow colour represents relative decrease.

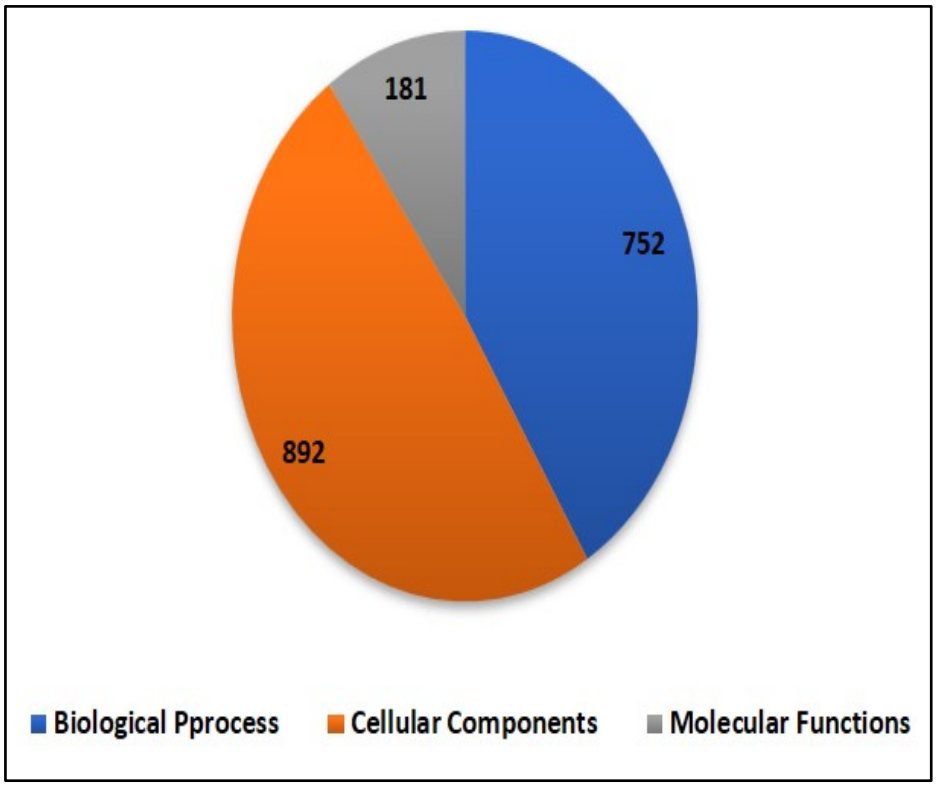
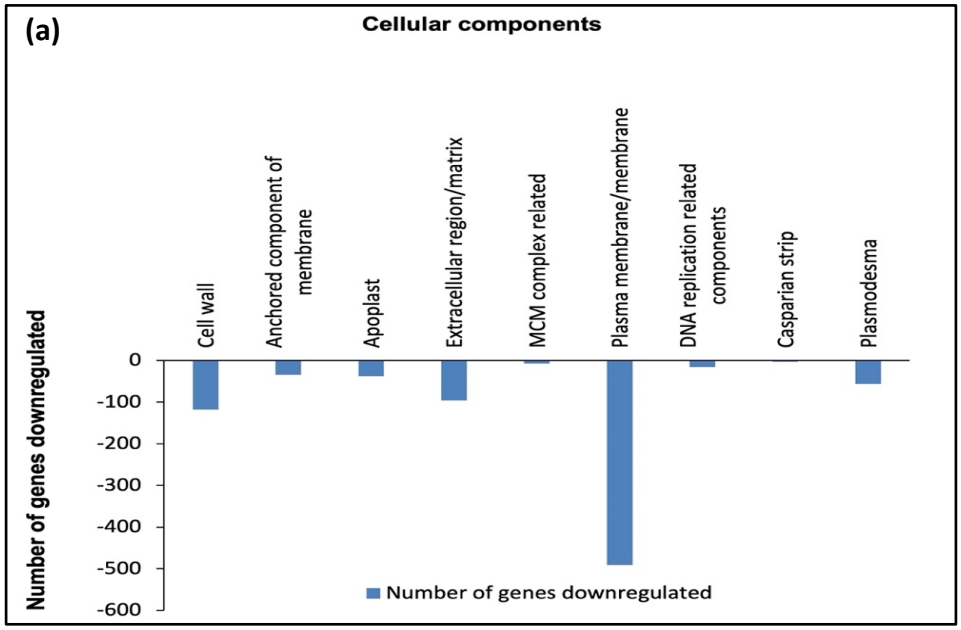


Figure 4.3 Venn diagrams representing the DEGs involved in different gene ontology components detected in *Trichoderma* treated roots of castor DCS-107 at 48hpi. The classification includes three GO categories - cellular component (CC), Biological process (BP) and Molecular function (MF).

GO analysis of plant DEGs in the cellular components (CC) category revealed that a high number of gene transcripts involved in cellular activities which include cell wall or plasma membrane or other membrane formation and transport activity to extracellular region or apoplast were downregulated (**Figure 4.4**). Likewise, the genes with DNA binding transcription factor activity (GO:0003700) and transferase activity (GO:0046527) were found to be downregulated in the category of molecular function (MF). However, both upregulation and downregulation was observed (**Figure 4.5**) for few genes with putative enzymatic roles like hydrolase and oxidoreductase activities along with transmembrane transport suggesting the possibility of multiple isoforms for these genes.



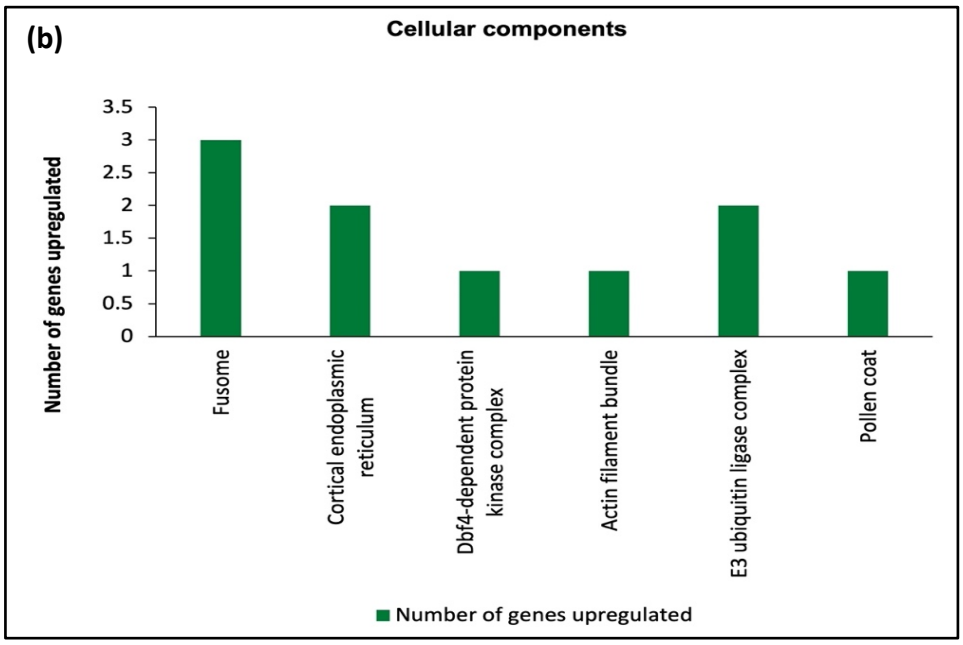


Figure 4.4 Gene enrichment analysis of plant DEGs in DCS-107 by GO term classification –Cellular components:
a – Downregulated,
b - Upregulated.

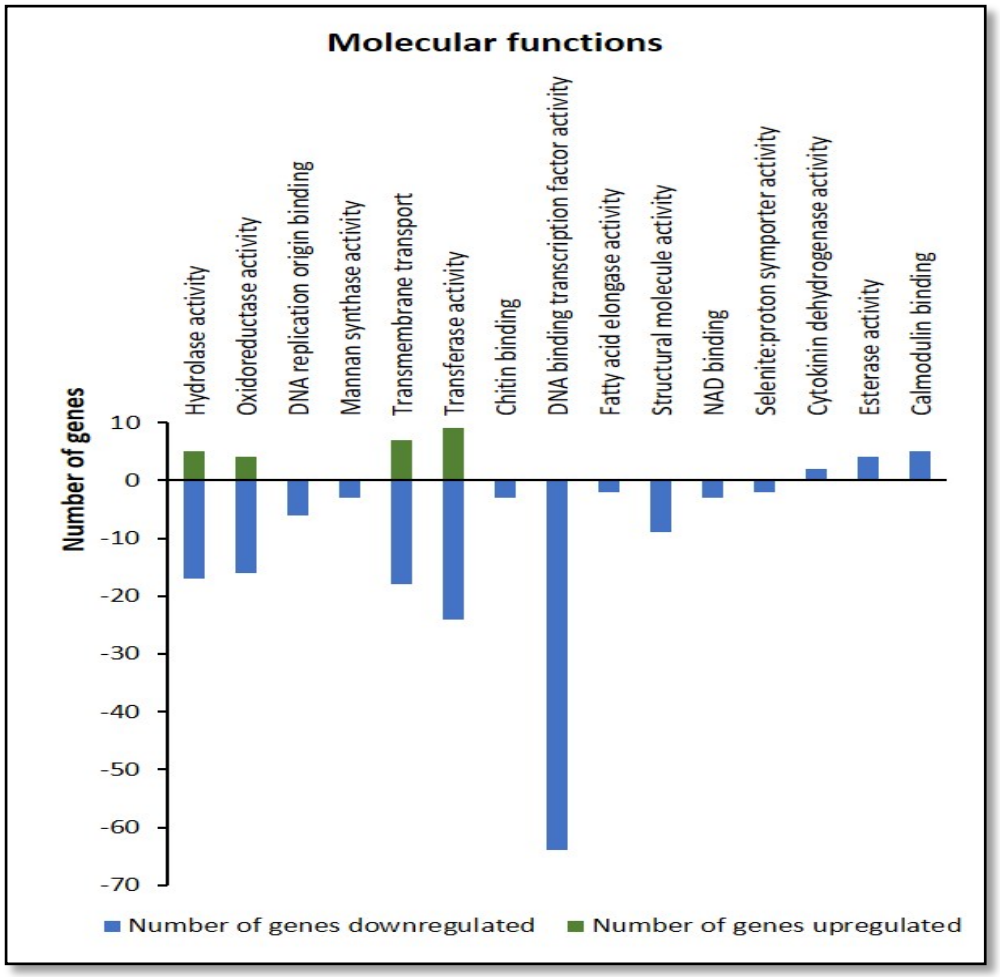


Figure 4.5 Gene enrichment analysis of plant DEGs in 7316 treated roots of castor DCS-107 by GO term classification – Molecular functions.

The number of genes downregulated were found to be greater than the number of genes upregulated in *Trichoderma*-treated castor roots of DCS-107. On the contrary, the mRNA transcripts of genes involved in biological process (BP) category were predominantly upregulated with the highest for cellular responses followed by the genes involved in signal transport (**Figure 4.6**). Whereas, the downregulated DEGs under biological process (BP) category were related to cell component organization, oxidation-reduction process, multicellular organismal process and cytoskeleton organization (**Figure 4.7**). Minimal enrichment with basal expression was observed for the gene transcripts related to response to chitin.

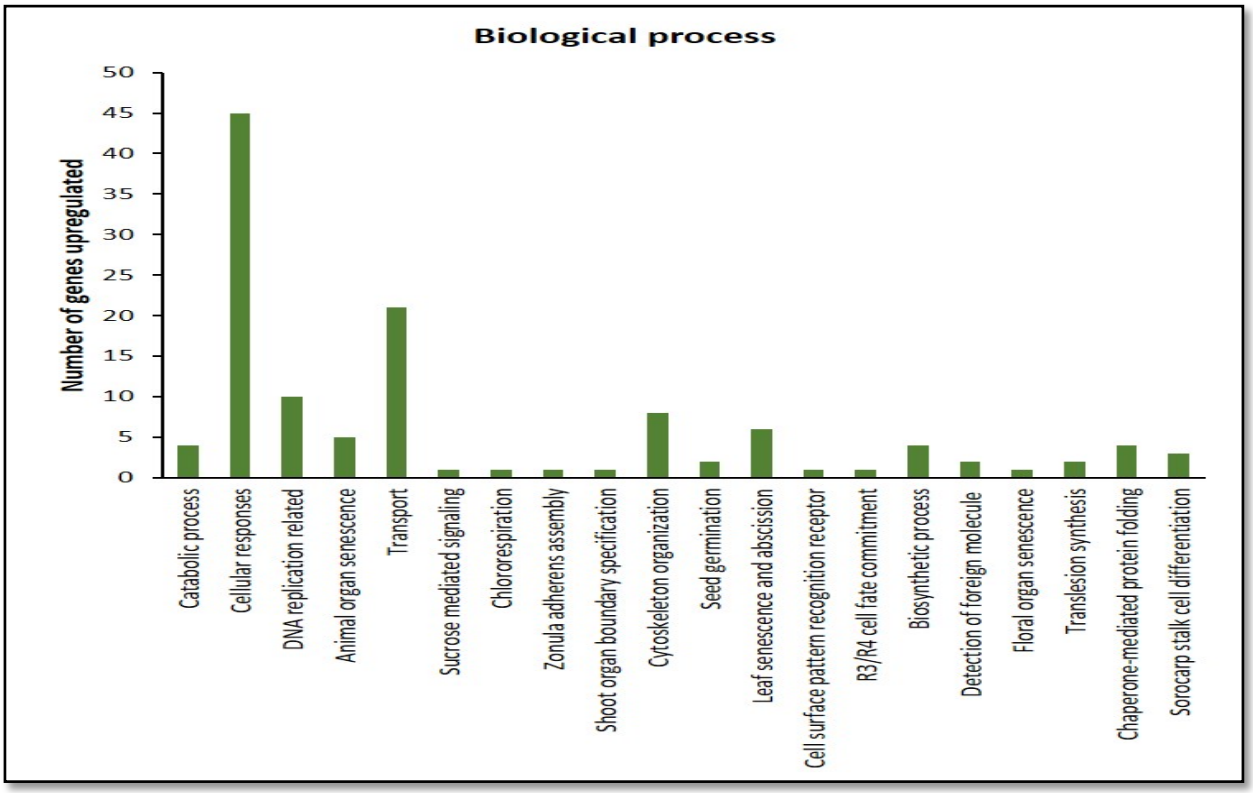


Figure 4.6 Gene enrichment analysis of plant DEGs in 7316 treated roots of castor DCS-107 by GO term classification – Biological process Upregulated genes).

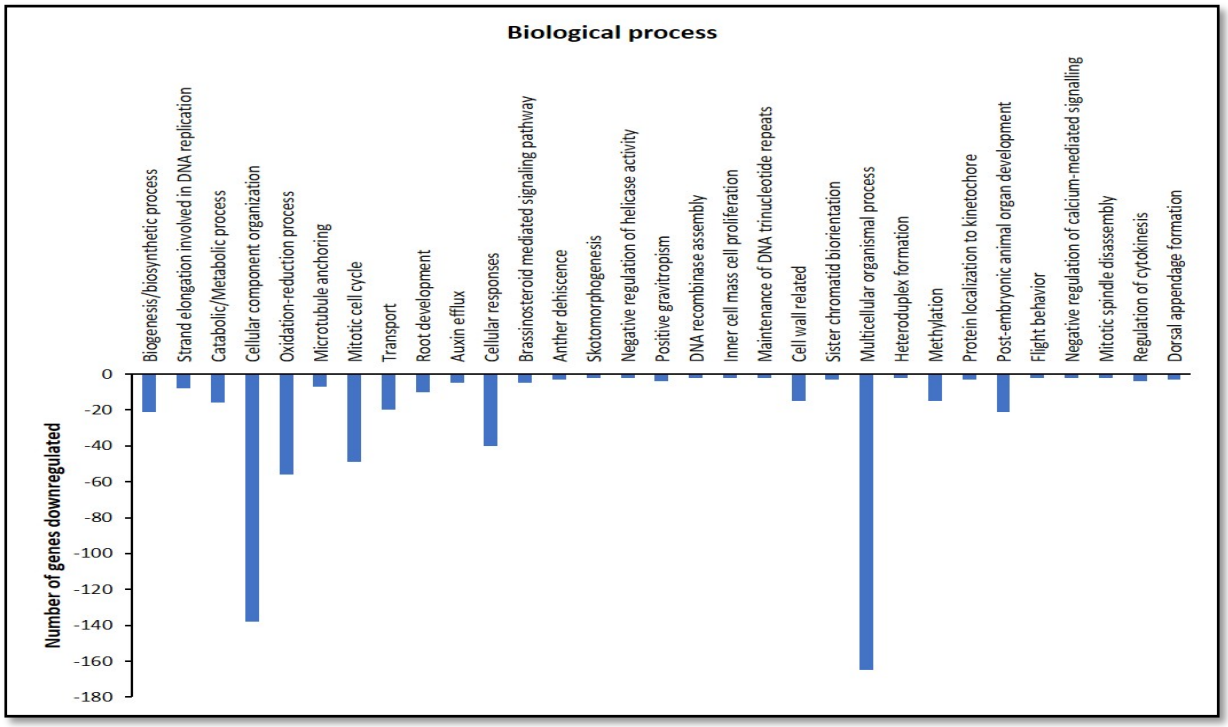


Figure 4.7 Gene enrichment analysis of plant DEGs in 7316 treated roots of castor DCS-107 by GO term classification – Biological process (downregulated genes).

4.3.3. Differential gene expression of castor treated with *Trichoderma* at 48 hpi

The findings from the transcriptome profiling analysis revealed that several of the gene transcripts were downregulated in *Trichoderma*-treated castor roots (**Table 4.5**) compared to the upregulated genes as presented in **Table 4.6**. The gene transcripts that were altered were primarily related to protein kinases with a putative role in recognition and *Trichoderma* colonization. Majority of the DEGs detected in the study are candidate genes that function in stress response, hypersensitive response, ROS changes, phenylpropanoid pathway, secondary metabolite biosynthesis, carbohydrate and amino acid biosynthesis/metabolism, ABC transporters, transcription factors along with proteins involved in electron transport and respiration.

Table 4.5 List of plant gene transcripts down regulated in the roots of castor DCS-107 in response to *T. asperellum 7316* at 48hpi.

Transcript ID	Predicted protein function (Transcript annotation)	logFC
Protein kinases		
RCOM_1593890	Probable serine/threonine protein kinase IRE4	-9.68
RCOM_0807920	MAP3K epsilon protein kinase 1	-8.97
RCOM_1340560	Serine/threonine-protein kinase ATG1a	-8.96
RCOM_1494420	Proline-rich receptor-like protein kinase PERK15	-8.73
RCOM_0906180	Cysteine-rich repeat secretory protein 38-like	-8.14
RCOM_0126270	Serine Threonine protein kinase	-7.95
RCOM_1355230	Phosphoglycerate kinase	-7.91
RCOM_0654970	Casein kinase 1-like protein 2	-7.87
RCOM_0906170	Cysteine-rich receptor-like protein kinase 44	-7.82
RCOM_0811450	Receptor protein kinase-like protein At4g34220	-7.82
RCOM_0912240	Probable serine/threonine-protein kinase WNK9	-7.48
RCOM_0901470	Serine threonine protein kinase bri1/*R*eceptor-like protein 15	-7.37
RCOM_1432170	Serine/threonine-protein kinase ZRK1	-7.31
XP_015574890.1	Glycogen recognition site of AMP-activated protein kinase	-7.18
-3.271728098	Leucine-rich repeat receptor-like tyrosine-protein kinase PXC3	-7.18
RCOM_1684990	Probable serine/threonine-protein kinase SIS8	-7.11
RCOM_0913550	Somatic embryogenesis receptor kinase 1	-6.70
RCOM_1050860	Protein phosphatase 2C and cyclic nucleotide-binding/kinase domain containing protein	-6.60
XP_015573292.1	Serine threonine-protein kinase	-6.60
RCOM_0295930	Probable inactive receptor kinase At5g58300	-6.49
RCOM_1602240	Cyclin-dependent kinase B2-2	-4.98
RCOM_0920850	Early nodulin-like protein 1	-4.70
RCOM_1340570	Probable inactive receptor-like protein kinase At2g46850	-3.57
RCOM_1022390	Leucine-rich repeat receptor protein kinase EXS, putative	-3.56
RCOM_1596350	LRR receptor-like serine/threonine-protein kinase SIK1	-3.52
RCOM_1080800	Serine/threonine-protein kinase bri1/receptor-like protein EBX1	-3.32
RCOM_1371710	Receptor-like protein 14	-3.32
RCOM_1310170	Probable leucine-rich repeat receptor-like protein kinase At1668400	-3.29
RCOM_1768760	Serine threonine-protein kinase SAPK7	-3.27

RCOM_0988670	Serine threonine-protein kinase AGC1-7	-3.17
RCOM_2139480	Receptor-like kinase TMK4	-3.09
RCOM_0712120	MOB kinase activator-like 1A	-3.09
RCOM_1486440	LRR receptor-like serine/threonine-protein kinase At1g51860	-3.08
RCOM_0779050	FLS2/53	-3.01
RCOM_0610070	Leucine-rich repeat receptor-like protein kinase PXL1	-3.0
RCOM_0052400	Receptor protein kinase TMK1	-3.0
RCOM_0853370	Serine/threonine-protein kinase D6PKL2	-2.93
RCOM_1454170	Serine/threonine-protein kinase	-2.91
RCOM_1442820	Leucine-rich repeat receptor protein kinase EXS, putative	-2.81
RCOM_1250190	Receptor-like protein 51	-2.76
RCOM_1333310	Probable LRR receptor-like serine/threonine-protein kinase At3g47570	-2.66
RCOM_1721670	LRR receptor-like serine/threonine-protein kinase RGI2	-2.56
RCOM_1509620	Leucine-rich repeat receptor-like serine/threonine-protein kinase RGI4	-2.55
RCOM_0797340	Probable leucine-rich repeat receptor-like protein kinase At1g68400	-2.50
RCOM_0647000	LRR receptor-like serine/threonine-protein kinase ERL2	-2.46
RCOM_0687670	Nodulation receptor kinase precursor	-2.39
RCOM_2032810	Leucine-rich repeat receptor-like protein kinase	-2.34
RCOM_1427830	Serine/threonine-protein kinase Nek1	-2.30
RCOM_0840960	Leucine-rich repeat receptor-like protein kinase PXC1	-2.20
RCOM_0848330	Systemin receptor SR160/ Probably inactive leucine- rich repeat receptor-like protein kinase IMK2 isoform X2	-2.23
RCOM_0814340	Leucine-rich repeat receptor-like serine/threonine kinase At1g60630	-2.17
RCOM_0799040	Serine/threonine-protein kinase Aurora-2	-2.17
ROS related proteins		
RCOM_0923970	Putative L-ascorbate peroxidase 6	-7.78
RCOM_0172310	Peroxidase 16	-7.74
RCOM_0635750	Flavonol synthase/flavanone 3-hydroxylase, putative / protein SRG1	-7.24
RCOM_0903900	Putative uncharacterized protein	-7.11
RCOM_0647160	Laccase	-7.11
RCOM_1433130	Respiratory burst oxidase homolog protein B	-6.96
RCOM_0774370	Lignin forming anionic Peroxidase	-5.20
RCOM_0602380	L-ascorbate oxidase	4.98
RCOM_0296590	Peroxidase 12	-4.92
RCOM_1600150	L-ascorbate oxidase	-4.23
RCOM_0774380	Lignin forming anionic Peroxidase	-4.19
RCOM_0414390	Peroxidase 57, putative/ Probable peroxidase 61	-3.86
RCOM_0296870	Laccase 9	-3.29
RCOM_0647190	Laccase 21	-3.25
RCOM_0687550	Laccase 12	-2.50
RCOM_0562170	Putative uncharacterized protein	-2.50
RCOM_1278030	Peroxidase 20	-2.48
RCOM_0231780	Peroxidase 27	-2.39
RCOM_0808690	Peroxidase 50Peroxidase 50 [Ricinus communis]- 100% identity- NCBI	-2.32
RCOM_0138860	Peroxidase 43 precursor, putative	-2.32
RCOM_0896640	Putative uncharacterized protein	-2.33
RCOM_1464960	Peroxidase 11	-2.25
RCOM_1402420	Laccase 13	-2.25
Defence response		
RCOM_1595930	Jacalin-related lectin 3	-11.06
RCOM_0658810	Trigalactosyldiacylglycerol 4	-9.03
RCOM_1383950	Serine carboxypeptidase	-9.03
RCOM_0337100	Thaumatin-like protein	-8.80
RCOM_0628760	Unannotated/ hypothetical protein	-7.59
RCOM_2159030	Elongation factor 1-alpha	-7.10

RCOM_1450190	Endoglucanase 24	-7.17
RCOM_0446390	Thaumatin-like protein 1	-3.64
RCOM_0896630	Gibberellin 20 oxidase, putative	-5.30
RCOM_1179080	Endoglucanase 17	-3.60
RCOM_0999860	Chitinase-like protein 2	-3.49
RCOM_1348140	Endoglucanase 25	-3.32
RCOM_1383810	Serine carboxypeptidase-like 2	-2.94
RCOM_1593590	Pathogenesis-related protein 5, Zeamatin precursor, putative	-2.81
RCOM_0484460	Wound-induced protein WIN2	-2.81
RCOM_1383690	Serine carboxypeptidase	-2.66
RCOM_1633620	Serine carboxypeptidase-like 45-like	-2.46
RCOM_1440410	Chitinase 2	-2.32
RCOM_0137950	Putative uncharacterized protein	-2.29
Phenylpropanoid metabolism		
RCOM_1299060	ATRAD3, putative/ Probable methyltransferase At1g29790	-8.20
RCOM_1616760	Probable methyltransferase At1g29790	-7.95
RCOM_0154700	tRNA (uracil-5-)-methyltransferase	-7.31
RCOM_0308380	O-methyltransferase, putative/ PREDICTED: *Ricinus communis* probable caffeine synthase MTL2	-7.03
RCOM_0938330	S-adenosylmethionine-dependent methyltransferase, putative /PREDICTED:*Ricinus communis* EEF1A lysine methyltransferase 4	-6.96
RCOM_0161380	Phosphomethylethanolamine N-methyltransferase isoform X2	-4.70
RCOM_1015530	Trans-resveratrol di-O-methyltransferase	-3.69
RCOM_0854630	Arginine methyltransferase NDUFAF7 homolog	-3.36
RCOM_1266090	Probable methyltransferase PMT19	-3.32
RCOM_1410160	Caffeoyl-CoA O-methyltransferase	-2.39
RCOM_0554590	Trans-resveratrol di-O-methyltransferase	-2.44
Secondary metabolite Biosynthesis		
RCOM_0896400	Probable 2-oxoglutarate-dependent dioxygenase AOP1	-7.48
RCOM_0866620	Probable terpene synthase 8	-5.01
RCOM_0306870	Ent-kaurene synthase B, chloroplast precursor, putative	-4.81
RCOM_1447050	Omega-hydroxypalmitate O-feruloyl transferase Anthranilate N-benzoyltransferase protein, putative	-3.14
RCOM_1045160	Probable terpene synthase 3	-3.04
RCOM_0823080	Ent-kaurene synthase B, chloroplast precursor, putative	-2.81
Cell wall modifications		
RCOM_0342250	Expansin-A1 or A10 or A15	-7.03
RCOM_1599330	Expansin A11	-4.62
RCOM_0550800	Protein IRX15-like	-4.46
RCOM_0184760	Pectinesterase	-4.10
RCOM_1500020	Pctinesterase inhibitor 4	-3.91
RCOM_1443780	Xyloglucan endotransglucosylase/hydrolase protein A precursor,	-3.83
RCOM_1194430	Xyloglucan endotransglucosylase/hydrolase 2	-3.44
RCOM_1541960	Probable pectinesterase/pectinesterase inhibitor 25	-3.32
RCOM_1179070	Pectinesterase	-3.32
RCOM_0708470	Probable pectinesterase/pectinesterase inhibitor 12	-3.09
RCOM_1003640	Pectinesterase	-2.73
RCOM_0299440	Casparian strip membrane protein 5	-2.72
RCOM_1773310	Putative uncharacterized protein	-2.64
RCOM_0417480	Pectinesterase	-2.51
RCOM_0635740	Xyloglucan endotransglucosylase/hydrolase 2/REPEAT	-2.32
RCOM_1565850	Expansin-A20	-2.25
RCOM_1438910	Xyloglucan endotransglucosylase/hydrolase 2/ REPEAT	-2.10
RCOM_1259260	Casparian strip membrane protein 2	-2.07
Signal transduction		
RCOM_0258090	Transferrin, putative	11.54

RCOM_0884410	Phosphoprotein phosphatase OR Disease resistance protein RPV1	11.54
RCOM_0884420	TIR domain containing protein	11.54
RCOM_1509380	Disease resistance protein RPP13, putative	10.55
Carbohydrate Biosynthesis/ metabolism		
RCOM_0542950	Cellulose synthase A catalytic subunit 6	-5.01
RCOM_0381780	Glucomannan 4-beta-mannosyltransferase	-3.80
RCOM_1180270	Cellulose synthase A catalytic subunit 3	-2.81
RCOM_1443660	Glyceraldehyde-3-phosphate dehydrogenase A	-2.18
RCOM_1186280	Glucomannan 4-beta-mannosyltransferase 2	-2.03
Nitrogen metabolism		
RCOM_1032820	Nitrate reductase	-5.63
Amino acid biosynthesis and metabolism		
RCOM_0907360	Arginine decarboxylase, putative	-8.24
RCOM_0592860	Anthranilate synthase alpha subunit 1	-3.46
RCOM_1445440	Aspartokinase 2	-2.36
Electron transport and membrane associated energy conservation/respiration		
RCOM_1084110	Cytochrome P450 71B2	-3.19
RCOM_1617460	Flavonoid 3-hydroxylase/cytochrome P450 CYP736A12	-3.09
RCOM_0405390	CYP93A1-3,9-dihydroxypterocarpan 6A-monooxygenase	-2.75
RCOM_0792010	Cytochrome P450 94C1	-2.58
RCOM_0585670	Cytochrome P450 716B1	-2.49
RCOM_1684620	Cytochrome P450 87A3	-2.46
RCOM_1376710	Cytochrome P450 86B1	-2.41
RCOM_0144700	Cytochrome P450 78A9	-2.30
RCOM_0841220	Cytochrome P450 76A1	-2.27
RCOM_1517630	cytochrome P450 89A2	-2.18
RCOM_1212380	Cytochrome P450 724B1	-2.11
ABC Transporters		
XP_025014341.1	ABC transporter G family member	-6.70
RCOM_0853020	ABC transporter B family member 15-like	-4.09
RCOM_0422670	ABC transporter G family member 22 isoform X1	-3.84
RCOM_0925270	ABC transporter G family member 32	-2.58
RCOM_1581560	ABC transporter G family member 8	-2.29
Transcription factors		
RCOM_1467110	Transcription factor *BIM1*, putative	-9.19
RCOM_0836650	Myb family transcription factor *PHL8*	-7.48
RCOM_0528090	Transcription factor *bHLH90*	-6.96
RCOM_1609660	GATA transcription factor 4	-4.13
RCOM_1586090	*Ricinus communis* transcription factor *bHLH74*	-3.27

Table 4.6 List of plant gene transcripts upregulated in the roots of castor DCS-107 in response to *T. asperellum 7316* at 48hpi.

Transcript ID	Predicted protein function (Transcript annotation)	logFC
Protein kinases		
RCOM_0815420	Probable serine/threonine-protein kinase WNK4	11.12
RCOM_0606150	Integrin-linked protein kinase 1	10.81
RCOM_1444750	Proline-rich receptor-like protein kinase PERK8	10.67
RCOM_1508280	Serine threonine-protein kinase	10.10
RCOM_0897280	Serine-threonine kinase receptor-associated protein	9.71
RCOM_1046950	Receptor-like serine threonine-protein kinase	9.44
RCOM_1267360	PTI1-like tyrosine-protein kinase 3	8.88
RCOM_0912240	Probable serine/threonine-protein kinase WNK9	8.56
RCOM_0546030	Leaf rust 10 disease-resistance locus receptor-like protein kinase-like 2.4	8.52
RCOM_0020950	Receptor-like cytosolic serine/threonine-protein kinase RBK1	8.32
RCOM_1173500	Checkpoint serine threonine-protein kinase	7.92
RCOM_1355230	Phosphoglycerate kinase	7.67
RCOM_1593890	Probable serine/threonine protein kinase IRE4	7.67
RCOM_0906040	Cysteine-rich receptor-like protein kinase 10	7.53
RCOM_1000600	Mitogen-activated protein kinase kinase kinase dlk-1	7.28
RCOM_0260330	Serine-threonine protein kinase 19	6.98
RCOM_1382770	Inositol-tetrakisphosphate 1-kinase 3	6.74
RCOM_1115620	LysM domain receptor-like kinase 3	3.79
RCOM_0646260	Serine/threonine-protein kinase STY13	2.78
RCOM_0206530	LRR receptor-like serine threonine-protein kinase 9DC3	3.40
RCOM_0905280	Probable serine/threonine-protein kinase PBL23 isoform X1	2.58
RCOM_0206830	Serine threonine-protein kinase	2.51
RCOM_1313140	Serine/threonine-protein kinase BLUS1	2.10
Cellular metabolism and homeostasis		
RCOM_0689940	Glycerol-3-phosphate dehydrogenase NAD(+) 2	9.25
RCOM_0574830	Probable glutathione peroxidase 2	9.22
RCOM_0923970	L-ascorbate peroxidase 6	8.18
RCOM_0819930	Glutathione S-transferase L3	7.80
RCOM_0259060	Glutathione gamma-glutamylcysteinyltransferase 1	7.28
RCOM_0550810	Probable 2-oxoglutarate-dependent dioxygenase At3g50210	7.28
RCOM_1685170	Peroxidase 5	3.17
RCOM_1232030	Cationic peroxidase 1	2.83
RCOM_0584650	1-acyl-sn-glycerol-3-phosphate acyltransferase	2.81
Phosphate transport		
RCOM_1342130	Protein phosphatase 2C	8.08
RCOM_1019210	Purple acid phosphatase	7.73
RCOM_1534250	Probable protein phosphatase 2C 8	7.60
RCOM_1355010	Acyl phosphatase	7.36
RCOM_0812230	Putative Protein phosphatase	3.00
RCOM_1602550	PhoD-like phosphatase	2.97
Metal ion transport and xenobiotics		
RCOM_1339960	Metal tolerance protein 1	8.66
RCOM_0632940	Potassium channel KAT2	8.66
RCOM_1352230	Cytochrome P450	8.66
RCOM_0707470	Copper-transporting ATPase Paa1 or Paa2	8.62
RCOM_0705970	Cytochrome P450 711A1	2.35
RCOM_0297800	Cytochrome P450 78A7	2.32

Plant growth promotion		
RCOM_1129090	YTH domain-containing protein ECT4	10.33
RCOM_0608010	GRF1-interacting factor 1	9.08
RCOM_0393280	WAT1-related protein At3g28050-like	8.66
RCOM_0393170	WAT1-related protein At4g15540	7.60
RCOM_1582420	Probable polygalacturonase	6.74
Stress responses		
RCOM_1595930	Jacalin-like lectin domain	11.42
RCOM_1037890	RING-H2 finger protein ATL11	9.48
RCOM_0304730	Nudix hydrolase 2	9.08
RCOM_1036630	F-box protein FBW2	7.28
RCOM_0550810	Ferrous ascorbate-dependent oxidoreductase family	7.28
RCOM_0572790	Receptor homology region, transmembrane domain- and RING domain-containing protein 1	6.86
RCOM_1615660	Protein of the SKP1 family	6.74
RCOM_0458380	UDP-glycosyltransferase 73C3	3.10
RCOM_1615660	SKP1-like protein 21	2.86
RCOM_0458380	UDP-glycosyltransferase 73C25	2.60
RCOM_0788110	RING-H2 finger protein ATL66	2.30
RCOM_0472870	UDP-glycosyltransferase 86A2	2.00
Defense responses		
RCOM_1514730	F-box/kelch-repeat protein At1g74510	8.88
RCOM_0812210	Disease resistance protein RPV1	7.28
RCOM_1383950	Serine carboxypeptidase-like 18	7.18
RCOM_2050290	Cold-regulated 413 plasma membrane protein 2	7.08
RCOM_0390850	TPL-binding domain in jasmonate signalling	7.08
RCOM_0697780	SNF1-related protein kinase regulatory subunit gamma-1-like	6.67
RCOM_0812230	Disease resistance protein RPS2	3.00
RCOM_1353410	Zinc finger protein ZAT5	2.60
Secondary metabolite synthesis		
RCOM_1034960	S-adenosylmethionine-dependent methyltransferase	8.76
RCOM_0160690	Probable methyltransferase PMT7	7.67
RCOM_0859900	Squalene monooxygenase SE1	7.44
RCOM_1063380	DNA (cytosine-5)-methyltransferase DRM2	7.52
RCOM_1171020	Probable O-methyltransferase 3	2.10
RCOM_0004120	Limonene synthase/probable terpene synthase 9	2.00
Molecular Chaperones		
RCOM_0569180	Hsc70-interacting protein, putative	9.64
RCOM_0663360	Peptidyl-prolyl cis-trans isomerase CYP37	6.98
RCOM_1039200	Universal stress protein PHOS34	6.98
RCOM_0850710	Peptidyl-prolyl cis-trans isomerase CYP38, chloroplast	6.86
RCOM_0547660	Bacterial trigger factor protein (TF)	6.86
Nucleic acid synthesis and modelling		
RCOM_0854630	Arginine methyltransferase NDUFAF7	8.18
RCOM_0500140	Putative lysine-specific demethylase JMJ16	8.03
RCOM_1593990	Deoxyuridine 5'-triphosphate nucleotidohydrolase	3.80
RCOM_1432610	Lysine-specific demethylase JMJ25	3.65
Carbohydrate and starch metabolism		
RCOM_1018060	Beta-galactosidase	11.38
RCOM_0831760	Probable glucan 1,3-beta-glucosidase A	7.18
RCOM_1177990	Beta-glucosidase 11	2.87
RCOM_0711410	Beta-galactosidase 15	2.30
RCOM_0526780	Alpha-amylase	2.24
Lipid and fatty acid synthesis and metabolism		
RCOM_0511110	Putative BPI/LBP family protein At1g04970	9.36

RCOM_0614020	Phosphatidylinositol-glycan biosynthesis class X	9.30
RCOM_0653990	Phospholipid:diacylglycerol acyltransferase 1	8.70
RCOM_1614440	Acyl-coenzyme A thioesterase 13	8.27
RCOM_1478210	Phospholipase A22	7.44
RCOM_1047790	Acyl- acyl-carrier-protein --UDP-N-acetylglucosamine O-acyltransferase	6.70
RCOM_1347470	Phospholipase A1 PLIP2	6.74
RCOM_1027640	TLC domain-containing protein 4-B	3.65
Amino acid Biosynthesis and metabolism		
RCOM_1579610	Glutamate synthase (NADH)	11.67
RCOM_1435660	Xaa-Pro aminopeptidase 3/intermediate cleaving peptidase 55, mitochondrial	9.40
RCOM_0611460	Phosphomethylpyrimidine synthase	8.76
RCOM_0907360	Arginine decarboxylase	8.32
RCOM_0904170	5'-adenylylsulfate reductase	7.08
RCOM_0321500	Thiamine biosynthetic bifunctional enzyme TH1	3.04
Electron transport, energy conservation & respiration		
RCOM_0689940	Glycerol-3-phosphate dehydrogenase NAD(+)	9.25
RCOM_2104740	NADH dehydrogenase (quinone) activity	6.60
RCOM_0028700	NADP-dependent glyceraldehyde-3-phosphate dehydrogenase	2.90
Transcription factors		
RCOM_1282600	Transcription factor *E2FB*	9.88
RCOM_0558970	Transcription factor *LRL1*	8.70
RCOM_0837230	Agamous-like MADS-box protein *AGL30*	8.52
RCOM_0339020	MADS-box protein *AGL29*	8.08
RCOM_1492980	Transcription factor *bHLH68*	7.36
RCOM_1315820	Probable transcription factor *KAN2*	7.28
RCOM_1436840	Transcription factor *PIF3*	3.54
RCOM_1211150	Transcription elongation factor s-II (*TFIIS*)	2.80
RCOM_0921060	WRKY transcription factor, *WRKY71*/ WRKY transcription factor,*WRKY40*	2.30
RCOM_0921060	WRKY transcription factor, *WRKY55*	2.30
RCOM_1211150	Transcription elongation factor, *ELF*	2.30
XP_025014933.1	Myb-like DNA-binding domain	2.30
RCOM_0937560	Transcription factor, G-box-binding factor	2.30

4.3.4. Detection of putative genes in castor in response to *Trichoderma*

4.3.4.1. Putative kinase and hypersensitive response genes in *Trichoderma*-treated castor

Out of an estimated number of 50 downregulated putative kinase genes, three genes-serine/threonine protein kinase IRE4, MAP3K epsilon protein kinase1 and Serine/threonine-protein kinase ATG1a were predominantly downregulated with a fold-change expression of -9.68, -8.97 and -8.96 respectively. A candidate stress responsive factor, Flavonol synthase/flavanone 3-hydroxylase gene was also found to be significantly downregulated (-7.24 fold-change) compared to control suggesting that the *Trichoderma* colonization negates inflammatory or hypersensitive responses in castor.

Similarly genes involved in reactive oxygen species (ROS) generation were found to be significantly downregulated which include; Putative L-ascorbate peroxidase 6, Peroxidase 16, Respiratory burst oxidase homolog protein B, Peroxidase 12 (with a fold-change of -7.78, -7.74, -6.96 and -4.92 respectively). Gene expression of two lignin forming peroxidases and 8 other Class III peroxidases were seen to be downregulated. Peroxidase 12, Peroxidase 57 and Peroxidase 20 were found to be downregulated with a fold change expression of -4.92, -3.86 and -2.48 fold respectively. Similar to the peroxidases, laccases were also found to be downregulated.

In addition, mRNA abundance levels of defense response genes- Jacalin-related lectin 3 with a fold-change of -11.06, Trigalactosyldiacylglycerol 4 and Serine carboxypeptidase with fold-change of -9.03 each were observed to be significantly lower compared to the control. Furthermore, pathogenesis-related proteins like Thaumatin-like protein (-8.80), Thaumatin-like protein 1 (-3.64) Endoglucanase 24 (-7.17), Endoglucanase 17 (-3.60), Endoglucanase 25 (-3.32) Pathogenesis-related protein 5 (-2.81) and Wound-induced protein WIN2 (-2.81) were significantly downregulated in *Trichoderma*-treated castor confirming restraining of these genes with a role in antimicrobial protein expression.

Likewise, a minimum of 11 gene transcripts with probable role as methyl transferases were found to be significantly downregulated with a fold change of -8.20 to -2.44 in *Trichoderma*-treated root sample compared to control. A few of the ABC transporter members of G and B classes and transcription factors with putative role in defense against pathogens were found to be significantly downregulated suggesting that the host favours *Trichoderma* colonization in the roots by negatively regulating plant defense responses.

Further, the putative transcription factors which include; putative transcription factor BIM1, myb family transcription factor PHL8, transcription factor bHLH90, GATA transcription factor 4 and transcription factor bHLH74 with putative roles in brassinosteroid signaling and response to biotic and abiotic stresses were found to be down regulated suggesting that *Trichoderma*-treatment is perceived as non-pathogenic or non-alarming biocontrol agent (BCA) by the host.

4.3.5. Gene transcripts upregulated in DCS-107 in response to *Trichoderma*

4.3.5.1. Upregulation of gene transcripts involved in cellular metabolism and detoxification

The mRNA transcripts of Glycerol-3-phosphate dehydrogenase NAD(+) 2 gene with a putative role in glycolysis and homeostasis was observed to be highly expressed with a fold-change of 9.25 followed by the probable glutathione peroxidase 2 gene with 9.22 fold-change expression level in response to *Trichoderma* indicating enhanced cellular metabolism and energy production. The gene transcripts of Glutathione S-transferase L3 (7.8 fold-change) indicated enhanced cellular metabolism as well as in the detoxification of a wide variety of xenobiotic compounds produced in response to *Trichoderma*. Likewise, mRNA transcripts of few of the peroxidases which include L-ascorbate peroxidase 6, Peroxidase 5, Cationic peroxidase 1 (8.18, 3.17 and 2.83 fold-change) were upregulated as a natural response against an invading organism to minimise cell damage caused due to ROS accumulation. The mRNA abundance levels of a probable 2-oxoglutarate-dependent dioxygenase was observed to be 7.28 fold-change higher compared to control indicating its role in phytohormone and secondary metabolite synthesis in response to *Trichoderma*.

4.3.5.2. Upregulated putative receptor-like kinases and resistance genes in castor

Among the mRNA transcripts with abundance, the gene transcripts of putative receptors with a role in extracellular recognition were found to significantly higher in *Trichoderma*-treated castor compared to control plants. The probable serine/threonine-protein kinase *WNK4* showed highest fold change expression (11.12) and is reported to play a role in diverse ion transport pathways in plants. The mRNA transcripts accumulation of integrin-linked protein kinase 1 gene with a putative role in root elongation and gravitropism was detected with a high fold-change of 10.81. Likewise, a proline-rich receptor-like protein kinase PERK8 with a fold-change expression of 10.67 was observed with a putative role in pollen development, increased lateral shoot production and seed set in plants.

The mRNA abundance levels of cysteine-rich receptor-like protein kinase 10 (*CRK*) was observed to be 7.53 fold higher in *Trichoderma*-treated plants compared to control suggesting its unique role in symbiosis of arbuscular mycorrhiza and rhizobia association in plants. The mRNA transcripts of mitogen-activated protein kinase kinase kinase dlk-1 gene, a prime component in protein phosphorylation and signal transduction was observed with a 7.28 fold-change to affect coordinated intracellular responses. Another receptor, inositol-

tetrakisphosphate 1-kinase 3 with a 6.74 fold-change expression was recorded with a role in signal transduction in mediating host responses. The receptor gene, LysM domain receptor-like kinase 3 was upregulated (3.79 fold-change) in response to *Trichoderma*, suggesting it as a candidate in mediating symbiosis establishment in castor.

4.3.5.3. Upregulation of genes involved in stress responses and defense signaling

The putative gene, Jacalin-like lectin domain was up regulated with 11.42 fold-change in castor in response to *Trichoderma* with a putative role in plant growth regulation and signaling. Similarly putative RING-H2 finger protein ATL11, Receptor homology region, transmembrane domain- and RING domain-containing protein 1 and RING-H2 finger protein ATL66 (9.48, 6.86 and 2.3 fold-change respectively) were upregulated along with a candidate Nudix hydrolase 2 gene (9.08 fold-change) confirming their role in housecleaning to maintain cellular homeostasis of the host. Further, a putative enzyme belonging to the ferrous ascorbate-dependent oxidoreductase family was 7.28 fold-change upregulated which plays a role in reactive oxygen species (ROS) scavenging to maintain the cellular homeostasis. An F-box protein FBW2 (7.28 fold-change), protein of the SKP1 family (6.74), SNF1-related protein kinase regulatory subunit gamma-1-like (6.67 fold-change) and SKP1-like protein 21 (2.86 fold-change) were upregulated at 48hpi in *Trichoderma*-treated castor compared to control plants. Further, a minimum of three UDP-glycosyltransferase genes (73C3, 73C25 and 86A2) were found to be upregulated with a crucial role in cellular detoxification and homeostasis.

Similarly, several putative genes involved in defense signaling were also upregulated in castor in response to *Trichoderma*. The mRNA transcripts of F-box/kelch-repeat protein At1g74510 were highly expressed with 8.88 fold-change with a role in negative regulation of phenylpropanoid biosynthesis thereby promoting JA mediated responses in *Trichoderma*-treated castor. Also, serine carboxypeptidase-like 18 gene transcripts, a candidate gene whose promoter sequences are enriched in abscisic acid (ABA)- and methylated jasmonic acid (MeJA)-responsive elements was upregulated with 7.18 fold-change expression. Similarly, two putative gene transcripts, cold-regulated 413 plasma membrane protein 2 and TPL-binding domain in jasmonate signalling (7.08 fold-change each) with a role in ABA and JA respectively were predominant. The finding is confirmed by the hike in expression level (6.67) of a SNF1-related protein kinase regulatory subunit gamma-1 (SnRK-like) gene, a global positive regulator of ABA signaling. Further, a Zinc finger protein ZAT5 was also found to be upregulated whose promoter sequences are enriched with *cis*-elements responsive to phytohormones suggesting that it is a potential candidate for analysing *Trichoderma*-induced responses.

Interestingly, two putative disease resistance proteins, RPV1 and RPS2 with 7.28 and 3.00 fold-change expression respectively were also found to be upregulated indicating that resistance to biotic stress was also activated along with growth regulation at 48 hpi.

4.3.5.4. Upregulation of phosphatases, transporter and plant growth promoting factors

The mRNA abundance levels of several putative protein phosphatases including purple acid phosphatases were higher in *Trichoderma* treated castor suggesting that these phosphatases are secreted to utilize organic phosphorus for plant growth and development. Likewise, metal tolerance protein1, potassium channel KAT2 and copper-transporting ATPase Paa1/Paa2 with fold-change of 8.66, 8.66 and 8.62 respectively were observed indicating that these proteins served as cation diffusion facilitator (CDF) for metal efflux from the cytoplasm into either extracellular space or organelles. Further, putative cytochrome P450 genes (cytochrome P450, Cytochrome P450 711A1 and Cytochrome P450 78A7 with 8.66, 2.35 and 2.32 fold-change expression respectively were observed indicating their role in detoxification of xenobiotics, cellular metabolism and homeostasis. The gene transcript accumulation of YTH domain-containing protein ECT4 with a role in biological timing and leaf formation peaked with a 10.33 fold-change expression. The mRNA transcripts of a growth regulating factor (*GRF1*)-interacting factor1 were upregulated with 9.08 fold change followed by WAT1-related protein gene At3g28050-like and WAT1-related protein gene At4g15540 with 8.66 and 7.6 fold change respectively with a role in plant development. The gene transcripts of probable polygalacturonase showed 6.74 fold-change upregulated suggesting its role in promoting plant growth which involves hypocotyl elongation and in floral organ patterning to produce higher proportions of flowers.

4.3.5.6. Upregulated secondary metabolites, molecular chaperoning and nuclear modelling

The mRNA abundance levels of S-adenosylmethionine-dependent methyltransferase and probable methyltransferase PMT7 were upregulated 8.76 and 7.67 fold-change respectively indicating their prominent role in biosynthesis of bioactive compounds and/or modification of biopolymers in response to *Trichoderma*. Likewise, Squalene monooxygenase SE1 with a putative role in biosynthesis of triterpenoid saponins showed 7.44 fold-expression.

The mRNA transcripts for several molecular chaperones-like, Hsc70-interacting protein, putative Peptidyl-prolyl cis-trans isomerase CYP37, Universal stress protein PHOS34, Peptidyl-prolyl cis-trans isomerase CYP38, chloroplast and bacterial trigger factor protein (TF) were

found to be highly upregulated with the highest fold-change for Hsc70-interacting protein (9.64) indicating that chaperone surveillance functions to ensure protein homeostasis, also known as proteostasis. Whereas, the putative DNA (cytosine-5)-methyltransferase DRM2 transcripts with a role in in de novo DNA methylation showed a 7.52 fold-change expression, Arginine methyltransferase NDUFAF7 with 8.18 fold-change expression indicated its role in DNA repair to regulate transcription, RNA splicing and protein stability. The transcripts of two putative metalloenzymes encoding lysine-specific demethylase JMJ16 (8.03 fold-change) and Lysine-specific demethylase JMJ25 (3.65 fold-change) indicated that these genes are essential for chromatin remodelling. The transcripts of Deoxyuridine 5'-triphosphate nucleotidohydrolase gene (3.8 fold-change) with a role in de-nova nucleotide synthesis were also upregulated in response to *Trichoderma* suggesting the activation of regulatory gene networks involved in plant growth and development.

4.3.5.6. Upregulation of genes for cellular macronutrient biosynthesis and metabolism

The mRNA abundance for two putative genes; β-galactosidase and β-galactosidase15 with 11.38 and 2.30 fold-change respectively were observed. Likewise, mRNA transcripts for probable glucan 1,3-β-glucosidase A and β-glucosidase 11 with 7.18 and 2.87 fold-change were recorded suggesting the elevated level of carbohydrate metabolism induced by *Trichoderma* treatment. Similarly, α-amylase gene transcripts were found to be marginally upregulated (2.24 fold change) which is essential for conversion of starch into oligosaccharides in plant cells.

A putative BPI/LBP family protein At1g04970 transcripts showed elevated accumulation with 9.36 fold-change followed by elevated mRNA levels of Phosphatidylinositol-glycan biosynthesis class X (9.3 fold-change) indicating the possibility of a lipopolysaccharide (LPS) based elicitation by *Trichoderma.* Phospholipid:diacylglycerol acyltransferase1 transcripts were found to be 8.70 fold-change with a role in membrane and storage lipid synthesis whereas, acyl-coenzyme A thioesterase 13 with 8.27 fold-change indicate that it is vital in regulating the free fatty acids in plant cells, The gene transcripts of phospholipase A22 (7.44) and phospholipase A1 PLIP2 (6.74) were upregulated with a putative roles in signal transduction and catalysing the initial step of oxylipins and JA biosynthesis. A TLC domain-containing protein 4-B gene also known as transmembrane protein56 with putative role in lipid homeostasis was elevated with 3.65 fold-change.

The gene transcripts of glutamate synthase (NADH) peaked with fold-change expression of 11.67 which facilitates the ammonium assimilation pathway followed by an amino peptidase

(9.40) which catalyses cleavage of amino acids from the amino (N-) terminus of the protein or peptide substrates. Phosphomethylpyrimidine synthase with a role in thiamine biosynthesis was found to be upregulated (with 8.76 fold-change) accompanied by another gene, a putative thiamine biosynthetic bifunctional enzyme TH1 with 3.04 fold-change expression. Likewise, Arginine decarboxylase (8.32 fold-change) which modulates proline metabolism was upregulated in response to *Trichoderma* in castor. Further, a 5'-Adenylyl sulfate reductase gene which catalyzes sulfate assimilation pathway leading to the synthesis of cysteine and the antioxidant glutathione was also found to be upregulated with 7.08 fold-change level expression in DCS-107 castor treated with *Trichoderma* compared to controls.

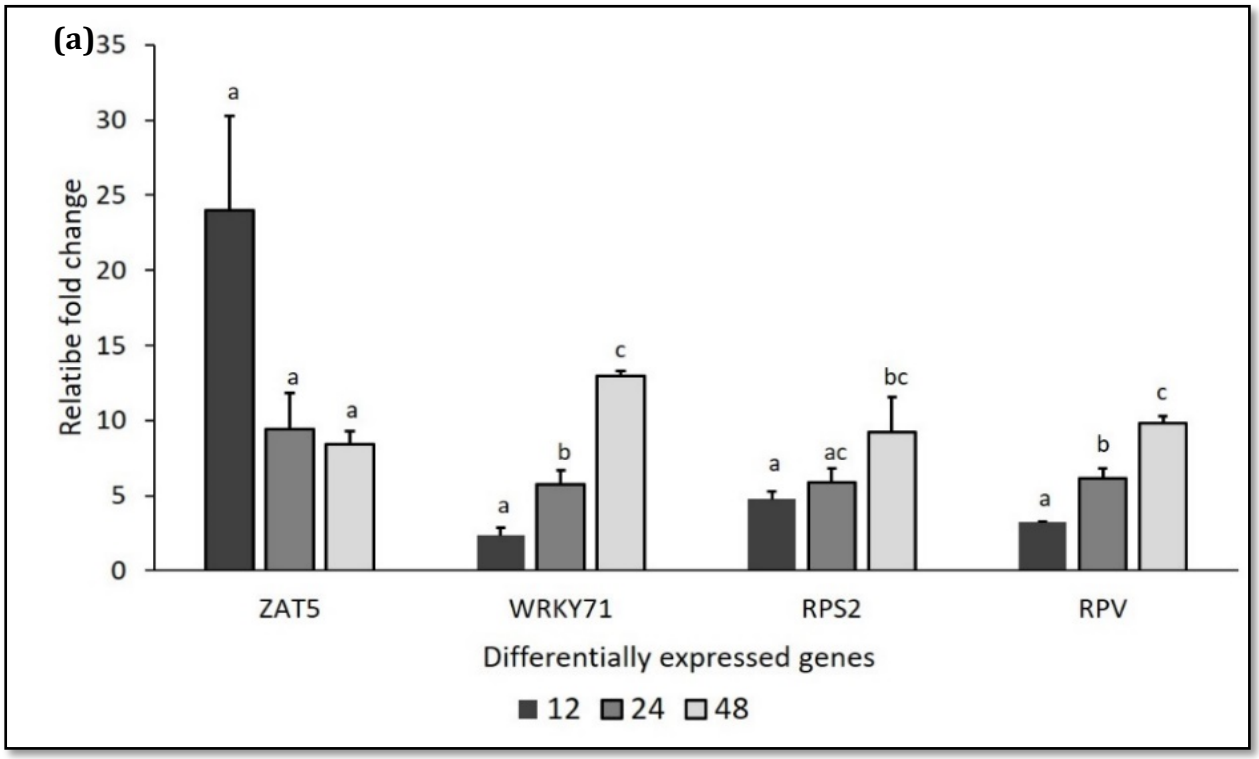
The mRNA transcripts of Glycerol-3-phosphate dehydrogenase NAD(+), NADH dehydrogenase (quinone) activity, NADP-dependent glyceraldehyde-3-phosphate dehydrogenase with high fold-change gene expression of 9.25, 6.6 and 2.9 were observed indicating their implication in glycolysis, lipid synthesis, and energy metabolism by electron transfer to mitochondria in plant cells.

4.3.5.7. Differential expression of putative transcription factors in response to *Trichoderma*

The mRNA levels of the putative transcription factor (TF), *E2FB* peaked with 9.88 fold-change in response to *Trichoderma* indicating its regulatory role for coordinating cell proliferation with embryonic differentiation whereas, *LRL1* that regulates the development of root hairs was upregulated with 8.70 fold-change expression. Likewise, agamous-like MADS-box protein AGL30 (8.52) which regulates pollen maturation, MADS-box protein AGL29 (8.08) which controls flower development, putative TF bHLH68 (7.36) crucial for photo morphogenesis and light signal transduction, probable transcription factor KAN2 (7.28) required for lateral organ polarity were upregulated in response to *Trichoderma*. Transcription factor PIF3 (3.54) to promote and optimize growth under photoperiodic conditions, transcription elongation factors; s-II (TFIIS) with 2.8 fold change expression for coordinating transcription initiation, and several *WRKY* transcription factors which mediate ethylene (ET) signaling and ET synthesis to hasten leaf senescence were also upregulated along with Myb-like DNA-binding domain and G-box-binding factor required in developmental and physiological processes in response to major cues such as light or hormones.

4.3.6. Validation of transcriptome data by quantitative Real Time- PCR (RT-qPCR)

To validate plant DEGs detected in the present study, RT-qPCR was performed for a set of 9 putative genes involved in defense and stress responses at 12, 24 and 48 hpi (**Figure 4.8**). Of these 9 genes, 4 genes were upregulated and 5 genes where downregulated in the DEG analysis. The qRT results of these 9 genes were consistent with transcriptome profiling data, suggesting high reliability and good quality of the data. Five genes that were found to be downregulated were Peroxidase12 (*PER12*), serine/threonine-protein kinase (*FLS2)*, pathogenesis related protein5 (*PR5)*, Endoglucanase (*ENDO*), Wound induced protein2 (*WIN2)*, *w*hereas the 4 putative genes which were upregulated were WRKY transcription factor (*WRKY71*), disease resistance protein1 (*RPV1*), zinc finger protein5 (*ZAT5*) and disease resistance gene, *RPS2.* The putative genes, *PER12*, *FLS2*, *PR5*, *ENDO* and *WIN2* confirmed to be downregulated play a crucial role in pathogen recognition and defense signaling suggesting that *Trichoderma* is perceived as a beneficial microbe by the host, castor.



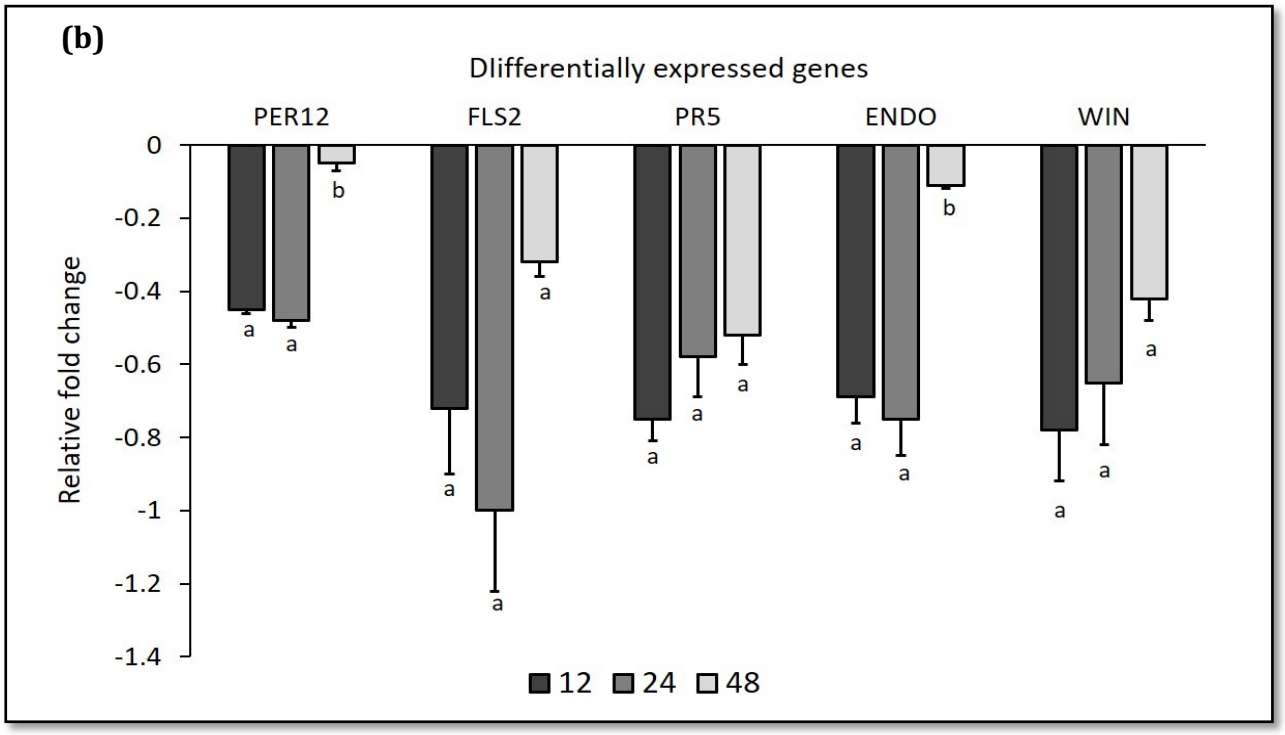


Figure 4.8 Validation of plant DEGs by quantitative Real Time-Polymerase Chain Reaction (RT-qPCR). The relative level of mRNA transcript accumulation of 9 stress and defense-related genes at 12, 24 and 48 hpi in 7316 treated castor DCS-107 roots. Confirmation of (a) upregulated and (b) downregulated plant DEGs using plant *Actin* as an internal control and non-template DNA control (NTC) is detected in the study.. Statistical difference between the time-points is displayed at Tukey p≤0.05. Vertical bars represent ±SE of the mean values. Statistical significance levels indicated by case letters: a-c.

4.4 DISCUSSION

The interaction between *Trichoderma asperellum* 7316, a promising strain and the host, castor (*Ricinus communis* L.) has been explored to understand the nature of transcriptional modulation induced by *Trichoderma*. The transcriptome profiling of *Trichoderma*-treated and control roots of DCS-107 genotype at 48 hpi plants provided a detailed insight into the systemic changes that occurred in castor roots in response to *Trichoderma*. It is interesting to note that majority of gene transcripts were observed to be downregulated and these putative DEGs were predominantly related to stress responses suggesting that the host recognized *Trichoderma* as a non-pathogenic but a beneficial organism.

4.4.1. Putative genes downregulated in castor in response to *Trichoderma*

The DEGs that were downregulated were primarily comprising of the family of kinases which include putative receptor-like protein kinases and LRR receptor-like serine/threonine-protein kinases. These receptors have been reported to play a crucial role in pathogen recognition and pattern associated molecular pattern (PAMP)-triggered immunity (Boller and Felix, 2009) and their negative regulation suggests that *Trichoderma* colonization is recognized as a non-pathogen by the host. Moreover, the putative genes involved in downstream functions like activating stress-related signaling, ROS generation, hypersensitive response and secondary metabolite production were also predominantly downregulated indicating that the host might be negatively regulating stress-related genes to promote *Trichoderma* colonization in the host.

Further, a downregulation of several of the peroxidases and laccases which play a vital role in plant defense response against pathogen attack, indicated that *Trichoderma* is sensed as a non-alarming entity by the host. Peroxidase (POX) not only helps in ROS scavenging but also aids to deter the spread of a pathogen through the formation of polymerized phenolic barriers around the sites of infection by pathogens (Siddaiah et al., 2017) resulting in cell wall reinforcement thereby triggering the synthesis of anti-nutritive, antibiotic, and cytotoxic compounds causing enhanced resistance against pathogens (Smit and Dubery, 1997).

Similar to peroxidases, laccases are key enzymes involved in lignification. A 20–40% reduction in lignin content has been observed in the knockout mutants of two laccase genes (*LAC4* and *LAC17*) in Arabidopsis (Berthet et al., 2011). Moreover, the triple mutant of *LAC4*, *LAC11*, and *LAC17* completely lost lignin deposition in roots (Zhao et al., 2013). Thus it is understandable that downregulation of lignin forming peroxidases and laccase allows colonization of *Trichoderma* inside the roots of DCS-107. In general, plants appear to balance generation of ROS leading to activation of peroxidases as the first line of defence and reducing

cell wall reinforcements after perceiving *Trichoderma* as no obvious threat in order to allow the symbiotic relationship to be established between them.

The jacalin-like mannose-binding lectin domain containing proteins which are reported to bind to the T-antigen and act as an agglutinin in higher organisms, were found to interact with endogenous carbohydrates especially in disease signaling pathway (Naithani et al., 2021). However, in response to *Trichoderma*, the putative lectin domain gene was observed to be down regulated in agreement that *Trichoderma* is recognized as a non-pathogen. Likewise, Serine carboxypeptidases like proteins (SCPLs) which were upregulated against *Magnaporthe grisea* infection in rice (Liu et al., 2008) were found to be downregulated in response to *Trichoderma*.

Conversely, a reduced number of the putative methyl transferases related to the family of *O*-methyltransferases (OMTs) with a putative role in secondary metabolites including phenylpropanoids, flavonoids, and alkaloids were observed. In addition, the genes involved in secondary metabolite biosynthesis, cell wall modifications, disease signaling and transduction were also downregulated confirming that *Trichoderma* is regarded by the host plant as a non-harmful agent.

Likewise downregulation of the putative transcription factors which include *BIM1*, myb family transcription factor *PHL8*, transcription factor *bHLH90*, GATA transcription factor4 indicated the repression of brassinosteroid signaling in response to *Trichoderma*. The putative *BIM1*, a bHLH protein is involved in brassinosteroid signaling and is reported to control Arabidopsis embryonic patterning via interaction with DORNROSCHEN (DRN) and DORNROSCHEN-LIKE (DRNL) transcription factors (Chandler et al., 2009, Jiang et al., 2015). The multimeric transcription factor complex formed by the trio genes suggested not only a role of brassinosteroids in embryonic development but also as a possible point of hormonal crosstalk with auxin in embryonic patterning, since DRN is involved in auxin signaling as well.

Similar to *BIM1*, the downregulation of other members of *bHLH* transcription factors, *bHLH90* and *bHLH74* confirmed the repression of brassinosteroid signaling which functions in photomorphogenesis, light signal transduction and secondary metabolism in response to stress (Guo et al., 2021). Likewise, downregulation of a myb family transcription factor *PHL8*, indicated that *Trichoderma* colonization is perceived as beneficial to the host, since *MYB* family of transcription factors are involved in controlling various cellular responses to biotic and abiotic stresses (Ambawat et al., 2013). Whereas GATA transcription factor4 which is known to be involved in light-dependent gene regulation and nitrate assimilation was observed to be

downregulated in agreement with studies revealing that repression of the transcription factor *bHLH74* by a miR396a promoted root growth in Arabidopsis seedlings (Bao et al., 2014).

4.4.2. Putative genes upregulated in castor in response to *Trichoderma*

A predominant number of serine threonine-protein kinase members were upregulated suggesting their role in plant growth and development, besides aiding in recognition of plant invaders comprising of both pathogenic as well as non-pathogenic organisms. The upregulated serine/threonine-protein kinase *WNK4* might be essential to act as a molecular switch that can alter the balance between NaCl reabsorption and K^+ secretion to maintain integrated homeostasis of the host cells (Kahle et al., 2005). Further, WINK4 gene has been reported as a key player in regulating plant growth and development in maize (Patil and Senthil-Kumar, 2020).

Likewise, upregulation of a putative inositol-tetrakisphosphate 1-kinase 3 gene, which plays a fundamental role in phosphate signaling to connect cell wall and membrane sensors with ion homeostasis and transport-mediated processes has previously been demonstrated in *Arabidopsis thaliana t*o catalyse the synthesis of phytate (inositol hexakisphosphate; $InsP_6$) synthesis and is indispensable for maintaining P_i homeostasis (Stevenson-Paulik et al., 2005). Recent studies have demonstrated that Arabidopsis inositol 1,3,4-trisphosphate 5/6 kinase 2 is required for the permeability of seed coat and seed coat development (Tang et al., 2013). The elevated gene expression levels of a putative proline-rich receptor-like protein kinase *PERK8* observed in the present study might be required for the floral organ development as demonstrated Chen and associates (2020) by a proline-rich extension-like receptor protein kinase (*PERK*) in *Brassica rapa* and its association with the pollen development. Likewise, an increased mRNA levels of a putative 2-oxoglutarate-dependent dioxygenase which aids in enhanced phytohormone formation such as ethylene, gibberellins, anthocyanidins and pigments that are catalysed by the enzymes containing 2OG dioxygenase domains were also observed in Arabidopsis with its importance in not only plant growth, development and metabolism but also in adaptive responses to low oxygen conditions (Iacopino et al., 2020).

Besides plant growth, the receptor-like protein kinases with a role in symbiotic association were also upregulated which include cysteine-rich receptor-like protein kinase 10 (*CRK*), and LysM domain receptor-like kinase 3 suggesting the recognition of *Trichoderma* by the host as a endosymbiont. The findings are in accordance with the study on the biological roles of *CRKs* in various tissues of the plants belonging to the genus, *Phaseolus* during diverse biological processes including *Phaseolus*-mycorrhiza/rhizobia symbiosis (Quezada et al.,

2019). Another potential candidate with a unique role in both the arbuscular mycorrhizal (AM) and the rhizobium-legume (RL) symbioses in response to signal molecules was detected in the present study similar to the reported the LysM receptor-like kinases (LysM-RLKs), known as *NFP/NFR5*, *LYK3/NFR1*, and *LYR3/LYS12* which were detected for root endosymbiosis in *Medicago truncatula* and *Lotus japonicus* (Gough et al., 2018; Buendia et al., 2018).

4.4.2.1. Putative genes upregulated with a role in cellular metabolism and detoxification

Glutathione S-transferases are one of the most important detoxifying enzymes that play a major role in stress tolerance in plants and systemic infection by rice black streaked dwarf virus (RBSDV) in rice showed an induction of GST 23 gene (Xu et al., 2013, Hasanuzzaman et al., 2017). In agreement, an upregulation of GST which helps to combat oxidative stress caused due to interaction with *Trichoderma* was observed for limiting ROS triggered by Pathogen triggered immunity (PTI).

The mRNA transcripts of Glycerol-3-phosphate dehydrogenase NAD(+) 2 gene with a putative role in glycolysis and homeostasis, a probable glutathione peroxidase 2 gene to function in cellular metabolism and energy production, Glutathione S-transferase L3 with a role in cellular metabolism and detoxification of a variety of xenobiotic compounds and few peroxidases which include L-ascorbate peroxidase 6, Peroxidase 5, Cationic peroxidase 1 were upregulated as a natural response against an invading organism to minimise cell damage caused due to ROS accumulation. Further, the findings from the present study were in agreement with the previous report on *Trichoderma* inoculation in tomato (Chen et al., 2019). Chen and co-workers (2019) reported a significant increase in the glutathione (*GSH*) content, the activity of glutathione S-transferase (GST) and the transcript levels of *GSH*, *GST1*, *GST2* and *GST3* along with the activity of peroxidase and polyphenol peroxidase that are involved in the xenobiotic conversion. In addition, expression of several detoxification genes such as Cytochrome P450 suggests that *Trichoderma asperellum* stimulates plant detoxification potential in all three phases (conversion, conjugation and sequestration) of xenobiotc metabolism in the roots of castor.

Both plants and microbes encode for phosphatases to mineralize organic phosphate (P) compounds. However, purple acid phosphatases (PAPs) an important class of plant APases that are secreted by plants into the rhizosphere to utilize organic phosphorus (Po) for plant growth and development were found to be upregulated in castor roots in response to *Trichoderma*. The upregulation of YTH domain-containing protein ECT4 gene in our study with a putative role in leaf organ formation has been demonstrated to be associated with developmental timing and

morphogenesis in Arabidopsis (Arribas-Hernández et al., 2018). Likewise, growth regulating factor (GRF1)-interacting factor1 which was upregulated in the study have been presented as positive regulators of cell proliferation and are involved in the regulation of stem and leaf development (Zhang et al., 2018), whereas *WALLS ARE THIN1* (*WAT1*), a plant-specific protein which was also upregulated controls secondary cell wall thickness of wood fibres and facilitates auxin export required for auxin homoeostasis as demonstrated from isolated Arabidopsis vacuoles into yeast and Xenopus oocytes (Ranocha et al., 2013). A putative polygalacturonase upregulated might be involved in promoting plant growth and floral organ patterning to produce higher proportions of flowers (Xiao et al., 2014).

Ubiquitination and subsequent proteasomal degradation of target proteins are essential for molecular processing and housecleaning to maintain homeostasis of plant cells. Several proteins which include, RING-H2 finger protein ATL11, Receptor homology region, transmembrane domain- and RING domain-containing protein 1, RING-H2 finger protein ATL66, Nudix hydrolase 2 gene, ferrous ascorbate-dependent oxidoreductase family, F-box protein FBW2, protein of the SKP1 family, SNF1-related protein kinase regulatory subunit gamma-1-like, SKP1-like protein 21 and UDP-glycosyltransferase with a role in regulating mechanisms involving proteasomal degradation, cellular detoxification and homeostasis in the host (Hacquard et al., 2022; Guzmán et al., 2012; Ge et al., 2008; Zhao et al., 2003).

4.4.2.2. Upregulated genes with a role in defense responses and signaling

While majority of the genes involved in ROS and hypersensitive responses were downregulated, it is interesting to note that a few of the defense response genes were upregulated in *Trichoderma*-treated castor plants along with the two putative resistance genes (*RPV1* and *RPS2*) indicating that a basal level of response was activated at 48 hpi to an incoming foreign organism. The upregulation of F-box/kelch-repeat protein, known as KFB1 is a member of a group of Kelch repeat F-box proteins that negatively regulate phenylpropanoid biosynthesis by targeting the phenypropanoid biosynthesis enzyme phenylalanine ammonia-lyase suggested its role in the downregulation of salicylic acid (SA)-mediated responses. This is consistent with the work done by Zhang et al., 2013 where upregulation or downregulation of KFB1 reciprocally affects the phenylpropanoid pathway. Also, Thaumatin-like protein are classified into the PR-5 protein family which is a characteristic of the SA pathway (Anisimova et al., 2021). Downregulation of such Thaumatin-like proteins also indicate a possible downregulation of SA-mediated protein response in *Trichoderma* treated roots of DCS-107. Likewise, elevated expression of putative gene transcripts of cold-regulated 413 plasma

membrane protein 2, a positive regulator of ABA responses (Hu et al., 2021), TPL-binding domain as a repressor of auxin signaling (Navarrete et al., 2022) and a plant-specific Zinc finger protein ZAT5 responsive to multiple plant hormones (Fan et al., 2021) suggested interplay of different phytohormones in *Trichoderma*-mediated defense signaling in castor. Further, a SNF1-related protein kinase regulatory subunit gamma-1-like gene, a member of SnRK2 which is reported as a global positive regulator of ABA signaling was upregulated. In addition, a hike in the Serine carboxypeptidase-like 18 gene transcripts, a candidate with promoter elements responsive to both ABA and MeJA confirmed that *Trichoderma* induced both ABA and JA mediated responses in castor. Our findings are in agreement with the studies of Moura and associates (2001) which identified the type I SCP gene in tomato (*Lycopersicon esculentum* Mill.) as one of the "late wound-inducible genes" based on its induced expression by wounding, systemin and MeJA. Likewise, a recent studies on functional analysis of *cis*-acting elements of promoter sequences of *TaSCPL* genes in wheat (*Triticum aestivum* L.) confirmed that those sequences are enriched in drought-, ABA- and MeJA-responsive elements (Xu et al., 2021). *WRK71*, belonging to a large family of transcription factors was seen upregulated. *WRK71* protein that is usually upregulated by several signalling molecules like salicylic acid, methyl jasmonate or on wounding and pathogen invasion has shown an enhanced resistance in rice in response to *Xanthomonas oryzae* pv. *oryzae* (Lie et al., 2007).

4.4.2.3. *Trichoderma*-induced molecular remodelling, chaperones and transcription factors

S-adenosylmethionine (SAM) is a dominant metabolic intermediate and ubiquitous cofactor and SAM-dependent methyltransferases (MTases) are responsible for methylation affecting several pathways involving macromolecules like lipids, proteins and nucleic acids in addition to the biosynthesis of small-molecule metabolites (Struck et al., 2012; Bennett et al., 2017; Luo et al., 2019). Our study also revealed several methy transferases including the highly upregulated S-adenosylmethionine-dependent methyltransferase with putative role in methylation processes of key regulatory genes involved in plant growth and development.

A few molecular chaperone genes like hsc70-interacting protein, peptidyl-prolyl cis-trans isomerase CYP37 and Peptidyl-prolyl cis-trans isomerase CYP38, chloroplast were upregulated suggesting that heat shock proteins (hsp) which include Hsc70-interacting protein are essential to aid in folding of newly synthesized polypeptide chains and translocation of proteins across membranes (Berka et al., 2022). Also, a wheat gene, cyclophilin, TaCypA-1

which encodes Peptidyl-prolyl cis-trans isomerase enzyme has been demonstrated as essential to induce thermo tolerance in *Escherichia coli* (Kaur et al., 2015).

Of the several upregulated transcription factors with a putative role in plant growth and development, the putative Transcription Factor, *E2FB* predominantly expressed followed by Lipid remodeling regulator1 (*LRL1*). *E2FB* is reported as a key target for auxin to determine whether cells should proliferate or exit the cell cycle, enlarge, and endoreduplicate their DNA (Magyar et al., 2005) and also in coordinating cell proliferation with seed maturation (Leviczky et al., 2019). The transcription factor, lipid remodeling regulator1 (*LRL1*) is shown to be differently involved in the phosphorus-depletion response in *Chlamydomonas reinhardtii* (Hidayati et al., 2019). A putative BPI/LBP family protein At1g04970 transcript accumulation indicated the possibility of a lipopolysaccharide (LPS)-based elicitation by *Trichoderma* which in turn upregulated phosphatidylinositol-glycan biosynthesis to generate the lipid anchor protein, glycophosphatidylinositol (GPI) suggesting that *Trichoderma* treatment not only induced lipid biosynthesis but also lipid based signaling in castor.

The other transcription factors, Agamous-like MADS-box protein AGL30 and MADS-box protein AGL29 play a crucial role in pollen maturation and flower development (Roy et al., 2012; Alvarez-Buylla et al., 2019). The other transcription factors that were upregulated include *bHLH68*, *KAN2* and *PIF3* which are required for photo morphogenesis, light signal transduction, lateral organ polarity and to promote and optimize growth under different photoperiodic and phytohormonal conditions while the *WRKY* transcription factors; *WRKY71*, *WRKY40* and *WRKY55* were found to be marginally upregulated in response to *Trichoderma*. Our findings are in accordance with the previous studies suggesting the alteration of stress and defense response genes in response to *Trichoderma*, though the level of the change remains quantitatively marginal (Alfano et al., 2007; Shoresh and Harman, 2010; Morán-Diez et al., 2012).

Chapter 5

Summary and conclusion

Trichoderma fungi have been intensively studied for their biocontrol and growth promotion abilities. Our research was aimed to screen six newly isolated strains of *Trichoderma* beginning from identification through systematic characterization of ITS, D1-D2, *Trichoderma* specific sequences and molecular markers using RAPD and SCAR marker techniques. Additionally, SCAR markers were developed in this study that could be utilized in further studies involving the screening of *Trichoderma* strains to detect potential fungal strains to serve as biocontrol agents in crop breeding programs. The identification of molecular variations by RAPD data profiling has opened a new possibility of detecting more efficient strain(s) of *Trichoderma* for formulating effective biopesticides to improve the productivity potential of crop plants. *Trichoderma* has been reported as a mycoparasitic agent, able to directly attack other fungi. Our results observed in the detached leaf assay also showed that leaves sprayed with *Trichoderma* are resistant to the fungal pathogen, *A. ricini*. Further, an in-depth study of the *Trichoderma* strains to synergize the effect of all toxic metabolites and hydrolytic enzymes may lead to formulating a complex strain that would enhance the antagonistic potential of *Trichoderma* as a potential biocontrol agent (BCA).

Trichoderma asperellum demonstrated both root colonizing and biocontrol properties. Biopriming with *T. asperellum* enhanced seed germination and root growth besides promoting antagonism against *Fusarium oxysporum ricini*. In our study, three strains of *Trichoderma asperellum*: 7316, N13 and TV5 showed varying levels of rhizosphere competence, antagonism and growth promotional response, which could be utilized by employing the strains either singly or in combination to increase plant growth and biocontrol potential in castor. Real Time gene expression analysis of host defence showed a complex reprograming of the defense gene pathways suggesting a role of *Trichoderma* in eliciting ISR in combating biotic stress, where *T. asperellum* 7316 was observed to be a promising strain in facilitating protection against *Fusarium* wilt disease in castor.

The study revealed that *Trichoderma* association with castor resulted in vast transcriptomic reprogramming of the plant genome which lead to the alteration of genes associated with stress and defense in castor. Together, the pattern of altered gene expression observed in castor roots due to *Trichoderma* colonization suggests a complex system of communication involving genetic cross talk between various molecular and biological processes. As explained in the graphical abstract, *Trichoderma* interaction leads to a complex reprogramming of stress response genes, in a way that would not inhibit its own colonization in the plant roots, but at the same time would be able to prompt an induced defense response. Downregulation of peroxidases, laccase, PR proteins, methyltransferase, endoglucanase along

with WIN2 enables the development of an efficient mutualistic relationship between castor and *Trichoderma* that also protects castor from oxidative damage. At the same time, early colonization causes upregulation of certain genes like At1g74510, serine carboxypeptidase-like 18, cold-regulated 413 plasma membrane protein 2 and TPL-binding domain and SNF1-related protein kinase that point towards the promotion of JA mediated ISR responses in *Trichoderma*-treated castor. Thus, a strong endophytic association between the host, castor and the BCA, *Trichoderma,* is not only mutually beneficial to both the interacting members, but also aids in priming the host to elicit faster and enhanced immune response to subsequent pathogen attack. Along with genes involved in elevated ISR response, low molecular weight secondary metabolites with antimicrobial properties were also upregulated in response to *Trichoderma* in castor. Therefore, the preliminary response of the plant to *Trichoderma* invasion involves the activation of several physical and biochemical responses to ensure persistent endophytic relation with the host.

Chapter 6

Bibliography

1. Aebi H. Catalase in vitro. 1984. Methods in Enzymol. 105:121–126.
2. Aghcheh RK, Németh Z, Atanasova L, Fekete E, Paholcsek M, Sándor E, Aquino B, Druzhinina IS, Karaffa L, Kubicek CP. The VELVET A orthologue VEL1 of *Trichoderma reesei* regulates fungal development and is essential for cellulase gene expression. 2014. PLoS One. 11:9(11):e112799.
3. Ahmad A, Javeed MT. Effects of different inoculum densities of *Trichoderma harzianum* and *Trichoderma viride* against *Meloidogyne javanica* on tomato. 2016. Saudi Journal of Biological Sciences. 23(2):288–292.
4. Alfano G, Ivey ML, Cakir C, Bos JI, Miller SA, Madden LV, Kamoun S, Hoitink HA. Systemic Modulation of Gene Expression in Tomato by *Trichoderma hamatum* 382. 2007. Phytopathol. 97:429–37.
5. Alsohaili SA, Hasan BMB. Morphological and Molecular Identification of Fungi Isolated from Different Environmental Sources in the Northern Eastern Desert of Jordan. 2018. J. of Biol. Sci1:329–337.
6. Alvarez-Buylla E.R, García-Ponce B, Sánchez MP, Espinosa Soto C, García-Gómez ML, Piñeyro-Nelson A, Garay-Arroyo A. MADS-box genes underground becoming mainstream: plant root developmental mechanisms. 2019. New Phytologist. 223:1143–1158.
7. Ambawat S, Sharma P, Yadav NR, Yadav RC. MYB transcription factor genes as regulators for plant responses: an overview. 2013. Physiol Mol Biol Plants. 19: 307–21.
8. Anisimova OK, Shchennikova AV, Kochieva EZ, Filyushin MA. Pathogenesis-Related Genes of PR1, PR2, PR4, and PR5 Families Are Involved in the Response to *Fusarium* Infection in Garlic (*Allium sativum* L.). 2021. Int J Mol Sci. 22(13):6688.
9. Anjani K, Pallavi M, Sudhakara Babu SN. Biochemical basis of resistance to leaf miner in castor (*Ricinus communis* L.). 2010. Industrial Crops and Products. 31: 192–196.
10. Anke, H., Kinn, J., Bergquist, KE. et al. Production of siderophores by strains of the genus *Trichoderma*. 1991. Biol Metals 4:176–180.
11. Arribas-Hernández L, Bressendorff S, Hansen MH, Poulsen C, Erdmann S, Brodersen P. An m6A-YTH Module Controls Developmental Timing and Morphogenesis in Arabidopsis. P2018. Plant Cell 30:952–967.
12. Atanasova L, Knox BP, Kubicek CP, Druzhinina IS, Baker SE. The polyketide synthase gene pks4 of *Trichoderma reesei* provides pigmentation and stress resistance. 2013. Eukaryot Cell. 11:1499-508.

13. Baek JM, Howell CR, Kenerley CM. The role of an extracellular chitinase from *Trichoderma virens* Gv29-8. 1999. Curr Genet. 35: 41–50.
14. Baker SE, Perrone G, Richardson NM, Gallo A, Kubicek CP. Phylogenomic analysis of polyketide synthase-encoding genes in *Trichoderma*. 2012. Microbiology. 158(Pt 1):147-154.
15. Bao M, Bian H, Zha Y, Li F, Sun Y, Bai B, Chen Z, Wang J, Zhu M, Han N. miR396a- mediated basic helix-loop-helix transcription factor bHLH74 repression acts as a regulator for root growth in Arabidopsis seedlings. 2014. Plant Cell Physiol. 55:1343–53.
16. Barrera VA, Lannone L, Romero AI, Chaverri P. Expanding the *Trichoderma harzianum* species complex: Three new species from Argentine natural and cultivated ecosystems. 2021. Mycologia 113(6):1136–1155.
17. Basappa H. Validation of integrated pest management modules for castor (*Ricinus communis*) in Andhra Pradesh. 2007. Indian Journal of Agricultural Sciences. 77 (6): 357–62.
18. Bautista-Muñoz C, Boldo XM, Villa-Tanaca L, Hernández-Rodríguez C. Identification of Candida spp. by randomly amplified polymorphic DNA analysis and differentiation between *Candida albicans* and *Candida dubliniensis* by direct PCR methods. 2003. J Clin Microbiol. 41(1):414–20.
19. Begum MF, Rahman MA, Alam MF. Biological Control of *Alternaria* Fruit Rot of Chili by *Trichoderma* Species under Field Conditions. 2021. Mycobiol. 38:113–117.
20. Bennett MR, Shepherd SA, Cronin VA, Micklefield J. Recent advances in methyltransferase biocatalysis. 2017. Curr Opin Chem Biol. 37:97–106.
21. Benítez T, Rincón AM, Limón MC, Codón AC. Biocontrol mechanisms of *Trichoderma* strains. 2004. Int Microbiol. 7:249–60.
22. Berka M, Kopecká R, Berková V, Brzobohatý B, Černý M. Regulation of heat shock proteins 70 and their role in plant immunity. 2022. J of Experimental Botany. 1894–1909.
23. Berthet S, Demont-Caulet N, Pollet B, Bidzinski P, Cézard L, Le Bris P, Borrega N, Hervé J, Eddy BE, Balzergue S, Lapierre C, Jouanin L. Disruption of LACCASE4 and 17 Results in Tissue-Specific Alterations to Lignification of *Arabidopsis thaliana* Stems. 2011. The Plant Cell. 23:1124–1137.
24. Beyer Jr. WF, Fridovich F. Assaying for superoxide dismutase activity: some large consequences of minor changes in conditions. 1987. Analytical Biochem. 161:559–566.

25. Bigirimana J, Meyer GD, Poppe J, Elad Y, Höfte M. Induction of systemic resistance on bean (*Phaseolus vulgaris*) by *Trichoderma harzianum*. 1997. Mededelingen van de Faculteit Landbouwwetenschappen - Rijksuniversiteit Gent 62(3B):1001-–007.
26. Bissett J. 1984. A revision of the genus *Trichoderma* I. Sect. Longibrachiatum sect. nov. Canadian J. of Bot. 62:924–931.
27. Bissett J. A revision of the genus *Trichoderma* II. Infrageneric classification. 1991a. Canadian J. of Bot. 69:2357–2372.
28. Bissett J. A revision of the genus *Trichoderma* III. Sect. Pachybasium. 1991b. Canadian J. of Bot. 69:2373–2417.
29. Bissett J. A revision of the genus *Trichoderma* IV. Additional notes on section Longibrachiatum. 1991c. Canadian J. of Bot. 69:2418–2420.
30. Bolger AM, Lohse M, Usadel B. Trimmomatic: a flexible trimmer for illumina sequence data. 2014. Bioinformatics 30, 2114–2120.
31. Boller T, Felix G. A renaissance of elicitors: Perception of microbe-associated molecular patterns and danger signals by pattern-recognition receptors. 2009. Annu Rev Plant Biol. 60, 379–406.
32. Brotman Y, Landau U, Alvaro CI, Takayuki T, Fernie AR, Chet I, Viterbo A, Willmitzer L. *Trichoderma*-Plant Root Colonization: Escaping Early Plant Defense Responses and Activation of the Antioxidant Machinery for Saline Stress Tolerance. 2013. PLOS Pathogens. 9(3): e1003221.
33. Buendia L, Girardin A, Wang T, Cottret L, Lefebvre B. LysM Receptor-Like Kinase and LysM Receptor-Like Protein Families: An Update on Phylogeny and Functional Characterization. 2018. Front Plant Sci, 9, 1531.
34. Buysens C, César V, Ferrais F, Boulois HD, Declerck S. Inoculation of *Medicago sativa* cover crop with *Rhizophagus irregularis* and *Trichoderma harzianum* increases the yield of subsequently-grown potato under low nutrient conditions. 2016. Applied Soil Ecology. 105: 137–143.
35. Cai F, Druzhinina IS. In honor of John Bissett: authoritative guidelines on molecular identification of *Trichoderma.* 2018. Fungal Diversity. 107:1–69.
36. Cai F, Yu G, Wang P, Wei Z, Fu L, Shen Q, Chen W. Harzianolide, a novel plant growth regulator and systemic resistance elicitor from *Trichoderma harzianum*. 2013. Plant Physiol Biochem.. 73:106–13.
37. Caldelari D, Wang G, Farmer EE, Dong X. *Arabidopsis lox3 lox4* double mutants are male sterile and defective in global proliferative arrest. 2010. Plant Mol. Biol. 75:25–33.

38. Chance B, Maehly AC. Assay of Catalase and Peroxidase. 1955. Methods in Enzymol. 2:764–775.
39. Caligiorne RB, Resende MA, Paiva E, Azevedo V. Use of RAPD (random amplified polymorphic DNA) to analyse genetic diversity of dematiaceous fungal pathogens. 1999. Can J Microbiol. 45(5):408–12.
40. Cardoza RE, Hermosa MR, Vizcaíno JA, González F, Llobell A, Monte E, Gutiérrez S. Partial silencing of a hydroxy-methylglutaryl-CoA reductase-encoding gene in *Trichoderma harzianum* CECT 2413 results in a lower level of resistance to lovastatin and lower antifungal activity. 2007. Fungal Genet Biol. 44(4):269–83.
41. Chakraborty MR and Chatterjee NC. Control of *Fusarium* wilt of *Solanum melongena* by *Trichoderma* spp. 2008. Biol Plant. 52: 582–586.
42. Chakraborty BN, Chakraborty U, Dey PL, Sunar K. Phylogenetic Relationships of *Trichoderma* isolates of North Bengal Based on Sequence Analysis of ITS Region of rDNA. 2010. Journal of Applied Sciences Research. 6(10):1477–1482.
43. Chandulal K, John P, Gopal C. 2016. Genetic diversity of *Trichoderma* sp. obtained from Tomato Rhizosphere using RAPD. Int. J. of Sci. Env. and Tech. 5: 2101–2108.
44. Chandler JW, Cole M, Flier A, Werr W. BIM1, a bHLH protein involved in brassinosteroid signalling, controls Arabidopsis embryonic patterning via interaction with DORNROSCHEN and DORNROSCHEN-LIKE. 2009. Plant Mol Biol. 69:57–68.
45. Chaverri P, Branco-Rocha F, Jaklitsch W, Gazis R, Degenkolb T, Samuels GJ. Systematics of the *Trichoderma harzianum* species complex and the re-identification of commercial biocontrol strains. 2015. Mycologia. 107(3):558–590.
46. Chen JL, Liu K, Miao CP. Salt tolerance of endophytic *Trichoderma koningiopsis* YIM PH30002 and its volatile organic compounds (VOCs) allelopathic activity against phytopathogens associated with *Panax notoginseng*. 2016. Ann Microbiol. 66, 981–990.
47. Chen G, Wang J, Wang H, Wang C, Tang X, Li J, Zhang L, Song J, Hou J, Yuan L. Genome-wide analysis of proline-rich extension-like receptor protein kinase (PERK) in *Brassica rapa* and its association with the pollen development. 2020. BMC Genomics. 21, 401.
48. Chen S, Yan Y, Wang Y, Wu M, Mao Q, Chen Y, Ahammed GJ. *Trichoderma asperellum* reduces phoxim residue in roots by promoting plant detoxification potential in *Solanum lycopersicum* L. 2019. Environmental Pollution 259, 113893.
49. Crutcher FK, Moran-Diez ME, Ding S, Liu J, Horwitz BA, Mukherjee PK, Kenerley CM. A paralog of the proteinaceous elicitor SM1 is involved in colonization of maize roots by *Trichoderma virens*. Fungal Biol. 2015. 119(6):476–86.

50. Crutcher FK, Parich A, Schuhmacher R, Mukherjee PK, Zeilinger S, Kenerley CM. A putative terpene cyclase, vir4, is responsible for the biosynthesis of volatile terpene compounds in the biocontrol fungus *Trichoderma virens*. 2013. Fungal Genet Biol. 56:67–77.
51. Devi TP, Prabhakaran N, Kamil D. Development of Species-Specific Markers for the identification of *Trichoderma asperellum* and *Trichoderma harzianum*. 2017. Vegetos- An International J. of Plant Res. 30:94–100.
52. Devi TP, Prabhakaran N, Kamil D, Pandey P. Borah JL. Characterization of Indian native isolates of *Trichoderma* spp. and assessment of their bio-control efficiency against plant pathogens. 2012. Afr. J. Biotechnol. 11(85):15150–15160.
53. Dou K, Lu Z, Wu Q, Ni M, Yu C, Wang M, Li Y, Wang X, Xie H, Chen J. A novel polyphasic identification system for genus *Trichoderma.* 2021. BioRxiv. 481382.
54. Daniel JF, Filho ER. Peptaibols of *Trichoderma*. 2007. Nat Prod Rep. 24(5):1128-–41.
55. Daryaei A, Jones EE, Ghazalibiglar H, Glare TR, Falloon RE. Effects of temperature, light and incubation period on production, germination and bioactivity of *Trichoderma atroviride*. 2016. J Appl Microbiol. 120(4): 999–1009.
56. Devi TP, Prabhakaran N, Kamil D. Development of Species-Specific Markers for the identification of *Trichoderma asperellum* and *Trichoderma harzianum*. 2017. Vegetos- An Int. J. of Plant Res. 30:94–100.
57. Djonović S, Pozo MJ, Dangott LJ, Howell CR, Kenerley CM. Sm1, a proteinaceous elicitor secreted by the biocontrol fungus *Trichoderma virens* induces plant defense responses and systemic resistance. 2006. Mol Plant Microbe Interact. 19(8):838–53.
58. Djonović S, Pozo MJ, Kenerley CM. Tvbgn3, a beta-1,6-glucanase from the biocontrol fungus, *Trichoderma virens* is involved in mycoparasitism and control of *Pythium ultimum*. 2006. Appl Environ Microbiol. 72(12):7661-70.
59. Doni F, Isahak A, Zain C, Sulaiman N, Fathurrahman F, Zain W, Kadhimi A, Alhasnawi A, Anhar A, Yusoff W. Increasing rice plant growth by *Trichoderma* sp. 2021.
60. Doni F, Zain CRCM, Isahak A. et al. Relationships observed between *Trichoderma* inoculation and characteristics of rice grown under System of Rice Intensification (SRI) vs. conventional methods of cultivation. 2017. Symbiosis 72:45–59.
61. Dubey MK, Jensen DF, Karlsson M. Hydrophobins are required for conidial hydrophobicity and plant root colonization in the fungal biocontrol agent *Clonostachys rosea*. 2014. BMC Microbiol 14:18.

62. Duclohier H. Peptaibiotics and peptaibols: an alternative to classical antibiotics? 2007. Chem Biodivers. 4(6):1023–6.
63. Elad Y. Biological control of foliar pathogens by means of *Trichoderma harzianum* and potential modes of action. 2000. Crop Protect. 19:709–714.
64. El-Hasan A, Walker A, Buchenauer H. 2007. *Trichoderma harzianum* and its Metabolite 6-Pentyl-alpha-pyrone Suppress Fusaric Acid Produced by *Fusarium moniliforme*. 2007. Journal of Phytopathology. 156: 79–87.
65. Engelberth J, Koch T, Schüler G, Bachmann N, Rechtenbach J, Boland W. Ion channel-forming alamethicin is a potent elicitor of volatile biosynthesis and tendril coiling. Cross talk between jasmonate and salicylate signalling in lima bean. 2001. Plant Physiol. 125(1):369–77.
66. Evidente A, Cabras A, Maddau L, Serra S, Andolfi A, Motta A. Viridepyronone, a new antifungal 6-substituted 2H-pyran-2-one produced by *Trichoderma v*iride. 2003. J Agric Food Chem. 51(24):6957–60.
67. Fan Y, Zhang Y, Rui C, Nan X, Zhang H, Wang J, Malik WA, Han M, Zhao L, Lu X, Chen X, Chen C. Zinc finger transcription factor ZAT family genes confer multi-tolerances in *Gossypium hirsutum* L. 2021. J Cotton Res. 4:24.
68. Flores SC, Momberg MR, Bibbins M, Noyola PP, Estrella AH. BLR-1 and BLR-2, key regulatory elements of photoconidiation and mycelial growth in *Trichoderma atroviride.* 2004. Microbiology. 150:3561–3569.
69. Gaderer R, Lamdan NL, Frischmann A, Sulyok M, Krska R, Horwitz BA, Seidl-Seiboth V. Sm2, a paralog of the *Trichoderma* cerato-platanin elicitor Sm1, is also highly important for plant protection conferred by the fungal-root interaction of *Trichoderma* with maize. 2015. BMC Microbiol. 15(1):2.
70. Gajera HP, Katakpara ZA, Patel SV, Golakiya BA. Antioxidant defense response induced by *Trichoderma viride* against *Aspergillus niger* Van Tieghem causing collar rot in groundnut (*Arachis hypogaea* L.). 2016. Microb Pathog. 91:26-–4.
71. Gawade D, Pawar BH, Gawande S Vasekar V. Antagonistic Effect of *Trichoderma* Against *Fusarium moniliformae* the Causal of Sugarcane Wilt. 2012. 12. 1236-–1241.
72. Ge X, Xia Y. The role of AtNUDT7, a Nudix hydrolase, in the plant defense response. 2008. Plant Signal Behav. 3:119–20.
73. Ghosh SK, Pal S. Entomopathogenic potential of *Trichoderma longibrachiatum* and its comparative evaluation with malathion against the insect pest *Leucinodes orbonalis*. 2016. Environ Monit Assess. 188(1):37.

74. Gomes EV, Costa Mdo N, de Paula RG, de Azevedo RR, da Silva FL, Noronha EF, Ulhoa CJ, Monteiro VN, Cardoza RE, Gutiérrez S, Silva RN. The Cerato-Platanin protein Epl-1 from *Trichoderma harzianum* is involved in mycoparasitism, plant resistance induction and self-cell wall protection. 2015. Sci Rep. 5:17998.
75. Gopal K, Sreenivasulu Y, Gopi V, Prasad Babu G, Kumar BT, Madhusudhan P, Ahmed SK, Palanivel SG. Genetic variability and Relationships among seventeen *Trichoderma* Isolates to Control Dry Root Rot Disease using RAPD markers. Z Naturforsch C J Biosci. 63C:740–746.
76. Gough C, Cottret L, Lefebvre B, Bono JJ. Evolutionary History of Plant LysM Receptor Proteins Related to Root Endosymbiosis. 2018. Front Plant Sci. 9:923.
77. Gressel JB and Hartmann KM. Morphogenesis in *Trichoderma:* Action Spectrum of Photo-induced Sporulation. 1968. Planta (Berl.) 79:271–274.
78. Grondona I, Hermosa R, Tejada M, Gomis MD, Mateos PF, Bridge PD, Monte E, Garcia-Acha I. Physiological and Biochemical Characterization of *Trichoderma harzianum*, a Biological Control Agent against Soilborne Fungal Plant Pathogens. 1997. Applied and Environmental Microbiol. 63:3189–3198.
79. Guo J, Sun B, He H, Zhang Y, Tian H, Wang B. Current Understanding of bHLH Transcription Factors in Plant Abiotic Stress Tolerance. 2021. Int J Mol Sci. 22:4921.
80. Guler NS, Pehlivan N, Karaoglu SA, Guzel S, Bozdeveci S. *Trichoderma atroviride* ID20G inoculation ameliorates drought stress-induced damages by improving antioxidant defence in maize seedlings. 2016. Acta Physiol Plant. 38:132.
81. Gupta R, Bar M. Plant Immunity, Priming, and Systemic Resistance as Mechanisms for *Trichoderma* spp. 2020. *Trichoderma* Rhizosphere Biology. Pp: 81–110.
82. Gupta VK, Misra AK, Gupta A, Pandey BK, Gaur RK. RAPD-PCR of *Trichoderma* isolates and in vitro antagonism against *Fusarium* wilt pathogens of *Psidium guajava*. L. 2010. J. of Plant Protect. Res. 50:256–262.
83. Guzmán P. The prolific ATL family of RING-H2 ubiquitin ligases. 2012. Plant Signal Behav. 7:1014–21.
84. Guzmán-Guzmán P, Alemán-Duarte MI, Delaye L, Herrera-Estrella A, Olmedo-Monfil V. Identification of effector-like proteins in *Trichoderma* spp. and role of a hydrophobin in the plant-fungus interaction and mycoparasitism. 2015. BMC Genet. 15–18(1):16.
85. Guzman-Guzman P, Troncoso MDP, Monfil VO. *Trichoderma* Species: Versatile Plant Symbionts. 2018. Phytopathol. 109:6–16.

86. Hacquard T, Clavel M, Baldrich P, Lechner E, Pérez-Salamó I, Schepetilnikov M, Derrien B, Dubois M, Hammann P, Kuhn L, Brun D, Bouteiller N, Baumberger N, Vaucheret H, Meyers BC, Genschik P. The Arabidopsis F-box protein FBW2 targets AGO1 for degradation to prevent spurious loading of illegitimate small RNA. 2022. Cell Rep. 39:110671.
87. Hajieghrari B. Effects of some Iranian *Trichoderma* isolates on maize seed germination and seedling vigor. 2010. Afr. J. Biotechnol. 9:4342–4347.
88. Hajieghrari B, Mohammadi M. Growth-promoting activity of indigenous *Trichoderma* isolates on wheat seed germination, seedling growth and yield. 2016. Australian Journal of Crop Science. 10(9):1339–1347.
89. Harman GE, Howell CR, Viterbo A, Chet I, Lorito M. *Trichoderma* species-opportunistic, avirulent plant symbionts. 2004. Nature Rev. Microbiol. 2:43–56.
90. Harman GE, Lorito M, Lynch JM. Uses of *Trichoderma* spp. to Alleviate or Remediate Soil and Water Pollution. 2004. Adv Appl Microbiol. 56:313–30.
91. Hasanuzzaman M, Nahar K, Anee TI, Fujita M. Glutathione in plants: biosynthesis and physiological role in environmental stress tolerance. 2017. Physiol Mol Biol Plants. 23:249–268.
92. Hermosa R, Viterbo A, Chet I, Monte E. Plant-beneficial effects of *Trichoderma* and of its genes. 2012. Microbiol. 158, 17–25.
93. Hidayati NA, Yamada-Oshima Y, Iwai M, Yamano T, Kajikawa M, Sakurai N. Lipid remodeling regulator 1 (*LRL1*) is differently involved in the phosphorus-depletion response from PSR1 in *Chlamydomonas reinhardtii*. 2019. Plant J. 100:610–626.
94. Hima VM and Beena S. In vitro antagonism of *Trichoderma* spp. against six soil borne fungal pathogens. 2016. Int. J. of Applied and Pure Science and Agriculture. 2:3.
95. Holzlechner M, Reitschmidt S, Gruber S, Zeilinger S, Marchetti-Deschmann M. Visualizing fungal metabolites during mycoparasitic interaction by MALDI mass spectrometry imaging. 2016. Proteomics. 16(11-12):1742–6.
96. Howell CR, Hanson LE, Stipanovic RD, Puckhaber LS. Induction of Terpenoid Synthesis in Cotton Roots and Control of *Rhizoctonia solani* by Seed Treatment with *Trichoderma virens*. 2000. Phytopathology. 90(3):248–52.
97. Hu X, Liu J, Liu E, Qiao K, Gong S, Wang J, Zhang J. Arabidopsis cold-regulated plasma membrane protein Cor413pm1 is a regulator of ABA response. 2021. Biochem and Biophysical Res Commun. 561:88–92.

98. Iacopino S, Licausi F. The Contribution of Plant Dioxygenases to Hypoxia Signalling. 2020. Front. Plant Sci. 11:1008.
99. Idris M, Mudawi H. The Efficacy of *Trichoderma* spp. and *Bacillus* Isolates in the Control of Chickpea Wilt Pathogens. 2014. Agriculture, Forestry and Fisheries.
100. Inbar J, Chet I. The Role of Lectins in Recognition and Adhesion of the Mycoparasitic Fungus *Trichoderma* spp. to its Host. 1996. Advances in Experimental Medicine and Biology. 408:229–231.
101. Jahan N, Sultana S, Adhikary SK, Rahman S, Yasmin S. Evaluation Of The Growth Performance Of *Trichoderma harzianum* (Rifai.) On Different Culture Media. 2018. Journal of Agriculture and Veterinary Science. 3(4): 44–50.
102. Jain D, Khurana JP. Role of Pathogenesis-Related (PR) Proteins in Plant Defense Mechanism. 2018. Molecular Aspects of Plant-Pathogen Interaction. pp 265–281.
103. Jaisani P, Pandey RN. Morphological and molecular characterization for identification of isolates of *Trichoderma* spp. from rhizospheric soils of crops in middle Gujarat. 2017. Indian Phytopathol. 70:238–245.
104. Jiang, J, Zhang C, Wang X. A recently evolved isoform of the transcription factor BES1 promotes brassinosteroid signaling and development in *Arabidopsis thaliana*. 2015. Plant Cell 27:361–74.
105. Jimtha JC, Jishma P, Arathy GB, Anisha C, Radhakrishnan EK. Identification of plant growth promoting Rhizosphere *Bacillus* sp. WG4 antagonistic to *Pythium myriotylum* and its enhanced antifungal effect in association with *Trichoderma*. 2016. Journal of soil science and plant nutrition. 16(3):578–590.
106. Kahle KT, Wilson FH, Lifton RP. Regulation of diverse ion transport pathways by WNK4 kinase: a novel molecular switch. 2005. Trends Endocrinol Metab. 16:98–103.
107. Kale SK, Pradeeprao KT, Dnyanobarao GS, & Agrawal T, Kotasthane AS. Efficiency of Different *Trichoderma* Isolates on Plant Growth Promoting Activity in Rice (*Oryza sativa* L.). 2016. International Journal of Bio-resource and Stress Management. 7(3):489–500.
108. Kaur G, Singh S, Dutta T, Kaur H, Singh B, Pareek A, Singh P. The peptidyl-prolyl cis-trans isomerase activity of the wheat cyclophilin, TaCypA-1, is essential for inducing thermotolerance in *Escherichia coli*. Biochem Open. 2:9–15.
109. Kamaruzzaman M, Hossain MD, Hossain I.. Antifungal and Morphological Assay of Selective *Trichoderma* Isolates Against Soil Borne Plant Pathogenic Fungi. 2016. International Journal of Innovation and Applied Studies 16(2):409–417.

110. Karuppiah V, Li T, Vallikkannu M, Chen J. Co-cultivation of *Trichoderma asperellum* GDFS1009 and *Bacillus amyloliquefaciens* 1841 causes differential gene expression and improvement in the wheat growth and biocontrol activity. 2019. Front. Microbiol. 1068:1–16.
111. Keswani C, Bisen K, Chitara MK, Sarma BK, Singh HB. Exploring the Role of Secondary Metabolites of *Trichoderma* in Tripartite Interaction with Plant and Pathogens. 2017. Agro-Environmental Sustainability. Pp:63–79.
112. Khan RAA, Najeeb S, Hussain S, Xie B, Li Y. Bioactive Secondary Metabolites from *Trichoderma* spp. against Phytopathogenic Fungi. 2020a. Microorganisms. 8: 817.
113. Khan, RAA, Najeeb S, Mao Z, Ling J, Yang Y, Li Y, Xie B. Bioactive secondary metabolites from *Trichoderma* spp. against phytopathogenic bacteria and koot-Knot nematode. 2020b. Microorganisms. 8:401.
114. Kim DS and Hwang BK. An important role of the pepper phenylalanine ammonia-lyase gene (PAL1) in salicylic acid-dependent signalling of the defence response to microbial pathogens. 2014. J Exp Bot 65(9), 2295–2306.
115. Kowsari M, Zamani MZ, Motallebi M. Enhancement of *Trichoderma harzianum* Activity Against *Sclerotinia sclerotiorum* by Overexpression of Chit42. 2014. Iran J Biotech. 12(2): e13869.
116. Kubicek CP, Herrera-Estrella A, Seidl-Seiboth, V. et al. Comparative genome sequence analysis underscores mycoparasitism as the ancestral life style of *Trichoderma*. 2011. Genome Biology. 12:R40.
117. Kumagai T , Oda Y. An action spectrum for photo-induced sporulation in the fungus *Trichoderma viride*. 1969. *Plant and Cell Physiology.* 10(2): 387–392.
118. Kumar M, Ashraf S. Role of *Trichoderma* spp. as a Biocontrol Agent of Fungal Plant Pathogens. 2017. Probiotics and Plant Health. 497–506.
119. Kullnig-Gradinger CM, Szakacs G, Kubicek CP. Phylogeny and evolution of the fungal genus *Trichoderma*—A multigene approach. 2002. Mycological Res. 106:757–767.
120. Kwiatkowski NP, Babiker WM, Merz WG, Carroll KC, Zhang SX. Evaluation of Nucleic Acid Sequencing of the D1/D2 region of the large subunit of the 28S rDNA and the Internal Transcribed Spacer Region using Smart Gene IDNS software for Identification of filamentous fungi in a clinical laboratory. 2012. The J. of Mol. Diagnost. 14:393–401.
121. Lee DH, Lee SK, Lee SY, Lee JK. 2013. Development of SCAR Markers for the Identification of *Phytophthora katsurae* Causing Chestnut Ink Disease in Korea. Mycobiology. 41(2):86–93.

122. Lehner SM, Atanasova L, Neumann NK, Krska R, Lemmens M, Druzhinina IS, Schuhmacher R. Isotope-assisted screening for iron-containing metabolites reveals a high degree of diversity among known and unknown siderophores produced by *Trichoderma* spp. 2013. Appl Environ Microbiol. 79(1):18–31.
123. Leviczky T, Molnár E, Papdi C, Őszi E, Horváth GV, Vizler C, Nagy V, Pauk J, Bögre L, Magyar Z. E2FA and E2FB transcription factors coordinate cell proliferation with seed maturation. 2019. Development 146:179333.
124. Li RX, Cai F, Pang G, Shen QR, Li R, Chen W. Solubilisation of Phosphate and Micronutrients by *Trichoderma harzianum* and Its Relationship with the Promotion of Tomato Plant Growth. 2015. PLoS One. 10:e0130081.
125. Li Y, Sun R, Yu J, Saravanakumar K, Chen J. Antagonistic and Biocontrol Potential of *Trichoderma asperellum* ZJSX5003 against the Maize Stalk Rot Pathogen *Fusarium graminearum*. 2016. Indian J Microbiol. 56(3):318–27.
126. Lima LH, Ulhoa CJ, Fernandes AP, Felix CR. Purification of a chitinase from *Trichoderma* sp. and its action on *Sclerotium rolfsii* and *Rhizoctonia solani* cell walls. 1997. J Gen Appl Microbiol. 43(1):31–37.
127. Linder MB, Szilvay GR, Nakari-Setälä T, Penttilä ME. Hydrophobins: the protein-amphiphiles of filamentous fungi. 2005. FEMS Microbiol Rev. 29(5):877–96.
128. Liu X, Bai X, Wang X, Chu C. OsWRKY71, a rice transcription factor, is involved in rice defense response. 2007. J Plant Physiol. 164:969–79.
129. Liu Q, Meng X, Li T, Raza W, Liu D, Shen Q. The Growth Promotion of Peppers (*Capsicum annuum* L.) by *Trichoderma guizhouense* NJAU4742-Based Biological Organic Fertilizer: Possible Role of Increasing Nutrient Availabilities. 2020. Microorganisms. 9:1296.
130. Liu YJ, Whelen S, Hall BD. Phylogenetic relationships among ascomycetes: evidence from an RNA polymerse II subunit. 1999. Molecular Biology and Evolution. 16(12): 1799–1808.
131. Liu H, Wang X, Zhang H, Yang Y, Ge X, Song F. A rice serine carboxypeptidase-like gene OsBISCPL1 is involved in regulation of defense responses against biotic and oxidative stress. 2008. Gene. 420:57–65.
132. Livak KJ, Schmittgen TD. Analysis of relative gene expression data using real-time quantitative PCR and the 2-ΔΔCT method. 2001. Methods 25(4):402–8.
133. Lo CT, Nelson EB, Harman GE. Biological control of turfgrass diseases with a rhizosphere competent strain of *Trichoderma harzianum*. 1996. Plant Disease. 80:736–741.

134. Luo H, Hansen ASL, Yang L, SchneiderK, Kristensen, M, Christensen U. Coupling S-adenosylmethionine-dependent methylation to growth: design and uses. 2019. PLoS Biol. 17:e2007050.

135. Luo Y, Zhang DD, Dong XW, Zhao PB, Chen LL, Song XY, Wang XJ, Chen XL, Shi M, Zhang YZ. Antimicrobial peptaibols induce defense responses and systemic resistance in tobacco against tobacco mosaic virus. 2010. FEMS Microbiol Lett. 313(2):120–6.

136. Lu Z, Tombolini R, Woo S, Zeilinger S, Lorito M, Jansson JK. In vivo study of *Trichoderma*-pathogen-plant interactions, using constitutive and inducible green fluorescent protein reporter systems. Appl Environ Microbiol. 2004. 70(5):3073–81.

137. Magyar Z, De Veylder L, Atanassova A, Bakó L, Inzé D, Bögre L. The role of the Arabidopsis *E2FB* transcription factor in regulating auxin-dependent cell division. 2005. Plant Cell. 17(9):2527–41.

138. Malmierca MG, Cardoza RE, Alexander NJ, McCormick SP, Collado IG, Hermosa R, Monte E, Gutiérrez S. Relevance of trichothecenes in fungal physiology: disruption of tri5 in *Trichoderma arundinaceum*. 2013. Fungal Genet Biol.

139. Malmierca MG, Cardoza RE, Alexander NJ, McCormick SP, Hermosa R, Monte E, Gutiérrez S. Involvement of *Trichoderma* trichothecenes in the biocontrol activity and induction of plant defense-related genes. 2012. Appl Environ Microbiol. 14:4856–68.

140. Malmierca MG, McCormick SP, Cardoza RE, Alexander NJ, Monte E, Gutiérrez S. Production of trichodiene by *Trichoderma harzianum* alters the perception of this biocontrol strain by plants and antagonized fungi. 2015. Environ Microbiol. (8):2628–46.

141. Martínez-Medina, A, Fernández I, Sánchez-Guzmán MJ, Jung SC, Pascual JA, Pozo MJ. Deciphering the hormonal signalling network behind the systemic resistance induced by *Trichoderma harzianum* in tomato. 2013. Front. Plant Sci. 4:206.

142. Matarese F, Sarrocco S, Gruber S, Seidl-Seiboth V, Vannacci G. Biocontrol of *Fusarium* head blight: interactions between *Trichoderma* and mycotoxigenic *Fusarium*. 2012. Microbiology (Reading). 158(Pt 1):98–106.

143. Mathys J, De CK, Timmermans P, Van KS., Lievens B, Vanhaecke M, Cammue BP, De CB. Genome-Wide Characterization of ISR Induced in *Arabidopsis thaliana* by *Trichoderma hamatum* T382 Against *Botrytis cinerea* Infection. 2012. Front. Plant Sci. 3:108.

144. Maurya MK, Mukesh S, Singh A, Pandey S, Ratan V. Effect of Different Temperature and Culture Media on the Mycelia Growth of *Trichoderma viride* Isolates. International Journal of Current Microbiology and Applied Sciences. 2017. 6(2):266–269.

145. Mazzei P, Vinale F, Woo SL, Pascale A, Lorito M, Piccolo A. Metabolomics by Proton High-Resolution Magic-Angle-Spinning Nuclear Magnetic Resonance of Tomato Plants Treated with Two Secondary Metabolites Isolated from *Trichoderma*. 2016. J Agric Food Chem. 64(18):3538–45.
146. Meng X, Miao Y, Liu Q, Ma L, Gua K, Liu, D, Ran W, Shen Q. TgSWO from *Trichoderma guizhouense* NJAU4742 promotes growth in cucumber plants by modifying the root morphology and the cell wall architecture. 2019. Microb Cell Fact. 18:148.
147. Mishra PK, Khan FN. Effect of Different Growth Media and Physical Factors on Biomass Production of *Trichoderma Viride*. 2015. People's Journal of Scientific Research. 8:2.
148. Modrzewska M, Marta MB, Joanna K, Pierzgalski A. *Trichoderma* as a biostimulator and biocontrol agent against Fusarium in the production of cereal crops: Opportunities and possibilities. 2022. Plant Pathology. 71:1471–1485.
149. Mohapatra S, Mittra B. Alleviation of *Fusarium oxysporum* induced oxidative stress in wheat by *Trichoderma viride*. 2017. Archives of Phytopathology and Plant Protection. 50(1-2): 84–96.
150. Morán-Diez E, Rubio B, Domínguez S, Hermosa R, Monte E, Nicolás C. Transcriptomic response of Arabidopsis thaliana after 24 h incubation with the biocontrol fungus *Trichoderma harzianum*. 2012. Journal of plant physiology. 169(6):614–20.
151. Morán-Diez ME, Alba AEM, Rubio MB, Hermosa R, Monte E.. *Trichoderma* and the Plant Heritable Priming Responses. 2021. J Fungi (Basel). 7: 318.
152. Morris JB, Morse SA, Navas AA, Soares DJ, Sofiatti V, Wang ML, Zanotto MD, Zieler H. A Review on the Challenges for Increased Production of Castor. 2012. Agronomy J. 104, 853–880.
153. Mota PR, Ribeiro MS, Georg RC, Silva GR, Paula RG, Silva RN, Ulhoa CJ. Expression analysis of the α-1,2-mannosidase from the mycoparasitic fungus *Trichoderma harzianum*. 2016. Biological Control. 95:1–4.
154. Moura DS, Bergey DR, Ryan CA. Characterization and localization of a wound-inducible type I serine-carboxypeptidase from leaves of tomato plants (*Lycopersicon esculentum* Mill.). 2001. Planta. 212:222–30.
155. Mukherjee PK, Buensanteai N, Moran-Diez ME, Druzhinina IS, Kenerley CM. Functional analysis of non-ribosomal peptide synthetases (NRPSs) in *Trichoderma virens* reveals a polyketide synthase (PKS)/NRPS hybrid enzyme involved in the induced systemic resistance response in maize. 2012. Microbiology (Reading). 158(Pt 1):155–165.

156. Mukhopadhyay R & Kumar D. *Trichoderma*: a beneficial antifungal agent and insights into its mechanism of biocontrol potential. 2020. Egyptian Journal of Biological Pest Control. 30:133.

157. Naithani S, Komath SS, Nonomura A, Govindjee G. Plant lectins and their many roles: Carbohydrate-binding and beyond. 2021. J. of Plant Physiol. 266:153531.

158. Navarrete F, Gallei M, Kornienko AE, Saado I, Khan M, Chia KS, Darino MA, Bindics J, Djamei A. TOPLESS promotes plant immunity by repressing auxin signaling and is targeted by the fungal effector Naked1. 2022. Plant Commun. 3: 100269.

159. Neumann NK, Stoppacher N, Zeilinger S, Degenkolb T, Brückner H, Schuhmacher R. The peptaibiotics database--a comprehensive online resource. 2015. Chem Biodivers. 12(5):743–51.

160. Nishad R, Ahmed T, Rahman VJ, Kareem A. Modulation of Plant Defense System in Response to Microbial Interactions. 2020. Front. Microbiol. 3:1298.

161. Nunzio F, Valeria V, Sheridan L W, Olimpia P, Armando DR, Laura G, Ida R, Nadia L, Mauro N, Giuseppe C, Youssef R. *Trichoderma*-Based Biostimulants Modulate Rhizosphere Microbial Populations and Improve N Uptake Efficiency, Yield, and Nutritional Quality of Leafy Vegetables. 2018. Frontiers in Plant Science. Vol 9.

162. Nwankiti AO, Gwa VI. Evaluation of antagonistic effect of *Trichoderma harzianum* against *Fusarium oxysporum* causal agent of white yam (*Dioscorea rotundata*) tuber rot. 2018. Trends in Technical & Scientific Res. 1:0012–0018.

163. Oljira AM, Hussain T, Waghmode TR, Zhao H, Sun H, Liu X, Wang X, Liu B. *Trichoderma* Enhances Net Photosynthesis, Water Use Efficiency, and Growth of Wheat (*Triticum aestivum* L.) under Salt Stress. 2020. Microorganisms. 8(10):1565.

164. Omann M, Lehner S, Brunner K, Delic M, Stoppacher N, Schuhmacher R, Pucher M, Zeilinger S. A cAMP receptor-like GPCR is involved in *Trichoderma atroviride* mycoparasitism. In Molecular Tools for Understanding and Improving BiocontroL. 2008. 45:103–108.

165. Pandey V, Ansari MW, Tula S, Yadav S, Sahoo RK, Shukla N, Bains G, Badal S, Chandra S, Gaur AK, Kumar A, Shukla A, Kumar J, Tuteja N. Dose-dependent response of *Trichoderma harzianum* in improving drought tolerance in rice genotypes. 2016. Planta. 243(5):1251–64.

166. Pandya JR, Sabalpara AN, Mahatma M. Randomly Amplified Polymorphic DNA Analysis of Native *Trichoderma* Isolates. 2017. Asian J. of Appl. Sci. and Technol. 1:147–150.

167. Park YS, Kunze S, Ni X, Feussner I, Kolomiets MV. Comparative molecular and biochemical characterization of segmentally duplicated 9-lipoxygenase genes ZmLOX4 and ZmLOX5 of maize. 2010. Planta. 231:1425–1437.
168. Patel PB and Pathak HC. Genetics of resistance to wilt in castor caused by *Fusarium oxysporum* f. sp. ricini Nanda and Prasad. 2011. Agric. Sci. Digest. 31 (1) : 30–34.
169. Patel VR, Dumancas GG, Viswanath LCK, Maples R and Subong BJJ. Castor Oil: Properties, Uses, and Optimization of Processing Parameters in Commercial Production. 2016. Lipid Insights. 9:1–12.
170. Patil M, Senthil-Kumar M. Role of Plant Kinases in Combined Stress. In: Protein Kinases and Stress Signaling in Plants: Functional Genomic Perspective. 2020. John Wiley & Sons, Ltd. Pp:445–458.
171. Perez G, Verdejo V, Gondim-Porto C, Orlando J, Caru M. Designing a SCAR molecular marker for monitoring *Trichoderma* cf. *harzianum* in experimental communities. 2014. J. of Zhejiang University-Science B (Biomed. & Biotechnol.). 15:966–978.
172. Qi W, Zhao L. Study of the siderophore-producing *Trichoderma asperellum* Q1 on cucumber growth promotion under salt stress. 2013. J Basic Microbiol. 53(4):355–64.
173. Qin WT and Zhuang WY. Seven wood-inhabiting new species of the genus *Trichoderma* (Fungi, Ascomycota) in *Viride* clade. 2016. Sci Rep. 6: 27074.
174. Qualhato TF, Cardoso Lopes FA, Steindorff AS, Brandao RS, Jesuino Amorim RS, Ulhoa CJ. Mycoparasitism studies of *Trichoderma* species against three phytopathogenic fungi: evaluation of antagonism and hydrolytic enzyme production. 2013. Biotechnol. Lett. 35, 1461–1468.
175. Quezada EH, García GX, Arthikala MK, Melappa G, Lara M, Nanjareddy K. Cysteine-Rich Receptor-Like Kinase Gene Family Identification in the Phaseolus Genome and Comparative Analysis of Their Expression Profiles Specific to Mycorrhizal and Rhizobial Symbiosis. 2019. Genes (Basel) 10:59.
176. Rahman MA, Begum MF, Alam MF. Screening of *Trichoderma* Isolates as a Biological Control Agent against *Ceratocystis paradoxa* Causing Pineapple Disease of Sugarcane. 2009. Mycobiol. 37, 2 77–285.
177. Rajani P, Rajasekaran C, Vasanthakumari, MM, Olsson SB, Ravikanth G, Shanker RU. Inhibition of plant pathogenic fungi by endophytic *Trichoderma* spp. through mycoparasitism and volatile organic compounds. 2021. Microbiol Res. 242:126595.

178. Rajput AQ, Khanzada MA, and Shahzad S. Effect of Different Organic Substrates and Carbon and Nitrogen Sources on Growth and Shelf Life of *Trichoderma harzianum*. 2014. J. Agr. Sci. Tech. 16: 731–745.
179. Ramalingam P. Isolation of *Trichoderma Viride* and *Pseudomonas Fluorescens* organism from soil and their treatment against rice pathogens. 2013. Journal of Microbiology and Biotechnology Research. 3:77–81.
180. Ramírez VR, Omero C, Chet I, Horwitz BA, Estrella AH. *Trichoderma atroviride* G-Protein α-Subunit Gene tga1 Is Involved in Mycoparasitic Coiling and Conidiation. 2002. Eukaryotic Cell. 594–605.
181. Ranocha P, Dima O, Nagy R, Felten J, Corratgé-Faillie C, Novák O, Morreel K, Lacombe B, Martinez Y, Pfrunder S, Jin X, Renou JP, Thibaud JB, Ljung K, Fischer U, Martinoia E, Boerjan W, Goffner D. Arabidopsis *WAT1* is a vacuolar auxin transport facilitator required for auxin homoeostasis. 2013. Nat Commun. 4:2625.
182. Redda ET, Jing M, Mei J, & Li M, & Wu B, & Jiang X. Antagonistic Potential of Different Isolates of *Trichoderma* against *Fusarium oxysporum*, *Rhizoctonia solani*, and *Botrytis cinerea*. 2018. European Journal of Experimental Biology. 8:2.
183. Reithner B, Brunner K, Schuhmacher R, Peissl I, Seidl V, Krska R, Zeilinger S. The G protein alpha subunit Tga1 of *Trichoderma atroviride* is involved in chitinase formation and differential production of antifungal metabolites. Fungal Genet Biol. 2005. 42(9):749–60.
184. Roberto AG, Gustavo HG, Jacobs D, Ardrtes W, Silvia BV, Montagu MV, Estrella AH. Molecular characterization of the proteinase-encoding gene, prb1, related to mycoparasitism by *Trichoderma harzianum*. 1993. Molecular Microbiology 8(3):603–13.
185. Robinson MD, McCarthy DJ, Smyth GK. edgeR: a bioconductor package for differential expression analysis of digital gene expression data. 2010. Bioinformatics. 26:139–40.
186. Rosado IV, Rey M, Codón AC, Govantes J, Moreno-Mateos MA, Benítez T. QID74 Cell wall protein of *Trichoderma harzianum* is involved in cell protection and adherence to hydrophobic surfaces. Fungal Genet Biol. 2007. 44(10):950–64.
187. Roy CS, Roy S, Nag A, Singh SK, Sengupta DN. Characterization of an AGAMOUS-like MADS box protein, a probable constituent of flowering and fruit ripening regulatory system in banana. 2012. PLoS One. 7:e44361.
188. Sabalpara AN, John P, Waghunde RR, Pandya JR. Antagonism of *Trichoderma* against Sugarcane wilt pathogen (*Fusarium moniliformae*). 2009. American-Eurasian Journal of Sustainable Agriculture, 3(4): 637–638.

189. Saber WIA, Ghoneem KM, Rashad YM, Al-Askar AA. *Trichoderma harzianum WKY1*: an indole acetic acid producer for growth improvement and anthracnose disease control in sorghum. 2017. Biocontrol Sci. and Technol. 27:654–676.
190. Sabrina S, Lorenzo M, Giampaola P, Antonio M, Antonio R, Giovanni V. 2013. Biological control of *Fusarium* Head Blight under field conditions. IOBC-WPRS. 86. 95–100.
191. Sagar MSI, Meah MB, Rahman MM, Ghose AK. Determination of genetic variations among different *Trichoderma* isolates using RAPD marker in Bangladesh. 2011. J. of Bangladesh Agril. Univ. 9:9–20.
192. Sain SK, Pandey AK. Biological spectrum of *Trichoderma harzianum* Rifai isolates to control fungal diseases of tomato (*Solanum lycopersicon* L.). 2016. Archives of Phytopathology and Plant Protection. 49(19-20): 507–521.
193. Salas-Marina MA, Isordia-Jasso MI, Islas-Osuna MA, Delgado-Sánchez P, Jiménez-Bremont JF, Rodríguez-Kessler M, Rosales-Saavedra MT, Herrera-Estrella A, Casas-Flores S. The Epl1 and Sm1 proteins from *Trichoderma atroviride* and *Trichoderma virens* differentially modulate systemic disease resistance against different life style pathogens in *Solanum lycopersicum*. 2015. Front Plant Sci. 23(6):77.
194. Saldaña MFR, Virelles PM, Torres EP, and Reyes YS. Compatibility Study of *Trichoderma harzianum* Rifai and Rice Fungicides, and Effects on Three Fungal Plant Pathogens. 2016. Agrisost. 22(2):46–58.
195. Saldaña-Mendoza SA, Pacios-Michelena S, Palacios-Ponce AS, Chávez-González ML, Cristóbal NA. *Trichoderma* as a biological control agent: mechanisms of action, benefits for crops and development of formulations. 2023. World J Microbiol Biotechnol. 39:269.
196. Samolski I, Rincón AM, Pinzón LM, Viterbo A, Monte E. The qid74 gene from *Trichoderma harzianum* has a role in root architecture and plant biofertilization. 2012. Microbiology. 158(Pt 1):129–138.
197. Samuels GJ, Dodd SL, Gams W, Castlebury LA, Petrini O. *Trichoderma* species associated with the green mold epidemic of commercially grown *Agaricus bisporus*. 2002. Mycology 94:146–170.
198. Sanz L, Montero M, Redondo J, Llobell A, Monte E. Expression of an alpha-1,3-glucanase during mycoparasitic interaction of *Trichoderma asperellum*. 2005. FEBS J. 272(2):493–9.
199. Saravanakumar K, Yu C, Dou K, Li MWY, Chen J. Synergistic effect of *Trichoderma*-derived antifungal metabolites and cell wall degrading enzymes on enhanced biocontrol of *Fusarium oxysporum* f. sp. *cucumerinum*. 2016. Biol. Control. 94:37–46.

200. Sarma AK, Singh MP, and Singh KI. Resistance of local castor genotypes to *Achaea janata* Linn. and *Spodoptera litura* Fabr. 2006. J. Applied Zool. Researchers. 17:179–181.

201. Saxena A, Raghuwanshi R, Singh HB. Elevation of Defense Network in Chilli Against *Colletotrichum capsici* by Phyllospheric *Trichoderma* Strain. 2016. J Plant Growth Regul 35:377–389.

202. Saxena D, Tewari AK, Dinesh R. In vitro antagonistic assessment of T. Harzianum PBT 23. 2014. Journal of Microbiology and Biotechnology Research 4 (3):59–65.

203. Scalschi L, Sanmartín M, Camañes G, Troncho P, PSánchez-Serrano JJ, García-Agustín P, Vicedo B. Silencing of OPR3 in tomato reveals the role of OPDA in callose deposition during the activation of defense responses against *Botrytis cinerea*. 2015. Plant J. 81, 304–15.

204. Schoch CL, Seifert KA, Huhndorf S, Robert V, Spouge JL, Levesque CA, Chen W. Fungal Barcoding, C.; Fungal Barcoding Consortium Author, L Proc. 2012. Natl. Acad. Sci. U.S.A.109:6241–6246.

205. Schoch CL, Seifert KA, Huhndorf S, Robert V, Spouge JL, Levesque CA, Chen W. Fungal Barcoding Consortium: Nuclear ribosomal internal transcribed spacer (ITS) region as a universal DNA barcode marker for Fungi. 2012. PNAS. 109:6241–6246.

206. Schuster A, Schmoll, M. Biology and biotechnology of *Trichoderma*. 2010. Appl Microbiol Biotechnol. 87:787–99.

207. Segarra G, Casanova E, Avilés M, Trillas I. *Trichoderma asperellum* strain T34 controls *Fusarium* wilt disease in tomato plants in soilless culture through competition for iron. 2010. Microb Ecol. 59(1):141–9.

208. Seibel C, Gremel G, Silva RN, Schuster A, Kubicek CP, Schmoll M. Light-dependent roles of the G-protein α subunit GNA1 of *Hypocrea jecorina* (anamorph *Trichoderma* reesei). 2009. BMC Biol 7:58.

209. Seidl V, Marchetti M, Schandl R, Allmaier G, Kubicek CP. Epl1, the major secreted protein of *Hypocrea atroviridis* on glucose, is a member of a strongly conserved protein family comprising plant defense response elicitors. 2006. FEBS J. 273(18):4346–59.

210. Seidl V, Song L, Lindquist E. *et al.* Transcriptomic response of the mycoparasitic fungus *Trichoderma atroviride* to the presence of a fungal prey. 2009. BMC Genomics. 10, 567.

211. Severino LS, Auld DL, Baldanzi M, Cândido MJD, Chen G, Crosby W, Tan D, He X, Lakshmamma P, Lavanya C, Machado OLT, Mielke T, Milani M, Miller TD, Morris JB, Morse

SA, Navas AA, Soares DJ, Sofiatti V, Wang ML, Zanotto MD and Zieler H. 2012. A Review on the Challenges for Increased Production of Castor. Agronomy Journal. 104:4.

212. Severino LS, Auld DL, Baldanzi M, Cândido MJD, Chen G, Crosby W, Tan D, He X, Lakshmamma P, Lavanya C, Machado OLT, Mielke T, Milani M, Miller TD, Morris JB, Morse SA, Navas AA, Soares DJ. A review on the challenges for increased production of castor. 2012. Agronomy J. 104, 853–880.
213. Sharma P, Kumar VP, Ramesh R, Saravanan K, Deep S, Sharma M, Mahesh S, Dinesh S. Biocontrol genes from *Trichoderma* species: A review. 2011. African J. of Biotechnol. 10:19898–19907.
214. Sharma PK, Gothalwala R. *Trichoderma*: A Potent Fungus as Biological Control Agent. 2017. Agro-Environmental Sustainability. 113–125.
215. Shoresh M, Yedidia I, Chet I. Involvement of Jasmonic Acid/Ethylene Signaling Pathway in the Systemic Resistance Induced in Cucumber by *Trichoderma asperellum* T203. 2005. Phytopathol. 95:76–84.
216. Shoresh M, Harman GE, Mastouri F. Induced systemic resistance and plant responses to fungal biocontrol agents. 2010. Annu Rev Phytopathol. 48:21–43.
217. Shi M, Chen L, Wang XW, Zhang T, Zhao PB, Song XY, Sun CY, Chen XL, Zhou BC, Zhang YZ. Antimicrobial peptaibols from *Trichoderma pseudokoningii* induce programmed cell death in plant fungal pathogens. 2012. Microbiology (Reading). 158(Pt 1):166–175.
218. Siddaiah CN, Satyanarayana NR, Mudili V, Gupta VK, Gurunathan S, Rangappa S, Huntrike SS, Srivastava RK. Elicitation of resistance and associated defense responses in *Trichoderma hamatum* induced protection against pearl millet downy mildew pathogen. 2017. Sci. Rep. 7:43991.
219. Singh A, Jain A, Sarma BK, Upadhyay RS, Singh HB. Rhizosphere competent microbial consortium mediates rapid changes in phenolic profiles in chickpea during *Sclerotium rolfsii* infection. 2014. Microbiological Research. 353–360.
220. Singh A, Shukla N, Kabadwal BC, Tewari AK and Kumar J. Review on Plant-*Trichoderma*-Pathogen Interaction. 2018. Int.J.Curr.Microbiol.App.Sci. 7(2): 2382–2397.
221. Singh A, Shahid M, Srivastava M, Pandey S, Sharma A, Kumar V. Optimal Physical Parameters for Growth of *Trichoderma* Species at Varying pH, Temperature and Agitation. 2014. Virology & Mycology. 3(1): 1000127.
222. Singh V, Upadhyay RS, Sarma B, Singh HB. Seed bio-priming with *Trichoderma asperellum* effectively modulate plant growth promotion in pea. 2016. International Journal of Agriculture, Environment and Biotechnology. 9(3):361.

223. Singh V, Upadhyay RS, Sarma BK, Singh HB. *Trichoderma asperellum* spore dose dependent modulation of plant growth in vegetable crops. 2016. Microbial Res. 193:74–86.

224. Skidmore AM, Dickinson CH. Colony interaction and hyphal interference between *Septoria nodorum* and phylloplane fungi. 1976. Trans. Br. Mycol. Soc 66:57–64.

225. Smit F, Dubery IA. Cell wall reinforcement in cotton hypocotyls in response to a *Verticillium dahliae* elicitor. 1997. Phytochemistry. 44:811–815.

226. Soares, DJ. 2012. The gray mold of castor bean: A review. In C.J.R. Cumagun, editor, Plant pathology. InTech Publisher, Rijeka, Croatia.

227. Souza Rd, Ambrosini A, Passaglia LM. Plant growth-promoting bacteria as inoculants in agricultural soils. 2015. Genet. Mol. Biol. 38(4):401–19.

228. Srinivasan U, Highley TL, Bruce A. The role of siderophore production in the biological control of wood decay fungi by *Trichoderma* spp. 1995.

229. Stempien E, Pierron RJG, Adendorff I, Van Jaarsveld WJ, Halleen F, Mostert L. Host defence activation and root colonization of grapevine rootstocks by the biological control fungus *Trichoderma atroviride*. 2020. Phytopathologia Mediterranea. 59:615–626.

230. Stevenson-Paulik J, Bastidas RJ, Chiou ST, Frye RA, York JD. Generation of phytate-free seeds in Arabidopsis through disruption of inositol polyphosphate kinases. 2005. PNAS. 102(35):12612–7.

231. Steyaert JM, Weld RJ, Mendoza-Mendoza A, Stewart A. Reproduction without sex: conidiation in the filamentous fungus *Trichoderma*. 2010. Microbiology. 156(10): 2887–2900.

232. Stielow JB, Lévesque CA, Seifert KA, Meyer W, Iriny L, Smits D, Renfurm R, Verkley GJ, Groenewald M, Chaduli D, Lomascolo A, Welti S, Lesage-Meessen L, Favel A, Al-Hatmi AM, Damm U, Yilmaz N, Houbraken J, Lombard L, Quaedvlieg W, Binder M, Vaas LA, Vu D, Yurkov A, Begerow D, Roehl O, Guerreiro M, Fonseca A, Samerpitak K, van Diepeningen AD, Dolatabadi S, Moreno LF, Casaregola S, Mallet S, Jacques N, Roscini L, Egidi E, Bizet C, Garcia-Hermoso D, Martín MP, Deng S, Groenewald JZ, Boekhout T, de Beer ZW, Barnes I, Duong TA, Wingfield MJ, de Hoog GS, Crous PW, Lewis CT, Hambleton S, Moussa TA, Al-Zahrani HS, Almaghrabi OA, Louis-Seize G, Assabgui R, McCormick W, Omer G, Dukik K, Cardinali G, Eberhardt U, de Vries M, Robert V. One fungus, which genes? Development and assessment of universal primers for potential secondary fungal DNA barcodes. 2015. Persoonia. 35:242–63.

233. Struck AW, Thompson ML, Wong LS, Micklefield J. S-adenosyl-methionine-dependent methyltransferases: highly versatile enzymes in biocatalysis, biosynthesis and other biotechnological applications. 2012. Chembiochem. 13:2642–2655.

234. Suresh N, Nelson R. Isolation of antagonistic fungi and evaluation of antifungal activity of the separated metabolite against the red rot of sugarcane pathogen. 2016. European Journal of Experimental Biology. 6(1):15–21.

235. Tamandegani PR, Marik T, Zafari D, Balázs D, Vágvölgyi C, Szekeres A, Kredics L. Changes in Peptaibol Production of Trichoderma Species during In Vitro Antagonistic Interactions with Fungal Plant Pathogens. 2020. Biomolecules. 10(5):730.

236. Tamura K, Peterson D, Peterson N, Stecher G, Nei M, Kumar S. MEGA5: Molecular Evolutionary Genetics Analysis using Maximum Likelihood, Evolutionary Distance, and Maximum Parsimony Methods. 2011. Mol. Biol. and Evol. 28:2731–2739.

237. Tang Y, Tan S, Xue H. Arabidopsis inositol 1,3,4-trisphosphate 5/6 kinase 2 is required for seed coat development. 2013. Acta Biochim Biophys Sin (Shanghai). 45(7):549–60.

238. Tijerino A, Cardoza RE, Moraga J, Malmierca MG, Vicente F, Aleu F, Collado IG, Gutiérrez S, Monte E, Hermosa R. Overexpression of the trichodiene synthase gene tri5 increases trichodermin production and antimicrobial activity in *Trichoderma brevicompactum*. 2011. Fungal Genetics and Biology. 48:3.

239. Tucci M, Ruocco M, De Masi L, De Palma M, Lorito M. The beneficial effect of *Trichoderma* spp. on tomato is modulated by the plant genotype. 2011. Mol Plant Pathol. 12(4):341–54.

240. Varón EH, Moreira MD, and Corredor JP. Effect of *Corythucha gossypii* on castor oil plant leaves: Sampling criteria and control by insecticides. 2010. Rev. Corpoica Ciencia Tecnol. Agropecu. 11:41–47.

241. Verma M, Brar S, Tyagi R, Surampalli R, Valero J. Antagonistic fungi, *Trichoderma* spp.: panoply of biological control. 2007. Biochem. Eng. J. 37:1–20.

242. Vinale F, Nigro M, Sivasithamparam K, Flematti G, Ghisalberti EL, Ruocco M, Varlese R, Marra R, Lanzuise S, Eid A, Woo SL, Lorito M. Harzianic acid: a novel siderophore from *Trichoderma harzianum*. 2013. FEMS Microbiol Lett. 347(2):123–9.

243. Vinale F, Sivasithamparam K, Ghisalberti EL, Marra R, Barbetti MJ, Li H, Woo SL, Lorito M. A novel role for *Trichoderma* secondary metabolites in the interactions with plants. 2008. Physiological and Molecular Plant Pathology. 72(1-3): 80–86.

244. Vinale F, Strakowska J, Mazzei P, Piccolo A, Marra R, Lombardi N, Manganiello G, Pascale A, Woo SL, Lorito M. Cremenolide, a new antifungal, 10-member lactone from

Trichoderma cremeum with plant growth promotion activity. 2016. Nat Prod Res. 30(22):2575–2581.

245. Viterbo A, Wiest A, Brotman Y, Chet I, Kenerley C. The 18mer peptaibols from *Trichoderma virens* elicit plant defence responses. 2007. Mol Plant Pathol. 8(6):737–46.
246. Větrovský T, Kolařík M, Žifčáková L, Zelenka T, Baldrian P. The rpb2 gene represents a viable alternative molecular marker for the analysis of environmental fungal communities. 2016. Mol Ecol Resour. 16(2):388–401.
247. Vitti A, Pellegrini E, Nali C, Lovelli S, Sofo A, Valerio M, Scopa A, Nuzzaci M. *Trichoderma harzianum* T-22 Induces Systemic Resistance in Tomato infected by Cucumber Mosaic Virus. 2016. Frontiers in Plant Sci. 7:1–11.
248. White TJ, Bruns T, Lee S, Taylor J. Amplification and direct sequencing of fungal ribosomal RNA genes for phylogenetics. 1990. In PCR Protocols: A Guide to Methods and Applications. 315–321.
249. Wiest A, Grzegorski D, Xu BW, Goulard C, Rebuffat S, Ebbole DJ, Bodo B, Kenerley C. Identification of peptaibols from *Trichoderma virens* and cloning of a peptaibol synthetase. J Biol Chem. 2002. 277(23):20862–8.
250. Woo SL, Donzelli B, Scala F, Mach R, Harman GE, Kubicek CP, Sorbo GD, Lorito, M. Disruption of the ech42 (Endochitinase-Encoding) Gene Affects Biocontrol Activity in *Trichoderma harzianum* P1. 1999. Molecular Plant-microbe Interactions. 12(5):419–429.
251. Xiao C, Somerville C, Anderson CT. POLYGALACTURONASE INVOLVED IN EXPANSION1 functions in cell elongation and flower development in Arabidopsis. Plant Cell. 2014. 26(3):1018–35.
252. Xie C, Mao X, Huang J, Ding Y, Wu J, Dong S, Kong L, Gao G, Li CY, Wei L. KOBAS 2.0: a web server for annotation and identification of enriched pathways and diseases. 2011. Nucleic Acids Res. 39:W316–22.
253. Xu Q, Ni H, Chen Q, Sun F, Zhou T, Lan Y, Zhou Y. Comparative proteomic analysis reveals the cross-talk between the responses induced by H_2O_2 and by long-term rice black-streaked dwarf virus infection in rice. 2013. PLoS One. 8(11): e81640.
254. Xu X, Zhang L, Zhao W, Fu L, Han Y, Wang K, Yan L, Li Y, Zhang XH, Min DH. Genome-wide analysis of the serine carboxypeptidase-like protein family in *Triticum aestivum* reveals *TaSCPL184-6D* is involved in abiotic stress response. 2021. BMC Genomics 22(1):350.

255. Xue AG, Guo W, Chen Y, Siddiqui I, Marchand G, Liu J, Ren C. Effect of Seed treatment with novel strains of *Trichoderma* spp on establishment and yield of spring wheat. 2017. Crop protect. 96:97–102.

256. Yamaguchi Y, Manita D, Takeuchi T, Kuramochi K, Kuriyama I, Sugawara F, Yoshida H, Mizushina Y. Novel terpenoids, trichoderonic acids A and B isolated from *Trichoderma virens*, are selective inhibitors of family X DNA polymerases. 2010. Biosci Biotechnol Biochem. 74(4):793–801.

257. Yang Y, Hu J, Chen F, Ding D, Zhou C. Development of a SCAR Marker-Based Diagnostic Method for the Detection of the Citrus Target Spot Pathogen *Pseudofabraea citricarpa*. 2018. Biomed Res Int. 7128903.

258. Yao Y, Li Y, Chen Z, Zheng B, Zhang L, Niu B, Meng J, Li A, Zhang J, Wang Q. Biological Control of Potato Late Blight Using Isolates of *Trichoderma*. 2016. Am. J. Potato Res. 93: 33–42.

259. Yan L, Khan RAA. Biological control of bacterial wilt in tomato through the metabolites produced by the biocontrol fungus *Trichoderma harzianum*. 2021. Egypt J Biol Pest Control 31:5.

260. Yassin MT, Mostafa AAF, Al-Askar AA, Sayed SRM, Rady AM. Antagonistic activity of *Trichoderma harzianum* and *Trichoderma viride* strains against some fungal pathogens causing stalk rot disease of maize, *in vitro*. 2021. J. of King Saud Univ. Sci33:101–363.

261. Zeilinger S, Galhaup C, Payer K, Woo SL, Mach RL, Fekete C, Lorito M, Kubicek CP. Chitinase gene expression during mycoparasitic interaction of *Trichoderma harzianum* with its host. 1999. Fungal Genet Biol.. 26(2):131–40.

262. Zeilinger S, Reithner B, Scala V, Peissl I, Lorito M, Mach RL. Signal transduction by Tga3, a novel G protein alpha subunit of *Trichoderma atroviride*. 2005. Appl Environ Microbiol.71(3):1591–7.

263. Zhang C, Wang W, Hu Y. et al. A novel salt-tolerant strain *Trichoderma atroviride* HN082102.1 isolated from marine habitat alleviates salt stress and diminishes cucumber root rot caused by *Fusarium oxysporum*. 2022. BMC Microbiol. 22:67.

264. Zhang F, Ge H, Zhang F, Guo N, Wang Y, Chen L, Ji X, Li C. Biocontrol potential of *Trichoderma harzianum* isolate T-aloe against *Sclerotinia sclerotiorum* in soybean. 2016. Plant Physiol Biochem. 100:64–74.

265. Zhang J, Zhang Y, Zhong Y, Qu Y, Wang T. Ras GTPases Modulate Morphogenesis, Sporulation and Cellulase Gene Expression in the Cellulolytic Fungus *Trichoderma reesei*. 2012. PLOS ONE. 7(11).

266. Zhang X, Gou M, Liu CJ. Arabidopsis Kelch repeat F-box proteins regulate phenylpropanoid biosynthesis via controlling the turnover of phenylalanine ammonia-lyase. 2013. Plant Cell:25(12):4994–5010.

267. Zhang D, Sun W, Singh R, Zheng Y, Cao Z, Li M, Lunde C, Hake S, Zhang Z. GRF-interacting factor1 Regulates Shoot Architecture and Meristem Determinacy in Maize. 2018. The Plant Cell. 30(2):360–374.

268. Zhao D, Ni W, Feng B, Han T, Petrasek MG, Ma H. Members of the Arabidopsis-SKP1-like gene family exhibit a variety of expression patterns and may play diverse roles in Arabidopsis. 2003. Plant Physiol. 133(1):203–17.

269. Zhao Q, Nakashima J, Chen F, Yin Y, Fu C, Yun J, Shao H, Wang X, Wang ZY, Dixon RA. Laccase is necessary and nonredundant with peroxidase for lignin polymerization during vascular development in Arabidopsis. 2013. Plant Cell. 25(10):3976–87.

270. Zheng H, Qiao M, Lv Y, Du X, Zhang K-Q, Yu Z. New Species of *Trichoderma* Isolated as Endophytes and Saprobes from Southwest China. 2021. Journal of Fungi. 7(6):467.

Supplementary Tables

Table S1 The GenBank accession numbers of submitted ITS and D1-D2 sequences amplified using ITS-1F/ITS-4R primers and NL-1/NL-4 primers respectively.

***Trichoderma* strains**	***Trichoderma* species**	**GenBank accession numbers for ITS sequences**	**GenBank accession numbers for D1-D2 sequences**
N13	*Trichoderma asperellum*	MH356723.1	MK411202.1
7316	*Trichoderma asperellum*	MH236427.1	MK411201.1
TV5	*Trichoderma asperellum*	MH393299.1	MK411216.1
TV2B16	*Trichoderma asperellum*	MH393229.1	MK411214.1
TV3	*Trichoderma harzianum*	MH393369.1	MK411220.1
TS4	*Trichoderma harzianum*	MH393371.1	MK411247.1

Table S2. List of RAPD primers used for PCR-based DNA amplification in *Trichoderma* strains.

S. No.	RAPD primers	Primer sequence 5'-3'	S. No.	RAPD primers	Primer sequence 5'-3'
1	OPA-13	CAGCACCCAC	31	OPY-09	AGCAGCGCAC
2	OPA-17	GACCGCTTGT	32	OPY-10	CAAACGTGGG
3	OPA-19	CAAACGTCGG	33	OPY-11	AGACGATGGG
4	OPA-20	GTTGCGATCC	34	OPY-12	AAGCCTGCGA
5	OPA-15	TTCCGAACCC	35	OPY-13	GGGTCTCGGT
6	OPA-03	AGTCAGCCAC	36	OPY-14	GGTCGATCTG
7	OPA-05	AGGGGTCTTG	37	OPY-15	AGTCGCCCTT
8	OPA-08	GTGACGTAGG	38	OPY-16	GGGCCAATGT
9	OPA-09	GGGTAACGCC	39	OPY-17	GACGTGGTGA
10	OPB-10	CTGCTGGGAC	40	OPY-18	GTGGAGTCAG
11	OPB-11	GTAGACCCGT	41	OPY-19	TGAGGGTCCC
12	OPB-12	CCTTGACGCA	42	OPY-20	AGCCGTGGAA
13	OPAJ-04	GAATGCGACC	43	OPZ-01	TCTGTGCCAC
14	OPB-14	TCCGCTCTGG	44	OPZ-02	CCTACGGGGA
15	OPB-15	GGAGGGTGTT	45	OPZ-03	CAGCACCGCA
16	OPX-11	GGAGCCTCAG	46	OPZ-04	AGGCTGTGCT
17	OPX-15	CAGACAAGCC	47	OPZ-05	TCCCATGCTG
18	OPX-16	CTCTGTTCGG	48	OPZ-06	GTGCCGTTCA
19	OPX-17	GACACGGACC	49	OPZ-07	CCAGGAGGAC
20	OPX-18	GACTAGGTGG	50	OPZ-08	GGGTGGGTAA
21	OPX-19	TGGCAAGGCA	51	OPZ-09	CACCCCAGTC
22	OPX-20	CCCAGCTAGA	52	OPZ-10	CCGACAAACC
23	OPY-01	GTGGCATCTC	53	OPZ-11	CTCAGTCGCA
24	OPY-02	CATCGCCGCA	54	OPZ- 12	TCAACGGGAC
25	OPY-03	ACAGCCTGCT	55	OPZ-13	GACTAAGCCC
26	OPY-04	GGCTGCAATG	56	OPZ-15	CAGGGCTTTC
27	OPY-05	GGCTGCGACA	57	OPZ-16	TCCCCATCAC
28	OPY-06	AAGGCTCACC	58	OPZ-17	CCTTCCCACT
29	OPY-07	AGAGCCGTCA	59	OPZ-18	AGGGTCTGTG
30	OPY-08	AGGCAGAGCA	60	OPZ-19	GTGCGAGCAA

61	OPZ-20	ACTTTGGCGG	93	OPE-06	AAGACCCCTC
62	OPC-01	TTCGAGCCAG	94	OPE-07	AGATGCAGCC
63	OPC-02	GTGAGGCGTC	95	OPE-08	TCACCACGGT
64	OPC-03	GGGGGTCTTT	96	OPE-09	CTTCACCCGA
65	OPC-04	CCGCATCTAC	97	OPE-10	CACCAGGTGA
66	OPC-07	GTCCCGACGA	98	OPE-11	GAGTCTCAGG
67	OPC-08	TGGACCGGTG	99	OPE-12	TTATCGCCCC
68	OPC-09	CTCACCGTCC	100	OPE-13	CCCGATTCGG
69	OPC-10	TGTCTGGGTG	101	OPE-14	TGCGGCTGAG
70	OPC-11	AAAGCTGCGG	102	OPE-15	ACGCACAACC
71	OPD-01	ACCGCGAAGG	103	OPE-16	GGTGACTGTG
72	OPD-02	GGACCCAACC	104	OPE-17	CTACTGCCGT
73	OPD-03	GTCGCCGTCA	105	OPE-18	GGACTGCAGA
74	OPD-04	TCTGGTGAGG	106	OPE-19	ACGGCGTATG
75	OPD-05	TGAGCGGACA	107	OPJ-01	CCCGGCATAA
76	OPD-06	ACCTGAACGG	108	OPJ-02	CCCGTTGGGA
77	OPD-07	TTGGCACGGG	109	OPJ-04	CCGAACACGG
78	OPD-08	GTGTGCCCCA	110	OPJ-05	CTCCATGGGG
79	OPD-09	CTCTGGAGAC	111	OPJ-06	TCGTTCCGCA
80	OPD-10	GGTCTACACC	112	OPJ-07	CCTCTCGACA
81	OPD-11	AGCGCCATTG	113	OPJ-08	CATACCGTGG
82	OPD-12	CACCGTATCC	114	OPJ-09	TGAGCCTCAC
83	OPD-13	GGGGTGACGA	115	OPJ-10	AAGCCCGAGG
84	OPD-14	CTTCCCCAAG	116	OPJ-11	ACTCCTGCGA
85	OPD-15	CATCCGTGCT	117	OPJ-12	GTCCCGTGGT
86	OPD-16	AGGGCGTAAG	118	OPJ-13	CCACACTACC
87	OPD-17	TTTCCCACGG	119	OPJ-14	CACCCGGATG
88	AP 106	AAGACCCCTC	120	OPJ-15	TGTAGCAGGG
89	OPD-20	ACCCGGTCAC	121	OPJ-16	CTGCTTAGGG
90	OPE-01	CCCAAGGTCC	122	OPJ-17	ACGCCAGTTC
91	OPE-04	GTGACATGCC	123	OPJ-18	TGGTCGCAGA
92	OPE-05	TCAGGGAGGT	124	OPJ-19	GGACACCACT

125	OPJ-20	AAGCGGCCTC	157	OPL-13	ACCGCCTGCT
126	OPK-01	CATTCGAGCC	158	OPL-14	GTGACAGGCT
127	OPK-02	GTCTCCGCAA	159	OPL-15	AAGAGAGGGG
128	OPK-04	CCGCCCAAAC	160	OPL-16	AGGTTGCAGG
129	OPK-05	TCTGTCGAGG	161	OPK-06	CACCTTTCCC
130	OPD-19	CTGGGGACTT	162	OPL-18	ACCACCCACC
131	OPK-07	AGCGAGCAAG	163	OPL-19	GAGTGGTGAC
132	OPK-08	GAACACTGGG	164	OPL-20	TGGTGGACCA
133	OPK-09	CCCTACCGAC	165	OPM-01	GTTGGTGGCT
134	OPK-10	GTGCAACGTG	166	OPM-02	ACAACGCCTC
135	OPK-11	AATGCCCCAG	167	OPM-03	GGGGGATGAG
136	OPK-12	TGGCCCTCAC	168	OPM-04	GGCGGTTGTC
137	OPK-13	GGTTGTACCC	169	OPM-05	GGGAACGTGT
138	OPK-14	CCCGCTACAC	170	OPM-06	CTGGGCAACT
139	OPK-15	CTCCTGCCAA	171	OPM-07	CCGTGACTCA
140	OPK-16	GAGCGTCGAA	172	OPM-08	TCTGTTCCCC
141	OPK-17	CCCAGCTGTG	173	OPM-09	GTCTTGCGGA
142	OPK-18	CCTAGTCGAG	174	OPM-10	TCTGGCGCAC
143	OPK-19	CACAGGCGGA	175	OPM-11	GTCCACTGTG
144	OPK-20	GTGTCGCGAG	176	OPM-12	GGGACGTTGG
145	OPL-01	GGCATGACCT	177	OPM-13	GGTGGTCAAG
146	OPL-02	TGGGCGTCAA	178	OPM-14	AGGGTCGTTC
147	OPL-03	CCAGCAGCTT	179	OPM-15	GACCTACCAC
148	OPL-04	GACTGCACAC	180	OPM-16	GTAACCAGCC
149	OPL-05	ACGCAGGCAC	181	OPM-17	TCAGTCCGGG
150	OPL-06	GAGGGAAGAG	182	OPM-18	CACCATCCGT
151	OPL-07	AGGCGGGAAC	183	OPM-19	CCTTCAGGCA
152	OPL-08	AGCAGGTGGA	184	OPM-20	AGGTCTTGGG
153	OPL-09	TGCGAGAGTC	185	OPN-01	CTCACGTTGG
154	OPL-10	TGGGAGATGG			
155	OPL-11	ACGATGAGCC			
156	OPL-12	GGGCGGTACT			

Table S3 Analysis of percentage polymorphism obtained with RAPD markers in six *Trichoderma* strains.

S. No.	RAPD marker	Total no. of amplified bands	Approximate band size (bp)		No. of Polymorphic bands	Polymorphism (%)
			Min	Max		
1.	OPA-13	23	250	1200	11	47.82
2.	OPA-17	22	150	1500	22	100
3.	OPA-19	22	200	650	22	100
4.	OPA-20	20	250	700	8	40
5.	OPA-15	0	0	0	0	0
6.	OPA-03	0	0	0	0	0
7.	OPA-05	6	450	850	6	100
8.	OPA-08	0	0	0	0	0
9.	OPA-09	0	0	0	0	0
10.	OPB-10	0	0	0	0	0
11.	OPB-11	0	0	0	0	0
12.	OPB-12	0	0	0	0	0
13.	OPAJ-04	0	0	0	0	0
14.	OPB-14	12	200	450	6	50
15.	OPB-15	0	0	0	0	0
16.	OPX-11	19	650	1500	7	36.84
17.	OPX-15	7	500	600	1	14.28
18.	OPX-16	14	450	950	14	100
19.	OPX-17	0	0	0	0	0
20.	OPX-18	28	250	1200	10	35.71
21.	OPX-19	32	250	1200	8	25
22.	OPX-20	18	500	1000	0	0
23.	OPY-01	20	450	1100	8	40
24.	OPY-02	46	250	1200	22	47.82
25.	OPY-03	26	350	1500	14	53.84
26.	OPY-04	28	400	1500	22	78.57
27.	OPY-05	40	100	1500	28	70
28.	OPY-06	40	200	1500	22	55

29.	OPY-07	12	250	1100	6	50
30.	OPY-08	10	350	550	10	100
31.	OPY-09	28	250	1200	22	78.57
32.	OPY-10	4	400	700	4	100
33.	OPY-11	22	300	1200	10	45.45
34.	OPY-12	15	450	1200	9	60
35.	OPY-13	28	500	1100	22	78.57
36.	OPY-14	28	350	1500	22	78.57
37.	OPY-15	28	300	850	16	57.14
38.	OPY-16	36	100	1200	36	100
39.	OPY-17	14	450	1200	14	100
40.	OPY-18	23	200	1000	23	100
41.	OPY-19	42	200	1000	24	57.14
42.	OPY-20	22	350	1200	10	45.45
43.	OPZ-01	16	400	1500	16	100
44.	OPZ-02	6	550	1200	6	100
45.	OPZ-03	22	300	1000	16	72.72
46.	OPZ-04	8	350	1100	8	100
47.	OPZ-05	6	450	850	6	100
48.	OPZ-06	15	150	1000	9	60
49.	OPZ-07	16	300	900	16	100
50.	OPZ-08	0	0	0	0	0
51.	OPZ-09	0	0	0	0	0
52.	OPZ-10	14	300	1100	14	100
53.	OPZ-11	0	0	0	0	0
54.	OPZ- 12	0	0	0	0	0
55.	OPZ-13	0	0	0	0	0
56.	OPZ-15	0	0	0	0	0
57.	OPZ-16	0	0	0	0	0
58.	OPZ-17	0	0	0	0	0
59.	OPZ-18	0	0	0	0	0
60.	OPZ-19	17	200	950	17	100
61.	OPZ-20	17	350	1200	17	100

62.	OPC-01	32	300	1100	20	62.5
63.	OPC-02	12	450	1500	12	100
64.	OPC-03	0	0	0	0	0
65.	OPC-04	23	300	1500	23	100
66.	OPC-07	39	300	1200	33	84.61
67.	OPC-08	17	450	1200	17	100
68.	OPC-09	25	200	1200	25	100
69.	OPC-10	10	300	1100	10	100
70.	OPC-11	38	200	1200	26	68.42
71.	OPD-01	0	0	0	0	0
72.	OPD-02	25	350	1200	19	76
73.	OPD-03	34	150	950	34	100
74.	OPD-04	4	850	120	4	100
75.	OPD-05	9	350	500	9	100
76.	OPD-06	6	600	1500	6	100
77.	OPD-07	11	350	900	11	100
78.	OPD-08	16	350	1200	10	62.5
79.	OPD-09	0	0	0	0	0
80.	OPD-10	9	500	1000	9	100
81.	OPD-11	15	300	1000	15	100
82.	OPD-12	4	450	750	4	100
83.	OPD-13	18	250	750	12	66.66
84.	OPD-14	0	0	0	0	0
85.	OPD-15	25	400	950	25	100
86.	OPD-16	2	500	-	2	100
87.	OPD-17	0	0	0	0	0
88.	OPD-18	4	300	400	4	100
89.	OPD-19	0	0	0	0	0
90.	OPD-20	4	450	750	4	100
91.	OPE-01	0	0	0	0	0
92.	OPE-04	30	250	1500	12	40
93.	OPE-05	26	3350	1500	26	100
94.	OPE-06	27	350	1500	21	77.78

95.	OPE-07	35	300	1200	11	31.43
96.	OPE-08	16	450	1500	10	62.50
97.	OPE-09	10	350	600	10	100
98.	OPE-10	6	1200	-	0	0
99.	OPE-11	9	550	750	9	100
100.	OPE-12	18	200	1200	12	66.66
101.	OPE-13	24	300	900	12	50
102.	OPE-14	21	300	1200	15	71.43
103.	OPE-15	14	450	900	14	100
104.	OPE-16	0	0	0	0	0
105.	OPE-17	0	0	0	0	0
106.	OPE-18	8	400	1000	8	100
107.	OPE-19	20	350	1500	14	70
108.	OPJ-01	6	500	1000	6	100
109.	OPJ-02	0	0	0	0	0
110.	OPJ-04	0	0	0	0	0
111.	OPJ-05	18	450	1200	12	66.66
112.	OPJ-06	16	600	1500	16	100
113.	OPJ-07	20	400	1200	8	40
114.	OPJ-08	22	400	1500	4	18.18
115.	OPJ-09	12	750	1100	6	50
116.	OPJ-10	23	350	1500	5	21.74
117.	OPJ-11	18	400	1200	12	66.66
118.	OPJ-12	12	500	1100	12	100
119.	OPJ-13	10	500	1000	10	100
120.	OPJ-14	0	0	0	0	0
121.	OPJ-15	0	0	0	0	0
122.	OPJ-16	16	400	900	16	100
123.	OPJ-17	20	600	1500	14	70
124.	OPJ-18	28	250	1500	28	100
125.	OPJ-19	28	400	1200	4	14.29
126.	OPJ-20	22	500	1500	16	72.72
127.	OPK-01	15	350	1000	15	100

128.	OPK-02	16	750	1500	4	25
129.	OPK-04	25	350	1000	7	28
130.	OPK-05	0	0	0	0	0
131.	OPK-06	0	0	0	0	0
132.	OPK-07	17	300	1200	17	100
133.	OPK-08	11	500	950	11	100
134.	OPK-09	0	0	0	0	0
135.	OPK-10	24	300	1500	24	100
136.	OPK-11	11	250	1500	11	100
137.	OPK-12	18	350	900	18	100
138.	OPK-13	0	0	0	0	0
139.	OPK-14	15	250	850	15	100
140.	OPK-15	14	250	1100	14	100
141.	OPK-16	16	300	1000	16	100
142.	OPK-17	14	200	550	14	100
143.	OPK-18	0	0	0	0	0
144.	OPK-19	36	350	900	12	33.33
145.	OPK-20	16	300	1500	16	100
146.	OPL-01	24	200	1000	18	75
147.	OPL-02	6	250	-	0	0
148.	OPL-03	20	500	1200	2	10
149.	OPL-04	17	200	1500	17	100
150.	OPL-05	14	500	650	2	14.29
151.	OPL-06	10	300	850	4	40
152.	OPL-07	18	400	750	6	33.33
153.	OPL-08	44	100	600	8	18.18
154.	OPL-09	0	0	0	0	0
155.	OPL-10	5	250	300	5	100
156.	OPL-11	25	250	1200	19	76
157.	OPL-12	14	300	1000	14	100
158.	OPL-13	27	250	1500	27	100
159.	OPL-14	22	300	1200	22	100
160.	OPL-15	29	350	1500	29	100

161.	OPL-16	26	300	1100	26	100
162.	OPL-18	17	300	1500	17	100
163.	OPL-19	16	200	650	16	100
164.	OPL-20	10	250	750	10	100
165.	OPM-01	34	200	900	34	100
166.	OPM-02	35	350	1100	23	65.71
167.	OPM-03	0	0	0	0	0
168.	OPM-04	24	450	1200	12	50
169.	OPM-05	26	200	1000	26	100
170.	OPM-06	34	200	1500	22	64.70
171.	OPM-07	0	0	0	0	0
172.	OPM-08	10	400	900	10	100
173.	OPM-09	10	300	550	4	40
174.	OPM-10	16	400	1000	10	62.5
175.	OPM-11	30	350	1100	0	0
176.	OPM-12	22	450	1200	16	72.72
177.	OPM-13	29	250	1200	29	100
178.	OPM-14	27	450	1200	9	33.33
179.	OPM-15	0	0	0	0	0
180.	OPM-16	0	0	0	0	0
181.	OPM-17	0	0	0	0	0
182.	OPM-18	0	0	0	0	0
183.	OPM-19	18	200	700	18	100
184.	OPM-20	12	500	800	12	100
185.	OPN-01	6	300	0	0	0

Table S4 The list of primers and internal controls used for quantitative Real Time-Polymerase Chain Reaction (RT-qPCR).

S. No.	Gene Name	Primer Sequences (5'to 3')	Amplicon Size (bp)
1	Peroxidase 12 (*PER12*)	F: TGAAGCACAAAGCAGACCAC R: ATCGCATCCCATAACAAAGC	181
2	Serine/threonine-protein kinase (*FLS2*)	F: AGAAAAGGCGTCCTTCCCTG R: GTGCTCTGCTAGTGGCTTCAC	179
3	Pathogenesis related protein 5 (*PR5*)	F: ATGCTGCTGTGTTTTCAATC R: GCTTGGATATTGACCGAGTA	133
4	Endoglucanase (*ENDO*)	F: TTTGCCAGTCACAACTACAGGGACG R:GAACACCCTGATAGCCCTCCTGACCA	350
5	Wound induced protein 2 (*WIN2*)	F: CCTAATAACCTATGTTGTAGCCAG R: AGTATTTGTCACCCTCAAGCACT	350
6	WRKY Transcription factor (*WRKY71*)	F: CAAGATGGAGTCTCTACAAGATGA R: ATTGGATTCATACACCTCATAGCAT	172
7	Disease resistance protein (*RPV1*)	F: ATTGAAGAGTCCAAAATCTCAGT R: CCACCCATTCCCCATATTCCAACA	498
8	Zinc finger protein (*ZAT5*)	F: GAAGAAGAGGATATGGCGAAT R: AATGAAAGTGTAGTGTTCGTAT	320
9	Disease resistance protein (*RPS2*)	F: TTGTTAGATGATGTTTGGGAAG R: TCCATTCTTCCTCAGTCTCTTTATT	327
10	Elongation Factor 1B (*EFB1*)	F: GAAAAAGTTGGAGGAGGCAG R: AGGGAGTCCACAGAAACAAG	144
11	Actin (*ACT*)	F: GAGAGGTTCCGGTGCCCAGA R: GGGATGCGAGGATGGATCCTC	450

Supplementary Figures

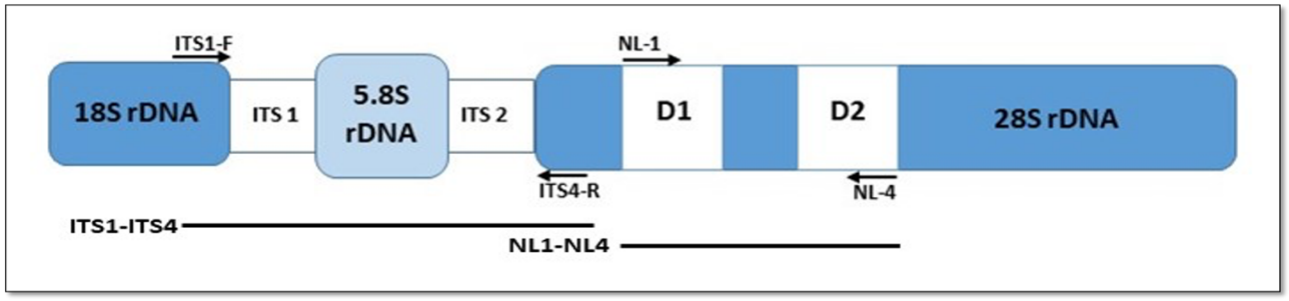


Figure S1 The Schematic diagram of the ITS and D1-D2 regions amplified using universal primers.

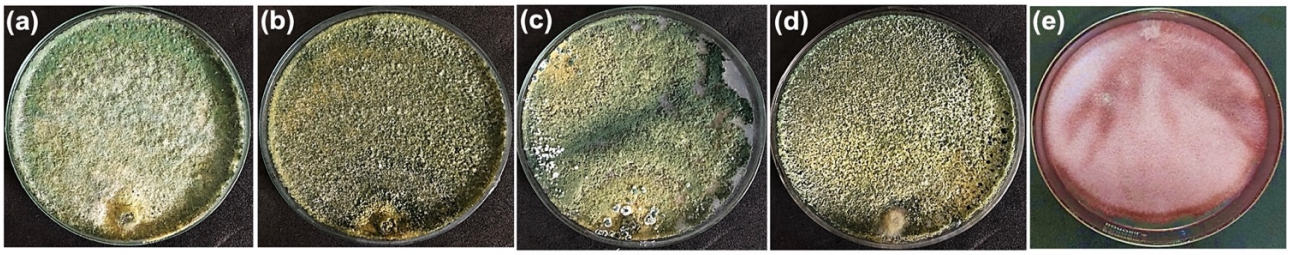


Figure S2 Fungal cultures of *Trichoderma asperellum* strains grown on Potato Dextrose Agar (PDA) and *Fusarium oxysporum ricini* grown on CMC medium 7 days-post plating. *Trichoderma asperellum* 7316 (a), *Trichoderma asperellum* N13 (b), *Trichoderma asperellum* TV5 (c), *Trichoderma asperellum* TV2B16 (d) and, *F. oxysporum ricini* (e).

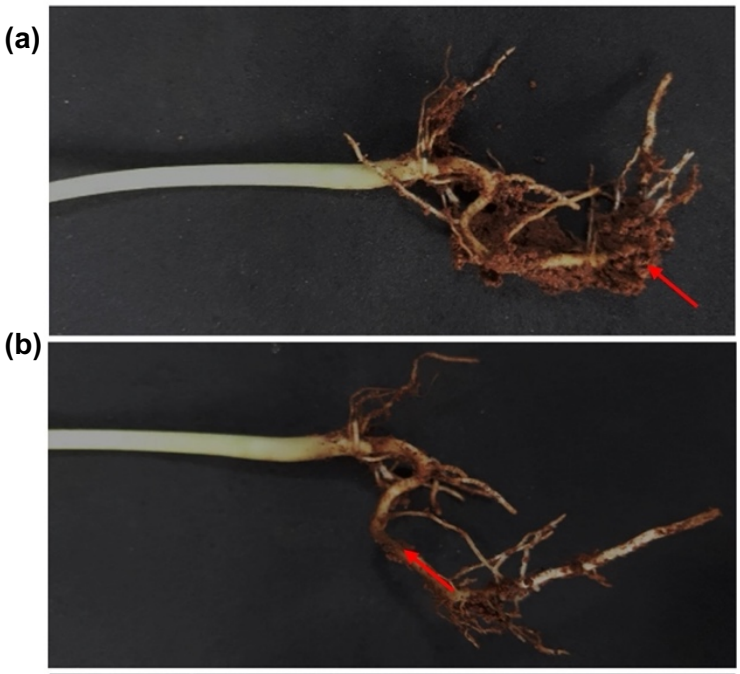


Figure S3 Bulk and rhizosphere soil collection from castor roots. Loosely adhering bulk soil that falls off from the root on shaking vigorously (a) and rhizosphere soil that tightly clings to the root surface (b).

Publications from the study

Biocatalysis and Agricultural Biotechnology 54 (2023) 102945



Contents lists available at ScienceDirect

Biocatalysis and Agricultural Biotechnology

journal homepage: www.elsevier.com/locate/bab





Characterization of *Trichoderma* strains for novel species-specific markers by multiplex PCR and antagonistic property against *Alternaria ricini* in castor (*Ricinus communis* L.)

Doris A Pradhan [a, 1], Prathyusha Bagagoni [a, 1], Saharika Slathia [a], R. Durga Prasad [b], Ragiba Makandar [a, *]

[a] *Department of Plant Sciences, School of Life Sciences, University of Hyderabad, Prof. C.R. Rao Road, Gachibowli, Hyderabad, 500046, India*
[b] *Indian Institute of Oilseeds Research, Rajendranagar, Hyderabad, Telangana, 500030, India*

ARTICLE INFO

Handling Editor: Dr. Ching Hou

Keywords:
Antimicrobial competence
Internal transcribed sequence
Multiplex PCR
Rhizosphere
Sequence characterized amplified region
Trichoderma

ABSTRACT

The study aimed at characterizing six *Trichoderma* strains isolated from the rhizospheric soil of castor growing region of Telangana, India. Microscopic examination and sequencing of ribosomal DNA (rDNA) using internal transcribed spacer (ITS) and D1-D2 region-specific primers revealed them as members of *Trichoderma* sp. Whereas the phylogenetic analysis revealed four of those strains as *Trichoderma asperellum,* two strains were confirmed as *Trichoderma harzianum* with a high sequence similarity of >99%. Further, multiplex PCR results with *Trichoderma*-specific primers; *TEF1* (translation elongation factor 1) and *rpb2* (the second largest subunit of RNA polymerase II) gene-specific primers confirmed the findings resulting from the phylogenetic analysis. To develop a set of sequence characterized amplified region (SCAR) markers, these strains were screened with 185 random amplified polymorphic DNA (RAPD) primers. A pairwise comparison of correlation of coefficient values determined from the RAPD-based genetic similarity analysis revealed that TV3 and TS4 strains were closely related to each other (0.98) confirming them as *T. harzianum* while N13, 7316, TV5, and TV2B16 strains formed a different cluster with *T. asperellum* strains. A set of novel SCAR markers were developed to distinguish these two species, *T. asperellum* and *T. harzianum* including the reported *Trichoderma* strains as Ex-type strains. *T. harzianum* strains had extremely low sporulation ability to be tested for biocontrol properties. Of the four *T. asperellum* strains, 7316 followed by N13 demonstrated high antagonistic ability against the fungal pathogen, *Alternaria ricini* indicating these strains as potential biocontrol agents to limit *Alternaria* infection in castor.

1. Introduction

The fungal members of the genus *Trichoderma* have been recognized as promising biological control agents (BCAs) to minimize pathogen attacks on plants. The *Trichoderma* fungi are mostly soil-borne, green spored, opportunistic and avirulent plant symbionts that are found to be harbouring predominantly in the plant-root ecosystems (Harman et al., 2004). Previous studies have demonstrated the ability of *Trichoderma* to promote growth and development by colonizing the roots of plants (Guzman-Guzman et al., 2018). Application of *Trichoderma harzianum* strain, T-22 induced systemic resistance in tomato against cucumber mosaic virus (Vitti

* Corresponding author.
E-mail address: mragiba@uohyd.ac.in (R. Makandar).
[1] Equal Contribution.

https://doi.org/10.1016/j.bcab.2023.102945
Received 2 August 2023; Received in revised form 8 October 2023; Accepted 12 November 2023
Available online 17 November 2023
1878-8181/© 2023 Elsevier Ltd. All rights reserved.

et al., 2016). Likewise, biopriming with *Trichoderma asperellum* showed dose-dependent modulation of plant growth in vegetable crops like cucumber, tomato, brinjal, chilli, guar, and okra (Singh et al., 2016). Further, seed treatment with *Trichoderma* spp. activated defence responses against pathogens, accompanied by an increase in the seed yield in wheat crops (Xue et al., 2017).

Trichoderma strains isolated from the rhizosphere may vary in their ability to perform the functions of a BCA. Therefore, it is necessary to screen *Trichoderma* strains to assess their genetic variability based on morphological and molecular differences. This enables the detection of potential strain(s) of *Trichoderma* to utilize them as a BCA for disease control. In order to do so, it is imperative to have precise molecular methods that can reveal reliable phylogenetic information. Though, assessing molecular differences through PCR-based amplification and sequencing of the internal transcribed spacer (ITS) region (White et al., 1990) and D1-D2 region of nuclear ribosomal DNA (Kwiatkowski et al., 2012) have been routinely used to conduct phylogenetic studies, it is important to include other gene loci as well to distinguish more closely interrelated species. Therefore, combining the information from other genetic loci data which include partial translation elongation factor 1-alpha (*TEF1*) and second largest subunit of RNA polymerase II (*rpb2*) sequences have been suggested for accurate phylogenetic analysis (Chaverri et al., 2015; Dou et al., 2018, 2020; Cai and Druzhinina, 2021). Further, investigating for DNA based polymorphism among the *Trichoderma* strains would not only reveal nucleotide level variability (Sagar et al., 2011) but also enable to develop markers for the detection of *Trichoderma* in samples. The study was aimed at morphological and molecular screening of *Trichoderma* strains using DNA-based markers which include random amplified polymorphic DNA (RAPD), sequence characterized amplified region (SCAR), and *Trichoderma* species-specific markers. The study also involved identification of a new set of SCAR markers to detect *Trichoderma* strains. Further, the antimicrobial competence of the *Trichoderma* strains was tested against *Alternaria ricini,* the leaf spot disease of castor through confrontation plate and detached leaf assays to identify the potential biocontrol agents against *A. ricini* and the findings are presented.

2. Materials and methods

2.1. Fungal isolation and culture conditions

Trichoderma strains; N13, 7316, TV5, TV2B16, TV3 and TS4 isolated from the rhizospheric soil of castor growing region in Telangana region in India were obtained from the Indian Institute of Oilseeds Research (IIOR), Hyderabad. Single-spored cultures were grown at 25 °C on Potato Dextrose Agar (PDA) for 7 days as shown in Fig. S1. Two strains of *Trichoderma*; *Trichoderma asperellum* Ta05 (JN104485, JN104500) and *Trichoderma harzianum* Th03 (JN039047, JN0390101) were obtained from Indian type Culture Collection (ITCC) (Devi et al., 2012) and included as controls.

The fungal pathogen, *Alternaria ricini* was isolated from the lesions of *Alternaria* leaf spot disease on castor, grown in greenhouse conditions at the University of Hyderabad (UoH) (Fig. S2). The diseased leaves were surface sterilized with 0.5% sodium hypochlorite solution for 2 min followed by washing three times with sterile distilled water. The mycelial growth from the pathogen infected leaves was streaked with a sterile loop on PDA plates and incubated at 25 °C. A single spore isolated from a single colony was plated on PDA medium for preparing a pure culture for inoculation. The spores were confirmed by examining with a light microscope (Leica model; make: Olympus-IX81) at 40X. For effective sporulation, *A. ricini* was cultured in a sporulation (S) medium prepared by dissolving 20 g sucrose and 30 g $CaCO_3$ per litre of distilled water and the media was autoclaved at 121 °C at 15 psi for 15 min before inoculation.

2.2. Microscopic examination of trichoderma strains

A specimen of each of the *Trichoderma* strains grown on PDA medium was transferred to sterilized glass slides using a sterilized inoculation loop and examined under the scanning confocal microscope (M/s Carl Zeiss make; Model no- LSM 880). Monitoring of mycelial growth rate, colony appearance, and structural features including phialides and spores as described previously (Bissett, 1984, 1991a, 1991b, 1991c) was carried out for phenotypic evaluation of the strains.

2.3. DNA extraction

Genomic DNA was extracted individually from the *Trichoderma* strains using CTAB buffer following the method given by Jaisani and Pandey (2017) with modifications. Fungal mycelia was ground to a fine powder using liquid nitrogen. CTAB buffer was added and the mixture was incubated for 15 min at room temperature with occasional mixing followed by centrifugation at 12,500 rpm for 10 min. The supernatant was transferred to a sterile 1.5 mL Eppendorf tube. An equal volume of phenol:chloroform:isoamyl alcohol (25:24:1) was added to the supernatant and gently mixed, followed by centrifugation at 12,500 rpm for 15 min. Genomic DNA was precipitated by adding an equal volume of isopropanol to the upper aqueous layer and the samples were chilled at −20 °C for 1 h followed by centrifugation at 12,500 rpm for 15 min. The precipitated DNA was washed in 70% ethanol and centrifuged at 12,500 rpm for 5 min. The DNA was air-dried and re-suspended in 1*X* Tris-EDTA (TE) buffer. The amount of DNA was quantified using UV Spectrophotometer (Hitachi-Hi Tech Co. Ltd.) at 260 nm absorbance and run on 0.8% agarose gel electrophoresis to assess the quality of the DNA.

2.4. PCR of ITS and D1-D2 regions of rDNA and sequencing

The schematic diagram of the ITS and D1-D2 regions amplified using universal primers is presented in Fig. S3A. The PCR amplification of the ITS region was carried out with the primer pair, 1 F (5′-TCCGTAGGTGAACCTTGCGG-3′) and 4 R (5′-TCCTCCGCTTATTGATATGC-3′) (White et al., 1990; Chakraborty et al., 2010) as shown in Fig. S3B. The PCR amplification of D1-D2 region was carried out using NL-1 (5′-GCATATCAATAAGCGGAGGAAAAG-3′) and NL-4 (5′-GGTCCGTGTTTCAAGACGG-3′) (Kwiatkowski et al., 2012) primers as shown in Fig. S3C. A 1:10 dilution of the genomic DNA (20 ng) from each of the *Trichoderma*

strains was used as a template in a 25 μLreaction mix containing 9 μL of PCR grade water, 2 μL each of the primers (10 pmol), 3 μL of 1:10 diluted genomic DNA and 9 μL of Emerald Master-mix (Emerald GT PCR MM – 2*X* premix; Takara brand).

The reaction cycle for ITS amplification was set as follows: an initial denaturation step at 95 °C for 5 min followed by 30 cycles with denaturation at 95 °C for 30 s, annealing at 55 °C for 45 s and extension at 72 °C for 30 s, followed with a final extension of 10 min at 72 °C and storage at 4 °C. The PCR conditions for D1-D2 region amplification were set at an initial denaturation step at 95 °C for 2 min, followed by 30 cycles with denaturation at 94 °C for 15 s, annealing at 55 °C for 30 s, extension at 68 °C for 2 min followed by a final extension of 5 min at 68 °C and storage at 4 °C. The PCR products were subjected to electrophoresis for 40 min on a 1.2% (w/v) agarose gel (HiMedia Laboratories Pvt. Ltd.), stained with ethidium bromide (HiMedia Laboratories Pvt. Ltd.) and observed under UV *trans*-illuminator. The resulting amplicons were excised and purified using Nucleospin Gel (Macherey-Nagel brand) and PCR Clean-up kit (Takara brand) according to the manufacturer's instructions and confirmed through a re-run on a 1.2% agarose gel. The amplified DNA products were sequenced and submitted to GenBank (Table S1).

2.5. In-silico and phylogenetic analysis of ITS and D1-D2 sequences

A homology-based search was carried out to compare ITS and D1-D2 DNA sequences of the *Trichoderma* strains against previously reported *Trichoderma* using BLASTn and multiple sequence alignment tool; Clustal Omega (EMBL-EBI). The ITS and D1-D2 sequence information of other reported *Trichoderma* strains were obtained from National Center for Biotechnology Information (NCBI) public domain. The phylogenetic tree was inferred based on the neighbour-joining method using sequences amplified with ITS-1F/ITS-4R and NL-1/NL-4 primers. Phylogenetic analyses was performed using MEGA10 (Molecular Evolutionary Genetics Analysis) program (Tamura et al., 2011). A parsimony analysis was performed using a heuristic search, with a starting tree obtained via stepwise addition, with random addition of sequences with 1000 replicates.

2.6. PCR for TEF1 and rpb2 genes

The primer pair, T2AF (5′-CTCTGCCGTTGACTGTGAACG-3′) and T2AR (5′-CGATAGTGGGGTTGCCGTCAA-3′) which is specific to *T. asperellum* (Devi et al., 2017) was used to amplify translation elongation factor1 (*TEF1*). As described previously, the PCR was set up using 10 pmol of primer concentration with optimal conditions of an initial denaturation step at 94 °C for 1 min followed by 30 cycles of 45 s at 94 °C, 45 s at 62 °C, and 1 min at 72 °C, followed by a final extension step for 10 min at 72 °C and storage at 4 °C. Similarly, the primer pair Th1F (5′-TTGCATGGGTTCGCTAAAGG-3′) and Th1R (5′-TCTTGTCAGCATCATGGCCGT-3′) which is specific to *T. harzianum* (Devi et al., 2017) was used to amplify the second largest subunit of RNA polymerase II (*rpb2*). The PCR reaction is as follows: an initial denaturation step at 94 °C for 2 min followed by 35 cycles of 30 s at 94 °C, 30 s at 57.30 °C, and 1 min at 72 °C, followed by a final extension step for 10 min at 72 °C and storage at 4 °C.

To verify the specificity and sensitivity of the primers along with simultaneous detection of PCR products from the two different loci, a multiplex PCR was carried out using both sets of primers simultaneously in the same PCR (Prabhakaran et al., 2015) for all the strains of *Trichoderma*. The multiplex PCR assay was repeated three times to ensure reproducibility of the results. The multiplex PCR conditions were same as those described above to amplify *TEF1* gene. The PCR products were resolved on a 1.2% agarose gel containing ethidium bromide. The PCR with non-template DNA was included as the negative control.

2.7. PCR for trichoderma specific SCAR markers

The SCAR primer sets; 2F2/2R2 and 2F2/2R3 (Perez et al., 2014) specific to *T. harzianum* were used. PCR conditions were set up as previously described with an initial denaturation step at 94 °C for 3 min, followed by 30 cycles with denaturation at 94 °C for 1 min, annealing at 62 °C for 1 min, extension at 72 °C for 1 min and a final extension of 7 min at 72 °C and storage at 4 °C. To confirm the specificity of primers, a multiplex PCR was carried out using both sets of primers simultaneously in the same PCR for all the strains of *Trichoderma* with the same PCR conditions. The PCR products were resolved on a 1.2% agarose gel containing ethidium bromide. The PCR with non-template DNA was included as the negative control.

2.8. Random amplified polymorphic DNA (RAPD) profiling and data analysis

A total of 185 oligonucleotide primers (ten-mers) (Table S2) obtained from Operon Technologies Inc., USA (synthesized by using M/s Bioserve Biotechnologies (I) Pvt. Ltd) were used to screen the *Trichoderma* strains. PCR reaction involved a 20 μL reaction mixture for each primer containing 100 ng of genomic DNA, 10 μL of Emerald master-mix (Emerald GT PCR MM – 2*X* premix; Takara brand), and 2.5 μL of the primer (5 pmol). The PCR parameters were as follows: initial denaturation at 94 °C for 5 min followed by 40 cycles: denaturation at 94 °C for 1 min, annealing at 36 °C for 1 min, extension at 72 °C for 2 min, with a final extension at 72 °C for 7 min and storage at 4 °C. Each reaction was repeated twice to assess the consistency of the DNA band profiles. The PCR products were resolved on a 1.2% agarose gel containing Ethidium bromide.

The PCR products from the gels were scored as ‘1’ and ‘0’ based on the presence or absence of bands respectively. The prominent and reproducible bands alone were considered for statistical analysis. The significance of polymorphism detected between the strains was tested by the DARwin program (version 6.0.18) and phylogenetic trees were drawn to analyse the relatedness among the fungal strains and with other reported *Trichoderma* strains as described previously. The correlation coefficients were calculated for the mean values of the size of amplicons.

2.9. Developing and testing new SCAR markers

The polymorphic DNA bands generated by RAPD primers; OPZ-06 and OPK-10 primers were excised from the gel and purified by Nucleospin Gel (Macherey-Nagel brand) and PCR Clean-up kit (Takara brand) according to manufacturer's instructions and after-

wards sequenced. The sequences obtained were aligned using Clustal Omega (EMBL-EBI). Primers were designed using the Primer3 tool from conserved regions of *T. asperellum* and *T. harzianum* strains respectively. The SCAR primer pairs; T1 and T2 was designed as forward and reverse primer pairs for *T. asperellum* while T3 and T4 was designed as forward and reverse primers for identification of *T. harzianum* respectively. The PCR parameters comprised an initial denaturation at 94 °C for 5 min followed by 40 cycles with denaturation at 94 °C for 1 min, annealing temperature gradient from 40 to 64 °C for 1 min, extension at 72 °C for 2 min, with a final extension at 72 °C for 7 min and storage at 4 °C. Multiplex PCR was performed using the two primer sets simultaneously in the same PCR for all the strains. *Trichoderma* strains; *T. asperellum* Ta05 and *T. harzianum* Th03 (ex-type strains) along with *T. longibrachiatum* and *T. virens* were used as to validate the specificity of the designed SCAR primers.

2.10. Confrontation plate assays

Trichoderma strains were tested for their antagonistic activity against *A. ricini,* causing leaf spot disease in castor-oil plant. 5 mm diameter mycelial discs were taken from the actively growing end of seven-day-old *Trichoderma* cultures and placed on Petri plates containing PDA (supplemented with CaCO3 0.03%). The fungal discs of *Alternaria* were placed opposite to the *Trichoderma* discs. Both *Trichoderma* and *Alternaria* discs were placed at equal distance from the periphery. Each of the *Trichoderma* strains was placed at the opposite periphery 48 h post inoculation (hpi) with *Alternaria* discs owing to the slow growth of the fungus. The PDA plates cultured only with *Trichoderma* and *Alternaria* discs were included as negative controls. The inoculated plates were incubated at 25 °C for 7 days. Radial growth of the fungal pathogen and *Trichoderma* was measured from 4 to 7 days post inoculation (dpi). The experiment was repeated three times with ten replications each and mean values were computed. The percentage inhibition was calculated as given below:

$$\% \text{ Inhibition } (\Delta) = \{(D1 - D2) / D1\} \text{ X } 100$$

wherein D1 is colony diameter in the control and D2 is colony diameter in the treated sample.

2.11. Detached leaf assays for antibiosis

Leaves from four-week-old castor plants of the two genotypes; DCS 107 and 48–1 were surface sterilized with 70% ethanol followed by 1% sodium hypochlorite solution for 2 min, followed by thorough rinsing three times with autoclaved double distilled water to remove traces of sodium hypochlorite from the leaves. Sterilized leaves were then dried on autoclaved blotting paper. The conidial suspension of 1×10^6 spores/ml was prepared for all four strains of *Trichoderma* and 1 mL of the spore suspension of each strain was sprayed on the entire leaf surface while the leaves of control plants were sprayed with autoclaved double distilled water. The *Trichoderma* inoculated and control leaves were maintained on moist cotton to avoid leaf drying and incubated for 24 h at 25 °C. After 24 h, the agar plugs of 5 mm diameter taken from growing margins of *Alternaria* were placed in the center of the leaves (adaxial surface) and incubated at 25 °C.

The *Alternaria* disease incidence was monitored at 3 dpi and 7 dpi and the experiments were repeated three times with five replicates. Inoculated leaf disks were visually rated based on lesion size and intensity of discoloration of leaves in comparison to control leaves. The leaves were rated on a scale of 0–5, where 0 indicates no symptoms and 5 indicates complete coverage with lesions with the following categories: 0: immune to pathogen with no lesions or chlorosis (–); 1: Not susceptible with a few lesions covering less than 10% of the leaf surface (+); 2: sparingly susceptible covering 1–25% of the leaf surface with lesions (++); 3: moderately susceptible to pathogen with 26–50% of the leaf surface covered with lesions (+++); 4: susceptible showing 51–75% of the leaf surface infected (++++); 5: highly susceptible showing <76% infection (+++++).

3. Results

3.1. Morphological characterization

Phenotyping of the *Trichoderma* strains for their growth pattern five days post culturing on PDA medium revealed the characteristic formation of green-colored mycelia and spores by the four strains– N13, 7316, TV5 and TV2B16. The strains, TV3 and TS4 appeared whitish-yellow to yellowish-green colour distinct from N13, 7316, TV5 and TV2B16 (Table 1). Variation in the conidiation pattern was also detected among the *Trichoderma* strains. The three *Trichoderma* strains– N13, 7316 and TV5 produced effusing concentric ring-like sporulation pattern whereas TV2B16 produced loose tufts with no ring formation. The strain, TS4 appeared to be fluffy and cottony while TV3 showed a radial growth pattern (Fig. S1).

Trichoderma strains varied for mycelial morphology, branching of conidiophores, sporulation pattern and shape of conidia. The conidiophores of the 4 fungal strains– N13, 7316, TV5 and TV2B16 showed alternating branching patterns with lateral branches.

Table 1
Morphological characteristics of six strains of *Trichoderma* spp. Cultured on potato dextrose agar (PDA) medium.

Trichoderma strain	Mycelium colour	Conidiation	Conidiophore	Conidia shape	Conidial colour
T. asperellum N13	Pale white	Concentric zones	Moderately branched	Globose to obovoid	Dark green
T. asperellum 7316	Snowy white	Effuse in concentric rings	Highly branched	Globose to sub-globose	Green
T. asperellum TV5	White	Effuse in concentric rings	Moderately branched	Globose to obovoid	Dark green
T. asperellum TV2B16	White	Lose tufts with no ring formation	Branched	Sub-globose to obovoid	Green
T. harzianum TV3	Watery white	Loose tufts in concentric rings	No branching	Globose to sub-globose	Yellow
T. harzianum TS4	White	Lose tufts in concentric zones	No branching	Globose to sub-globose	Whitish yellow

While the strains– N13, 7316 and TV5 showed predominant branching of the main axis with phialides forming penicillate heads at the tip of the branches, TV2B16 produced secondary branches with very few phialides. On the contrary, branching was absent in *Trichoderma* strains TS4 and TV3 thereby morphologically distinguishing them from the remaining four *Trichoderma* strains– N13, 7316, TV5 and TV2B16. Furthermore, N13, 7316, TV5 and TV2B16 sporulated profusely compared to TV3 and TS4 correlating with the branching pattern observed in these strains by phase-contrast microscopy (Fig. 1).

3.2. PCR-based amplification of ITS and D1-D2 region

The PCR amplicons of size ranging between 500 and 600 bp were obtained from ITS and D1-D2 regions of all the six strains; N13, 7316, TV5, TV2B16, TV3 TS4 along with the Ex-type strains; *T. asperellum* Ta05 and *T. harzianum* Th03 (Fig. S3). The Blast search result showed significant sequence similarity with the *Trichoderma* species *T. asperellum and T. harzianum* (Table 2). The ITS sequences of two strains, N13 and 7316 (MH356723.1 and MH236427.1 respectively) showed sequence similarity of 99.83% to *T. asperellum,* QT21984 (KY209917.1) whereas their D1-D2 sequences (MK411202.1 and MK411201.1) showed 99.82% and 99.65% similarity respectively with *T. asperellum,* CBS125571 (MH877858.1) indicating that these strains were related to *T. asperellum*. Likewise, the percentage similarity of the ITS sequences of the remaining strains; TV5 (MK411216.1) and TV2B16 (MH393229.1) also showed >99% similarity to *T. asperellum* confirming them as *T. asperellum* strains. On the contrary, ITS and D1-D2 sequences of the two strains, TV3 and TS4 showed >99 % similarity to *T. harzianum* strain, CBS 130681 (MH877292.1) indicating them as *T. harzianum* strains.

The phylogenetic relationship was assessed among the six *Trichoderma* strains by including the ex-type strains– *T. asperellum* Ta05 and *T. harzianum* Th03 along with other recently reported strains of *T. asperellum* and *T. harzianum* (Zheng et al., 2021). The *Trichoderma* strains from other species, *T. longibrachiatum* and *T. virens* were also included in the phylogenetic analysis. The fungal member, *Mycospharella etlingerae* strain, CBS 129062 (JF770452.1), a necrotroph was included as an out-group. The phylogenetic tree drawn for ITS (Fig. 2A) and D1-D2 (Fig. 2B) sequences by the neighbour joining tree method revealed that the ITS sequences of all the six strains grouped into two major clusters– cluster A and cluster B. The two strains *Trichoderma harzianum* TV3 and TS4 along with the ex-type strain *T. harzianum* Th03 fell into the cluster A. Cluster B included the four strains– *T. asperellum* 7316, N13, TV5 and TV2B16 along with the ex-type strain, *T. asperellum* Ta05.

Similarly, the dendrogram constructed using D1-D2 sequences of all six strains distributed into two major clusters– cluster D and cluster E. Cluster D included the four strains- *T. asperellum* 7316, N13, TV5 and TV2B16 along with the ex-type strain, *T. asperellum* Ta05. Cluster E consisted of the two strains *T. harzianum* TV3 and TS4 along with the ex-type strain, Th03. Therefore, both the dendrograms constructed using ITS and D1-D2 sequences revealed similar results wherein 7316, N13, TV5, and TV2B16 grouped together in one cluster, while the remaining two strains, TV3 and TS4 grouped together in a separate cluster.

To further validate the relatedness among the strains, dendrograms were drawn using complementary ITS (Fig. S4A) and D1-D2 (Fig. S4B) sequences of these six strains in comparison with the twenty previously reported *Trichoderma* strains whose ITS and D1-D2

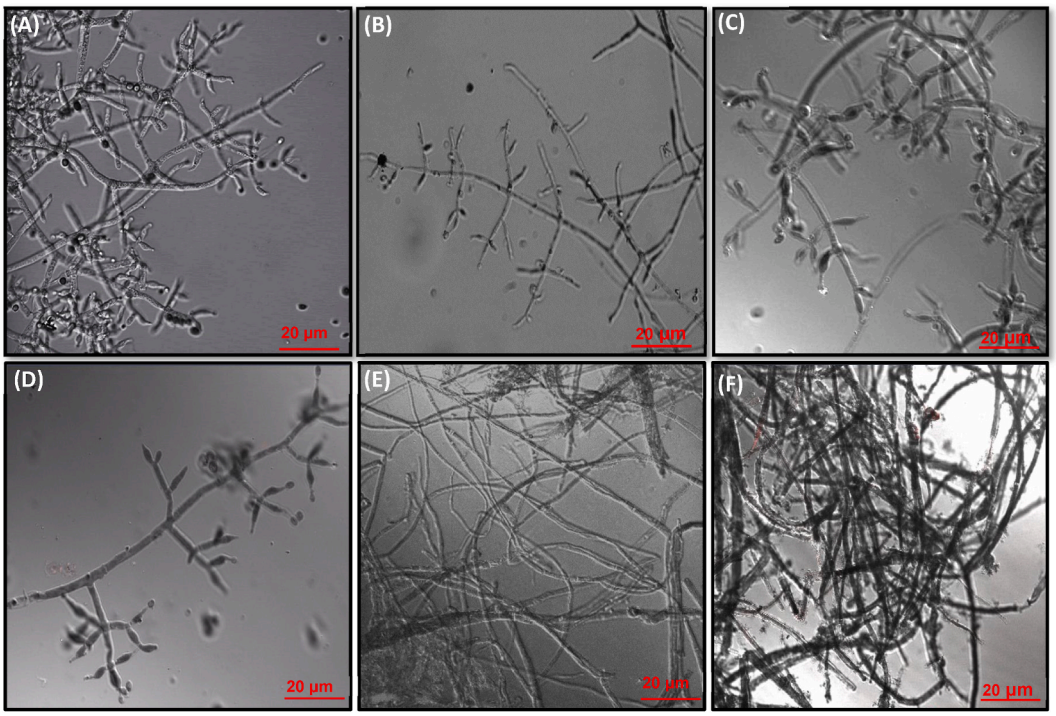


Fig. 1. Comparison of morphological states of six strains of *Trichoderma* using confocal scanning microscope at 20*x*. (**A**) *Trichoderma asperellum* 7316; (**B**) *Trichoderma asperellum* N13; (**C**) *Trichoderma asperellum* TV5; (**D**) *Trichoderma asperellum* TV2B16; (**E**) *Trichoderma harzianum* TV3; (**F**) *Trichoderma harzianum* TS4.

Table 2
BLAST-search results of ITS and D1-D2 sequences of *Trichoderma* strains amplified using ITS-1F/ITS-4R primers and NL-1/NL-4 primers respectively.

BLAST-search results of ITS sequences						BLAST-search results of D1-D2 sequences					
Trichoderma strains	Score values	Query cover %	E value	Similarity (%)	Accession No. Of highest similarity strain	Score values	Query cover %	E value	Similarity (%)	Accession No. Of highest similarity strain	Species
N13	1112	98	0	99.83	KY209917.1 (*T. asperellum* QT21984)	1038	97	0	99.82	MH877858.1 (*T. asperellum* CBS125571)	*Trichoderma asperellum*
7316	1112	98	0	99.83	KY209917.1 (*T. asperellum* QT21984)	1035	97	0	99.65	MH877858.1 (*T. asperellum* CBS125571)	*Trichoderma asperellum*
TV5	1101	98	0	99.51	KM268676.1 (*T. asperellum* DWG3)	1027	97	0	99.47	MH877858.1 (*T. asperellum* CBS125571)	*Trichoderma asperellum*
TV2B16	1094	98	0	99.34	MK691700.1 (*Trichoderma asperellum* T16)	1029	71	0	99.30	MH478122.1 (*T. asperellum* ERR11-12)	*Trichoderma asperellum*
TV3	1114	98	0	99.04	KY225678.1 (*T. harzianum* QT22144)	1031	97	0	99.65	MH877292.1 (*T. harzianum* CBS130681)	*Trichoderma harzianum*
TS4	1116	97	0	99.35	KY225678.1 (*T. harzianum* QT22144)	1037	98	0	99.65	MH877292.1 (*T. harzianum* CBS130681)	*Trichoderma harzianum*

sequences were available in public domain. The ITS sequence of the six strains was also compared with 100 reported *Trichoderma* sequences, which comprised 36 strains of *T. asperellum* and 49 strains of *T. harzianum*, along with strains of other distant *Trichoderma* species (Fig. S5). A significant level of similarity was observed among the *Trichoderma* strains under study with the other previously reported strains. In both the phylogenetic analyses 7316, N13, TV5 and TV2B16 strains grouped together in one cluster showing significant relatedness to *T. asperellum*, while TV3 and TS4 strains grouped together showing significant similarity to *T. harzianum*.

3.3. *Trichoderma spp. detection based on TEF1 and rpb2 genes*

To confirm the species of the six strains, *Trichoderma* species-specific primer pairs– T2AF/T2AR and TH1F/TH1R reported as specific to *T. asperellum and T. harzianum* respectively were selected for the PCR based amplification of *TEF1* (translation elongation factor 1) and *rpb2* (the second largest subunit of RNA polymerase II) gene sequences respectively. The primer pair, T2AF/T2AR amplified a monomorphic band of size 507 bp in the strains, 7316, N13, TV5, TV2B16 and Ta05 whereas no bands were observed for strains TV3, TS4 and Th03. (Fig. 3A). Similarly, an 824 bp amplicon was observed in TV3, TS4 and Th03 strains using Th1F/Th1R primer pair (Fig. 3B) while the band was absent in the strains, 7316, N13, TV5, TV2B16 and Ta05. Multiplex PCR using both the primer sets T2AF/T2AR and Th1F/Th1R simultaneously, confirmed the detection of *Trichoderma* spp. By amplifying the corresponding DNA amplicons (Fig. 3C).

3.4. *Trichoderma species-detection based on SCAR markers*

Further, to confirm the detected *Trichoderma* species, the SCAR markers specific to *T. harzianum* were tested by employing the two sets of primers– 2F2/2R2 and 2F2/2R3 in the screening of the strains under study. The 2F2/2R2 and 2F2/2R3 primer sets amplified 278 bp and 448 bp DNA fragments respectively in the strains, TV3, TS4 and Th03 while no amplification was observed in the strains–N13, 7316, TV5, TV2B16 and Ta05 (Fig. 3D–E). Multiplex PCR using 2F2/2R2 and 2F2/2R3 together also displayed a similar amplification pattern thereby confirming the findings that TV3 and TS4 were strains of *T. harzianum* (Fig. 3F).

3.5. *RAPD profiling and statistical analysis*

Genotyping of the six strains of *Trichoderma* was carried out using 185 Random Amplified Polymorphic DNA (RAPD) markers to analyse the variability among the *Trichoderma* strains. A distinct genetic make-up of the fungal strains was evident based on the polymorphic DNA markers. Out of a total of 185 primers, 136 primers showed reproducible polymorphic bands, wherein each primer showed 1–46 amplified bands. The approximate range of band size was 150–1500 bp, and 70.66% of the bands were polymorphic (Table S3). The remaining markers were all monomorphic either amplifying similar DNA bands or no band altogether in all the strains. The detected putative polymorphic and monomorphic markers are listed in (Table S4).

Among the monomorphic markers, 44 RAPD markers showed no amplification, while the remaining 5 markers showed uniform amplification generating a similar band size in all six *Trichoderma* strains. Relationships among the strains were evaluated by cluster analysis of the data based on the coefficients of the similarity matrix (Table 3). Maximum genetic similarity was obtained between *T. harzianum* TV3 *and T. harzianum* TS4 (0.98) followed by *T. asperellum* N13 and *T. asperellum* TV2B16 (0.92). Minimum genetic similarity was observed between N13 and TV3 and, N13 and TS4 with a coefficient value of 0.22 each. Further, to understand the genetic relatedness among the six strains of *Trichoderma,* a dendrogram constructed using RAPD marker data revealed that the strains were segregated into two major clusters. Cluster I consisting of the strains N13, 7316, TV5, and TV2B16 was distantly placed from cluster II

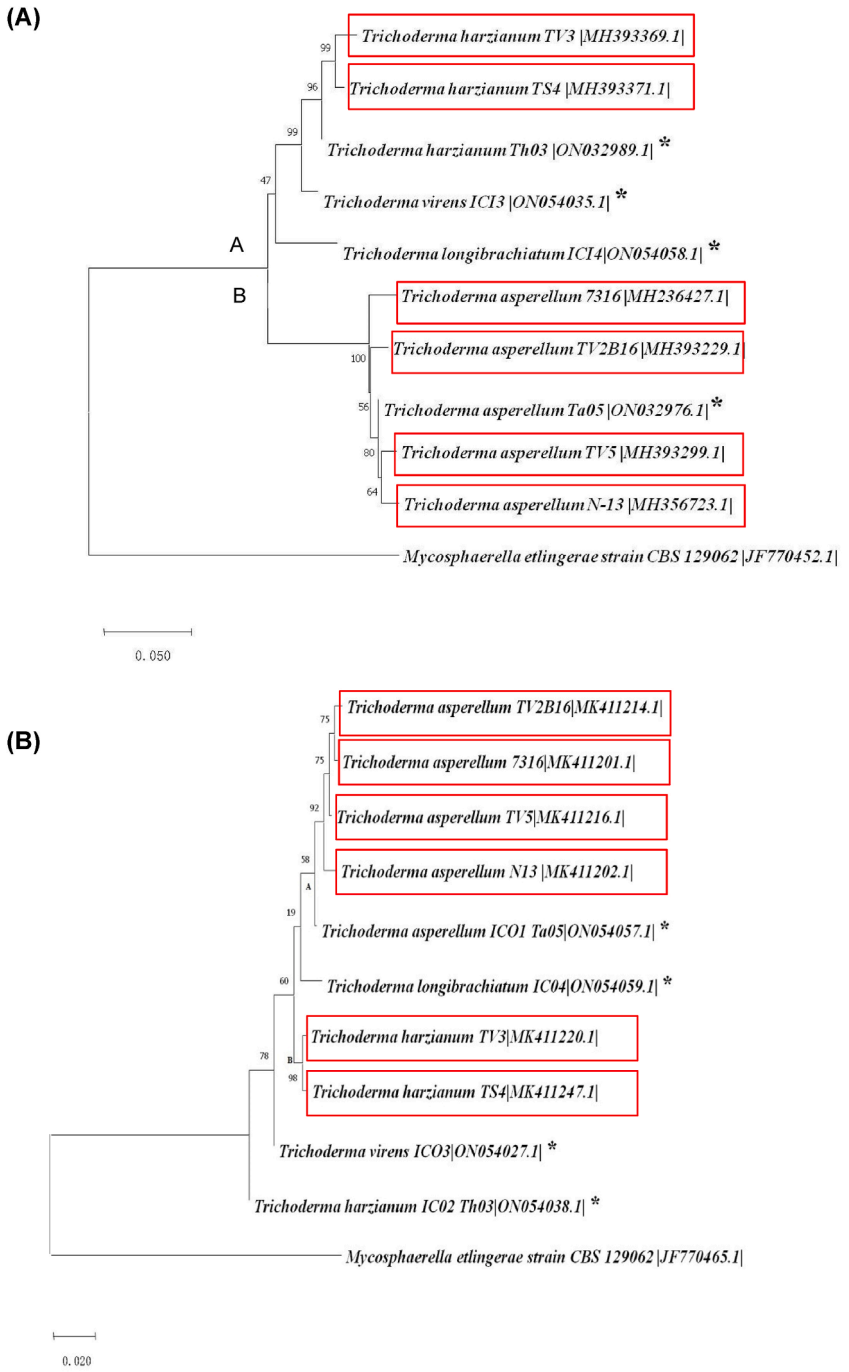


Fig. 2. Phylogenetic tree of *Trichoderma* strains based on ITS and D1-D2 sequences. (**A**) ITS sequences of six strains of *Trichoderma* including ex-type strains. (**B**) D1-D2 sequences of six strains of *Trichoderma* including ex-type strains. The ex-type strains of *Trichoderma* species are marked by asterisk. The six *Trichoderma* strains tested in the study are marked by red colored-boxes. (For interpretation of the references to colour in this figure legend, the reader is referred to the Web version of this article.)

which consisted of TV3 and TS4 and the findings were in accordance with the ITS and D1-D2 region-based phylogenetic profiling (Fig. S6).

Among the RAPD amplified sequences, OPZ-06 and OPK-10 were selected to develop SCAR markers due to their reproducibility and distinct polymorphism between the six *Trichoderma* strains. The marker, OPZ-06 produced a monomorphic band of 950 bp for strains N13, 7316, TV5 and TV2B16, whereas no bands were observed for strains TV3 and TS4 (Fig. 4A). On the contrary, OPK-10 showed a prominent band at 1400 bp for TV3 and TS4 with no amplification for N13, 7316, TV5 and TV2B16 respectively (Fig. 4B). The PCR amplicons generated by the RAPD markers, OPZ-06_{950} and OPK-10_{1400} were sequenced. The nucleotide sequences from the

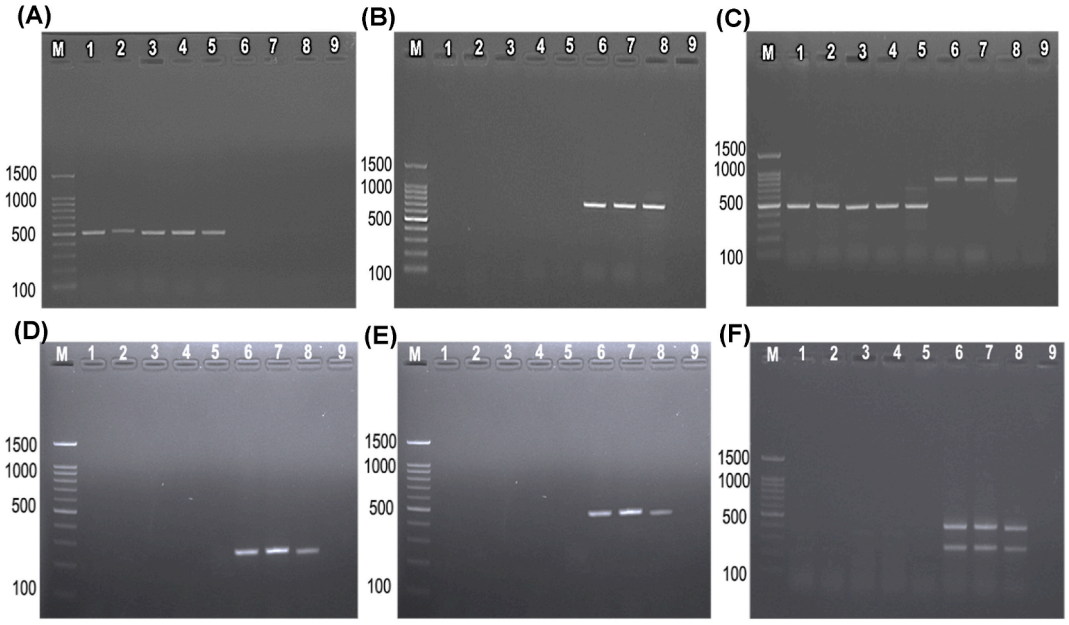


Fig. 3. *Trichoderma*-species specific PCR amplification. (**A**) T2AF/T2AR amplified *T. asperellum*-specific polymorphic band in N13, 7316, TV5, TV2B16 and Ta05 (L-1 to L-5) at 507 bp but absent in TV3, TS4 and Th03 (L-6 to L-8). (**B**) TH1F/TH1R amplified *T. harzianum*-specific polymorphic band in TV3, TS4 and Th03 at 824 bp (L-6 to L-8) but absent in N13, 7316, TV5, TV2B16 and Ta05 (L-1 to L-5). (**C**) Multiplex PCR confirmed the results. (**D**) 2F2/2R2 SCAR marker amplified *T. harzianum*-specific polymorphic band in TV3, TS4 and Th03 (L-6 to L-8) at 278 bp but absent in N13, 7316, TV5, TV2B16 and Ta05 (L-1 to L-5). (**E**) F2/2R3 also generated a polymorphic band with in TV3, TS4 and Th03 at 448 bp (L-6 to L-8) but absent in N13, 7316, TV5, TV2B16 and Ta05 (L-1 to L-5). (**F**) Multiplexing PCR confirmed the results. The *Trichoderma* strains; *T. asperellum* N13 (L-1), *T. asperellum* 7316 (L-2), *T. asperellum* TV5 (L-3), *T. asperellum* TV2B16 (L-4), *T. asperellum* Ta05 (L-5), *T. harzianum* TV3 (L-6), *T. harzianum* TS4 (L- 7), *T. harzianum* (L-8). L-9 is non-template control. M: DNA 100bp ladder.

Table 3
RAPD-based genetic similarity among the six strains of *Trichoderma* analyzed in a pairwise manner.

	N13	7316	TV5	TV2B16	TV3	TS4
N13	1.00					
7316	0.88	1.00				
TV5	0.81	0.85	1.00			
TV2B16	0.92	0.91	0.82	1.00		
TV3	0.22	0.23	0.25	0.22	1.00	
TS4	0.22	0.23	0.25	0.22	0.98	1.00

four strains related to *T. asperellum* amplified by the OPZ-06_{950} marker were aligned using the Clustal Omega program to test the nucleotide similarity among the strains. Likewise, the sequences amplified by OPK-10_{1400} marker from TV3 and TS4 strains were also aligned and significant level of similarity was observed in their nucleotide sequences (<99%).

3.6. Developing SCAR markers specific to T. asperellum and T. harzianum

Two sets of forward and reverse primers (T1/T2 and T3/T4) designed for identification of *T. asperellum* and *T. harzianum* strains were synthesized from the deciphered nucleotide sequences. They were evaluated using a gradient of annealing temperatures ranging from 40 to 64 °C. The details of the species-specific primers along with their sequence information are given in Table 4. The primer pair, T1/T2 showed a specific band of size 467 bp with uniform amplification in N13, 7316, TV5, TV2B16 and Ta05 strains which was absent in TV3, TS4, Th03, *T. longibrachiatum* and *T. virens* (Fig. 5A). Similarly, the primer pair T3/T4 amplified a unique 436 bp DNA band in TV3, TS4 and Th03 strains alone while no amplification was observed in N13, 7316, TV5, TV2B16, Ta05, *T. longibrachiatum* and *T. virens* (Fig. 5B). The annealing temperature was fixed at 55 °C to overcome non-specific amplification. Multiplexing PCR with T1/T2 and T3/T4 primers generated a similar amplification pattern confirming the specificity of the SCAR markers to detect *T. asperellum* or *T. harzianum* strains only. (Fig. 5C).

3.7. Antagonistic effect of trichoderma on alternaria through dual culturing

To study, the antagonistic property of *Trichoderma* against *A. ricini,* the *Trichoderma* strains N13, 7316, TV5, and TV2B16 were selected for confrontation plate assays. *Trichoderma harzianum* strains TV3 and TS4 were not included in this study due to its extremely low sporulation ability. The dual cultures were grown with the fungal pathogen, *A. ricini* along with each of the *T. asperellum* strains placed at equidistance from one another. Petri plates were monitored for the extent of mycelial spread. Petri plates growing *Trichoderma* and *Alternaria* alone were included as controls. All *T. asperellum* strains grew to at least two-third of the medium surface thus

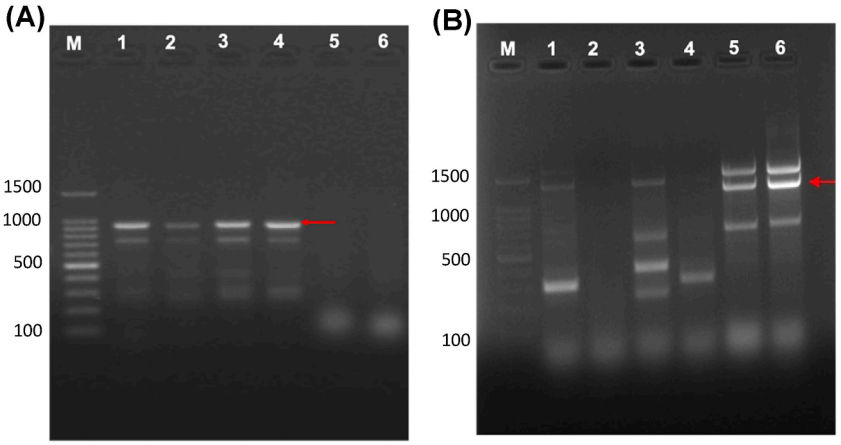


Fig. 4. Gel images showing the PCR amplification of the polymorphic RAPD markers which were developed into SCAR markers following DNA sequencing. (**A**) OPZ-06_{950} marker showed a polymorphic band with uniform amplification for N13, 7316, TV5 and TV2B16 at 950 bp (red arrow) but absent in TV3 and TS4. (**B**) OPK-10_{1400} marker showed a polymorphic band with uniform amplification for TV3 and TS4 at 1400 bp (red arrow) but absent in N13, 7316, TV5 and TV2B16. The lanes 1 to 6 represent the *Trichoderma* strains: *T. asperellum* N13 (L-1), *T. asperellum* 7316 (L-2), *T. asperellum* TV5 (L-3), *T. asperellum* TV2B16 (L-4), *T. harzianum* TV3 (L-5), *T. harzianum* TS4 (L- 6). M: DNA 100bp ladder. (For interpretation of the references to colour in this figure legend, the reader is referred to the Web version of this article.)

Table 4
Primer sequence information of SCAR primers designed for developing species-specific markers.

SCAR Primer	Forward/Reverse	Primer specific to the species	Sequence (5'→3')	GC (%)	T_m (^{0}C)
T1	Forward	*T. asperellum*	CTATTGAACTCTGGACTGCTT	42.86	56
T2	Reverse	*T. asperellum*	CAATCTCAGAAGACTGGCGAGCG	56.52	64
T3	Forward	*T. harzanium*	CATAGACATTGCTGCTAATATTGG	37.50	52
T4	Reverse	*T. harzanium*	AACAAAACAAAAGATGAGACGAAAG	32.00	51

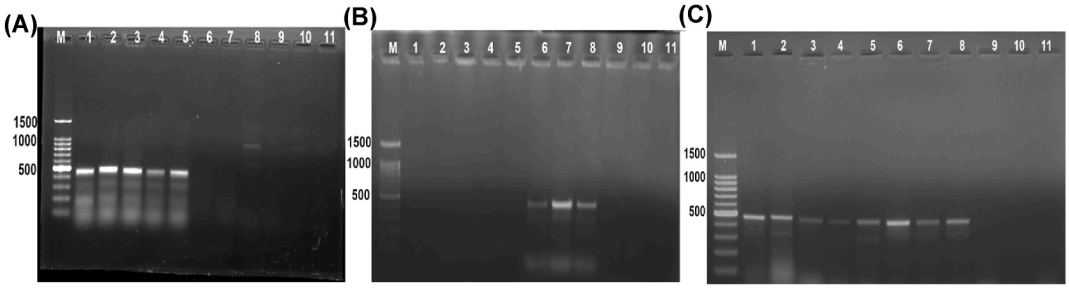


Fig. 5. Developing a new set of *Trichoderma* species-specific SCAR markers. (**A**) T1/T2 showed a specific band with uniform amplification at 467 bp in N13, 7316, TV5, TV2B16 and Ta05 but absent in the strains TV3, TS4, Th03, IC13 and IC14. (**B**) T3/T4 showed a band with uniform amplification at 436 bp in TV3, TS4 and Th03 but absent in N13, 7316, TV5, TV2B16, Ta05 and, IC13 and IC14. (**C**) Multiplex PCR amplification of the SCAR markers T1/T2 and T3/T4 simultaneously confirmed the results. T1/T2 and T3/T4 amplified the 467 bp (L-1 to L-5) and 436 bp (L-6 to L-8) bands respectively. The lanes representing the *Trichoderma* strains are: *T. asperellum* N13 (L-1). *T. asperellum* 7316 (L-2). *T. asperellum* TV5 (L-3). *T. asperellum* TV2B16 (L-4). *T. asperellum* Ta05 (L-5), *T. harzianum* TV3 (L-6), *T. harzianum* TS4 (L- 7), *T. harzianum* Th03 (L-8), *T. longibrachiatum* IC13 (L-9), *T. virens* IC14 (L-10). L-11 is non-template control. M: DNA 100bp ladder.

showing their broad antifungal activity. (Fig. 6). The growth inhibition (%) of *A. ricini* due to the antagonistic effect of *Trichoderma* strains was estimated based on the delta values of inhibition (Δ inhibition) as shown in Table 5. N13 and TV5 strains showed the highest percentage of inhibition of 59.54% and 59.48% respectively, followed by TV2B16 with an inhibition of 58%.

3.8. Effect of Trichoderma on Alternaria ricini-challenged castor leaves

To monitor the effect of *Trichoderma* treatment on *Alternaria* leaf spot disease, detached leaf assay was carried out on two castor genotypes, DCS 107 and 48–1 which were tolerant and susceptible to the *Alternaria* leaf spot respectively. Leaves pre-treated with each of the *Trichoderma* strains (N13, 7316, TV5, and TV2B16) in isolation for 24 h where challenged by the fungal pathogen, *A. ricini*. Disease scoring of *Alternaria* leaf spot incidence on *Trichoderma* treated and control castor genotypes was assessed visually by monitoring at 3 dpi and 7 dpi using a 0–5 scale. The leaves of DCS-107 and 48–1 pre-treated with the *Trichoderma* strain 7316 before challenge with *Alternaria* showed low susceptibility (+) compared to the controls of most strains. The leaves of both the castor genotypes, DCS-107 and 48–1 pre-treated with TV2B16 showed high susceptibility (+ + + + +) to Alternaria, similar to the untreated controls at 7 dpi (Table 6).

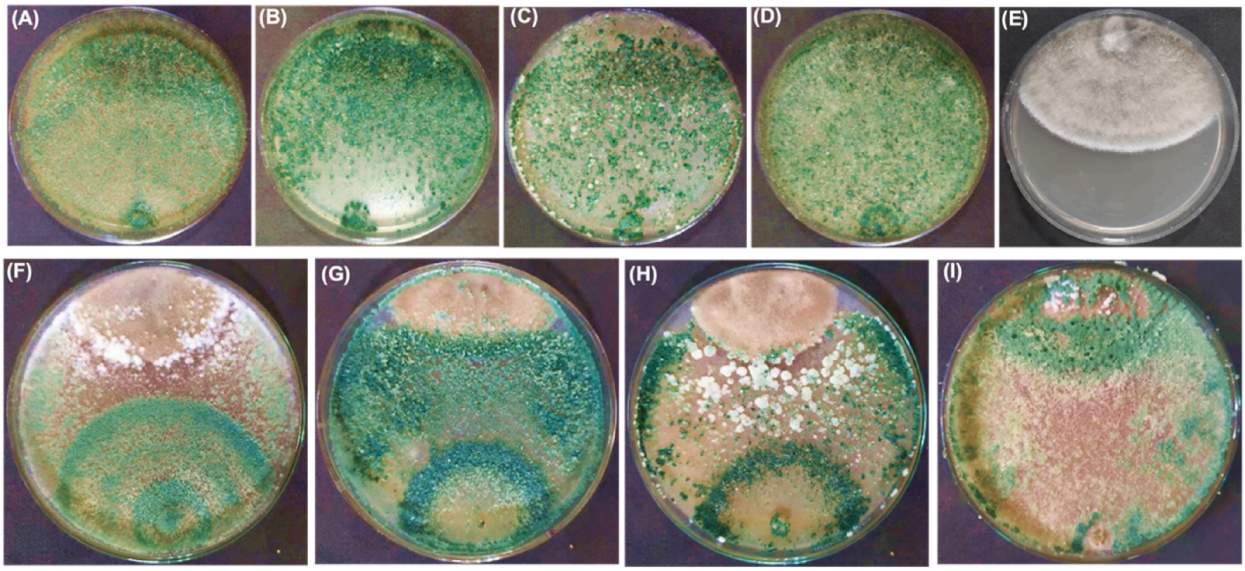


Fig. 6. Confrontation plate assays with dual cultures grown with *A. ricini* and *T. asperellum* strains at 7 dpi. Plates growing only *T. asperellum* 7316 (**A**), N13 (**B**), TV5 (**C**) and TV2B16 (**D**) and *A. ricini* (**E**) served as controls. Test plates included *Alternaria* grown with *T. asperellum* 7316 (**F**), *Alternaria* grown with *T. asperellum* N13 (**G**), *Alternaria* grown with *T. asperellum* TV5 (**H**) and *Alternaria* grown with *T. asperellum* TV2B16 (**I**).

Table 5
Percentage fungal pathogen growth inhibition by antagonistic effect of *Trichoderma* strains.

Trichoderma asperellum strains	Percentage inhibition of pathogen growth (%)	
	4 dpi	7 dpi
N13	28.56	59.54
7316	24.27	54.23
TV5	27.65	59.48
TV2B16	25.18	58.00

Table 6
Disease scoring of *Trichoderma*-treated castor genotypes through detached leaf assays for antibiosis against the leaf spot causing fungal pathogen, *Alternaria ricini* using 0–5 scale.

Trichoderma asperellum strains	Disease severity index (0–5 scale)[a]			
	DCS-107		48–1	
	3dpi	7dpi	3dpi	7dpi
N13	1 (+)	1 (+)	2 (++)	3 (+++)
7316	1 (+)	1 (+)	1 (+)	1 (+)
TV5	1 (+)	3 (+++)	2 (++)	4 (++++)
TV2B16	2 (++)	5 (+++++)	2 (++)	5 (+++++)
Untreated (Control)	3 (+++)	5 (+++++)	3 (+++)	5 (+++++)

[a] The scale 0: immune/highly resistant, (+): resistant, (++): moderately resistant, (+++): moderately susceptible, (++++): susceptible and (+++++): highly susceptible.

The typical disease phenotyping for leaf spot/lesion size with pathogen-induced necrosis of leaf tissues carried out to monitor the *Alternaria* pathogen spread in response to *Trichoderma* revealed variation among the strains. The leaves from the control plants which were pre-treated with sterile water alone, upon challenge with *Alternaria* pathogen showed a significant level of necrosis of the tissues at 7 dpi (Fig. 7). Priming of the castor genotype, DCS-107 with N13 showed significantly low susceptibility levels compared to the castor genotype, 48–1 which showed moderate level of susceptibility to *Alternaria* at 7 dpi. On the contrary, priming with 7316 exhibited a high level of antibiosis and disease control of *Alternaria* in both the castor genotypes at 3 and 7 dpi compared to the remaining *T. asperellum* strains. The research findings suggest the potential application of 7316 as a BCA followed by N13 strain.

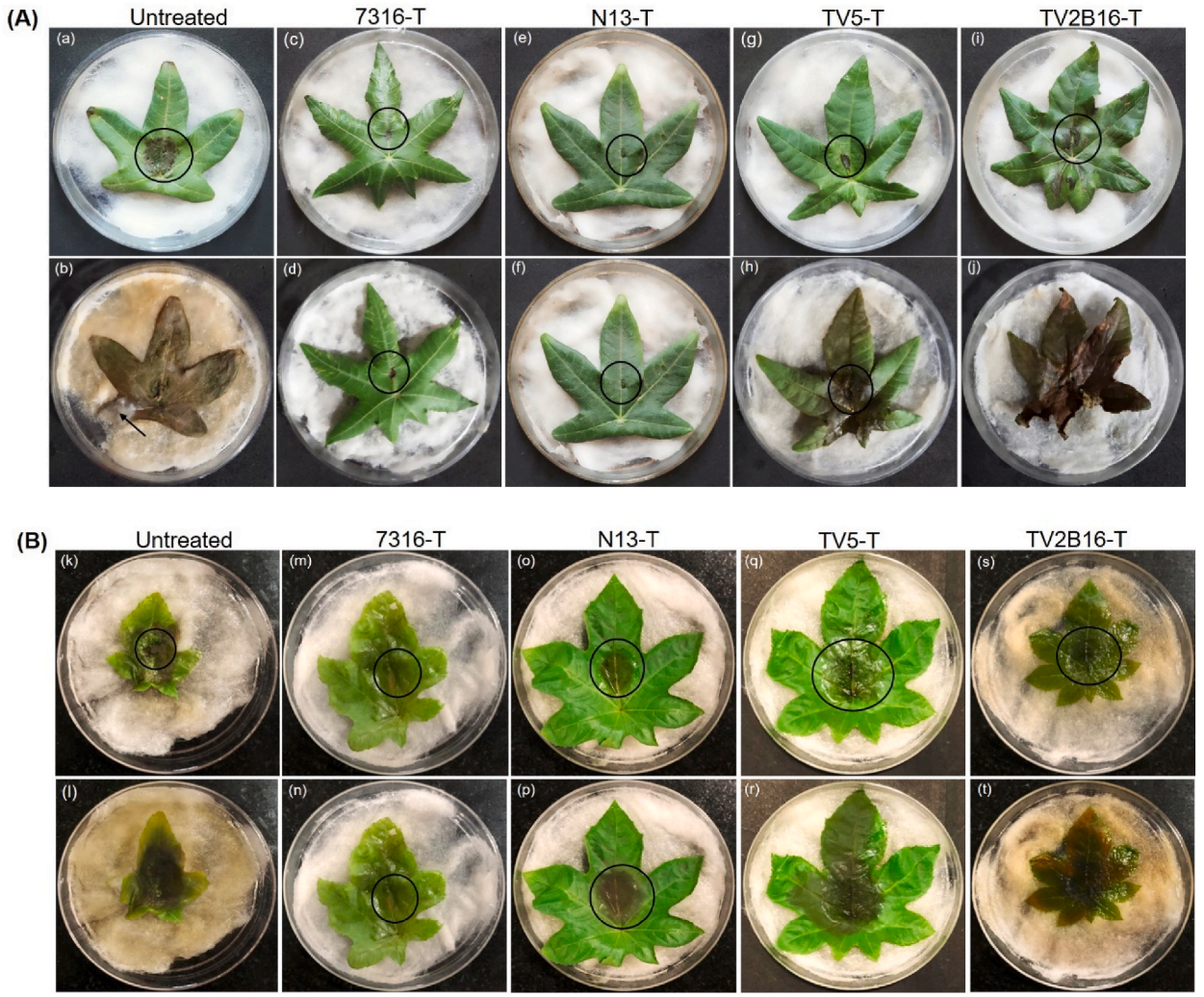


Fig. 7. Effect of *Trichoderma* treatment on *Alternaria* leaf spot in castor by detached leaf assays. Two castor genotypes; (**A**) DCS-107 and (**B**) 48–1 treated individually with each of the four strains of *T. asperelum;* 7316, N13, TV5, and TV2B16 were compared to untreated samples at 3 and 7 dpi. The *Alternaria* leaf spot spread was monitored at 3 dpi (**a, c, e, g, i, k, m, o, q, s**) and 7dpi (**b, d, f, h, j, l, n, p, r, t**) respectively.

4. Discussion

Trichoderma fungi have been reported as BCAs to promote growth and development by colonizing the roots of plants (Guzman-Guzman et al., 2018). To utilize *Trichoderma* as a BCA, it is necessary to identify and analyse the fungal strains for antagonistic ability against pathogens. The conventional methods employed to detect fungal members have been through phenotyping for morphological traits which include colony formation, mycelial growth rate, sporulation, branching pattern, phialides, and spore morphology (Bissett, 1984, 1991a, 1991b, 1991c). However, using morphological characteristics alone is inadequate due to the increasing number of species as well as dearth of the morphological characteristics (Devi et al., 2012). Of late, DNA-based sequencing methods have been utilized that reveal nucleotide variability with precision (Samuels et al., 2002). The ITS and D1-D2 regions of rDNA are considered as fungal barcode markers and have been extensively used in studying intraspecific fungal diversity (Kullnig-Gradinger et al., 2002; Chakraborty et al., 2010; Schoch et al., 2012; Chaverri et al., 2015). Besides, nucleotide sequence-based detection, species-specific marker assays were employed to accurately identify species within the genus, *Trichoderma* (Gupta et al., 2010; Devi et al., 2017). Previous studies have demonstrated that a combination of both traditional methods of morphological analysis as well as molecular analyses of fungal strains would enable in-depth and accurate detection of fungal members (Alsohaili and Hasan, 2018). Therefore, in the present study, evaluation of the six strains of *Trichoderma*–7316, N13, TV5, TV2B16, TV3 and TS4 were carried out for the above morphological traits through mmicroscopic examination followed by sequencing of the ribosomal DNA (rDNA) using internal transcribed spacer (ITS) and D1-D2 region-specific primers to confirm them as *Trichoderma* members.

Our findings from *in silico*-based BLAST search analysis as well as nucleotide diversity comparison analysis of ITS and D1-D2 sequences of the six strains with other reported *Trichoderma* species in a concatenated dendrogram also revealed that the four

strains–7316, TV2B16, N13 and TV5 were related to *T. asperellum* while the remaining two strains, TV3 and TS4 were related to *T. harzianum* thereby confirming the fungal strains as belonging to two different species.

The two genes– translation elongation factor1 (*TEF1*) and the second-largest subunit of RNA polymerase II (*rpb2*) have been reported to serve as markers to detect *Trichoderma asperellum* and *Trichoderma harzianum* species respectively due to highly conserved sequences to distinguish *T. asperellum* and *T. harzianum* strains (Barrera et al., 2021; Devi et al., 2017; Větrovský et al., 2016). To confirm the results from the ITS and D1-D2 region-based grouping of the strains, PCR was performed using the above markers. The findings revealed that the primer pair T2AF/T2AR specific to *TEF1* amplified a DNA band (507 bp) in the four strains– N13, 7316, TV5, TV2B16 (507 bp) that is specific to *T. asperellum.* Similarly the primer pair T2AF/T2AR specific to *rpb2* amplified a DNA band (824 bp) in TV3 and TS4 alone that is specific to *T. harzianum*.

According to Perez et al. (2014), the primer sets 2F2/2R2 and 2F2/2R3 reportedly amplified a 278 bp and 448 bp DNA band respectively in *T. harzianum.* To confirm the accuracy of the *Trichoderma* species detection, these SCAR markers were tested. As anticipated TV3 and TS4 showed prominent DNA bands each of size 278 bp and 448 bp confirming them as strains of *T. harzianum*. In addition to the separate PCRs, multiplex PCR assays reconfirmed the specificity of each of the amplicons and precision of both the primer sets. A multiplex PCR assay has been demonstrated as a powerful tool for accurate and rapid identification of fungal strains (Chanu et al., 2022). Further, Prabhakaran and associates (2015) developed a multiplex PCR assay for simultaneous detection of different species of *Trichoderma* in a single reaction.

Previous findings have demonstrated the applicability of Random Amplified polymorphic DNA (RAPD) markers to detect molecular variation among the *Trichoderma* strains (Perez et al., 2014; Gupta et al., 2010; Pandya et al., 2017). In our study also, characterization of the fungal strains with 185 random primers showed genetic variation among the strains. The polymorphic banding patterns detected in the study were indicative of molecular differences among the *Trichoderma* strains. The RAPD marker, OPY-02 showed the highest number of bands that ranged between 250bp to 1200bp. Further, statistical analysis by pairwise comparison of correlation of coefficient values obtained from RAPD profiling revealed that TV3 and TS4 were closely related to each other (0.98). Further, TV3 and TS4 fungal strains comprised one cluster distinct from the remaining four strains– N13, 7316, TV5, and TV2B16 which together formed one cluster. These results were in accordance with the findings revealed from the dendrograms obtained through ITS and D1-D2 sequences and RAPD sequences.

To convert RAPD assay into a more robust and accurate mode of strain characterization, the highly specific and reliable SCAR markers were generated using conserved sequences of *T. harzianum* and *T. asperellum*. The primer pair T1/T2 amplified a 467bp sequence exclusively in N13, 7316, TV5, TV2B16 and the ex-type strain Ta05 confirming its specificity to *T. asperellum.* The primer pair T3/T4 amplified a 436 bp sequence in TV3, TS4 and the ex-type strain, Th03 confirming its specificity to *T. harzianum*. The synthesized SCAR primers T1/T2 and T3/T4 are highly specific to *T. asperellum* and *T. harzianum* respectively and can be utilized as standard markers in *Trichoderma* species identification. The identification of molecular variations by RAPD data profiling would provide a new possibility of detecting *Trichoderma* strains to be utilized as biopesticides to improve the productivity potential of crop plants.

A significant level of mycoparasitism was revealed by the strain, N13 (59.54%) through confrontation plate assay. In agreement, priming with N13 also exhibited significant level of antibiosis in DCS-107, a tolerant genotype when compared to 48–1, a susceptible genotype suggesting that the interacting host factors might also influence the disease reaction. On the contrary, priming with 7316 exhibited a high level of antibiosis and disease control of *Alternaria* in both the castor genotypes suggesting a synergistic action between *Trichoderma* and the host. The favourable outcome could be resulting from the sequential expression of antimicrobial proteins which include chitinases, glucanases and proteases (Sharma et al., 2011; Mora and Earle, 2001). The reduced lesion size observed in response to the reaction to *Alternaria* fungus was correlating with the findings of the confrontation plate assay carried out with dual cultures to test fungal pathogen inhibition by *Trichoderma* via *in vitro* culture studies. The mycoparasitic ability of *Trichoderma* detected in the study to inhibit and confine the growth of *Alternaria* was in agreement with other reported findings (Begum et al., 2021; Nwankiti and Gwa, 2018; Yassin et al., 2021). Further, an in-depth study of *Trichoderma* fungi to synergize the effect of all toxic metabolites and hydrolytic enzymes may lead to formulating a complex strain that would enhance the antagonistic potential of *Trichoderma* as a potential biocontrol agent (BCA).

5. Conclusion

The study was carried out to identify the *Trichoderma* strain/s that could serve as a BCA. Screening of the fungal strains for morphological, molecular and antagonistic attributes revealed significant level of genetic variation among the *Trichoderma* strains isolated from the rhizosphere soil of castor-oil plant. The present study led to the detection of genus and/species of all six strains of *Trichoderma* through systematic characterization of ITS and D1-D2 sequences and molecular markers– RAPD and SCAR. A set of novel SCAR markers were developed to distinguish the two species– *T. asperellum* and *T. harzianum* including the reported *Trichoderma* strains as ex-type strains. Further, the findings were validated for their reproducibility and accuracy by multiplex PCR assay. *Trichoderma* has been reported as a mycoparasitic agent, able to directly attack other fungi. The findings from the present study also demonstrated that *Trichoderma* impeded the growth of *A. ricini* in castor. The confrontation plate assay and detached leaf assay revealed the mycoparasitic and antagonistic ability of *Trichoderma* strains to the fungal pathogen, *A. ricini*. 7316 followed by N13 demonstrated high antagonistic ability against the fungal pathogen, *A. ricini* indicating these strains as potential biocontrol agents to limit *Alternaria* infection in castor.

Authors contribution

Doris A. Pradhan (DP) has carried the experiments as part of her doctoral program under the guidance and supervision of the corresponding author, Prof. Ragiba Makandar (RM) at UoH. DP carried the experiments, data analysis, and drafting the manuscript. Prathyusha Bagagoni (PB) contributed equally to the MS in phylogenetic studies, PCRs, RAPD and SCAR marker analyses and plant bioassays. Saharika Slathia (SS) carried first round of the RAPD screening experiments. R. D. Prasad provided the fungal strains and castor genotypes-resource material. The corresponding author, RM has planned and supervised the research work, obtained funding, provided research inputs, suggestions, and revisions of the manuscript.

Declaration of competing interest

The authors declare that they have no known competing financial interests or personal relationships that could have appeared to influence the work reported in this paper. The authors declare no conflict of interest.

Data availability

Data will be made available on request.

Acknowledgements

This work was supported by the financial support received from the Indian Council of Agricultural Research (ICAR)-NFBSFARA with the grant No. NFBSFARA/BS-3007/2012–13 to RM. The authors acknowledge the Indian Institute of Oilseeds Research (IIOR), Hyderabad for providing castor genotypes, *Trichoderma* and *Fusarium oxysporum* cultures; Facilities at the University of Hyderabad (UoH); IOE, DBT-BUILDER; DBT-PURSE; DBT-FIST, DBT-CREBB, UGC-SAP, CIL, and Plant Culture Facility. The financial support in the form of fellowships - UGC-SRF to DAP and UoH-BBL to PB are also acknowledged.

Appendix A. Supplementary data

Supplementary data to this article can be found online at https://doi.org/10.1016/j.bcab.2023.102945.

References

Alsohaili, S.A., Hasan, B.M.B., 2018. Morphological and molecular identification of fungi isolated from different environmental sources in the northern eastern desert of Jordan. Jordan J. Biol. Sci. 1, 329–337.

Barrera, V.A., Lannone, L., Romero, A.I., Chaverri, P., 2021. Expanding the *Trichoderma harzianum* species complex: three new species from Argentine natural and cultivated ecosystems. Mycologia 113 (6), 1136–1155.

Begum, M.F., Rahman, M.A., Alam, M.F., 2021. Biological control of Alternaria fruit rot of chili by *Trichoderma* species under field conditions. MYCOBIOLOGY 38, 113–117.

Bissett, J., 1984. A revision of the genus *Trichoderma* I. Sect. Longibrachiatum sect. nov. Can. J. Bot. 62, 924–931.

Bissett, J., 1991a. A revision of the genus *Trichoderma* II. Infrageneric classification. Can. J. Bot. 69, 2357–2372.

Bissett, J., 1991b. A revision of the genus *Trichoderma* III. Sect. Pachybasium. Canadian J. Bot. 69, 2373–2417.

Bissett, J., 1991c. A revision of the genus *Trichoderma* IV. Additional notes on section Longibrachiatum. Can. J. Bot. 69, 2418–2420.

Cai, F., Druzhinina, I.S., 2021. In honor of John Bissett: authoritative guidelines on molecular identification of *Trichoderma*. Fungal Divers. 107, 1–69. https://doi.org/10.1007/s13225-020-00464-4.

Chakraborty, B.N., Chakraborty, U., Dey, P.L., Sunar, K., 2010. Phylogenetic relationships of *Trichoderma* isolates of north bengal based on sequence analysis of ITS region of rDNA. J. Appl. Sci. Res. 6 (10), 1477–1482.

Chanu, K.V., Thakuria, D., Pant, V., Bisht, S., Tandel, R.S., 2022. Development of multiplex PCR assay for species specific detection and identification of Saprolegnia parasitica. Biotechnology Reports. 35, e00758.

Chaverri, P., Branco-Rocha, F., Jaklitsch, W., Gazis, R., Degenkolb, T., Samuels, G.J., 2015. Systematics of the *Trichoderma harzianum* species complex and the re-identification of commercial biocontrol strains. Mycologia 107 (3), 558–590.

Devi, T.P., Prabhakaran, N., Kamil, D., 2017. Development of species-specific markers for the identification of *Trichoderma asperellum* and *Trichoderma harzianum*. Vegetos- An Int. J. of Plant Res. 30, 94–100.

Devi, P., Prabhakaran, N., Kamil, D., Pandey, P., Borah, J.L., 2012. Characterization of Indian native isolates of *Trichoderma* spp. and assessment of their bio-control efficiency against plant pathogens. Afr. J. Biotechnol. 11 (85), 15150–15160.

Dou, K., Lu, Z., Wu, Q., Ni, M., Yu, C., Wang, M., Li, Y., Wang, X., Xie, H., Chen, J., 2018. A novel polyphasic identification system for genus *Trichoderma*. bioRxiv 481382.

Dou, K., Lu, Z., Wu, Q., Ni, M., Yu, C., Wang, M., Li, Y., Wang, X., Xie, H., Chen, J., Zhang, C., 2020. MIST: a multilocus identification system for *Trichoderma*. Appl. Environ. Microbiol. 86. . e01532- 20.

Gupta, V.K., Misra, A.K., Gupta, A., Pandey, B.K., Gaur, R.K., 2010. RAPD-PCR of *Trichoderma* isolates and in vitro antagonism against *Fusarium* wilt pathogens of *Psidium guajava*. L. J. of Plant Protect. Res. 50, 256–262.

Guzman-Guzman, P., Troncoso, M.D.P., Monfil, V.O., 2018. Trichoderma species: versatile plant symbionts. Phytopathology 109, 6–16.

Harman, G.E., Howell, C.R., Viterbo, A., Chet, I., Lorito, M., 2004. *Trichoderma* species-opportunistic, avirulent plant symbionts. Nat. Rev. Microbiol. 2, 43–56.

Jaisani, P., Pandey, R.N., 2017. Morphological and molecular characterization for identification of isolates of *Trichoderma* spp. from rhizospheric soils of crops in middle Gujarat. Indian Phytopathol. 70, 238–245.

Kullnig-Gradinger, C.M., Szakacs, G., Kubicek, C.P., 2002. Phylogeny and evolution of the fungal genus *Trichoderma*—a multigene approach. Mycol. Res. 106, 757–767.

Kwiatkowski, N.P., Babiker, W.M., Merz, W.G., Carroll, K.C., Zhang, S.X., 2012. Evaluation of nucleic acid sequencing of the D1/D2 region of the large subunit of the 28S rDNA and the internal transcribed spacer region using smart gene IDNS software for identification of filamentous fungi in a clinical laboratory. J. Mol. Diagn. 14, 393–401.

Mora, A., Earle, E., 2001. Combination of *Trichoderma harzianum* endochitinase and a membrane-affecting fungicide on control of Alternaria leaf spot in transgenic broccoli plants. Appl. Microbiol. Biotechnol. 55, 306–310.

Nwankiti, A.O., Gwa, V.I., 2018. Evaluation of antagonistic effect of *Trichoderma harzianum* against *Fusarium oxysporum* causal agent of white yam (*Dioscorea rotundata*) tuber rot. Trends Tech. & Sci. Res. 1, 12–18.

Pandya, J.R., Sabalpara, A.N., Mahatma, M., 2017. Randomly amplified polymorphic DNA analysis of native *Trichoderma* isolates. Asian J. of Appl. Sci. and Technol. 1, 147–150.

Prabhakaran, N., Devi, T.P., Sathiyabama, M., Kamil, D., 2015. Multiplex PCR for detection and differentiation of diverse *Trichoderma* species. Ann. Microbiol. 65, 1591–1595.
Perez, G., Verdejo, V., Gondim-Porto, C., Orlando, J., Caru, M., 2014. Designing a SCAR molecular marker for monitoring *Trichoderma* cf. *harzianum* in experimental communities. J. of Zhejiang Univ.-Sci. B (Biomed. & Biotechnol.) 15, 966–978.
Sagar, M.S.I., Meah, M.B., Rahman, M.M., Ghose, A.K., 2011. Determination of genetic variations among different *Trichoderma* isolates using RAPD marker in Bangladesh. J. Bangladesh Agric. Univ. 9, 9–20.
Samuels, G.J., Dodd, S.L., Gams, W., Castlebury, L.A., Petrini, O., 2002. *Trichoderma* species associated with the green mold epidemic of commercially grown *Agaricus bisporus*. Mycology 94, 146–170.
Schoch, C.L., Seifert, K.A., Huhndorf, S., Robert, V., Spouge, J.L., Levesque, C.A., Chen, W., 2012. Fungal Barcoding Consortium: nuclear ribosomal internal transcribed spacer (ITS) region as a universal DNA barcode marker for Fungi. Proc. Natl. Acad. Sci. USA 109, 6241–6246.
Sharma, P., Kumar, V.P., Ramesh, R., Saravanan, K., Deep, S., Sharma, M., Mahesh, S., Dinesh, S., 2011. Biocontrol genes from *Trichoderma* species: a review. Afr. J. Biotechnol. 10, 19898–19907.
Singh, V., Upadhyay, R.S., Sarma, B.K., Singh, H.B., 2016. *Trichoderma asperellum* spore dose dependent modulation of plant growth in vegetable crops. Microbial. Res. 193, 74–86.
Tamura, K., Peterson, D., Peterson, N., Stecher, G., Nei, M., Kumar, S., 2011. MEGAX: molecular evolutionary genetics analysis using maximum likelihood, evolutionary distance, and maximum parsimony methods. Mol. Biol. Evol. 28, 2731–2739.
Větrovský, T., Kolařík, M., Žifčáková, L., Zelenka, T., Baldrian, P., 2016. The rpb2 gene represents a viable alternative molecular marker for the analysis of environmental fungal communities. Mol. Ecol. Resour. 16 (2), 388–401.
Vitti, A., Pellegrini, E., Nali, C., Lovelli, S., Sofo, A., Valerio, M., Scopa, A., Nuzzaci, M., 2016. *Trichoderma harzianum* T-22 induces systemic resistance in tomato infected by cucumber mosaic virus. Front. Plant Sci. 7, 1–11.
White, T.J., Bruns, T., Lee, S., Taylor, J., 1990. Amplification and direct sequencing of fungal ribosomal RNA genes for phylogenetics. In: PCR Protocols: A Guide to Methods and Applications. pp. 315–321.
Xue, A.G., Guo, W., Chen, Y., Siddiqui, I., Marchand, G., Liu, J., Ren, C., 2017. Effect of Seed treatment with novel strains of *Trichoderma* spp on establishment and yield of spring wheat. Crop Protect. 9, 97–102.
Yassin, M.T., Mostafa, A.A.F., Al-Askar, A.A., Sayed, S.R.M., Rady, A.M., 2021. Antagonistic activity of *Trichoderma harzianum* and *Trichoderma viride* strains against some fungal pathogens causing stalk rot disease of maize, *In vitro*. J. King Saud Univ. Sci. 33, 101–363.
Zheng, H., Qiao, M., Lv, Y., Du, X., Zhang, K.Q., Yu, Z., 2021. New species of *Trichoderma* isolated as endophytes and saprobes from southwest China. J. Fungi 7, 467.

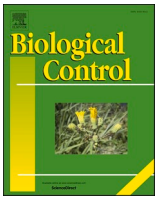
Biological Control 184 (2023) 105280



Contents lists available at ScienceDirect

Biological Control

journal homepage: www.elsevier.com/locate/ybcon



Assessing rhizosphere *Trichoderma asperellum* strains for root colonizing and antagonistic competencies against Fusarium wilt through molecular and biochemical responses in castor

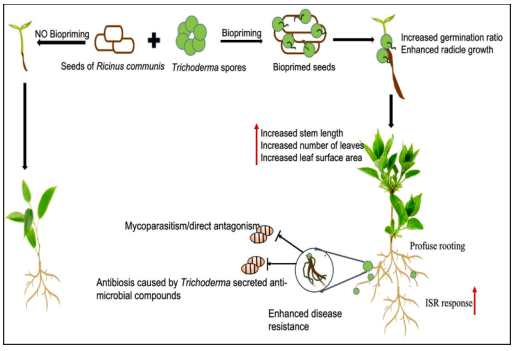
Doris A. Pradhan, Prathyusha Bagagoni, Ragiba Makandar *

Department of Plant Sciences, School of Life Sciences, University of Hyderabad, Prof. C.R. Rao Road, Gachibowli, Hyderabad 500046, India

HIGHLIGHTS

- *Trichoderma asperellum* demonstrated both root colonizing and biocontrol properties.
- Biopriming with *T. asperellum* enhanced seed germination and root growth in castor.
- *Trichoderma* treatment promoted antagonism against *Fusarium oxysporum ricini.*
- *Trichoderma* treatment elicited biochemical responses against *F. oxysporum ricini.*

GRAPHICAL ABSTRACT



ARTICLE INFO

Keywords:
Biocontrol agent
Castor
Fusarium oxysporum
Mycoparasitism
Trichoderma asperellum
Wilt

ABSTRACT

The study was aimed at identifying the effective strain(s) of *Trichoderma asperellum* to colonize castor roots, promote growth and limit pathogen infection. Two castor genotypes; DCS-107 and 48-1 varying for stress tolerance to Fusarium wilt were treated with four *Trichoderma asperellum* strains; 7316, N13, TV5 and TV2B16 to analyze root colonizing and antagonistic competencies. A significant decline in the colony-forming unit (CFU) counts was observed in *Trichoderma*-treated bulk and rhizosphere soil compared to controls indicating a high rhizosphere competence of the *Trichoderma asperellum* strains; 7316 followed by N13. These strains also showed high mycoparasitic propensity against *Fusarium oxysporum* through dual culture-confrontation and *in-planta* assays. Bio-priming with *Trichoderma* strains enhanced plant growth in the tolerant genotype, DCS-107 compared to the susceptible genotype, 48-1 suggesting differential responses of the host genotypes. An increase in shoot length by 46.2, 28.9 and 21.7% was observed upon treatment of DCS-107 genotype with the *Trichoderma* strains, 7316, N13 and TV5 respectively. Further, a quantitative polymerase chain reactions (qPCRs) of 13 stress and defence response genes revealed gene transcript reprogramming, causing a transient repression of the plant immune responses to enable root colonization. Further, biochemical analysis revealed higher antioxidant enzyme activity of catalase, superoxide dismutase and glutathione peroxidase and total phenol content in co-stressed conditions compared to the controls suggesting that *Trichoderma* confers protection against oxidative stress

* Correspondence author.
E-mail address: mragiba@uohyd.ac.in (R. Makandar).

https://doi.org/10.1016/j.biocontrol.2023.105280
Received 26 December 2022; Received in revised form 28 May 2023; Accepted 1 June 2023
Available online 7 June 2023
1049-9644/© 2023 Elsevier Inc. All rights reserved.

damage. *Trichoderma* strains, 7316, N13 and TV5, either individually or in combination could be utilized as potential biocontrol agents to enhance growth and confer resistance to wilt pathogen, *Fusarium oxysporum ricini*.

1. Introduction

Castor (*Ricinus communis* L.) is one of the most ancient non-edible oilseed crops with high oil content (50%) and utilitarian value in the farming, industrial and pharmaceutical sectors. Despite its importance, castor oil production represents only 0.15% of the total vegetable oil content produced annually worldwide (Severino et al., 2012; Morris et al., 2012). However, castor growing regions worldwide are restricted to marginal lands with very low yield potential. Therefore, it necessitates investigating other alternative measures to increase the productivity of castor plants. A promising approach to boost crop yield and minimize loss of productivity due to plant diseases is the use of biological control agents (BCA). The advantage of BCA over any chemical or synthetic fungicides/pesticides includes lesser side effects, their efficacy against fungicide-resistant pathogens and environment friendly nature.

The fungal members belonging to the genus, *Trichoderma* are fast growing and non-virulent symbiotic species. They are known to promote plant growth besides functioning as promising biological control agents (Hermosa et al., 2012). The potential of *Trichoderma* to minimize pathogen infection in plants under various soil conditions has been explored extensively as commercial biocontrol agents. The key strategies employed by *Trichoderma* in direct conflict with pathogens include competition, mycoparasitism and antibiosis (Elad, 2000; Karuppiah et al., 2019). Previous studies to screen *Trichoderma* strains revealed potential strain/s of *Trichoderma harzianum* to function effectively as a BCA when tested against various pathogenic fungi (Grondona et al., 1997; Elad, 2000; Qualhato et al., 2013). Apart from its fungicidal property, *Trichoderma* exerts numerous benefits to plants which includes better nutrient absorption, rhizosphere modification, enhanced tolerance to biotic and abiotic stress, promotes plant morphological traits like elongated root and shoot length, branches, number of leaves, lateral root formation and root hair numbers. The previous research finding demonstrated that application of *Trichoderma guizhouense* NJAU4742-based fertilizer into the soil showed enhanced yield of pepper (Liu et al., 2020). Similarly, root application of *Trichoderma* showed enhanced biomass and root architecture in cucumber (Meng et al., 2019) providing the rationale for the present study. It is hypothesized that the *Trichoderma* may exhibit the propensity as a BCA in castor and therefore, the present study has been carried to test *Trichoderma asperellum* strains detected from castor growing regions of Telangana, India for their root colonizing ability and antibiosis against fungal pathogens. The study was carried to identify the effective strain(s) that could be utilized for not only promoting plant growth but also conferring antibiosis against the root wilt-causing fungal pathogen, *Fusarium oxysporum ricini* using molecular and biochemical approaches and the findings are presented.

2. Materials and methods

2.1. Plant and fungal material

Seeds of the two castor (*Ricinus communis* L.) genotypes; DCS-107 and 48-1, the fungal strains of *Trichoderma asperellum*; 7316 (MH236427.1, MK411201.1), N13 (MH356723.1, MK411202.1), TV5 (MH393299.1, MK411216.1) and TV2B16 (MH393229.1, MK411214.1) and, *Fusarium oxysporum ricini* used for the study as shown in Fig. S1 were obtained from Indian Institute of Oilseeds Research (IIOR), Hyderabad in Telangana, India. The *T. asperellum* strains were isolated from the soil, whereas *F. oxysporum ricini* was isolated from the leaves of the castor plants grown in the field located at IIOR, Hyderabad at 17.3231 ^{0}N Longitude and 78.4096 ^{0}E latitude with an altitude of 528.3 m above the sea level.

2.2. Fungal inoculum preparation

Single-spored cultures were prepared by growing on Potato Dextrose Agar (PDA) as previously described (Devi et al., 2017). The medium was autoclaved at 121 °C and 15 psi for 15 min and plated before inoculation. The fungal cultures were incubated at 24 ± 2 °C and spores were harvested from 7 day-old cultures with a fine camel hair brush by rinsing with sterile water containing 0.02% (v/v) Tween 20 as a surfactant to disperse the spores in the solution. For effective sporulation, *F. oxysporum ricini* was cultured on carboxymethylcellulose (CMC) medium. The CMC medium was prepared by dissolving 1.5 g low viscosity CMC, 1 g yeast extract, 1 g KH_2PO_4, 1 g NH_4NO_3, and 0.5 g $MgSO_4{\cdot}7H_2O$ in a litre of distilled water. The chemical reagents were obtained from Hi-Media, India.

2.3. Soil sampling for rhizosphere and bulk soil

The seeds of DCS-107 and 48-1 castor genotypes were surface sterilized for 5 min with 1.5% sodium hypochlorite solution prepared in autoclaved water and thoroughly rinsed three times with sterile distilled water. The seeds were sown in twice autoclaved potting soil and grown until two leaf growth-stage in a plant growth chamber maintained at 28 °C and 14/10 day/night respectively under a PAR of 500 W m^{-2} with 55% relative humidity. The roots of the castor plants were treated with each of the four strains of *T. asperellum*; N-13, 7316, TV5 and TV2B16 in isolation at different concentrations (3×10^4, 6×10^4 and 9×10^4 spores/ml) by dipping the root system in falcon tubes containing the three different spore suspensions for 24 h and transplanted to pots containing un-autoclaved field soil. The mock (water)-treated plants of the same age, grown under similar plant growth conditions and transplanted in the same field soil served as controls. The rhizosphere and bulk soil samples were collected from *Trichoderma*-treated castor genotypes at 12, 24, 36, and 48-days post-inoculation (dpi).

The soil adhering to the roots was shaken vigorously until 80% of the loosely adhering soil fell off from the roots. The soil sample was collected and is referred to as bulk soil (Fig. S2a) while the soil that remains attached to the root is considered as rhizosphere soil as shown in Fig. S2b. Serial dilutions were prepared from the stock solution of bulk and rhizosphere soil samples by adding 1 g of each of the soil samples to 10 mL of autoclaved distilled water. A 100 μL of the solution per treatment was plated on Luria Bertani HiVeg media (LB) and the plates were incubated at 37 °C overnight. The colony-forming units (CFU) was counted 24 h post plating from 15 replicates for each of the treatments carried with three different spore concentrations at four different time points. The experiments were repeated three times to check for consistency of the results.

2.4. Biopriming with Trichoderma and seed germination assay

The surface-sterilized castor seeds were inoculated for 2 h at 28 °C with each of the four strains of *Trichoderma* in isolation. The spore concentration of 1x 10^6 spores/ml prepared in 1.5% CMC was used. Castor seeds treated with CMC alone served as control. The *Trichoderma*-treated seeds were placed in Petri plates on moist sterile filter paper in the growth chamber at 28 °C. The germinated seed count and radicle length were recorded for the *Trichoderma*-treated and control seedlings 4 days-post treatment. The experiment was repeated three times independently, each having fifteen replicates for each of the treatments tested in the study.

2.5. Trichoderma-treated plant assays through pot trial

The surface sterilized seeds of DCS-107 and 48-1 castor genotypes were treated with the *Trichoderma* strains as described above. Both treated and control seeds were sown in twice-autoclaved potting soil and the plants were grown in a plant growth chamber maintained at 28 °C and 14/10 day/night respectively with 25% relative humidity. The two-week-old plants were analyzed for the traits like the length of root and shoot, leaf size, fresh and dry weight of the plants. Fresh weight was measured immediately after sampling. To compute the dry weight, plants were oven-dried at 40 °C for 48 h before measuring the biomass of plants. The experiment was repeated three times independently, each having fifteen replicates for each of the treatments tested in the study.

2.6. Plate confrontation assay

Mycelia discs of size 5 mm diameter from the actively growing end of 7 day-old *F. oxysporum* fungal culture was placed juxtaposed to a 5 mm diameter discs of *Trichoderma* cultures on Petri plates containing PDA (supplemented with calcium carbonate). The mycelia discs were placed at 1 cm distance from the edge of the Petri plate. Each of the *Trichoderma* strains was placed at the opposite periphery 48 h post-inoculation (hpi) with *Fusarium* discs owing to the slow growth of the fungi. The PDA plates cultured with *Trichoderma* and *Fusarium* mycelia discs alone served as negative controls. The inoculated plates were incubated at 28 °C for 7 days. Radial growth of the fungal pathogen, *F. oxysporum* and the *Trichoderma* strain was measured from fourth day till 7 dpi. The experiment was repeated three times independently, each comprising of ten replicates for each of the pathogen antagonism treatment and the mean values were computed. The percentage inhibition of radial growth (PIRG) was calculated using the formula developed by Skidmore and Dickinson (1976) and Rahman and associates (2011) as given below:

$$PIRG = \{(R_1 - R_2)/R_1\} \times 100$$

whereas R_1 is Colony diameter in the control and R_2 is Colony diameter in treated.

2.7. Efficacy of Trichoderma treatment on Fusarium wilt

The roots of two-weeks-old castor plants of DCS-107 and 48-1 genotypes were treated with each of the *T. asperellum strains* - N13, 7316, TV5 and TV2B16 in isolation with a conidial suspension of 1×10^6 spores/ mL for 24 h. The *Trichoderma*-treated plants were transferred to Falcon tubes containing the conidial suspension of 1×10^6 spores/ml of *F. oxysporum*. Another set of plants of the same age, grown under similar growth conditions were treated with *F. oxysporum* spore suspension alone. The mock (water-treated) treated plants served as controls. The disease incidence was monitored at 7 and 21 dpi. The experiment was replicated three times independently with fifteen replicates for each of the strains of *Trichoderma* tested. Percentage wilt incidence was calculated at 21 dpi.

2.8. RNA isolation and cDNA synthesis

Total RNA was isolated from the roots and leaves of castor genotypes, DCS107 and 48-1 treated with the *T. asperellum* strains; 7316 and N13 respectively along with their controls at 48 h post inoculation (hpi). 500 mg of root sample was ground to a fine powder in liquid nitrogen using a mortar and pestle. The powdered sample was transferred into 2 mL microcentrifuge tubes treated with 0.1% (v/v) diethylpyrocarbonate (DEPC). 1 mL of the pre-heated (65 °C) Extraction buffer-I comprising of 2% cetyltrimethyl ammonium bromide (CTAB) (w/v), 2% polyvinylpolypyrrolidone (PVPP) (w/v), 100 mM Tris(hydroxymethyl)aminomethane hydrochloride (Tris–HCl; pH 8.0), 25 mM ethylenediaminetetraacetic acid (EDTA) and 2 M sodium chloride (NaCl) was added and mixed thoroughly by vortexing. To the contents of the tube, Beta-mercaptoethanol (2% final concentration) was added and incubated at 65 °C for 30 min, with occasionally mixing. 1 mL of chloroform:isoamyl alcohol (24:1/v:v) was added, mixed by brief vortexing and centrifuged at 13,000 rpm for 10 min at room temperature. The supernatant was transferred to fresh microcentrifuge tubes containing 1 mL of the Extraction buffer-II, comprising of phenol saturated Tris buffer of pH 6.7 (Sigma, USA) to which sodium dodecyl sulfate (SDS 0.1%; w/v), sodium acetate (NaOAc 0.32 M; w/v) and EDTA (0.01 M). 200 μL of chloroform was added to the contents of the tubes, vortexed for a few seconds and, incubated for 15 min at room temperature. The samples were centrifuged at 13,000 rpm for 10 min at 4 °C. The upper aqueous phase was transferred into fresh tubes containing 0.6 vol of chilled isopropanol and stored at –20 °C overnight. The samples were centrifuged at 13,000 rpm for 10 min at 4 °C. The supernatant was drained and the RNA pellet was washed with 70% ethanol followed by air drying and finally dissolved in 25 μL of DEPC treated autoclaved water and stored at –80 °C. The cDNA was synthesized from the total RNA using the cDNA synthesis kit (Takara, Shiga, Japan) according to the manufacturer's instructions.

2.9. Real-time quantitative PCR (qPCR)

Primers used for qPCR were designed by Oligo Analyzer 3.1 bioinformatics tool amplifying short fragments of 150–300 bp. Primers designed for 13 genes related to different defence response pathways and an internal control are listed in Table S1. Actin gene expression was monitored which served as a reference control. The PCR conditions used were set at an initial denaturation of 95 °C for 3 min followed by 95 °C for 15 s, an annealing temperature specific to the gene for 30 s, 72 °C for 20 s followed by 40 cycles of 95 °C for 15 s followed by 60 °C for 15 s. The qPCR reaction was performed using Applied Biosystems 7500 Real time PCR Systems. Experiment was repeated twice independently. Relative fold change gene expression was normalised against the reference control using the formula $2^{-\Delta\Delta CT}$.

2.10. Sampling of roots for biochemical and antioxidant activity assays

The treatments comprised of *Trichoderma*-treated alone (only T), *Fusarium*-treated alone (only F) and co-culturing with *Trichoderma* and *Fusarium* pathogen (T + F). 0.5 g of treated and untreated castor root samples at 3 dpi were frozen in liquid nitrogen to stop metabolism and then homogenized with 2 mL of extraction buffer that consists of 50 mM phosphate buffer (pH 7) containing 1 mM EDTA and 2% w/v PVP (polyvinyl pyrrolidone) at 4 °C. The sample was then centrifuged at 13000 rpm for 20 min at 4 °C. The supernatant (enzyme extract) was used for assay of catalase (CAT), glutathione peroxidase (GPX) and superoxide dismutase (SOD). Propagation, inoculation and sampling of plants were done independently with minimum of five replicates (plants) being evaluated for each experiment.

2.11. Catalase (CAT) activity assay

Catalase activity was measured following the method as described previously (Aebi, 1984). To 50 μL of enzyme extract, 2.9 mL of 50 mM phosphate buffer and 50 μL of 30 mM H_2O_2 was mixed rapidly at room temperature by adding H_2O_2 at the end of the reaction. The change in absorbance value was recorded at 240 nm at an interval of 30 sec for 3 min. The CAT activity was assayed by measuring the initial rate of H_2O_2 disappearance at 240 nm, using an extinction coefficient of 40 $mM^{-1}cm^{-1}$ and expressed as Enzyme Unit (EU) mg^{-1} fresh weight.

2.12. Glutathione peroxidase (GPX) activity assay

GPX activity was assayed as described previously by Chance and Maehly (1955). To 50 μL enzyme extract 2.75 mL of 50 mM phosphate

buffer (pH 7.0), 100 μL of 30 mM guaiacol and 40 mM H_2O_2 was added. The change in absorbance value was recorded at 470 nm at an interval of 30 sec for 3 min. GPX activity was determined following the formation of tetraguaiacol by measuring the absorbance at 470 nm and using an extinction coefficient of 26.6 $mM^{-1}cm^{-1}$. One unit (U) of peroxidase activity was represented by the amount of enzyme catalyzing the oxidation of l mol of guaiacol in 1 min and the enzyme activity was expressed as Enzyme unit (EU) mg^{-1} fresh weight.

2.13. Superoxide dismutase (SOD) activity assay

SOD activity was measured as described previously by Beyer and Fridovich (1987). To 50 μL enzyme extract, 1.5 mL of 50 mM phosphate buffer (pH 7.0), 0.3 mL of 100 μM ethylenediaminetetraacetic acid disodium salt (EDTA-Na2), 0.3 mL of 130 mM L-methionine, 0.3 mL of 750 μM nitro blue tetrazolium (NBT), 0.25 mL deionized water was added. Reaction was started by adding 0.3 mL of 20 μM riboflavin. Samples were incubated under a light source having two tungsten incandescent light bulbs having luminance of 8072.93 lx for 15 min. At the same time, a control without the enzyme extract was also prepared. Increase in absorbance due to the formation of formazan was measured at 560 nm using spectrophotometer.

2.14. Total phenol estimation

Total phenol content was extracted from 0.5 g of root tissue was homogenized in liquid nitrogen and extracted in 50% methanol at 80 °C for 90 min and centrifuged at 4000 rpm at 4 °C for 15 min. Saponification of the pellet was done by adding 0.5 N NaOH for 24 h at room temperature to remove the bound phenol and further neutralized with 0.5 mL (2 N) HCl after 24 h. The samples were centrifuged at 12000 rpm at 4 °C for 15 min. Further Folin-Ciocalteu's (FC) assay was performed by adding 100 μL of extracted supernatant diluted with water to make up volume of 1 mL and mixed with 0.5 mL 2 N FC reagent and 2.5 mL of 20% Na_2CO_3. The absorbance was measured at 725 nm. TPC was calculated by using gallic acid standard calibration curve. The result is expressed as mg gallic acid per mg fresh weight.

2.15. Statistical analysis

The data obtained is computed as the mean ± standard error of the mean. The data were statistically analysed by using one-way analysis of variance (ANOVA) and multiple mean comparisons were performed using Tukey's test at the $p \leq 0.05$ significance level. Differences at $p \leq 0.05$ were considered to be significant. In the figures, different letters above the bars indicate significant differences between the control and treatment groups at the $p \leq 0.05$ level according to Tukey's test.

3. Results

3.1. Monitoring the growth of Trichoderma and Fusarium fungal strains

The fungal cultures of four strains of *T. asperellum* (7316, N13, TV5 and TV2B16) and *F. oxysporum ricini* grown in isolation produced profuse mycelial growth and sporulation as shown in Fig. S1. The characteristic olive-green coloured spores of the *Trichoderma* fungal strains were visible at 7 days-post plating. Further, predominant mycelial proliferation and sporulation of *F. oxysporum* fungus was observed in CMC medium.

3.2. Bulk and rhizosphere soil assays to assess the effect of Trichoderma

Compared to the controls, a significant decline was observed in CFU count in *Trichoderma*-treated bulk (Fig. 1) and rhizosphere (Fig. 2) soil samples for all the *Trichoderma asperellum* strains demonstrating their competence ability to restrict the growth of other microorganisms. However, these *Trichoderma* strains exhibited varying levels of competence in both bulk and rhizosphere soil samples with an effective competence activity mostly observed at a concentration of 9×10^4 spores/ml at 36 and 48 dpi. The bulk soil analyzed from castor genotypes, DCS-107 (Fig. 1a) and 48-1 (Fig. 1b) treated with *Trichoderma asperellum* strain 7316 at a concentration of 9×10^4 spores/ml was found to be effective for DCS-107 compared to 48-1 genotype at an early point of 12 dpi suggesting that the differential response to *Trichoderma* might be resulting from the nature of the host genotypes (Fig. 1). Likewise, the CFU count from the bulk soil sample treated with *T. asperellum* strain N13 was found to be effective at a concentration of 9×10^4 at a later time point (36 dpi) for both the genotypes while the CFU count significantly reduced at 24 dpi when treated with TV5 strain in both the genotypes demonstrating its competing ability with other *Trichoderma* strains (Fig. 1c-f). Contrary to the above strains, bulk soil analysis for TV2B16 showed non-significant responses in the DCS-107 genotype (Fig. 1g) while 48-1 genotype (Fig. 1h) exhibited a significant reduction in the CFU count indicating variation in the response of the hosts to the treatment with *Trichoderma* strains.

A significant decrease in CFU count at all concentrations was observed in the rhizosphere soil collected from castor roots treated with the *Trichoderma* strain 7316 in 48-1 genotype compared to DCS 107, while the strain, N13 was more effective in DCS-107 compared to 48-1 suggesting variation among the strains for their rhizosphere competing ability (Fig. 2a-d). The strain, TV5 (Fig. 2e and f) was found to be more effective especially at the concentration of 6 $x10^4$ spores/ml at 36 dpi for both DCS-107 and 48-1 genotypes indicating its potential as the strain with high rhizosphere competing ability. The CFU count in rhizosphere soil treated with TV2B16 reduced significantly in 48-1 compared to DCS-107 suggesting variation in host responses to TV2B16 (Fig. 2g and h).

3.3. Effect of bio-priming with T. asperellum strains on seed germination and plant growth

To study the effect of *Trichoderma* treatment on castor plants, the percentage seed germination and radicle growth were monitored at 4 dpi for DCS-107 and 48-1 genotypes which were treated with *Trichoderma* strains individually with a concentration of 1×10^6 spores/ml (Table 1). The seeds treated with CMC solution alone served as controls. The highest percentage of germination was observed for *T. asperellum* strain, 7316 treated seeds showing a 23% and 33% spike in the germination of DCS-107 and 48-1 genotypes respectively compared to their controls. Treatment with TV2B16 showed a similar spike in the germination percentage of DCS-107 seeds, but no significant increase in 48-1. Treatment with *Trichoderma* strains; N13 and TV5 though increased the germination rate, the effect was less compared to 7316 (Fig. S3).

The effect of biopriming on the radicle length of DCS-107 and 48-1 seeds of castor 4 days-post treatment with the four strains is shown in Fig. S3. The radicle length of seedlings treated with 7316 showed an increase of 73% in DCS-107 and 67% in 48-1 compared to the controls of DCS-107 and 48-1 genotypes respectively. Likewise, an increase of 24% and 43% radicle growth in DCS-107 and 48-1 respectively was observed when treated with N13. While TV5 did not show any significant effect on radicle growth, TV2B16 displayed a 22% higher radicle length for 48-1 treated seeds compared to control as shown in Table 1.

3.4. Effect of biopriming seeds with Trichoderma on the growth of castor

A remarkable feature exhibited by the roots of *Trichoderma* treated DCS-107 genotype was luxuriant roots with higher number of secondary root formation (Fig. S4). The seeds of 48-1 genotype were also bioprimed with all four strains of *Trichoderma*, however, their mortality rate ranged between 75% and 80% within the first two weeks of biopriming thereby indicating the sensitivity of seeds of 48-1 to biopriming (data not shown). Since the effect of biopriming of the seeds with *Trichoderma* strains was predominant on the castor genotype, DCS-107,

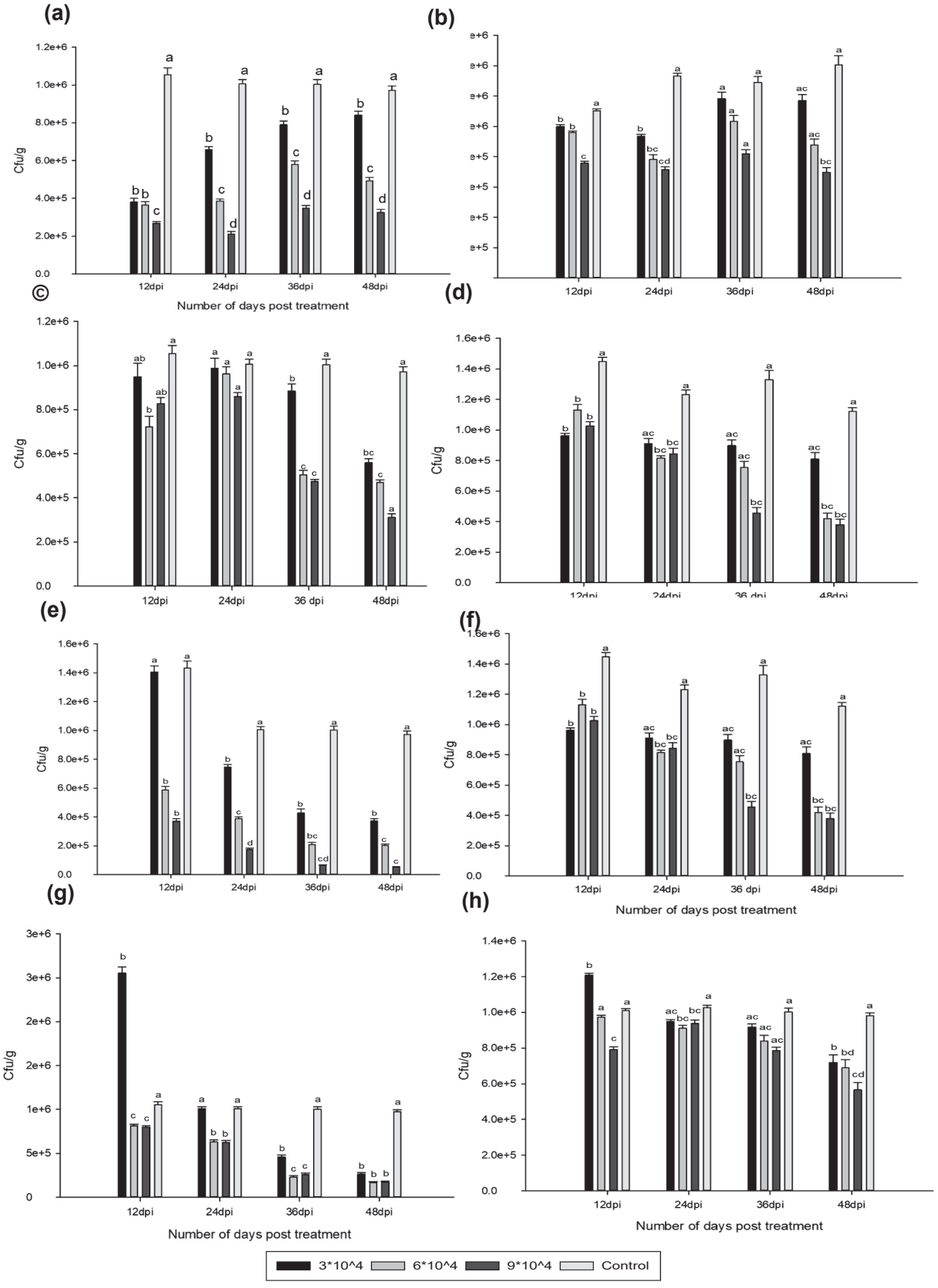


Fig. 1. Colony forming unit (CFU) counts of bulk soil of *Trichoderma* treated roots of DCS-107 and 48-1 respectively at 12, 24, 36 and 48-days post inoculation (dpi). *T. asperellum* 7316 treated DCS-107 (**a**), *T. asperellum* 7316 treated 48-1 (**b**), *T. asperellum* N13 treated DCS-107 (**c**), *T. asperellum* N13 treated 48-1 (**d**), *T. asperellum* TV5 treated DCS-107 (**e**), *T. asperellum* TV5 treated 48-1 (**f**), *T. asperellum* TV2B16 treated DCS-107 (**g**), and *T. asperellum* TV2B16 treated 48-1 (**h**). Statistical difference between treatments displayed at Tukey < 0.05. Vertical bars represent Mean $\pm$ standard error (SE).

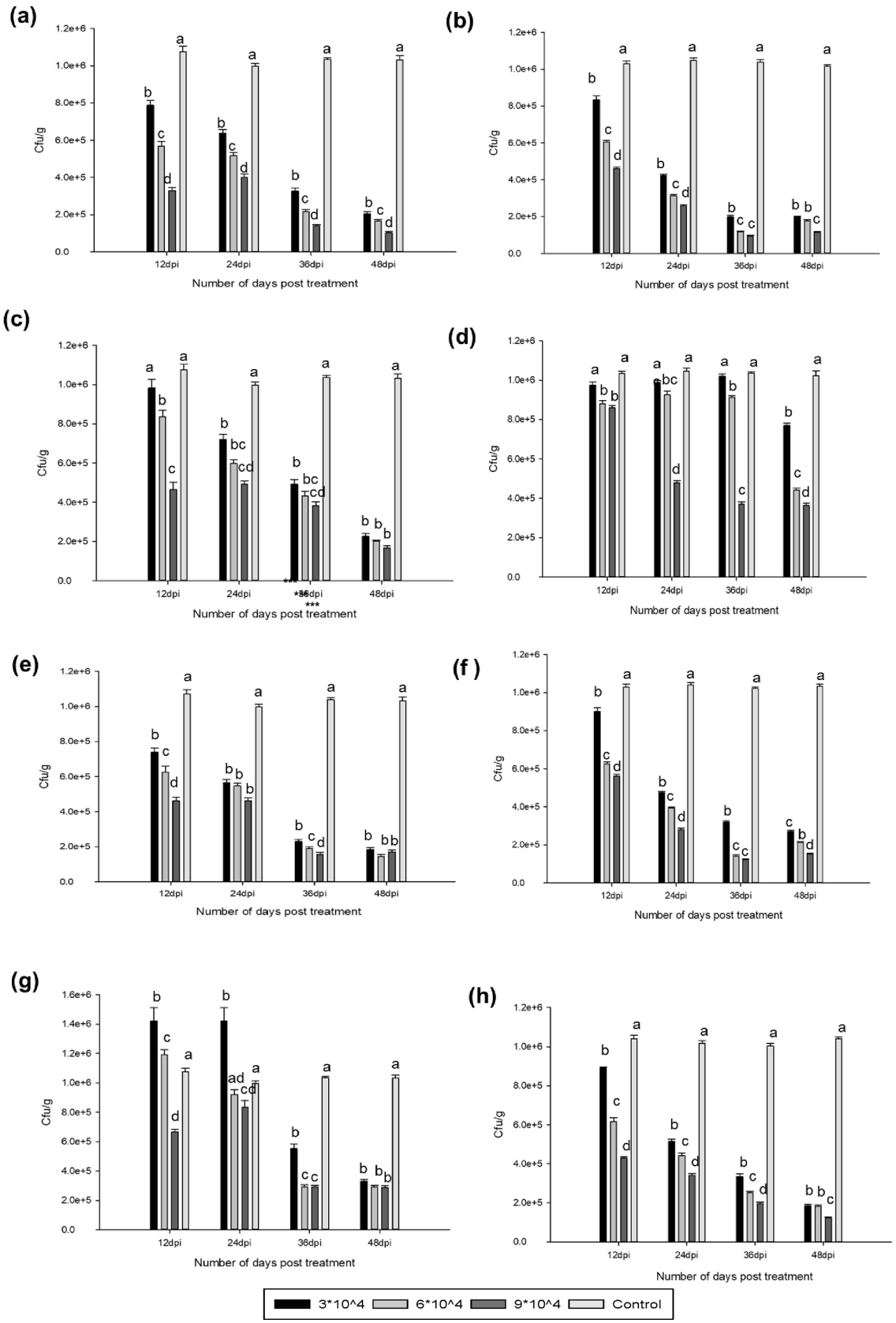


Fig. 2. Colony forming unit (CFU) counts of rhizosphere soil of *Trichoderma* treated roots of DCS-107 and 48-1 respectively at 12, 24, 36 and 48 dpi. *T. asperellum* 7316 treated DCS-107 (**a**), *T. asperellum* 7316 treated 48-1 (**b**), *T. asperellum* N13 treated DCS-107 (**c**), *T. asperellum* N13 treated 48-1 (**d**), *T. asperellum* TV5 treated DCS-107 (**e**), *T. asperellum* TV5 treated 48-1 (**f**), *T. asperellum* TV2B16 treated DCS-107 (**g**), and *T. asperellum* TV2B16 treated 48-1 (**h**). Statistical difference between treatments displayed at Tukey < 0.05. Vertical bars represent Mean $\pm$ standard error (SE).

Table 1
The effect of biopriming with *Trichoderma* strains on seed germination and radicle growth of castor genotypes at 4 dpi.

Biopriming with *Trichoderma* isolates	Percentage seed germination (%)		Radicle length (mm)	
	DCS-107	48-1	DCS-107	48-1
Trichoderma asperellum N13	85 ± 3.19^{c}	46.67 ± 2.72^{a}	49.77 ± 1.53^{c}	22.09 ± 0.56^{c}
Trichoderma asperellum 7316	96.67 ± 1.93^{b}	71.67 ± 3.19^{b}	69.56 ± 1.44^{b}	25.82 ± 0.62^{b}
Trichoderma asperellum TV5	81.67 ± 3.19^{acd}	41.67 ± 4.519^{a}	39.8 ± 1.18^{a}	16.76 ± 0.41^{a}
Trichoderma asperellum TV2B16	91.67 ± 1.67^{bcd}	40 ± 2.72^{a}	41.77 ± 1.72^{a}	18.83 ± 0.35^{d}
Untreated (Control)	73.33 ± 2.72^{a}	38.33 ± 3.19^{a}	40.13 ± 1.32^{a}	15.45 ± 0.59^{a}

^{a,b,c,d} Statistical significance levels for treatments with each of the *Trichoderma* isolates. Mean ± standard error (SE) with different letters indicate significance level at $P < 0.05$, according to Tukey test.

these plants were further analysed for other growth parameters.

Significant differences in the growth of roots (Fig. 3a), leaves (Fig. 3b), and shoot (Fig. 3c) was observed in DCS-107 in response to all the *Trichoderma* strains. A significant increase in plant growth demonstrated by an increase in shoot length by 46.5, 28.9, and 23% in 7316, N13, and TV5 treated DCS-107 respectively was noted when compared to untreated controls. Similarly, bio-priming led to enhanced plant fresh weight and dry weight in DCS-107. The total biomass calculated for *Trichoderma*-treated plants showed a 131, 85 and 60% increase in fresh weight and 84, 41, 31 % increase in dry weight in 7316, N13 and TV5 treated DCS-107 respectively when compared to untreated controls. TV2B16 treatment showed a marginal 13% increase in fresh weight for DCS-107 (Fig. 3d-f).

3.5. Antagonistic effect of Trichoderma on Fusarium through dual-fungal cultures

To study, the antagonistic properties of *Trichoderma* against *F. oxysporum ricini,* the fungal strains were tested through confrontation plate assays. The dual cultures grown with *F. oxysporum* along with each of the four strains of *T. asperellum,* kept at equidistance from one another in Petri plates were monitored for the extent of mycelia spread. Petri plates growing *Trichoderma* and pathogen discs alone served as controls. All the strains overgrew at least two-third of the medium surface thus showing a pronounced antifungal activity of *Trichoderma* (Fig. S5). TV2B16 showed profuse growth-inhibiting *Fusarium* fungal growth on 7 dpi while a clear zone of inhibition was observed for 7316 against *F. oxysporum.*

Percentage fungal pathogen growth inhibition caused by the antagonistic effect of *Trichoderma* strains was estimated based on the delta values of inhibition (Δ inhibition) as shown in Table. 2. The strains 7316 and TV2B16 showed a higher degree of antibiosis against *F. oxysporum* with a 9.38 and 7.5% pathogen growth inhibition respectively on the fourth day and 44.8 and 40.7 % inhibition by both the strains on the seventh day of plating (Fig. S5j).

Table 2
Percentage *Fusarium* pathogen growth inhibition by the antagonistic effect of *Trichoderma* strains.

Trichoderma isolates	Percentage inhibition of *Fusarium* growth (%)	
	4 dpi	7 dpi
Trichoderma aperellum N13	9.13 ± 0.49^{a}	40.69 ± 0.98^{ab}
Trichoderma asperellum 7316	9.761 ± 0.77^{a}	44.82 ± 0.43^{a}
Trichoderma asperellum TV5	5.9 ± 0.95^{a}	36.83 ± 1.08^{b}
Trichoderma asperellum TV2B16	7.51 ± 0.5^{a}	44.81 ± 0.48^{a}

^{a,b} Statistical significance levels for treatments with each of the *Trichoderma* isolates. Mean ± SE with different letters indicate significance level at $P < 0.05$, according to Tukey test.

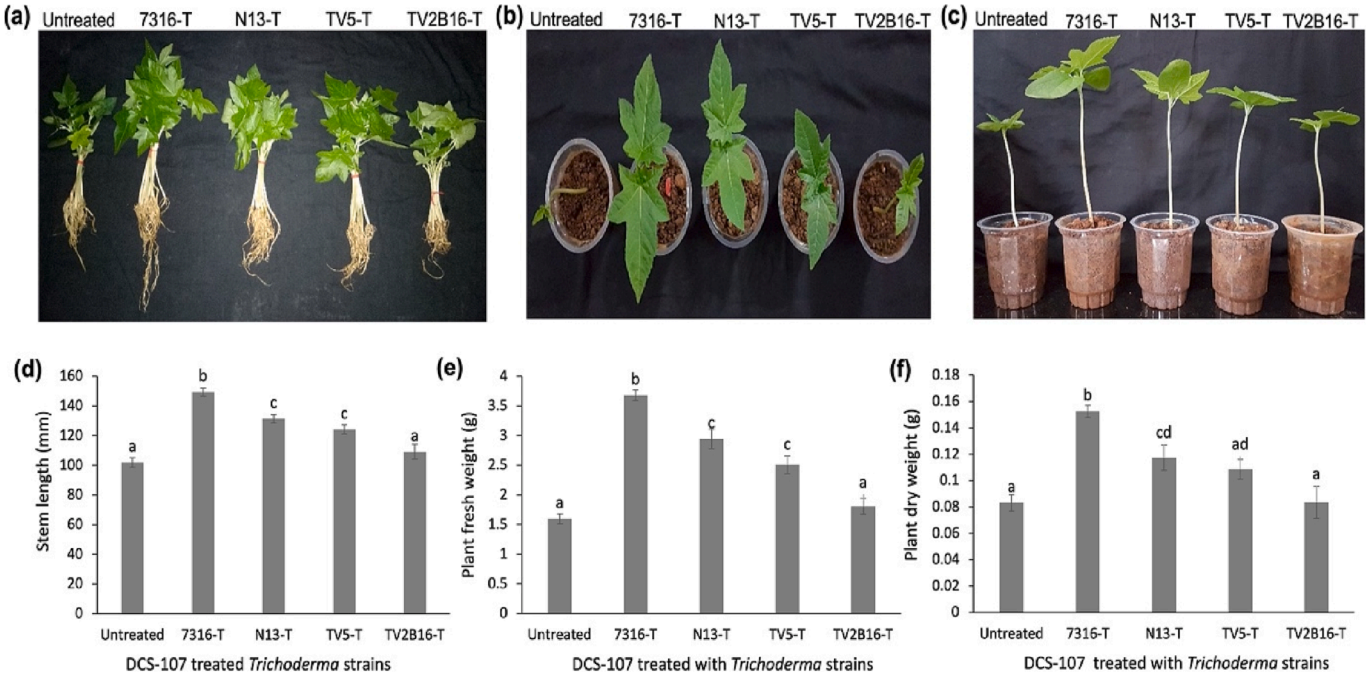


Fig. 3. Effect of *Trichoderma* treatment on plant growth of castor plants of DCS-107 genotype. The roots (**a**), leaves (**b**) and shoot (**c**) of two-week-old plants treated with *T. asperellum* strains; 7316, N13, TV5 and TV2B16. Graphical representation of length of the stem (**d**) measured in milli meters (mm), fresh weight (**e**) and dry weight (**f**) measured in grams (**g**) of castor plants. Untreated: Castor plants mock-treated with CMC solution alone; T: *Trichoderma*-treated plants. Statistical difference between the treatments displayed at Tukey < 0.05. Vertical bars represent Mean ± standard error (SE).

3.6. Effect of Trichoderma on castor challenged with Fusarium oxysporum

To test the effect of *Trichoderma* treatment on the root wilt disease caused by *F. oxysporum, Trichoderma* treated roots of DCS-107 and 48-1 were co-stressed with the fungal pathogen, *F. oxysporum.* Wilt disease symptoms along with plant growth were monitored at 7 and 21 dpi respectively (Fig. S6). The set of plants that were treated with *Fusarium* pathogen alone showed yellowing of roots and wilting at 7dpi (Fig. S6a), followed by complete death of the plant by 21 dpi (Fig. S6b). The *T. asperellum* strains; 7316 and N13- treated plants showed no major wilting at 7dpi, even though N13 showed yellow discoloration of the roots. Whereas both TV5 and TV2B16 treated plants showed slight drooping of leaves along with yellowed roots at 7dpi.

At 21 days, it was evident that 7316 showed elevated level of biocontrol compared to all the other strains used in the experiment with the lowest percentage of wilt incidence, which is 24% (Fig. 4). This is consistent with the results obtained in dual culture experiment where 7316 showed maximum antibiosis. Though TV5 showed relatively higher wilt disease incidence when compared to TV2B16, the level of disease incidence was significantly lower than that of the control plants. Moreover, the three strains; N13, TV5, and TV2B16 displayed a moderate level of resistance to *Fusarium* when compared to the pathogen-challenged plants. The castor genotype, 48-1 on the other hand did not withstand biopriming with *Trichoderma*, thus indicating the sensitivity of seeds of 48-1 to biopriming (data not shown).

3.7. Quantitative real time PCR for host response to Trichoderma treatment

To test host responses to *Trichoderma* treatment, the relative expression of 13 putative defence response genes comprising of Phenylalanine lyase (*PAL*), Pathogenesis Related Protein1 (*PR1*), Pathogenesis Related Protein2 (*PR2*), Pathogenesis Related Protein5 (*PR5*), 12-oxophytodienoate reductase (*OPR*), Responsive to Desiccation29 (*RD29*), Calreticulin (*CRT*), Glutaredoxin (*GRX*), Chalcone synthase (*CHS*), MYB (myeloblastosis) family of transcription factor (*MYB75*), UDP-glucose:flavonoid 3-o-glucosyltransferase (*UF3GT*), Lipoxegenase (*LOX*) and S-Adenosyl-L-methionine (*SAM*) genes were monitored in *Trichoderma*-treated DCS-107 and 48-1 plants with two strains, 7316 and N13 individually compared to the controls (mock-treated with water). Relative expression of defence response genes showed significant variation not only between the two strains of *Trichoderma*, but also between the two genotypes of castor (Fig. 5). 7316 treated roots of castor showed a down-regulation of majority of the defence response genes in both 48-1 and DCS-107. The *PR2* transcripts were up-regulated 3 fold-change in 7316 treated DCS-107 roots while its expression was down-regulated in N13. Though *OPR* was up-regulated in both 48-1 and DCS-107, a 4 fold-change up-regulation was observed in DCS-107 compared to 48-1. *LOX* and *SAM* showed prominent up-regulation only in DCS-107. Conversely, treatment with N13 showed up-regulation of all the twelve defence response genes in DCS-107 roots whereas all genes except GRX were down-regulated in 48-1 roots.

Interestingly, leaves of 7316 treated plants (root treatment) showed an enhanced expression of major defence related genes like *PAL*, *PR1*, *PR5*, *RD29*, *CRT*, and *GRX* in both the genotypes of castor (Fig. 6). The genes *PR2*, *CHS*, *MYB75*, *UF3GT*, *LOX5* and *SAM* were differentially regulated in the two genotypes while *OPR* remains down-regulated in both. Notably, leaves of N13 (root treatment) treated plants showed a down-regulation of most genes in 48-1 except *PR1*. The genes *PR2*, *RD29*, *CRT* and *LOX5* were up-regulated in DCS-107 leaves whereas PAL, *OPR*, *GRX* and *SAM* were down-regulated suggesting fine-tuning of the activation of different network pathways of defence genes. Together these data indicate that *Trichoderma* strains 7316 and N13 activate both localized and induced systemic resistance in the roots and leaves of castor respectively that shows substantial variation across the two genotypes of castor.

3.8. Biochemical analysis to evaluate host responses to Trichoderma treatment

To monitor the biochemical responses of *Trichoderma* against *Fusarium* wilt causing pathogen, *Fusarium oxysporum,* the DCS-107 plants were inoculated in isolation with three different treatments; *Trichoderma* alone, *Fusarium* alone and co-culturing with *Trichoderma* and *Fusarium* pathogen. Of the two strains used for testing the host response to

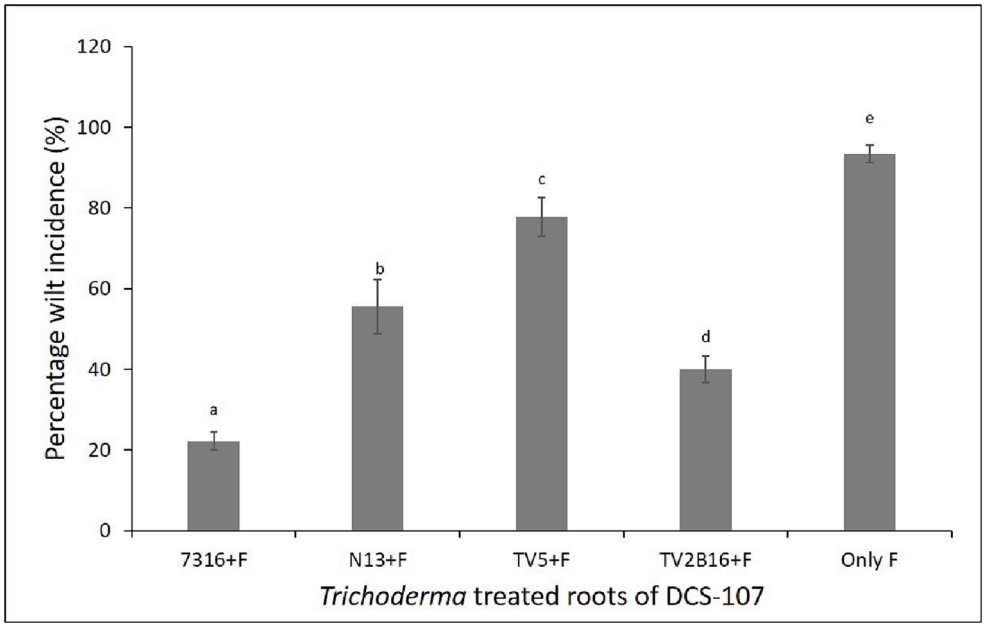


Fig. 4. Effect of *Trichoderma* treatment on *Fusarium* wilt disease in castor. Percentage *Fusarium* wilt incidence recorded in the roots of DCS-107 plants treated with *T. asperellum strains;* 7316, N13, TV5 and TV2B16 at 21 dpi. The data was normalized against the control/untreated samples for all treatments. Statistical difference between the treatments displayed at Tukey < 0.05. Vertical bars represent Mean $\pm$ standard error (SE).

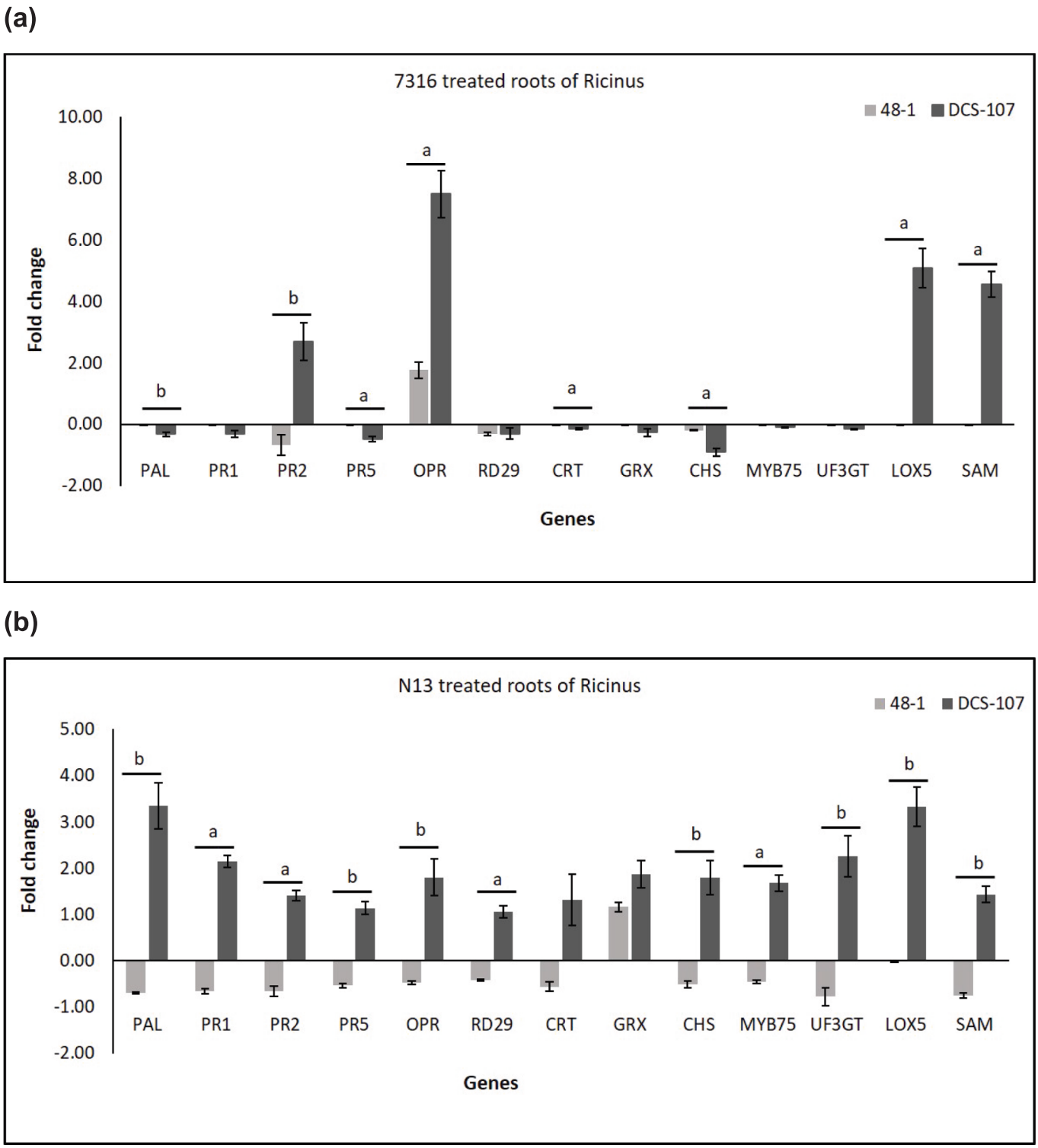


Fig. 5. Relative expression of defence response genes in roots of *Trichoderma* treated DCS-108 and 48-1 genotypes of castor. Relative levels of mRNA transcript accumulation of 13 genes in *T. asperellum* 7316-treated (**a**) and *T. asperellum* N13-treated (**b**) roots of castor at 48 hpi. Actin gene expression was used as control to normalize the expression of the defence genes, using the $2^{-\Delta\Delta CT}$ method. The graphs show the mean expression levels ± standard deviation (SD). The alphabets denote the level of significance of each gene amongst the two genotypes of castor. a: $p < 0.0$; b: $p < 0.05$.

Trichoderma treatment, it was noticed that for 7316, majority of the defence response genes were down-regulated. Further, 7316 has shown better growth promoting and antibiosis ability suggesting it's recognition by the host as not only non-threatening but also beneficial for plant growth. Hence our results narrowed down to 7316 which was chosen to carry forward further biochemical studies. The castor genotype, 48-1 on the other hand did not withstand biopriming with *Trichoderma*, thus indicating the sensitivity of seeds of 48-1 to biopriming (data not shown).

In *Trichoderma*-treated roots of DCS-107 plants, SOD and CAT levels were enhanced, though the up-regulation of SOD is lesser compared to CAT (Fig. 7). SOD level was even higher in case of co-stressed plants.

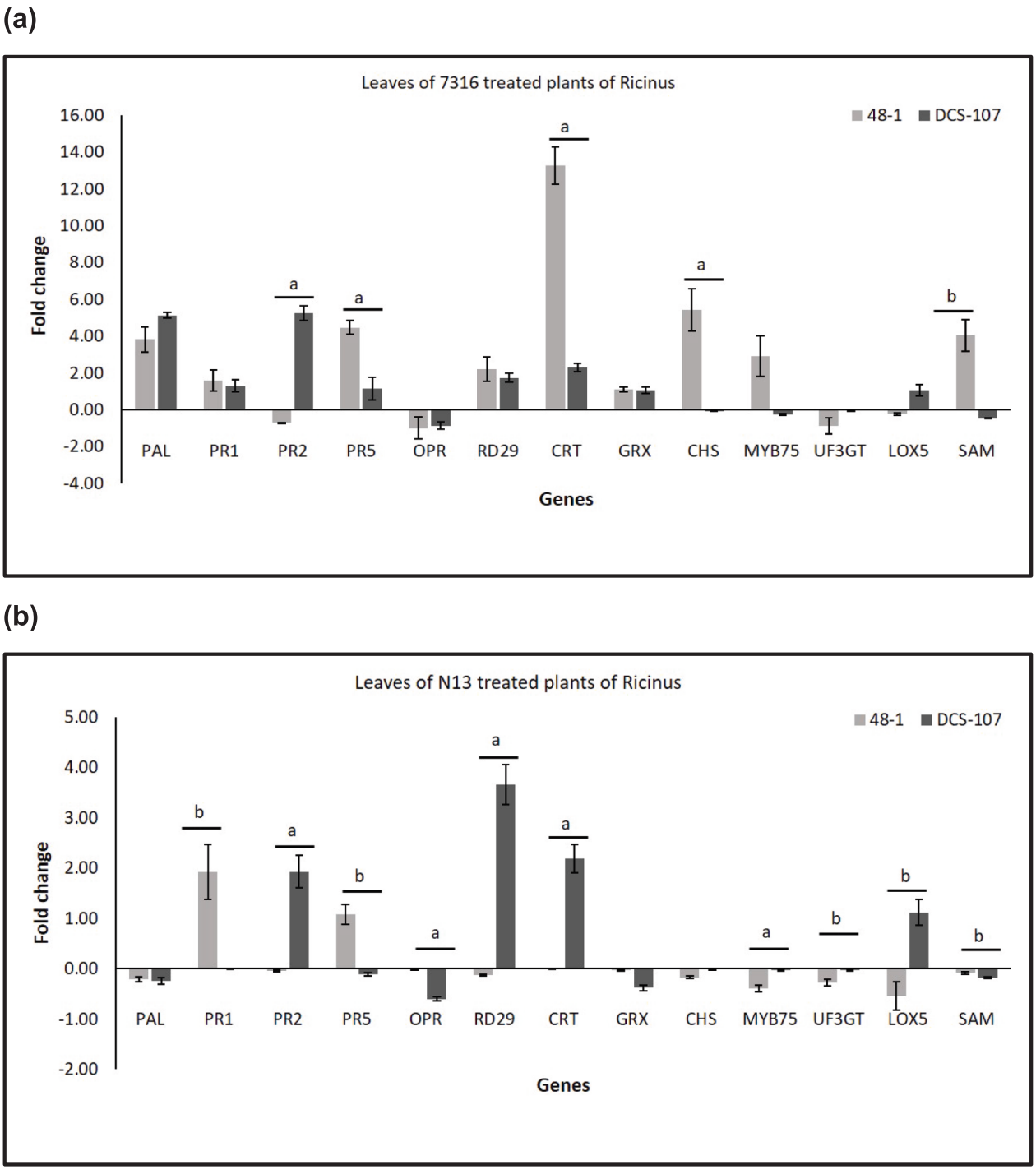


Fig. 6. Relative expression of defence response genes in leaves of *Trichoderma* treated DCS-108 and 48-1 genotypes of castor. Relative levels of mRNA transcript accumulation of 13 genes in *T. asperellum* 7316-treated (**a**) and *T. asperellum* N13-treated (**b**) leaves of castor at 48 hpi. Actin gene expression was used as control to normalize the expression of the defence genes, using the $2^{-\Delta\Delta CT}$ method. The graphs show the mean expression levels ± standard deviation (SD). The alphabets denote the level of significance of each gene amongst the two genotypes of castor. a: $p < 0.0$; b: $p < 0.05$.

CAT activity was observed to be elevated in *Fusarium*-infected plants as well as *Trichoderma*-inoculated and co-stressed samples compared to healthy controls which might be due to accumulation of excess H_2O_2 during pathogen infection.

GPX also plays an important role in the fine regulation of ROS levels in the cell through the activation and deactivation of H_2O_2. Just like SOD, GPX level was seen to be the highest in the case of co-stressed plants. Total phenol content (TPC) in *Trichoderma*-treated tissues was significantly higher than that in untreated castor plants, though the highest expression was seen in co-stressed samples. Synthesis of high amount of phenols by 7316, compared to the controls, suggests their role in inducing resistance against *Fusarium* wilt in castor.

4. Discussion

The genus, *Trichoderma* encompass promising biocontrol agents (BCA) to control phytopathogens. Identifying potential *Trichoderma* strain(s) would ensue an effective and economically viable biocontrol

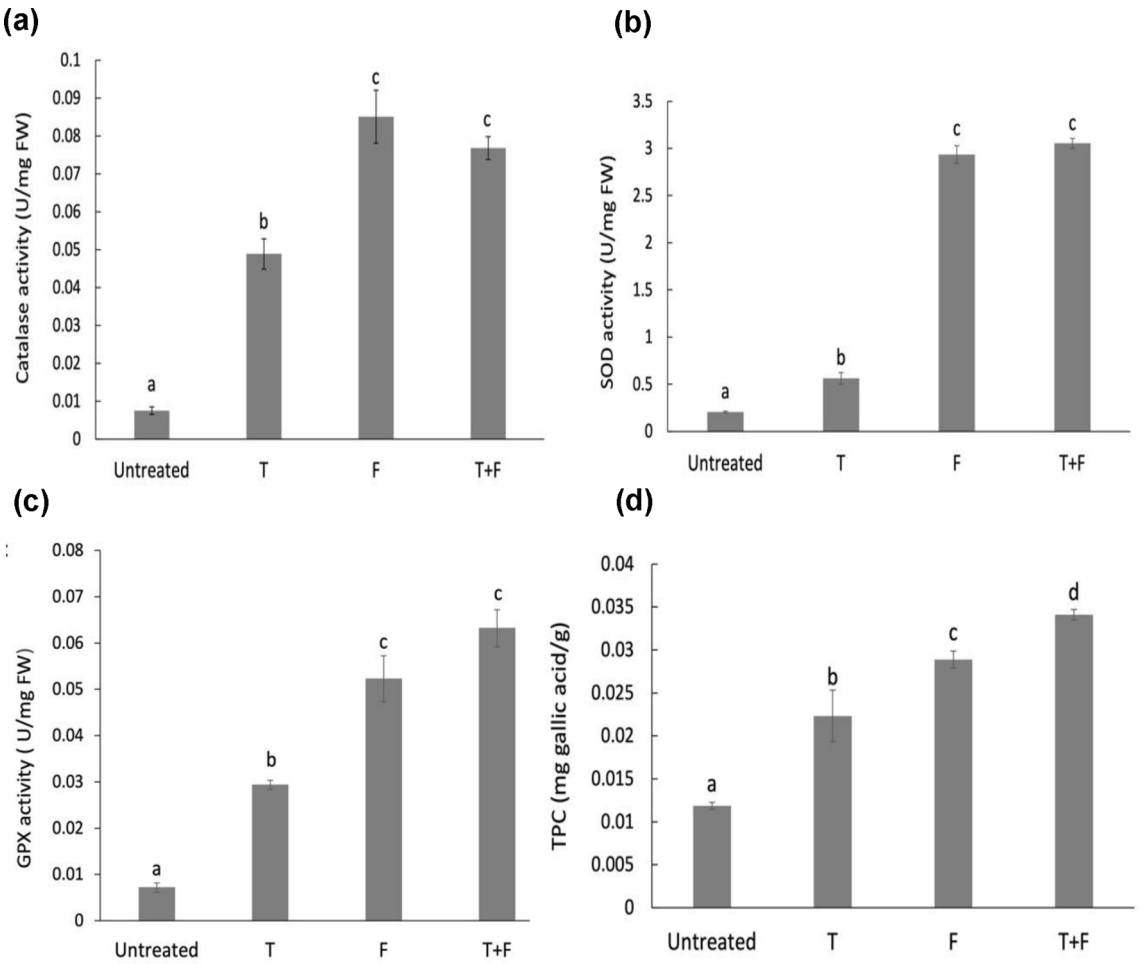


Fig. 7. Effect of *Trichoderma asperellum* 7316 on the accumulation of antioxidative enzymes CAT (**a**), SOD (**b**) and GPX (**c**) and, total phenol content (TPC) (**d**) either individually or in the combination with *Fusarium* in castor at 3 dpi. Histograms shown by different letters indicating statistical significance level between treatments displayed at Tukey < 0.05. Vertical bars represent Mean $\pm$ standard deviation (SE).

measure. Two castor genotypes; DCS-107 and 48-1 varying in tolerance to wilt disease were treated with *Trichoderma asperellum* strains to test their efficacy on plant growth and biocontrol of *Fusarium oxysporum,* the wilt causing fungal pathogen of castor. The seed treatment has been considered as one of the effective methods to confer resistance against biotic and abiotic stresses (Xue et al., 2017) and also to increase crop yield (Singh et al., 2016). The research findings have demonstrated that the strains of *T. asperellum* used in the study varied in their rhizosphere competency, biocontrol, and plant growth-promoting properties. Though all the strains showed efficient rhizosphere competence ability, two strains 7316 and TV5 showed significant competitive ability when compared to the other strains. N13 showed relatively effective results in the rhizosphere soil compared to bulk soil, though the effect was enhanced post 36 days. This could be due to a considerable amount of time required by N13 to establish and proliferate in the rhizosphere compared to other strains. The success of biocontrol agents depends on their ability to efficiently proliferate and colonize in the rhizosphere (Lo et al., 1996). Further, variation among the two genotypes has had been noticed when treated with the same *Trichoderma* strain indicating that either the gene products or the secondary metabolites produced by the host genotypes could be playing a critical role in its colonization and rhizosphere competence ability (Saravanakumar et al., 2016; Li et al., 2016; Kumar and Ashraf, 2017).

The significant reduction of CFU count by *Trichoderma* might be due to its high propensity to mobilize soil nutrients at a rapid rate divesting the uptake of nutrients, resulting in the limitation and starvation of other competing microorganisms (Benítez et al., 2004). The reduced CFU count also relates to effectual colonization on the roots of castor and the spread of *Trichoderma* in bulk and rhizosphere soil samples. Along with competitive nutrient uptake, *Trichoderma* appears to modify the environmental pH of the rhizosphere, along with its ability to survive in a wide range of pH conditions (Benítez et al., 2004; Sharma and Gothalwala, 2017) resulting in a decline of the CFU count in the rhizosphere of the plants. Being able to alter the surrounding pH, *Trichoderma* might be impeding the pathogens to secrete pathogenicity factors and thereby reducing their virulence in the host genotype (Saravanakumar et al., 2016; Li et al., 2016; Kumar and Ashraf, 2017).

In agreement with the previous studies, the *Trichoderma* strains impeded the growth of *F. oxysporum* in the present study. Though 7316 and TV2B16 showed better inhibition, the strain TV2B16 was highly proliferating and rapidly overgrowing on *Fusarium* pathogen which indicated the antibiosis effect of *Trichoderma.* The clear zone of inhibition observed in 7316 might be resulting from diffusible metabolites synthesized or secreted by *Trichoderma.* Previous studies reported that *Trichoderma* releases a wide range of secondary metabolites that are antifungal and antibacterial in nature which include epipolythiodioxopiperazines, peptaibols, pyrones, pyridones, butenolides, azaphilones, koninginins, lactones, steroids, anthraquinones and trichothecenes that inhibits the growth of various phytopathogens (Khan et al., 2020a,b; Schuster and Schmoll, 2010). The results obtained from challenging of *Trichoderma*-primed castor roots with *F. oxysporum* confirmed the role of *Trichoderma* in combating biotic stress, especially with the strain, 7316

which appeared to be effective in controlling *Fusarium* pathogen. In addition to the antagonistic property of *Trichoderma*, one of its major roles lies in plant growth promotion and development. Previous research studies have been able to strongly establish the growth promotion effect of *Trichoderma* on several economically important agricultural crops (Singh et al., 2016; Xue et al., 2017).

The biopriming of castor seeds with *Trichoderma asperellum* strain, 7316 enhanced the seed germination of *Trichoderma*-treated castor genotypes compared to the control samples similar to the findings by Hajieghrari and associates (2010). In our study, three strains, 7316, N13 and TV5 showed varying levels of rhizosphere competence, antagonism and growth promotional response in castor genotypes which could be utilized either singly or in combination to increase plant growth and biocontrol potential in castor.

Trichoderma spp. being opportunistic plant symbionts elicit a vast gene transcript reprogramming in plants (Brotman et al., 2013). A comparative analysis carried to understand the host response to two selected *Trichoderma* strains (7316 and N13) which demonstrated effective rhizosphere competence, plant growth and development, along with mycoparasitism and resistance to *Fusarium* revealed variation in the pattern of genetic reprogramming in castor. Phenylalanine ammonia lyase (*PAL*) is the first enzyme in the phenylpropanoid biosynthesis pathway which is involved in the biosynthesis of lignin, phenols and even salicylic acid (Kim and Hwang, 2014). *LOX5* plays an important role in defence response and lateral root development (Park et al., 2010; Caldelari et al., 2010). The gene 12-oxo-phytodienoic acid reductase (*OPR*) is important in the jasmonic acid (JA) biosynthesis pathway (Scalschi et al., 2015) and thus plays a vital role in plant defence. In DCS-107 treated with N13 strain showed up-regulated *PAL*, OPR and *LOX5* activity compared to 48-1 suggesting the activation of defence pathways were genotype dependent. 7316 treated plants of both the genotypes of castor showed down-regulated *PAL* activity but up-regulated *OPR* indicating the priming of JA related defence response by 7316, whereas *LOX5* up-regulated in DCS-107 alone.

Similarly, Pathogenesis-related (*PR*) proteins are a specific set of proteins that are induced on pathogen attack and play a very vital role in the defence response of plants (Jain and Khurana, 2018). Overexpression of *PAL* in pepper leads to enhanced production of *PR1* that plays a vital role in the SA dependent SAR response. This is vividly seen in N13 treated DCS-107 roots where up-regulated *PAL* activity coincides with elevated expression of *PR1*. This is consistent with findings of Shoresh and associates (2005) where *T. asperellum* T203 modulated the expression of major genes involved in the JA pathway. On the contrary, down-regulated *PAL* activity indicated that 7316 inoculation may have repressed the SAR response in DCS-107. N13 treated DCS-107 roots showed an up-regulation of the other PR genes as well (*PR2* and *PR5*) whereas in 48-1 all of the genes were down-regulated. 7316 treated roots of DCS-107 showed a 3 fold-change up-regulation of *PR2* gene. *PR2* (β-1,3 glucanase) is involved in increased lignin content and callose deposition which acts as a first line of defence response to pathogen entry. From the above observation, it is evident that different genotypes of castor show a diverse response to different strains of *Trichoderma*. *Trichoderma* is a plant-beneficial agent and for the fungus to be able to coexist as a symbiont in the roots, the down-regulation of most of the defence response genes indicates a strategy of the fungus to evade the innate immunity of the plant to allow the successful colonization of *Trichoderma* in the roots.

GRX acts an antioxidant and is involved in the cellular response to oxidative stress. Enhanced GRX activity in N13 treated roots compared to 7316 might be eliciting a higher oxidative burst compared to 7316. From the above observation, it can be said that compared to N13, colonization of 7316 results in modulating several defence genes to enable better colonization of the fungi in the host. Similar observations had been made by Brotman and associates (2013) in *Trichoderma* treated roots of *Arabidopsis thaliana* along with a range of other host plants (Morán-Diez et al., 2021). Previous study has shown that though *Trichoderma* is sensed by the plant as a "safe" organism it is able to prime the internal defence response of the plant that helps the plant combat any subsequent pathogen attack (Gupta and Bar 2020). Elevation of *OPR* shows that 7316 is able to trigger the JA-mediated signalling in the leaves of both the genotypes of castor. This could have been the reason why 7316 was the most efficient to combat the *Fusarium* infection in castor leading to better growth compared to the other strains tested.

Interestingly, out of the 13 defence response genes under study, 8 (*PAL*, *PR1*, *PR2*, *PR5*, *RD29*, *CRT*, *GRX* and *LOX5*) genes were up-regulated in leaves of DCS-107, whereas only 4 genes (*PR1*, *RD29*, *CRT* and *LOX5*) were up-regulated in N13 treated DCS-107. More so, the leaves of the 48-1 genotype of castor showed more up-regulation of genes by 7316 compared to N13. Similar result was seen in the leaves of grapevine on the root colonization by *Trichoderma atroviride* (Stempien et al., 2020). Elevated levels of *PAL* and *PR1* gene transcripts could indicate that root colonization of 7316 leads to elevated SA-mediated defence response in the leaves of castor, thus priming the plant from any subsequent pathogen infiltration.

Production of reactive oxygen species (ROS) comprising of hydrogen peroxide (H_2O_2) and superoxide (O_2^-) during an oxidative burst is one of the earliest defence responses elicited on the exposure to pathogen. However, overproduction of ROS is highly toxic and causes irreversible oxidative damage to cells. Our findings were in agreement with the findings by Shoresh et al. 2010 which have shown that *Trichoderma* protects plants against biotic stress by reducing ROS level. SOD, CAT and GPX are major ROS scavenging and antioxidant enzymes reported in plants in response to biotic stress. Though, SOD catalyses the dismutation of O_2^- which helps in reducing O_2^- content, it leads to the production of H_2O_2, whereas CAT enzyme catalyses H_2O_2 breakdown into water and oxygen in an energy-efficient manner.

GPX also plays an important role in the fine regulation of ROS levels in the cell through the activation and deactivation of H_2O_2. Just like SOD, GPX level was seen to be the highest in the case of co-stressed plants. The enhanced levels of antioxidative enzymes (SOD, CAT and GPX) in co-stressed castor plants compared to plants infected with *F. oxysporum*, suggested that protects castor from the damage of oxidative stress.

Total phenol content (TPC) in *Trichoderma*-treated tissues was significantly higher compared to untreated castor plants, though the highest expression was seen in co-stressed samples. The increase in phenolic content in plants is responsible for the deposition of lignin that acts as a physical barrier to pathogen entry. It also regulates molecules that are directly related to defence response (Keswani et al., 2017). Our results are in agreement with the findings reported by Bigirimana and associates (1997) and Singh and associates (2014) wherein inoculation of *Trichoderma* either alone or in consortium with other microbes caused enhanced phenolic accumulation. Synthesis of high amount of phenols by 7316, compared to the controls, suggests their role in inducing resistance against *Fusarium* wilt which might have elicited the production of sensing molecules in castor during disease resistance against wilt. Further, an in-depth study of the *Trichoderma* strains to synergize the effect of all toxic metabolites and hydrolytic enzymes may lead to formulating a complex strain that would enhance the antagonistic potential of *Trichoderma* as a BCA.

5. Conclusions

Trichoderma asperellum demonstrated both root colonizing and biocontrol properties. Biopriming with *T. asperellum* enhanced seed germination and root growth besides promoting antagonism against *Fusarium oxysporum ricini*. In our study, three strains of *Trichoderma. asperellum*; 7316, N13 and TV5 showed varying levels of rhizosphere competence, antagonism and growth promotional response, which could be utilized by employing the strains either singly or in combination to increase plant growth and biocontrol potential in castor. Real-Time gene expression analysis of host defence showed a complex

reprograming of the defence gene pathways suggesting a role of *Trichoderma* in eliciting Induced Systemic Response (ISR) in combating biotic stress, where *T. asperellum* 7316 was observed to be a promising strain in facilitating protection against *Fusarium* wilt disease in castor.

CRediT authorship contribution statement

Doris A. Pradhan: Methodology, Investigation, Formal analysis, Data curation, Writing – original draft. **Prathyusha Bagagoni:** Methodology, Investigation, Formal analysis, Manuscript review & editing. **Ragiba Makandar:** Conceptualization, Visualization, Investigation, Supervision, Resources, Funding acquisition, Project administration, Writing – review & editing.

Declaration of Competing Interest

The authors declare that they have no known competing financial interests or personal relationships that could have appeared to influence the work reported in this paper.

Acknowledgments

The funding from the Indian Council of Agricultural Research (ICAR)-NFBSFARA (F. No. NFBSFARA/BS-3007/2012-13 provided to RM is acknowledged. The Indian Institute of Oilseeds Research (IIOR), Hyderabad for providing castor genotypes and fungal cultures, Facilities at the University of Hyderabad (UoH) including UoH-IOE, DBT BUILDER, DBT-CREBB, DST-FIST, UGC-SAP, DST-PURSE, CIL, and Plant Culture Facility are acknowledged. Also, the financial support as fellowships to DAP (UGC-SRF) and PB (UoH-BBL fellowship) are acknowledged.

Appendix A. Supplementary material

Supplementary data to this article can be found online at https://doi.org/10.1016/j.biocontrol.2023.105280.

References

Aebi, H., 1984. [13] Catalase in vitro. Methods Enzymol. 105, 121–126.
Benítez, T., Rincón, A.M., Limón, M.C., Codón, A.C., 2004. Biocontrol mechanisms of *Trichoderma* strains. Int. Microbiol. 7, 249–260.
Beyer Jr., Wayne, F., Irwin, F., 1987. Assaying for superoxide dismutase activity: some large consequences of minor changes in conditions. Analytical Biochem. 161, 559–566.
Bigirimana, J., Meyer, G.D., Poppe, J., Elad, Y., Höfte, M., 1997. Induction of systemic resistance on bean (*Phaseolus vulgaris*) by *Trichoderma harzianum*. Mededelingen van de Faculteit Landbouwkundige en Toegepaste Biologische Wetenschappen 62, Universiteit Gent pp. 1001–1007.
Brotman, Y., Landau, U., Á Inostroza, I.C., Takayuki, T., Fernie, A.R., Chet, I., Viterbo, A., Willmitzer, L., 2013. Trichoderma-Plant Root Colonization: Escaping Early Plant Defense Responses and Activation of the Antioxidant Machinery for Saline Stress Tolerance. PLOS Pathogens. 9(3), e1003221.
Caldelari, D., Wang, G., Farmer, E.E., Dong, X., 2010. *Arabidopsis lox3 lox4* double mutants are male sterile and defective in global proliferative arrest. Plant Mol. Biol. 75, 25–33.
Chance, B., Maehly, A.C., 1955. Assay of Catalase and Peroxidase. Methods in Enzymol. 2, 764–775.
Devi, T.P., Prabhakaran, N., Kamil, D., 2017. Development of Species-Specific Markers for the identification of *Trichoderma asperellum* and *Trichoderma harzianum*. Vegetos-Int. J. Plant Res. 30, 94–100.
Elad, Y., 2000. Biological control of foliar pathogens by means of *Trichoderma harzianum* and potential modes of action. Crop Protect. 19, 709–714.
Grondona, I., Hermosa, R., Tejada, M., Gomis, M.D., Mateos, P.F., Bridge, P.D., Monte, E., Garcia-Acha, I., 1997. Physiological and Biochemical Characterization of *Trichoderma harzianum*, a Biological Control Agent against Soilborne Fungal Plant Pathogens. Appl. Environ. Microbiol. 63, 3189–3198.
Gupta, R., Bar, M., 2020. Plant Immunity, Priming, and Systemic Resistance as Mechanisms for *Trichoderma* spp. Trichoderma Rhizosphere Biol. 81–110.
Hajieghrari, B., 2010. Effects of some Iranian *Trichoderma* isolates on maize seed germination and seedling vigor. Afr. J. Biotechnol. 9, 4342–4347.
Hermosa, R., Viterbo, A., Chet, I., Monte, E., 2012. Plant-beneficial effects of *Trichoderma* and of its genes. Microbiol. 158, 17–25.
Jain, D., Khurana, J.P., 2018. Role of Pathogenesis-Related (PR) Proteins in Plant Defense Mechanism. Mol. Aspects Plant-Pathogen Interaction 265–281.
Karuppiah, V., Li, T., Vallikkannu, M., Chen, J., 2019. Co-cultivation of *Trichoderma asperellum* GDFS1009 and *Bacillus amyloliquefaciens* 1841 causes differential gene expression and improvement in the wheat growth and biocontrol activity. Front. Microbiol. 1068, 1–16.
Keswani, C., Bisen, K., Chitara, M.K., Sarma, B.K., Singh, H.B., 2017. Exploring the Role of Secondary Metabolites of *Trichoderma* in Tripartite Interaction with Plant and Pathogens. In: Singh J., Seneviratne G. (eds) Agro-Environmental Sustainability. Springer pp 63–79.
Khan, R.A.A., Najeeb, S., Hussain, S., Xie, B., Li, Y., 2020a. Bioactive Secondary Metabolites from *Trichoderma* spp. against Phytopathogenic Fungi. Microorganisms. 8, 817.
Khan, R.A.A., Najeeb, S., Mao, Z., Ling, J., Yang, Y., Li, Y., Xie, B., 2020b. Bioactive secondary metabolites from *Trichoderma* spp. against phytopathogenic bacteria and koot-Knot nematode. Microorganisms 8, 401.
Kim, D.S., Hwang, B.K., 2014. An important role of the pepper phenylalanine ammonia-lyase gene (PAL1) in salicylic acid-dependent signalling of the defence response to microbial pathogens. J. Exp. Bot. 65 (9), 2295–2306.
Kumar, M., Ashraf, S., 2017. Role of *Trichoderma* spp. as a Biocontrol Agent of Fungal Plant Pathogens. Probiotics and Plant Health, pp. 497–506.
Li, Y., Sun, R., Yu, J., Saravanakumar, K., Chen, J., 2016. Antagonistic and Biocontrol Potential of *Trichoderma asperellum* ZJSX5003 against the Maize Stalk Rot Pathogen *Fusarium graminearum*. Indian J Microbiol. 56, 318–327.
Liu, Q., Meng, X., Li, T., Raza, W., Liu, D., Shen, Q., 2020. The Growth Promotion of Peppers (*Capsicum annuum* L.) by *Trichoderma guizhouense* NJAU4742-Based Biological Organic Fertilizer: Possible Role of Increasing Nutrient Availabilities. Microorganisms. 9, 1296. doi: 10.3390/microorganisms 8091296.
Lo, C.T., Nelson, E.B., Harman, G.E., 1996. Biological control of turfgrass diseases with a rhizosphere competent strain of *Trichoderma harzianum*. Plant Disease. 80, 736–741.
Meng, X., Miao, Y., Liu, Q., Ma, L., Gua, K., Liu, D., Ran, W., Shen, Q., 2019. TgSWO from *Trichoderma guizhouense* NJAU4742 promotes growth in cucumber plants by modifying the root morphology and the cell wall architecture. Microb Cell Fact. 18, 148. https://doi.org/10.1186/s12934-019-1196-8.
Morán-Diez, M.E., Alba, A.E.M., Rubio, M.B., Hermosa, R., Monte, E., 2021. *Trichoderma* and the Plant Heritable Priming Responses. J Fungi (Basel). 7, 318.
Morris, J.B., Morse, S.A., Navas, A.A., Soares, D.J., Sofiatti, V., Wang, M.L., Zanotto, M. D., Zieler, H., 2012. A Review on the Challenges for Increased Production of Castor. Agronomy J. 104, 853–880.
Park, Y.S., Kunze, S., Ni, X., Feussner, I., Kolomiets, M.V., 2010. Comparative molecular and biochemical characterization of segmentally duplicated 9-lipoxygenase genes ZmLOX4 and ZmLOX5 of maize. Planta. 231, 1425–1437.
Qualhato, T.F., Cardoso, L.F.A., Steindorff, A.S., Brandao, R.S., Jesuino Amorim, R.S., Ulhoa, C.J., 2013. Mycoparasitism studies of *Trichoderma* species against three phytopathogenic fungi: evaluation of antagonism and hydrolytic enzyme production. Biotechnol. Lett. 35, 1461–1468.
Rahman, M.A., Begum, M.F., Alam, M.F., 2009. Screening of Trichoderma Isolates as a Biological Control Agent against *Ceratocystis paradoxa* Causing Pineapple Disease of Sugarcane. Mycobiol. 37 (2), 77–285.
Saravanakumar, K., Yu, C., Dou, K., Li, M.W.Y., Chen, J., 2016. Synergistic effect of *Trichoderma*-derived antifungal metabolites and cell wall degrading enzymes on enhanced biocontrol of *Fusarium oxysporum* f. sp. *cucumerinum*. Biol. Control. 94, 37–46.
Scalschi, L., Sanmartín, M., Camañes, G., Troncho, P., PSánchez-Serrano, J.J., García-Agustín, P., Vicedo, B., 2015. Silencing of OPR3 in tomato reveals the role of OPDA in callose deposition during the activation of defense responses against *Botrytis cinerea*. Plant J. 81, 304–15.
Schuster, A., Schmoll, M., 2010. Biology and biotechnology of *Trichoderma*. Appl Microbiol Biotechnol. 87, 787–799.
Severino, L.S., Auld, D.L., Baldanzi, M., Cândido, M.J.D., Chen, G., Crosby, W., Tan, D., He, X., Lakshmamma, P., Lavanya, C., Machado, O.L.T., Mielke, T., Milani, M., Miller, T.D., Morris, J.B., Morse, S.A., Navas, A.A., Soares, D.J., Sofiatti, 2012. A review on the challenges for increased production of castor. Agronomy J. 104, 853–880.
Sharma, P.K., Gothalwala, R., 2017. Trichoderma: A Potent Fungus as Biological Control Agent. Agro-Environ. Sustain.. 113–125.
Shoresh, M., Yedidia, I., Chet, I., 2005. Involvement of Jasmonic Acid/Ethylene Signaling Pathway in the Systemic Resistance Induced in Cucumber by *Trichoderma asperellum* T203. Phytopathol. 95, 76–84.
Shoresh, M., Harman, G.E., Mastouri, F., 2010. Induced systemic resistance and plant responses to fungal biocontrol agents. Annu. Rev. Phytopathol. 48, 21–43.
Singh, A., Jain, A., Sarma, B.K., Upadhyay, R.S., Singh, H.B., 2014. Rhizosphere competent microbial consortium mediates rapid changes in phenolic profiles in chickpea during *Sclerotium rolfsii* infection. Microbiol. Res. 353–360.
Singh, V., Upadhyay, R.S., Sarma, B.K., Singh, H.B., 2016. *Trichoderma asperellum* spore dose depended modulation of plant growth in vegetable crops. Microbiol Res. 193, 74–86.
Skidmore, A.M., Dickinson, C.H., 1976. Colony interaction and hyphal interference between *Septoria nodorum* and phylloplane fungi. Trans. Br. Mycol. Soc 66, 57–64.
Stempien, E., Pierron, R.J.G., Adendorff, I., Van, J.W.J., Halleen, F., Mostert, L., 2020. Host defence activation and root colonization of grapevine rootstocks by the biological control fungus *Trichoderma atroviride*. Phytopathologia Mediterranea. 59, 615–626.
Xue, A.G., Guo, W., Chen, Y., Siddiqui, I., Marchand, G., Liu, J., Ren, C., 2017. Effect of seed treatment with novel strains of *Trichoderma* spp. on establishment and yield of spring wheat. Crop Protect. 96, 97–102.

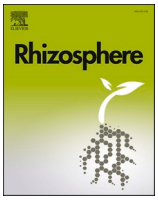
Rhizosphere 27 (2023) 100745



Contents lists available at ScienceDirect

Rhizosphere

journal homepage: www.elsevier.com/locate/rhisph





Delineating host responses induced by *Trichoderma* in castor through comparative transcriptome analysis

Doris A Pradhan, Ragiba Makandar *

Department of Plant Sciences, School of Life Sciences, University of Hyderabad, Prof. C.R. Rao Road, Gachibowli, Hyderabad 500046, India

ARTICLE INFO

Keywords:
Castor
Differentially expressed genes
Host defense
Next generation sequencing
Trichoderma
Transcriptome analysis

ABSTRACT

Trichoderma has been recognized as a beneficial fungus to promote crop growth and resistance against pathogens in plants. However, our understanding about the underling molecular mechanism is limited. Delineating the plant's responses to *Trichoderma* colonization is crucial to understand the molecular basis of their interaction. Therefore, to detect the key differentially expressed genes (DEGs), a pairwise transcriptome analysis was carried at 48 h post inoculation (hpi) between control and *Trichoderma*-treated roots of castor (*Ricinus communis* L.). A total of 20,696 plant transcripts were detected using EdgeR software, of which 1508 were DEGs. 474 of these putative DEGs were upregulated while the remaining were downregulated ($p < 0.05$) in the root samples of the castor genotype, DCS107 treated with *Trichoderma asperellum* strain 1736. Majority of the DEGs that were downregulated were related to stress, hypersensitive response, reactive oxygen species (ROS), phenylpropanoid pathway, secondary metabolite biosynthesis, carbohydrate and amino acid biosynthesis/metabolism, ABC transporters and transcription factors accompanied by proteins involved in electron transport. Further, to confirm the findings, Real Time-quantitative Polymerase Chain Reaction (RT-qPCR) was carried at 12, 24 and 48 hpi for a set of 9 DEGs with a putative role in stress and defense responses. 5 of these genes involved in stress response were found to be downregulated, similar to the transcriptome result. Likewise, the expression of the remaining genes- *WRKY71*, *RPV*, *ZAT5* and *RPS2* with a function in defense were found to be upregulated suggesting that these genes might be playing a crucial role in *Trichoderma*-mediated responses in castor.

1. Introduction

The fungal members of the genus, *Trichoderma* have been recognized as biocontrol agents due to their ability to exhibit efficient mycoparasitism against various pathogens (Rajani et al., 2021). The mycoparasitism of *Trichoderma* has been attributed to its ability to secrete various hydrolytic enzymes, ABC transporter membrane pumps and secondary metabolites accompanied by rhizosphere modification and competition for nutrients (Qualhato et al., 2013). Besides its parasitic nature, many rhizosphere competent strains of *Trichoderma* are able to colonize the roots of plants, an association that leads to overall plant growth promotion and productivity potential (Benítez et al., 2004). In addition to enhanced growth and development, *Trichoderma*'s association with plants has been demonstrated to induce both local and induced systemic resistance (ISR) responses in a variety of crops like pepper, tomato, pea, tobacco and sorghum (Liu et al., 2020; Singh et al., 2016; Li et al., 2015; Saber et al., 2017). Though previous studies have evaluated the ability of *Trichoderma* to promote antibiosis and plant growth, our understanding about the underlying mechanism is limited.

Identifying the key genetic components altered by *Trichoderma* in the host would reveal the mechanism employed by *Trichoderma* to modulate the plant's defense response to ensure their long-lasting beneficial association. Therefore, the present study was aimed at identifying the key components altered by *Trichoderma* treatment in castor in controlled conditions. In recent years, transcriptome studies have been extensively employed to identify key signaling components to decipher host-microbe interactions. Though, previous studies revealed that induced systemic resistance (ISR) gets activated by *Trichoderma* treatment in crop plants as well as model plants like, *Arabidopsis thaliana* and tomato (Alfano et al., 2007; Tucci et al., 2011; Mathys et al., 2012; Martínez-Medina et al., 2013), however, recent studies have indicated that partial suppression of salicylic acid (SA)-dependent responses in plants is necessary to form a symbiotic association between mycorrhiza and the host (Nishad et al., 2020).

India contributes about 85% of the global production of castor (*Ricinus communis* L.) However over the last couple of years there has

* Corresponding author.
E-mail address: mragiba@uohyd.ac.in (R. Makandar).

https://doi.org/10.1016/j.rhisph.2023.100745
Received 4 May 2023; Received in revised form 3 July 2023; Accepted 4 July 2023
Available online 13 July 2023
2452-2198/© 2023 Elsevier B.V. All rights reserved.

been a drop in the overall production of castor due to various biotic and abiotic factors. The rapid growth in population and the crop losses caused by emerging plant pathogens are major hindrances that require immediate action to ensure crop security in the coming years. Also, eco-friendly, non-hazardous practices for crop production are being promoted to achieve sustainability. *Trichoderma* has displayed such promising results for many agricultural crops. From an applicative perspective, sufficient evidence of a strong mutualistic relation between host and microorganism is necessary, before any biocontrol organism can be introduced to a crop. Hence, a better understanding of what really happens during *Trichoderma*'s interaction with the host, will undeniably open new ways to explore the potential of *Trichoderma* for better performance in agriculture.

We hypothesized that colonization of *Trichoderma* in castor involved alteration in host responses and defense signaling. To delineate the changes induced by *Trichoderma* colonization in the roots of castor, transcriptome study was carried by treating the roots of the castor genotype, DCS-107 grown in controlled conditions with *Trichoderma asperellum* strain, 7316 compared to the control (mock-treated) castor plants and the research findings are presented.

2. Materials and methods

2.1. Plant material and growth conditions

Seeds of castor genotype, DCS-107 were obtained from Indian Institute of Oilseeds Research (IIOR), Hyderabad, India. Surface sterilized seeds were germinated on sterile filter paper for 4 days. The germinated seedlings were grown hydroponically in autoclaved Hoagland's nutrient solution (Table S1) for 14 days in a plant growth chamber maintained at 28 °C and 14-day/10-night hour regime under a PAR of 500 W m^{-2} with 55% relative humidity (RH).

2.2. Culturing Trichoderma and plant inoculation

Trichoderma asperellum 7316 (MH236427.1, MK411201.1) isolated from arable soils of Telangana region of India, was obtained from IIOR, Hyderabad, India. Purified culture of *Trichoderma* streaked from a single spore was maintained on Potato Dextrose Agar (PDA) at 24±2 °C. The media was autoclaved at 121 °C and 15 psi for 15 min before inoculation. *Trichoderma* spores were harvested from 7-day old culture by rinsing with sterile water containing 0.02% (v/v) Tween 20 to disperse the spores in the solution.

Trichoderma inoculum was added to the 14-day-old castor plants grown in Hoagland's liquid plant growth medium under aseptic conditions following three washes to remove traces of Tween 20. The hydroponic cultures were adjusted to a final concentration of 10^5 germinated spores per ml. Castor plants treated with sterile distilled water alone served as controls. Three biological replicates for each of the treatments were collected at 48 hpi and the root samples were quick-frozen in liquid nitrogen for RNA isolation.

2.3. Microscopic examination of Trichoderma root colonization

To monitor the growth and colonization of *Trichoderma*, roots of *Trichoderma*-treated castor plants harvested at 48 hpi were stained with trypan blue in lactic acid. Root samples were cleared in 5% potassium hydroxide (KOH), stained in 0.1% trypan blue and stored at room temperature. The root samples were cut longitudinally into one cm-long fragments. The samples were mounted on a clean glass slides containing 20 μL of autoclaved 70% glycerol, covered with a cover slip and observed under the light microscope (Make: Olympus U-Cmad3).

2.4. Gene expression profiling using RNA-Seq

2.4.1. RNA isolation

Total RNA was isolated from control and *Trichoderma*-treated castor roots at 12, 24 and 48 hpi. The solutions and buffers were prepared in water pre-treated with 0.1% (v/v) diethylpyrocarbonate (DEPC) overnight and autoclaved at 121 °C at 15 psi for 15 min. 500 mg of root sample was ground to a fine powder in liquid nitrogen using a pestle and mortar. The powdered sample was transferred into 2 mL microcentrifuge tubes containing 1 mL of the extraction buffer-I which was pre-heated at 65 °C. Extraction buffer-I comprised of 2% cetyltrimethylammonium bromide (CTAB) (w/v), 2% polyvinylpolypyrrolidone (PVPP) (w/v), 100 mM tris(hydroxymethyl) aminomethane (Tris–HCl; pH 8.0), 25 mM ethylenediamine tetra-acetic acid (EDTA; pH, 8.0) and 2 M sodium chloride (NaCl) that were mixed and autoclaved. Beta-mercaptoethanol (2% final concentration) was added just before use. The samples were briefly mixed and incubated at 65 °C for 30 min. One mL of chloroform:isoamyl alcohol (24; v:v) was added and the samples were gently mixed and centrifuged at 13,000 rpm for 10 min at room temperature. The supernatant from the tubes was transferred to fresh micro centrifuge tubes. 1 mL of extraction buffer-II comprising of phenol saturated with Tris buffer (Sigma, USA; pH 6.7), sodium dodecyl sulfate (SDS; 0.1% w/v), sodium acetate (NaOAc; 0.32 M) and EDTA (0.01 M; pH 8.0) was added to the above supernatant and vortexed briefly. A 200 μL of chloroform was added per sample, vortexed for a few seconds, and incubated for 15 min at room temperature. The samples were centrifuged at 13,000 rpm for 10 min at 4 °C. The upper aqueous phase was transferred into fresh tubes containing. A 0.6 volume of isopropanol was added to the samples and mixed gently before storing at −80 °C for 15 min. The samples were centrifuged at 13,000 rpm for 10 min at 4 °C. The supernatant was decanted and the RNA pellet was washed with 70% ethanol followed by air drying and suspending in 25 μL of DEPC treated autoclaved water. The samples were stored at −80 °C.

2.4.2. RNA-Seq library construction

Total RNA of the samples was quantified by Agilent 2100 Bioanalyzer (Agilent Technologies, Palo Alto, CA, USA), NanoDrop (Thermo Fisher Scientific Inc.) and resolution on 1% agarose gel. One μg the total RNA with RIN value above 7 was used for following library preparation. Next generation sequencing library preparations were carried according to the manufacturer's protocol (NEBNext® UltraTM RNA Library Prep Kit for Illumina®). Total RNA was treated with Oligo (dT) beads (Magnetic mRNA Isolation Kit from NEB, Hyderabad, India) for mRNA enrichment and Ribo-Zero kit (TruSeq Stranded Total RNA with Ribo-Zero Plant from Illumina, San Diego, USA) to remove rRNA from the samples. The double stranded cDNA library was prepared through size selection and PCR enrichment. Quality control was evaluated by Qubit 3.0, Agilent 2100 system and Q-PCR and sequenced on Illumina HiSeq 2500 using SBS kit V4 at Nucleome Informatics Ltd., Hyderabad, India.

2.4.3. Read mapping and data analysis

Raw sequence reads in the FASTQ format were processed to remove Illumina adaptor sequences by Trimmomatic program (Bolger et al., 2014). After filtering approximately 21–25 million paired-reads were retained. The reads were mapped with HISAT2 program. The mapped reads were aligned to the reference genome. The tool feature counts was used to get the total number of reads that were aligned to the reference genes. EdgeR software (Robinson et al., 2010) was used to detect differential expression between the samples. The assembled genes with log fold-change 2 and >2 with the p-adj value < 0.05 were considered to be significant. The enriched genes were then checked for GO enrichments using KOBAS 3.0 (Xie et al., 2011). The transcriptome obtained from *Trichoderma*-treated castor plants has been deposited at Gene Expression Omnibus (GEO) GSE198090.

2.5. Transcriptome data validation by Real Time-quantitative PCR (RT-qPCR)

The first strand cDNA was synthesized using 2 μg/μL of total RNA from *Trichoderma*-treated and control samples collected at 12, 24 and 48 hpi using cDNA synthesis kit (Takara, Shiga, Japan). Primers were designed by Oligo Analyzer 3.1 bioinformatics tool amplifying short fragments of 100–250 bp. Primers designed for the 9 stress- and defense-related genes along with the 2 internal controls- Elongation Factor β1 (*EFB1*) and Actin (*ACT*)) are listed in Table S2.

The RT-qPCR reaction was performed in 96-well PCR plates on the Eppendorf gradient with gene specific primers. The 10 μL reaction mixture comprises of 5.2 μL of 1× SYBR mix, 0.5 μL of 0.25 μM of each primers, 1 μL of 1:20 diluted cDNA and 2.8 μL of water to make up the volume. The cycling conditions used were initial denaturation of 95 °C for 3 min followed by 95 °C for 15 s, specific annealing temperature for the specific gene for 30 s, 72 °C for 20 s followed by 40 cycles of 95 °C for 15 s, 60 °C for 15 s. The expression of relative fold change was calculated by 2ˆ-ΔΔCt at (Livak and Schmittgen, 2001). Statistical analysis was carried using SigmaPlot 11.0. The RT-qPCR values were plotted to compare gene expression using student t-test at 12, 24 and 48 hpi. The statistical significance of variation between the different time-points was displayed at Tukey $p \leq 0.05$. Vertical bars represent ±SE of the mean values of the replicates.

3. Results

3.1. Colonization by Trichoderma in castor roots

Trichoderma-treated roots of castor were monitored by light microscopy to visualize the colonization of the fungus in the root tissue. Longitudinal sections of root samples taken from *Trichoderma*-treated roots of castor showed both external and internal growth of *Trichoderma*. Trypan blue-stained roots of castor at 48 hpi showed predominant growth of the mycelium and vesicle formation in the root tissue. The microscopic images confirmed complete attachment of the fungal hyphae to the surface of castor (Fig. 1). Along with mycelial spread on the roots surface (Fig. 1A) and penetration into the roots (Fig. 1B), enlargement of hyphal tips into vesicles (Fig. 1C) was observed at 48 hpi indicating intracellular colonization of *Trichoderma*.

3.2. Genome-wide mRNA abundance levels in Trichoderma-treated castor

To delineate the changes in castor gene expression induced by *Trichoderma* colonization, the transcriptome profiles of castor roots grown in hydroponic cultures treated with and without *Trichoderma* were compared. The differentially expressed genes (DEGs) were detected by pairwise comparison of mRNA transcript abundance levels between *Trichoderma*-treated and control castor roots. The total raw sequences generated by RNA sequencing from both control and *Trichoderma*-treated root samples were estimated to be 21–25 million reads (Table S3). The reads were filtered using stringent parameters and the read map distribution generated by computational analysis is listed in Table S4. Following the alignment of the sequence reads to the reference genome, the tool feature counts was used to get the total number of reads that were aligned to the reference genes.

A total of 20,696 plant transcripts were detected in the roots of *Trichoderma*-treated castor at 48 hpi. Of these gene transcripts, a total of 1825 differentially expressed genes (DEGs) were detected using DEGSeq software. A hierarchical clustering of the DEGs of castor plants was performed as shown in Fig. S1 (Supporting Information). Gene ontology (GO) analysis is presented as Venn diagrams showing three GO categories; cellular component (CC), biological process (BP) and molecular function (MF) as shown in Fig. S2 (Supporting Information). Using EdgeR software (Robinson et al., 2010), the assembled genes with log fold-change 2 and >2 with the p-adj value < 0.05 were considered to be significant which revealed a total of 1508 DEGs, of which 474 DEGs alone were found to be upregulated in *Trichoderma*-treated castor roots at 48 hpi.

GO analysis of plant DEGs in the cellular components (CC) category revealed that a high number of gene transcripts involved in cellular activities which include cell wall or plasma membrane or other membrane formation and transport activity to extracellular region or apoplast were downregulated (Fig. 2A). On the contrary, a few of the genes like putative fusome, cortical endoplasmic reticulum and E3 ubiquitin ligase were found to be upregulated (Fig. 2B) which play a critical role in synchronizing cell divisions, trafficking membrane-bound proteins and regulating protein homeostasis respectively. In the category of molecular function (MF), majority of the genes with a role in DNA binding transcription factor activity (GO:0003700) and transferase activity (GO:0046527) were found to be downregulated. However, both upregulation and downregulation was also observed (Fig. 3) for few genes with putative enzymatic roles like hydrolase and oxidoreductase activities along with transmembrane transport suggesting the possibility of multiple isoforms for these genes.

The number of genes downregulated were found to be greater than the number of genes upregulated in *Trichoderma*-treated castor roots of DCS-107. On the contrary, the mRNA transcripts of genes involved in biological process (BP) category were predominantly upregulated with the highest number for cellular responses followed by the genes involved in signal transport (Fig. 4). Whereas, the downregulated DEGs under biological process (BP) category were related to cell component organization, oxidation-reduction process, multicellular organismal process and cytoskeleton organization (Fig. 5). Minimal enrichment with basal expression was observed for the gene transcripts related to response to chitin.

3.3. Differential gene expression of castor treated with Trichoderma at 48 hpi

The findings from the transcriptome profiling analysis revealed that several of the gene transcripts were downregulated in *Trichoderma*-

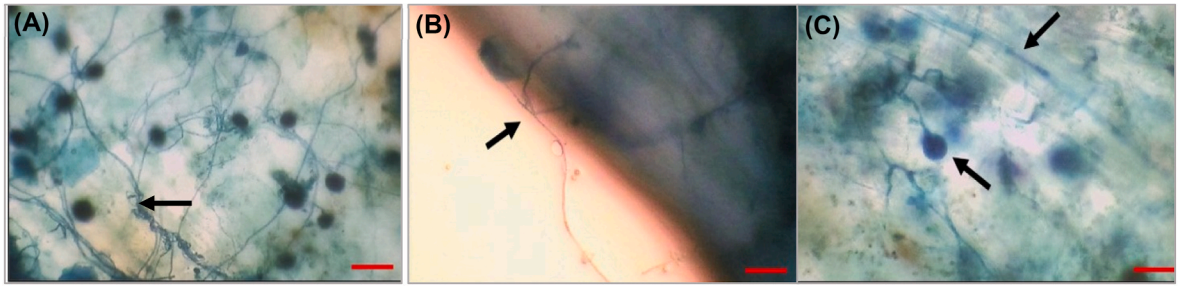


Fig. 1. Colonization of DCS 107 roots by *Trichoderma asperellum* 7316 observed through light microscopy. A visual representation of fungal growth in trypan-blue stained DCS roots inoculated with *T. asperellum* 7316 at 48 h post inoculation (hpi); (A) mycelial spread on the root surface, (B) penetration into the roots and (C) enlargement of hyphal tips into vesicles was observed. Arrows indicate *Trichoderma* colonization in root samples. Scale bar 20 μm.

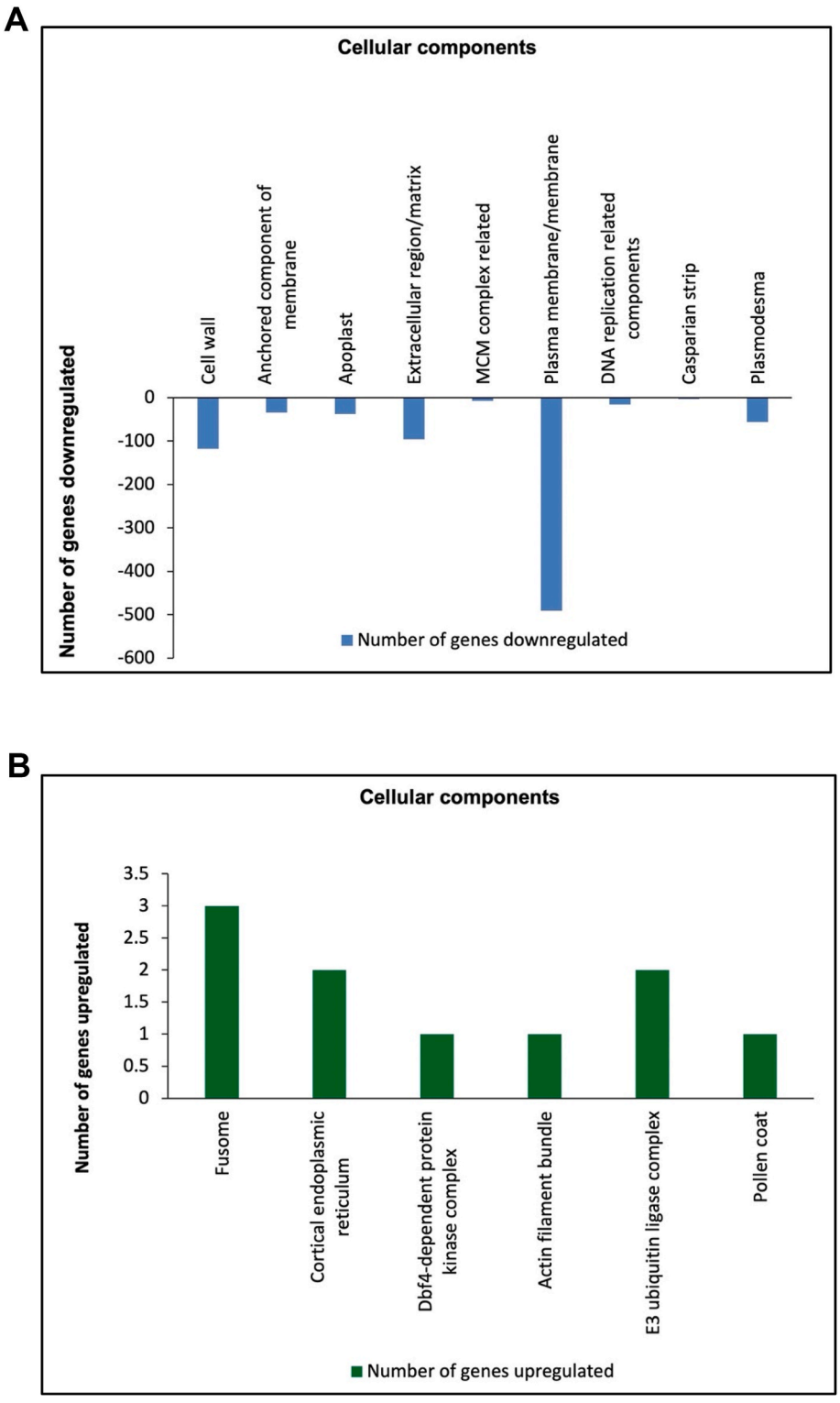


Fig. 2. Gene enrichment analysis of plant DEGs in DCS-107 by GO term classification – Cellular components; (A) number of genes downregulated were related to plasma membrane or membrane associated functions and (B) number of genes upregulated were related to cellular homeostasis and cell division regulation.

treated castor roots (Table 1) compared to the upregulated genes as presented in Table 2. The gene transcripts that were altered were primarily related to protein kinases with a putative role in recognition and *Trichoderma* colonization. Majority of the DEGs detected in the study are candidate genes that function in stress response, hypersensitive response, ROS changes, phenylpropanoid pathway, secondary metabolite biosynthesis, carbohydrate and amino acid biosynthesis/ metabolism, ABC transporters, transcription factors along with proteins involved in electron transport and respiration.

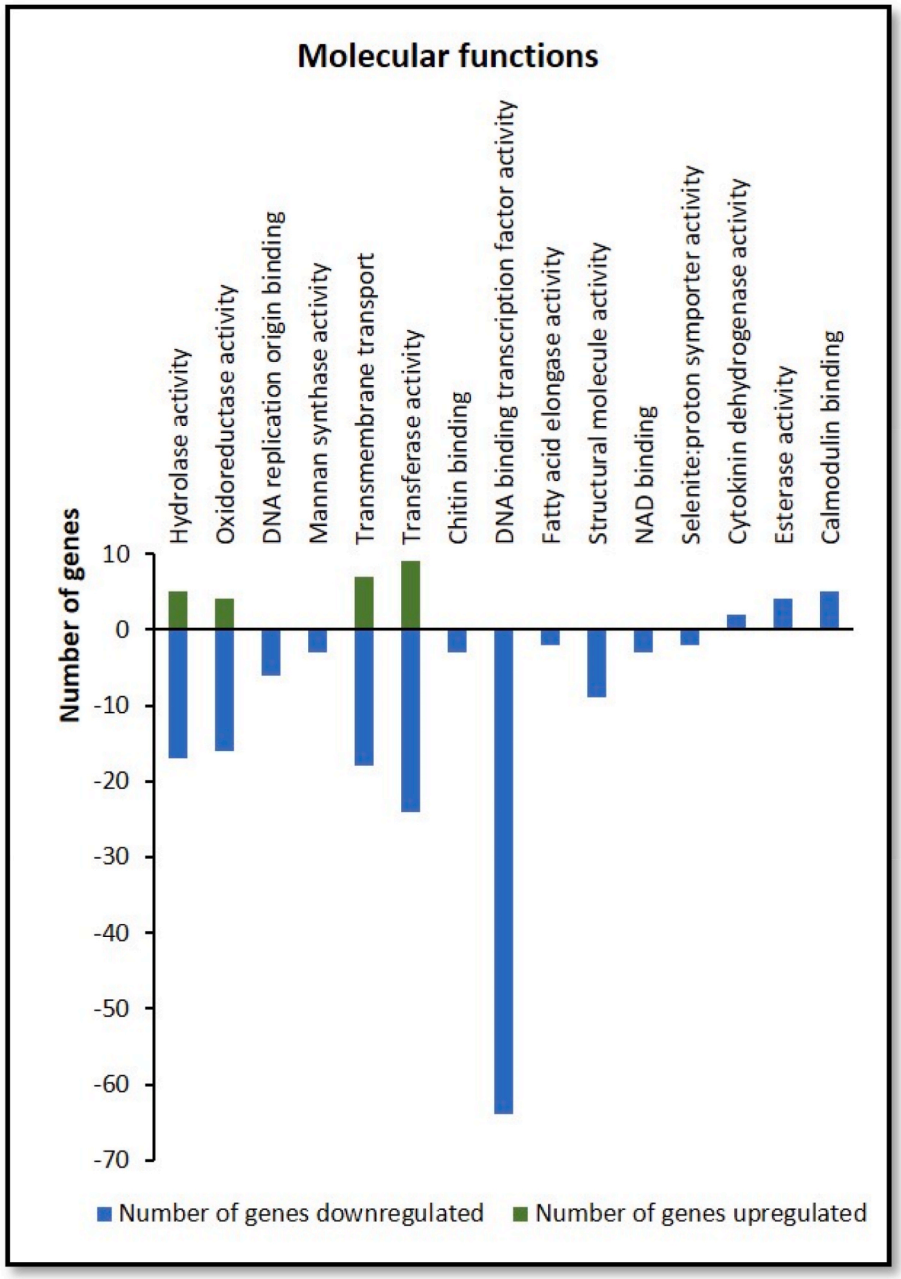


Fig. 3. Gene enrichment analysis of plant DEGs in 7316 treated roots of castor DCS-107 by GO term classification – Molecular functions. The highest number of downregulated genes comprised of genes involved in DNA binding transcription factor activity.

3.4. Detection of putative genes in castor in response to Trichoderma

3.4.1. Putative kinase and hypersensitive response genes in Trichoderma-treated castor

Of an estimated number of 50 downregulated putative kinase genes, three genes-serine/threonine protein kinase IRE4, MAP3K epsilon protein kinase1 and Serine/threonine-protein kinase ATG1a were predominantly downregulated with a fold-change expression of −9.68, −8.97 and −8.96 respectively. A candidate stress responsive factor, Flavonol synthase/flavanone 3-hydroxylase gene was also found to be significantly downregulated (−7.24 fold-change) compared to control suggesting that the *Trichoderma* colonization negates inflammatory or hypersensitive responses in castor.

Similarly genes involved in reactive oxygen species (ROS) generation were found to be significantly downregulated which include; Putative L-ascorbate peroxidase 6, Peroxidase 16, Respiratory burst oxidase homolog protein B, Peroxidase 12 (with a fold-change of −7.78, −7.74, −6.96 and −4.92 respectively). Gene expression of two lignin forming peroxidases and 8 other Class III peroxidases were seen to be downregulated. Peroxidase 12, Peroxidase 57 and Peroxidase 20 were found to be downregulated with a fold change expression of −4.92, −3.86 and −2.48 fold respectively. Similar to the peroxidases, laccases were also found to be downregulated.

In addition, mRNA abundance levels of defense response genes-Jacalin-related lectin 3 with a fold-change of −11.06, Trigalactosyldiacylglycerol 4 and Serine carboxypeptidase with fold-change of −9.03 each were observed to be significantly lower compared to the control. Furthermore, pathogenesis-related proteins like Thaumatin-like protein (−8.80), Thaumatin-like protein 1 (−3.64) Endoglucanase 24 (−7.17), Endoglucanase 17 (−3.60), Endoglucanase 25 (−3.32)

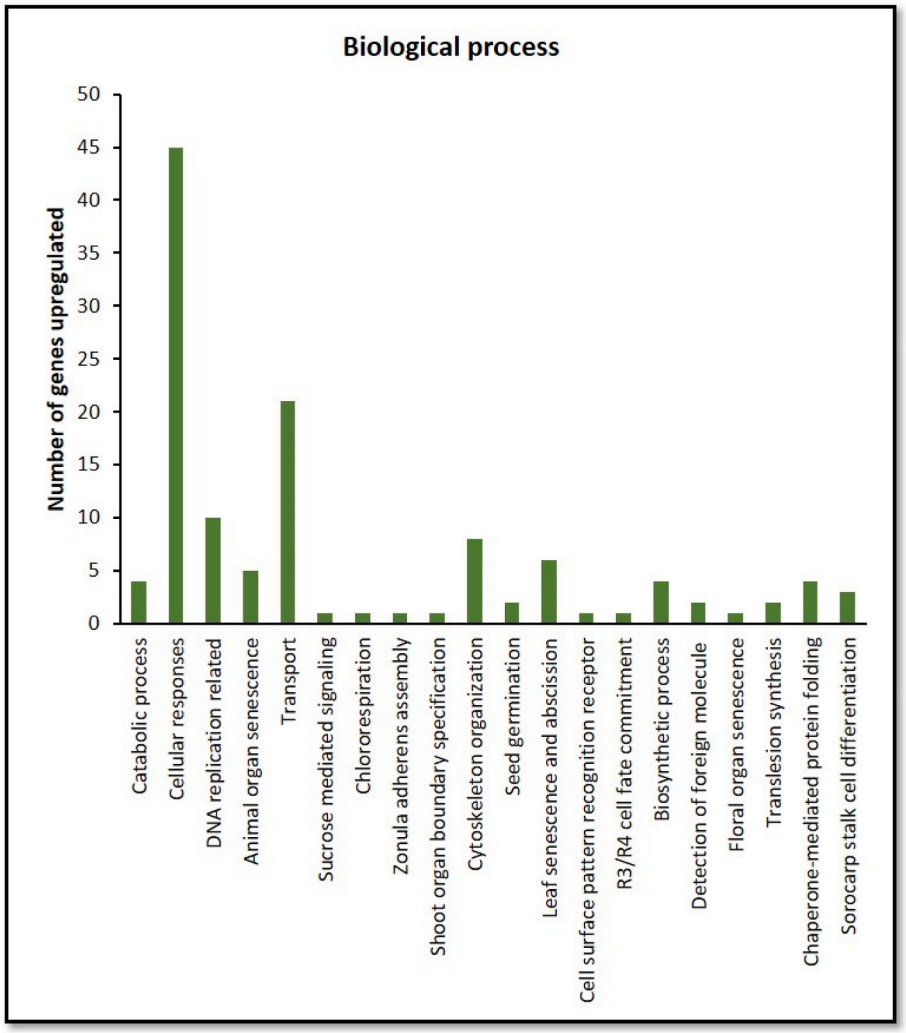


Fig. 4. Gene enrichment analysis of plant DEGs in 7316 treated roots of castor DCS-107 by GO term classification – Biological process (upregulated genes). The highest number of genes that were upregulated were observed with a function in cellular responses followed by the genes involved in signal transport.

Pathogenesis-related protein 5 (−2.81) and Wound-induced protein WIN2 (−2.81) were significantly downregulated in *Trichoderma*-treated castor confirming restraining of these genes with a role in antimicrobial protein expression.

Likewise, a minimum of 11 gene transcripts with probable role as methyl transferases were found to be significantly downregulated with a fold change of −8.20 to −2.44 in *Trichoderma*-treated root sample compared to control. A few of the ABC transporter members of G and B classes and transcription factors with putative role in defense against pathogens were found to be significantly downregulated suggesting that the host favours *Trichoderma* colonization in the roots by negatively regulating plant defense responses.

Further, the putative transcription factors which include; putative transcription factor BIM1, myb family transcription factor PHL8, transcription factor bHLH90, GATA transcription factor 4 and transcription factor bHLH74 with putative roles in brassinosteroid signaling and response to biotic and abiotic stresses were found to be down regulated suggesting that *Trichoderma*-treatment is perceived as non-pathogenic or non-alarming biocontrol agent (BCA) by the host.

3.5. Gene transcripts up regulated in DCS-107 in response to Trichoderma

3.5.1. Upregulated putative receptor-like kinases and resistance genes in castor

Among the mRNA transcripts with abundance, the gene transcripts of putative receptors with a role in extracellular recognition were found to significantly higher in *Trichoderma*-treated castor compared to control plants. The probable serine/threonine-protein kinase WNK4 showed highest fold change expression (11.12) and is reported to play a role in diverse ion transport pathways in plants. The mRNA transcripts accumulation of integrin-linked protein kinase 1 gene with a putative role in root elongation and gravitropism was detected with a high fold-change of 10.81. Likewise, a proline-rich receptor-like protein kinase PERK8 with a fold-change expression of 10.67 was observed with a putative role in pollen development, increased lateral shoot production and seed set in plants.

The mRNA abundance levels of cysteine-rich receptor-like protein kinase 10 (*CRK*) was observed to be 7.53 fold higher in *Trichoderma*-treated plants compared to control suggesting its unique role in symbiosis of arbuscular mycorrhiza and rhizobia association in plants. The mRNA transcripts of mitogen-activated protein kinase kinase dlk-1 gene, a prime component in protein phosphorylation and signal transduction was observed with a 7.28 fold-change to affect coordinated intracellular responses. Another receptor, inositol-tetrakisphosphate 1-kinase 3 with

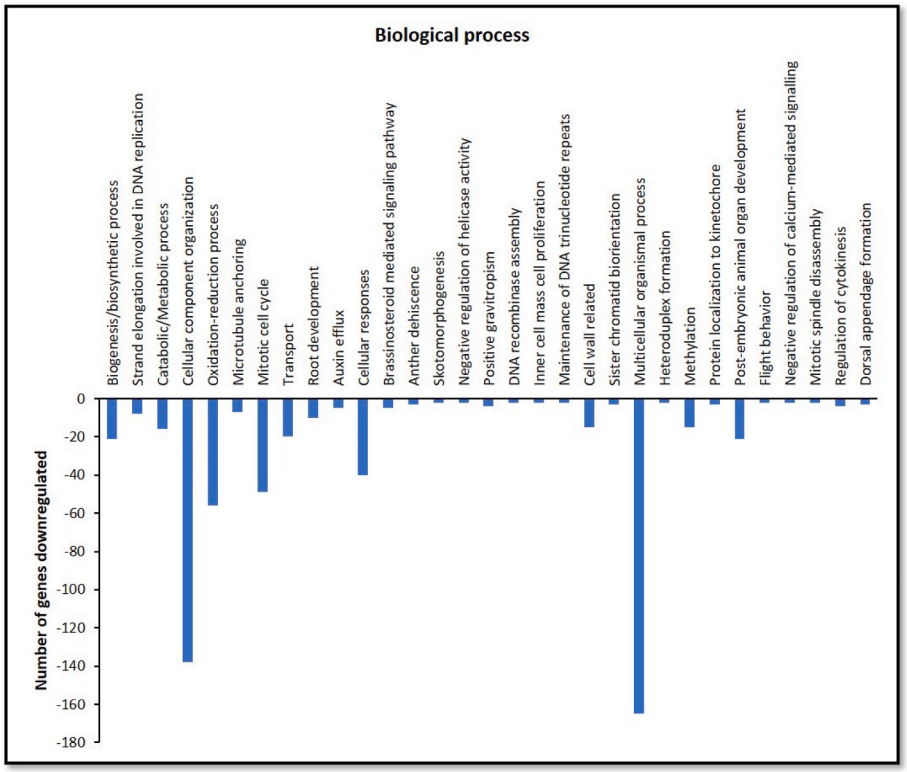


Fig. 5. Gene enrichment analysis of plant DEGs in 7316 treated roots of castor DCS-107 by GO term classification – Biological process (downregulated genes). The highest number of downregulated DEGs were related to cell component organization followed by multicellular organismal process and oxidation-reduction processes.

a 6.74 fold-change expression was recorded with a role in signal transduction in mediating host responses. The receptor gene, LysM domain receptor-like kinase 3 was up regulated (3.79 fold-change) in response to *Trichoderma*, suggesting it as a candidate in mediating symbiosis establishment in castor.

3.5.2. Up regulation of gene transcripts involved in cellular metabolism and detoxification

The mRNA transcripts of Glycerol-3-phosphate dehydrogenase NAD (+) 2 gene with a putative role in glycolysis and homeostasis was observed to be highly expressed with a fold-change of 9.25 followed by the probable glutathione peroxidase 2 gene with 9.22 fold-change expression level in response to *Trichoderma* indicating enhanced cellular metabolism and energy production. The gene transcripts of Glutathione S-transferase L3 (7.8 fold-change) indicated enhanced cellular metabolism as well as in the detoxification of a wide variety of xenobiotic compounds produced in response to *Trichoderma*. Likewise, mRNA transcripts of few of the peroxidases which include L-ascorbate peroxidase 6, Peroxidase 5, Cationic peroxidase 1 (8.18, 3.17 and 2.83 fold-change) were upregulated as a natural response against an invading organism to minimise cell damage caused due to ROS accumulation. The mRNA abundance levels of a probable 2-oxoglutarate-dependent dioxygenase was observed to be 7.28 fold-change higher compared to control indicating its role in phytohormone and secondary metabolite synthesis in response to *Trichoderma*.

3.5.3. Upregulation of phosphatases, transporter and plant growth promoting factors

The mRNA abundance levels of several putative protein phosphatases including purple acid phosphatases were higher in *Trichoderma* treated castor suggesting that these phosphatases are secreted to utilize organic phosphorus (Po) for plant growth and development. Likewise, metal tolerance protein1, potassium channel KAT2 and copper-transporting ATPase Paa1/Paa2 with fold-change of 8.66, 8.66 and 8.62 respectively were observed indicating that these proteins served as cation diffusion facilitator (CDF) for metal efflux from the cytoplasm into either extracellular space or organelles. Further, putative cytochrome P450 genes-cytochrome P450, Cytochrome P450 711A1 and Cytochrome P450 78A7 with 8.66, 2.35 and 2.32 fold-change expression respectively were observed indicating their role in detoxification of xenobiotics, cellular metabolism and homeostasis.

The gene transcript accumulation of YTH domain-containing protein ECT4 with a role in biological timing and leaf formation peaked with a 10.33 fold-change expression. The mRNA transcripts of a growth regulating factor (*GRF1*)-interacting factor1 were upregulated with 9.08 fold change followed by WAT1-related protein gene At3g28050-like and WAT1-related protein gene At4g15540 with 8.66 and 7.6 fold change respectively with a role in plant development. The gene transcripts of probable polygalacturonase showed 6.74 fold-change upregulated suggesting its role in promoting plant growth which involves hypocotyl elongation and in floral organ patterning to produce higher proportions of flowers.

3.5.4. Up regulation of genes involved in stress responses and defense signaling

The putative gene, Jacalin-like lectin domain was up regulated with 11.42 fold-change in castor in response to *Trichoderma* with a putative role in plant growth regulation and signaling. Similarly putative RING-H2 finger protein ATL11, Receptor homology region, transmembrane domain- and RING domain-containing protein 1 and RING-H2 finger protein ATL66 (9.48, 6.86 and 2.3 fold-change respectively) were upregulated along with a candidate Nudix hydrolase 2 gene (9.08 fold-change) confirming their role in housecleaning to maintain cellular homeostasis of the host. Further, a putative enzyme belonging to the ferrous ascorbate-dependent oxidoreductase family was 7.28 fold-change upregulated which plays a role in reactive oxygen species (ROS) scavenging to maintain the cellular homeostasis.

An F-box protein FBW2 (7.28 fold-change), protein of the SKP1

Table 1
List of plant gene transcripts down regulated in the roots of the castor genotype, DCS-107 in response to *T. asperellum* 7316 at 48hpi.

Transcript ID	Predicted protein function (Transcript annotation)	logFC (Fold change)
Protein kinases		
RCOM_1593890	Probable serine/threonine protein kinase IRE4	−9.68
RCOM_0807920	MAP3K epsilon protein kinase 1	−8.97
RCOM_1340560	Serine/threonine-protein kinase ATG1a	−8.96
RCOM_1494420	Proline-rich receptor-like protein kinase PERK15	−8.73
RCOM_0906180	Cysteine-rich repeat secretory protein 38-like	−8.14
RCOM_0126270	Serine Threonine protein kinase	−7.95
RCOM_1355230	Phosphoglycerate kinase	−7.91
RCOM_0654970	Casein kinase 1-like protein 2	−7.87
RCOM_0906170	Cysteine-rich receptor-like protein kinase 44	−7.82
RCOM_0811450	Receptor protein kinase-like protein At4g34220	−7.82
RCOM_0912240	Probable serine/threonine-protein kinase WNK9	−7.48
RCOM_0901470	Serine/threonine-protein kinase bri1, putative/ *Ricinus communis* receptor-like protein 15	−7.37
RCOM_1432170	Serine/threonine-protein kinase ZRK1	−7.31
XP_015574890.1	Glycogen recognition site of AMP-activated protein kinase	−7.18
−3.271728098	Leucine-rich repeat receptor-like tyrosine-protein kinase PXC3	−7.18
RCOM_1684990	Probable serine/threonine-protein kinase SIS8	−7.11
RCOM_0913550	Somatic embryogenesis receptor kinase 1	−6.70
RCOM_1050860	Protein phosphatase 2C and cyclic nucleotide-binding/kinase domain-containing protein	−6.60
XP_015573292.1	Serine threonine-protein kinase	−6.60
RCOM_0295930	Probable inactive receptor kinase At5g58300	−6.49
RCOM_1602240	Cyclin-dependent kinase B2-2	−4.98
RCOM_0920850	Early nodulin-like protein 1	−4.70
RCOM_1340570	Probable inactive receptor-like protein kinase At2g46850	−3.57
RCOM_1022390	Leucine-rich repeat receptor protein kinase EXS, putative	−3.56
RCOM_1596350	LRR receptor-like serine/threonine-protein kinase SIK1	−3.52
RCOM_1080800	Serine/threonine-protein kinase bri1-UNIPROT/receptor-like protein EIX1 - NCBI	−3.32
RCOM_1371710	Receptor-like protein 14	−3.32
RCOM_1310170	Probable leucine-rich repeat receptor-like protein kinase At1g68400	−3.29
RCOM_1768760	Serine threonine-protein kinase SAPK7	−3.27
RCOM_0988670	Serine threonine-protein kinase AGC1-7	−3.17
RCOM_2139480	Receptor-like kinase TMK4	−3.09
RCOM_0712120	MOB kinase activator-like 1A	−3.09
RCOM_1486440	LRR receptor-like serine/threonine-protein kinase At1g51860	−3.08
RCOM_0779050	FLS2/53	−3.01
RCOM_0610070	Leucine-rich repeat receptor-like protein kinase PXL1	−3.0
RCOM_0052400	Receptor protein kinase TMK1	−3.0
RCOM_0853370	Serine/threonine-protein kinase D6PKL2	−2.93
RCOM_1454170	Serine/threonine-protein kinase	−2.91
RCOM_1442820	Leucine-rich repeat receptor protein kinase EXS, putative	−2.81
RCOM_1250190	Receptor-like protein 51	−2.76
RCOM_1333310	Probable LRR receptor-like serine/threonine-protein kinase At3g47570	−2.66
RCOM_1721670	LRR receptor-like serine/threonine-protein kinase RGI2	−2.56
RCOM_1509620	Leucine-rich repeat receptor-like serine/ threonine-protein kinase RGI4	−2.55
RCOM_0797340	Probable leucine-rich repeat receptor-like protein kinase At1g68400	−2.50
RCOM_0647000	LRR receptor-like serine/threonine-protein kinase ERL2	−2.46
RCOM_0687670	Nodulation receptor kinase precursor	−2.39
RCOM_2032810	Leucine-rich repeat receptor-like protein kinase	−2.34
RCOM_1427830	Serine/threonine-protein kinase Nek1	−2.30
RCOM_0840960	Leucine-rich repeat receptor-like protein kinase PXC1	−2.20
RCOM_0848330	Systemin receptor SR160- UNIPROT/Probably inactive leucine-rich repeat receptor-like protein kinase IMK2 isoform ×2 [Ricinus communis] - NCBI	−2.23
RCOM_0814340	Inactive leucine-rich repeat receptor-like serine/threonine-protein kinase At1g60630	−2.17
RCOM_0799040	Serine/threonine-protein kinase Aurora-2	−2.17
ROS related proteins		
RCOM_0923970	Putative L-ascorbate peroxidase 6	−7.78
RCOM_0172310	Peroxidase 16	−7.74
RCOM_0635750	Flavonol synthase/flavanone 3-hydroxylase, putative -UNIPROT/protein SRG1	−7.24
RCOM_0903900	Putative uncharacterized protein	−7.11
RCOM_0647160	Laccase	−7.11
RCOM_1433130	Respiratory burst oxidase homolog protein B	−6.96
RCOM_0774370	Lignin forming anionic Peroxidase	−5.20
RCOM_0602380	L-ascorbate oxidase	4.98
RCOM_0296590	Peroxidase 12	−4.92
RCOM_1600150	L-ascorbate oxidase	−4.23
RCOM_0774380	Lignin forming anionic Peroxidase	−4.19
RCOM_0414390	Peroxidase 57, putative/Probable peroxidase 61	−3.86
RCOM_0296870	Laccase 9	−3.29
RCOM_0647190	Laccase 21	−3.25
RCOM_0687550	Laccase 12	−2.50
RCOM_0562170	Putative uncharacterized protein	−2.50
RCOM_1278030	Peroxidase 20	−2.48
RCOM_0231780	Peroxidase 27	−2.39
RCOM_0808690	Peroxidase 50 [Ricinus communis]- 100% identity- NCBI	−2.32
RCOM_0138860	Peroxidase 43 precursor, putative (Ricinus communis)-100%/peroxidase 43 (Ricinus communis)-99.689% identity- NCBI	−2.32
RCOM_0896640	Putative uncharacterized protein	−2.33
RCOM_1464960	Peroxidase 11	−2.25
RCOM_1402420	Laccase 13	−2.25
Defense response		
RCOM_1595930	Jacalin-related lectin 3	−11.06
RCOM_0658810	Trigalactosyldiacylglycerol 4	−9.03
RCOM_1383950	Serine carboxypeptidase	−9.03
RCOM_0337100	Thaumatin-like protein	−8.80
RCOM_0628760	Unannotated/hypothetical protein	−7.59
RCOM_2159030	Elongation factor 1-alpha	−7.10
RCOM_1450190	Endoglucanase 24	−7.17
RCOM_0446390	Thaumatin-like protein 1	−3.64
RCOM_0896630	Gibberellin 20 oxidase, putative	−5.30
RCOM_1179080	Endoglucanase 17	−3.60
RCOM_0999860	Chitinase-like protein 2	−3.49
RCOM_1348140	Endoglucanase 25	−3.32
RCOM_1383810	Serine carboxypeptidase-like 2	−2.94
RCOM_1593590	Pathogenesis-related protein 5 [Ricinus communis] −100% identity, Zeamatin precursor, putative [Ricinus communis]	−2.81
RCOM_0484460	Wound-induced protein WIN2	−2.81
RCOM_1383690	Serine carboxypeptidase	−2.66
RCOM_1633620	Serine carboxypeptidase-like 45-like	−2.46
RCOM_1440410	Chitinase 2	−2.32
RCOM_0137950	Putative uncharacterized protein	−2.29
Phenylpropanoid metabolism		
RCOM_1299060	ATRAD3, putative/PREDICTED: *Ricinus communis* probable methyltransferase At1g29790	−8.20
RCOM_1616760	probable methyltransferase At1g29790	−7.95
RCOM_0154700	tRNA (uracil-5-)-methyltransferase	−7.31
RCOM_0308380	O-methyltransferase, putative – UNIprot/ PREDICTED: *Ricinus communis* probable caffeine synthase MTL2	−7.03
RCOM_0938330	S-adenosylmethionine-dependent methyltransferase, putative/PREDICTED: *Ricinus communis* EEF1A lysine methyltransferase 4	−6.96
RCOM_0161380	Phosphomethylethanolamine N-methyltransferase isoform ×2 [*Ricinus communis*]	−4.70
RCOM_1015530	Trans-resveratrol di-O-methyltransferase	−3.69

(*continued on next page*)

Table 1 (*continued*)

Transcript ID	Predicted protein function (Transcript annotation)	logFC (Fold change)
RCOM_0854630	Arginine methyltransferase NDUFAF7 homolog	−3.36
RCOM_1266090	Probable methyltransferase PMT19	−3.32
RCOM_1410160	Caffeoyl-CoA O-methyltransferase	−2.39
RCOM_0554590	Trans-resveratrol di-O-methyltransferase	−2.44
Secondary metabolite Biosynthesis		
RCOM_0896400	Probable 2-oxoglutarate-dependent dioxygenase AOP1	−7.48
RCOM_0866620	Probable terpene synthase 8	−5.01
RCOM_0306870	Ent-kaurene synthase B, chloroplast precursor, putative	−4.81
RCOM_1447050	Omega-hydroxypalmitate O-feruloyl transferase [*Ricinus communis*]/Anthranilate N-benzoyltransferase protein, putative [*Ricinus communis*]	−3.14
RCOM_1045160	Probable terpene synthase 3	−3.04
RCOM_0823080	Ent-kaurene synthase B, chloroplast precursor, putative	−2.81
Cell wall modifications		
RCOM_0342250	Expansin-A1 or A10 or A15	−7.03
RCOM_1599330	Expansin A11	−4.62
RCOM_0550800	Protein IRX15-like	−4.46
RCOM_0184760	Pectinesterase	−4.10
RCOM_1500020	Pctinesterase inhibitor 4	−3.91
RCOM_1443780	Xyloglucan endotransglucosylase/hydrolase protein A precursor, putative	−3.83
RCOM_1194430	Xyloglucan endotransglucosylase/hydrolase 2	−3.44
RCOM_1541960	Probable pectinesterase/pectinesterase inhibitor 25	−3.32
RCOM_1179070	Pectinesterase	−3.32
RCOM_0708470	Probable pectinesterase/pectinesterase inhibitor 12	−3.09
RCOM_1003640	Pectinesterase	−2.73
RCOM_0299440	Casparian strip membrane protein 5	−2.72
RCOM_1773310	Putative uncharacterized protein	−2.64
RCOM_0417480	Pectinesterase	−2.51
RCOM_0635740	Xyloglucan endotransglucosylase/hydrolase 2/ REPEAT	−2.32
RCOM_1565850	Expansin-A20	−2.25
RCOM_1438910	Xyloglucan endotransglucosylase/hydrolase 2/ REPEAT	−2.10
RCOM_1259260	Casparian strip membrane protein 2	−2.07
Signal transduction		
RCOM_0258090	Transferrin, putative	−11.54
RCOM_0884410	Phosphoprotein phosphatase OR Disease resistance protein RPV1 (previous showed DSC)	−11.54
RCOM_0884420	TIR domain containing protein	−11.54
RCOM_1509380	Disease resistance protein RPP13, putative	−10.55
Carbohydrate Biosynthesis/metabolism		
RCOM_0542950	Cellulose synthase A catalytic subunit 6	−5.01
RCOM_0381780	Glucomannan 4-beta-mannosyltransferase	−3.80
RCOM_1180270	Cellulose synthase A catalytic subunit 3	−2.81
RCOM_1443660	Glyceraldehyde-3-phosphate dehydrogenase A	−2.18
RCOM_1186280	Glucomannan 4-beta-mannosyltransferase 2	−2.03
Nitrogen metabolism		
RCOM_1032820	Nitrate reductase	−5.63
Amino acid biosynthesis and metabolism		
RCOM_0907360	Arginine decarboxylase, putative	−8.24
RCOM_0592860	Anthranilate synthase alpha subunit 1	−3.46
RCOM_1445440	Aspartokinase 2	−2.36
Electron transport and membrane associated energy conservation/respiration		
RCOM_1084110	Cytochrome P450 71B2	−3.19
RCOM_1617460	Flavonoid 3-hydroxylase- UNIPROT/ cytochrome P450 CYP736A12	−3.09
RCOM_0405390	CYP93A1-3,9-dihydroxypterocarpan 6A-monooxygenase	−2.75
RCOM_0792010	Cytochrome P450 94C1	−2.58
RCOM_0585670	Cytochrome P450 716B1	−2.49
RCOM_1684620	Cytochrome P450 87A3	−2.46
RCOM_1376710	Cytochrome P450 86B1	−2.41
RCOM_0144700	Cytochrome P450 78A9	−2.30
RCOM_0841220	Cytochrome P450 76A1	−2.27
RCOM_1517630	cytochrome P450 89A2	−2.18
RCOM_1212380	Cytochrome P450 724B1	−2.11

Table 1 (*continued*)

Transcript ID	Predicted protein function (Transcript annotation)	logFC (Fold change)
ABC Transporters		
XP_025014341.1	ABC transporter G family member	−6.70
RCOM_0853020	ABC transporter B family member 15-like	−4.09
RCOM_0422670	ABC transporter G family member 22 isoform ×1	−3.84
RCOM_0925270	ABC transporter G family member 32	−2.58
RCOM_1581560	ABC transporter G family member 8	−2.29
Transcription factors		
RCOM_1467110	Transcription factor *BIM1*, putative	−9.19
RCOM_0836650	Myb family transcription factor *PHL8*	−7.48
RCOM_0528090	Transcription factor *bHLH90*	−6.96
RCOM_1609660	GATA transcription factor 4	−4.13
RCOM_1586090	*Ricinus communis* transcription factor *bHLH74*	−3.27

family (6.74), SNF1-related protein kinase regulatory subunit gamma-1-like (6.67 fold-change) and SKP1-like protein 21 (2.86 fold-change) were upregulated at 48hpi in *Trichoderma*-treated castor compared to control plants. Further, a minimum of three UDP-glycosyltransferase genes (73C3, 73C25 and 86A2) were found to be upregulated with a crucial role in cellular detoxification and homeostasis.

Similarly, several putative genes involved in defense signaling were also upregulated in castor in response to *Trichoderma*. The mRNA transcripts of F-box/kelch-repeat protein At1g74510 were highly expressed with 8.88 fold-change with a role in negative regulation of phenylpropanoid biosynthesis thereby promoting jasmonic acid (JA) mediated responses in *Trichoderma*-treated castor. Also, serine carboxypeptidase-like 18 gene transcripts, a candidate gene whose promoter sequences are enriched in abscisic acid (ABA)- and methylated jasmonic acid (MeJA)- responsive elements was upregulated with 7.18 fold-change expression. Similarly, two putative gene transcripts, cold-regulated 413 plasma membrane protein 2 and TPL-binding domain in jasmonate signaling (7.08 fold-change each) with a role in ABA and JA respectively were predominant. The finding is confirmed by the hike in expression level (6.67) of a SNF1-related protein kinase regulatory subunit gamma-1 (SnRK-like) gene, a global positive regulator of ABA signaling.

Further, a Zinc finger protein ZAT5 was also found to be upregulated whose promoter sequences are enriched with *cis*-elements responsive to phytohormones suggesting that it is a potential candidate for analysing *Trichoderma*-induced responses. Interestingly, two putative disease resistance proteins, RPV1 and RPS2 with 7.28 and 3.00 fold-change expression respectively were also found to be upregulated indicating that resistance to biotic stress was also activated along with growth regulation at 48 hpi.

3.5.5. Upregulated secondary metabolites, molecular chaperoning and nuclear modelling

The mRNA abundance levels of S-adenosylmethionine-dependent methyltransferase and probable methyltransferase PMT7 were upregulated 8.76 and 7.67 fold-change respectively indicating their prominent role in biosynthesis of bioactive compounds and/or modification of biopolymers in response to *Trichoderma*. Likewise, Squalene monooxygenase SE1 with a putative role in biosynthesis of triterpenoid saponins showed 7.44 fold-expression.

The mRNA transcripts for several molecular chaperones-like, Hsc70-interacting protein, putative Peptidyl-prolyl cis-trans isomerase CYP37, Universal stress protein PHOS34, Peptidyl-prolyl cis-trans isomerase CYP38, chloroplast and bacterial trigger factor protein (TF) were found to be highly upregulated with the highest fold-change for Hsc70-interacting protein (9.64) indicating that chaperone surveillance functions to ensure protein homeostasis, also known as proteostasis. Whereas, the putative DNA (cytosine-5)-methyltransferase DRM2 transcripts with a role in de novo DNA methylation showed a 7.52 fold-change expression, Arginine methyltransferase NDUFAF7 with 8.18

Table 2
List of plant gene transcripts upregulated in the roots of castor genotype, DCS-107 in response to *T. asperellum* 7316 at 48hpi.

Transcript ID	Predicted protein function (Transcript annotation)	logFC (Fold change)
Protein kinases		
RCOM_0815420	Probable serine/threonine-protein kinase WNK4	11.12
RCOM_0606150	Integrin-linked protein kinase 1	10.81
RCOM_1444750	Proline-rich receptor-like protein kinase PERK8	10.67
RCOM_1508280	Serine threonine-protein kinase	10.10
RCOM_0897280	Serine-threonine kinase receptor-associated protein	9.71
RCOM_1046950	Receptor-like serine threonine-protein kinase	9.44
RCOM_1267360	PTI1-like tyrosine-protein kinase 3	8.88
RCOM_0912240	Probable serine/threonine-protein kinase WNK9	8.56
RCOM_0546030	Leaf rust 10 disease-resistance locus receptor-like protein kinase-like 2.4	8.52
RCOM_0020950	Receptor-like cytosolic serine/threonine-protein kinase RBK1	8.32
RCOM_1173500	Checkpoint serine threonine-protein kinase	7.92
RCOM_1355230	Phosphoglycerate kinase	7.67
RCOM_1593890	Probable serine/threonine protein kinase IRE4	7.67
RCOM_0906040	Cysteine-rich receptor-like protein kinase 10	7.53
RCOM_1000600	Mitogen-activated protein kinase kinase dlk-1	7.28
RCOM_0260330	Serine-threonine protein kinase 19	6.98
RCOM_1382770	Inositol-tetrakisphosphate 1-kinase 3	6.74
RCOM_1115620	LysM domain receptor-like kinase 3	3.79
RCOM_0646260	Serine/threonine-protein kinase STY13	2.78
RCOM_0206530	LRR receptor-like serine threonine-protein kinase 9DC3	3.40
RCOM_0905280	Probable serine/threonine-protein kinase PBL23 isoform ×1	2.58
RCOM_0206830	Serine threonine-protein kinase	2.51
RCOM_1313140	Serine/threonine-protein kinase BLUS1	2.10
Cellular metabolism and homeostasis		
RCOM_0689940	Glycerol-3-phosphate dehydrogenase NAD (+) 2	9.25
RCOM_0574830	Probable glutathione peroxidase 2	9.22
RCOM_0923970	L-ascorbate peroxidase 6	8.18
RCOM_0819930	Glutathione S-transferase L3	7.80
RCOM_0259060	Glutathione gamma-glutamylcysteinyltransferase 1	7.28
RCOM_0550810	Probable 2-oxoglutarate-dependent dioxygenase At3g50210	7.28
RCOM_1685170	Peroxidase 5	3.17
RCOM_1232030	Cationic peroxidase 1	2.83
RCOM_0584650	1-acyl-sn-glycerol-3-phosphate acyltransferase	2.81
Phosphate transport		
RCOM_1342130	Protein phosphatase 2C	8.08
RCOM_1019210	Purple acid phosphatase	7.73
RCOM_1534250	Probable protein phosphatase 2C 8	7.60
RCOM_1355010	Acyl phosphatase	7.36
RCOM_0812230	Putative Protein phosphatase	3.00
RCOM_1602550	PhoD-like phosphatase	2.97
Metal ion transport and xenobiotics		
RCOM_1339960	Metal tolerance protein 1	8.66
RCOM_0632940	Potassium channel KAT2	8.66
RCOM_1352230	Cytochrome P450	8.66
RCOM_0707470	Copper-transporting ATPase Paa1 or Paa2	8.62
RCOM_0705970	Cytochrome P450 711A1	2.35
RCOM_0297800	Cytochrome P450 78A7	2.32
Plant growth promotion		
RCOM_1129090	YTH domain-containing protein ECT4	10.33
RCOM_0608010	GRF1-interacting factor 1	9.08
RCOM_0393280	WAT1-related protein At3g28050-like	8.66
RCOM_0393170	WAT1-related protein At4g15540	7.60
RCOM_1582420	Probable polygalacturonase	6.74
Stress responses		
RCOM_1595930	Jacalin-like lectin domain	11.42
RCOM_1037890	RING-H2 finger protein ATL11	9.48
RCOM_0304730	Nudix hydrolase 2	9.08
RCOM_1036630	F-box protein FBW2	7.28
RCOM_0550810	Ferrous ascorbate-dependent oxidoreductase family	7.28
RCOM_0572790	Receptor homology region, transmembrane domain- and RING domain-containing protein 1	6.86
RCOM_1615660	Protein of the SKP1 family	6.74
RCOM_0458380	UDP-glycosyltransferase 73C3	3.10

Table 2 (*continued*)

Transcript ID	Predicted protein function (Transcript annotation)	logFC (Fold change)
RCOM_1615660	SKP1-like protein 21	2.86
RCOM_0458380	UDP-glycosyltransferase 73C25	2.60
RCOM_0788110	RING-H2 finger protein ATL66	2.30
RCOM_0472870	UDP-glycosyltransferase 86A2	2.00
Defense responses		
RCOM_1514730	F-box/kelch-repeat protein At1g74510	8.88
RCOM_0812210	Disease resistance protein RPV1	7.28
RCOM_1383950	Serine carboxypeptidase-like 18	7.18
RCOM_2050290	Cold-regulated 413 plasma membrane protein 2	7.08
RCOM_0390850	TPL-binding domain in jasmonate signaling	7.08
RCOM_0697780	SNF1-related protein kinase regulatory subunit gamma-1-like	6.67
RCOM_0812230	Disease resistance protein RPS2	3.00
RCOM_1353410	Zinc finger protein ZAT5	2.60
Secondary metabolite synthesis		
RCOM_1034960	S-adenosylmethionine-dependent methyltransferase	8.76
RCOM_0160690	Probable methyltransferase PMT7	7.67
RCOM_0859900	Squalene monooxygenase SE1	7.44
RCOM_1063380	DNA (cytosine-5)-methyltransferase DRM2	7.52
RCOM_1171020	Probable O-methyltransferase 3	2.10
RCOM_0004120	Limonene synthase/probable terpene synthase 9	2.00
Molecular Chaperones		
RCOM_0569180	Hsc70-interacting protein, putative	9.64
RCOM_0663360	Peptidyl-prolyl cis-trans isomerase CYP37	6.98
RCOM_1039200	Universal stress protein PHOS34	6.98
RCOM_0850710	Peptidyl-prolyl cis-trans isomerase CYP38, chloroplast	6.86
RCOM_0547660	Bacterial trigger factor protein (TF)	6.86
Nucleic acid synthesis and modelling		
RCOM_0854630	Arginine methyltransferase NDUFAF7	8.18
RCOM_0500140	Putative lysine-specific demethylase JMJ16	8.03
RCOM_1593990	Deoxyuridine 5′-triphosphate nucleotidohydrolase	3.80
RCOM_1432610	Lysine-specific demethylase JMJ25	3.65
Carbohydrate and starch metabolism		
RCOM_1018060	Beta-galactosidase	11.38
RCOM_0831760	Probable glucan 1,3-beta-glucosidase A	7.18
RCOM_1177990	Beta-glucosidase 11	2.87
RCOM_0711410	Beta-galactosidase 15	2.30
RCOM_0526780	Alpha-amylase	2.24
Lipid and fatty acid synthesis and metabolism		
RCOM_0511110	Putative BPI/LBP family protein At1g04970	9.36
RCOM_0614020	Phosphatidylinositol-glycan biosynthesis class X	9.30
RCOM_0653990	**Phospholipid:diacylglycerol acyltransferase 1**	8.70
RCOM_1614440	Acyl-coenzyme A thioesterase 13	8.27
RCOM_1478210	Phospholipase A22	7.44
RCOM_1047790	Acyl- acyl-carrier-protein –UDP-N-acetylglucosamine O-acyltransferase	6.70
RCOM_1347470	Phospholipase A1 PLIP2	6.74
RCOM_1027640	TLC domain-containing protein 4-B	3.65
Amino acid Biosynthesis and metabolism		
RCOM_1579610	Glutamate synthase (NADH)	11.67
RCOM_1435660	Xaa-Pro aminopeptidase 3/intermediate cleaving peptidase 55, mitochondrial	9.40
RCOM_0611460	Phosphomethylpyrimidine synthase	8.76
RCOM_0907360	Arginine decarboxylase	8.32
RCOM_0904170	5′-adenylylsulfate reductase	7.08
RCOM_0321500	Thiamine biosynthetic bifunctional enzyme TH1	3.04
Electron transport, energy conservation & respiration		
RCOM_0689940	Glycerol-3-phosphate dehydrogenase NAD (+)	9.25
RCOM_2104740	NADH dehydrogenase (quinone) activity	6.60
RCOM_0028700	NADP-dependent glyceraldehyde-3-phosphate dehydrogenase	2.90
Transcription factors		
RCOM_1282600	Transcription factor *E2FB*	9.88
RCOM_0558970	Transcription factor *LRL1*	8.70
RCOM_0837230	Agamous-like MADS-box protein *AGL30*	8.52
RCOM_0339020	MADS-box protein *AGL29*	8.08
RCOM_1492980	Transcription factor *bHLH68*	7.36
RCOM_1315820	Probable transcription factor *KAN2*	7.28
RCOM_1436840	Transcription factor *PIF3*	3.54
RCOM_1211150	Transcription elongation factor s-II (*TFIIS*)	2.80

(*continued on next page*)

Table 2 (*continued*)

Transcript ID	Predicted protein function (Transcript annotation)	logFC (Fold change)
RCOM_0921060	WRKY transcription factor, *WRKY71*/probable WRKY transcription factor, *WRKY40*	2.30
RCOM_0921060	WRKY transcription factor, *WRKY55*	2.30
RCOM_1211150	Transcription elongation factor, *ELF*	2.30
XP_025014933.1	Myb-like DNA-binding domain	2.30
RCOM_0937560	Transcription factor, G-box-binding factor	2.30

fold-change expression indicated its role in DNA repair to regulate transcription, RNA splicing and protein stability.

The transcripts of two putative metalloenzymes encoding lysine-specific demethylase JMJ16 (8.03 fold-change) and Lysine-specific demethylase JMJ25 (3.65 fold-change) indicated that these genes are essential for chromatin remodeling. The transcripts of Deoxyuridine 5′-triphosphate nucleotidohydrolase gene (3.8 fold-change) with a role in de-nova nucleotide synthesis were also upregulated in response to *Trichoderma* suggesting the activation of regulatory gene networks involved in plant growth and development.

3.5.6. Upregulation of genes for cellular macronutrient biosynthesis and metabolism

The mRNA abundance for two putative genes; β-galactosidase and β-galactosidase15 with 11.38 and 2.30 fold-change respectively were observed. Likewise, mRNA transcripts for probable glucan 1,3-β-glucosidase A and β-glucosidase 11 with 7.18 and 2.87 fold-change were recorded suggesting the elevated level of carbohydrate metabolism induced by *Trichoderma* treatment. Similarly, α-amylase gene transcripts were found to be marginally upregulated (2.24 fold change) which is essential for conversion of starch into oligosaccharides in plant cells.

A putative BPI/LBP family protein At1g04970 transcripts showed elevated accumulation with 9.36 fold-change followed by elevated mRNA levels of Phosphatidylinositol-glycan biosynthesis class X (9.3 fold-change) indicating the possibility of a lipopolysaccharide (LPS) based elicitation by *Trichoderma.* Phospholipid:diacylglycerol acyltransferase1 transcripts were found to be 8.70 fold-change with a role in membrane and storage lipid synthesis whereas, acyl-coenzyme A thioesterase 13 with 8.27 fold-change indicate that it is vital in regulating the free fatty acids in plant cells, The gene transcripts of phospholipase A22 (7.44) and phospholipase A1 PLIP2 (6.74) were upregulated with a putative roles in signal transduction and catalysing the initial step of oxylipins and jasmonic acid (JA) biosynthesis. A TLC domain-containing protein 4-B gene also known as transmembrane protein56 with putative role in lipid homeostasis was elevated with 3.65 fold-change.

The gene transcripts of glutamate synthase (NADH) peaked with fold-change expression of 11.67 which facilitates the ammonium assimilation pathway followed by an amino peptidase (9.40) which catalyzes cleavage of amino acids from the amino (N-) terminus of the protein or peptide substrates. Phosphomethylpyrimidine synthase with a role in thiamine biosynthesis was found to be upregulated (with 8.76 fold-change) accompanied by another gene, a putative thiamine biosynthetic bifunctional enzyme TH1 with 3.04 fold-change expression. Likewise, Arginine decarboxylase (8.32 fold-change) which modulates proline metabolism was upregulated in response to *Trichoderma* in castor. Further, a 5′-Adenylyl sulfate reductase gene which catalyzes sulfate assimilation pathway leading to the synthesis of cysteine and the antioxidant glutathione was also found to be upregulated with 7.08 fold-change level expression in DCS-107 castor treated with *Trichoderma* compared to controls.

The mRNA transcripts of Glycerol-3-phosphate dehydrogenase NAD (+), NADH dehydrogenase (quinone) activity, NADP-dependent glyceraldehyde-3-phosphate dehydrogenase with high fold-change gene expression of 9.25, 6.6 and 2.9 were observed indicating their implication in glycolysis, lipid synthesis, and energy metabolism by electron transfer to mitochondria in plant cells.

3.5.7. Differential expression of putative transcription factors in response to Trichoderma

The mRNA levels of the putative transcription factor (TF), *E2FB* peaked with 9.88 fold-change in response to *Trichoderma* indicating its regulatory role for coordinating cell proliferation with embryonic differentiation whereas, *LRL1* that regulates the development of root hairs was upregulated with 8.70 fold-change expression. Likewise, agamous-like MADS-box protein AGL30 (8.52) which regulates pollen maturation, MADS-box protein AGL29 (8.08) which controls flower development, putative TF bHLH68 (7.36) crucial for photo morphogenesis and light signal transduction, probable transcription factor KAN2 (7.28) required for lateral organ polarity were upregulated in response to *Trichoderma*.

Transcription factor PIF3 (3.54) to promote and optimize growth under photoperiodic conditions, transcription elongation factors; s-II (TFIIS) with 2.8 fold change expression for coordinating transcription initiation, and several *WRKY* transcription factors which mediate ethylene (ET) signaling and ET synthesis to hasten leaf senescence were also upregulated along with Myb-like DNA-binding domain and G-box-binding factor required in developmental and physiological processes in response to major cues such as light or hormones.

3.6. Validation of transcriptome data by quantitative Real Time- PCR (RT-qPCR)

To validate plant DEGs detected in the present study, RT-qPCR was performed for a set of 9 putative genes involved in defense and stress responses at 12, 24 and 48 hpi (Fig. 6). Of these 9 genes, 4 genes were upregulated and 5 genes where down regulated in the DEG analysis. The qRT results of these 9 genes were consistent with transcriptome profiling data, suggesting high reliability and good quality of the data. Five genes that were found to be downregulated were Peroxidase12 (*PER12*), serine/threonine-protein kinase (*FLS2*), pathogenesis related protein5 (*PR5*), Endoglucanase (*ENDO*), Wound induced protein2 (*WIN2*), *w*hereas the 4 putative genes which were upregulated were WRKY transcription factor (*WRKY71*), disease resistance protein1 (*RPV1*), zinc finger protein5 (*ZAT5*) and disease resistance gene, *RPS2.* The putative genes, *PER12*, *FLS2*, *PR5*, *ENDO* and *WIN2* confirmed to be downregulated play a crucial role in pathogen recognition and defense signaling suggesting that *Trichoderma* is perceived as a beneficial microbe by the host, castor.

4. Discussion

Fungal biocontrol agents have been reported to protect plants against abiotic stresses, such as high temperatures and saline conditions (Kashyap et al., 2017, 2020). They are also utilized to promote plant defense owing to their ability to induce ISR protecting them against several pathogens and, all of which resulting in an increase in plant yield. In this regard, *Trichoderma* fungal members have played important roles in enhancing plant growth and crop production (Alfano et al., 2007; Alvarez-Buylla et al., 2019). In this study, an attempt is made to understand the molecular basis of the *Trichoderma*-mediated host responses in castor by analysing castor-*Trichoderma* interaction through transcriptome profiling studies. It is interesting to note that majority of gene transcripts were observed to be downregulated and these putative DEGs were predominantly related to stress responses suggesting that the host recognized *Trichoderma* as a non-pathogenic but a beneficial organism.

4.1. Putative genes downregulated in castor in response to Trichoderma

The DEGs that were downregulated were primarily comprising of the family of kinases which include putative receptor-like protein kinases and LRR receptor-like serine/threonine-protein kinases. These receptors have been reported to play a crucial role in pathogen recognition and

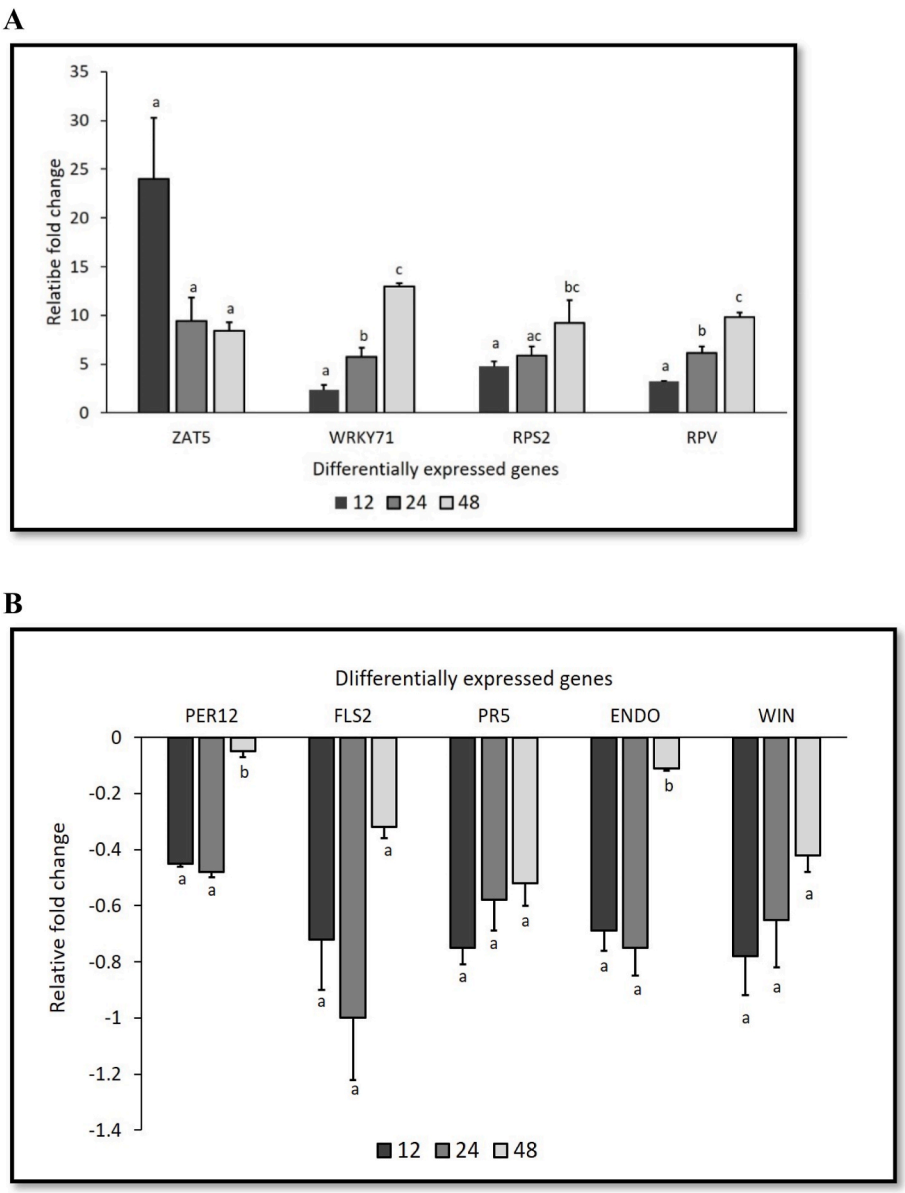


Fig. 6. Validation of plant DEGs by Real Time-quantitative Polymerase Chain Reaction (RT-qPCR). The relative level of mRNA transcript accumulation of 9 stress and defense-related genes at 12, 24 and 48 hpi in *T. asperellum* 7316-treated castor (DCS-107) roots. Confirmation of (A) upregulated and (B) downregulated plant DEGs using plant *Actin* as an internal control and non-template DNA control (NTC). Statistical significance of variation between the different time-points was displayed at Tukey $p \leq 0.05$. Vertical bars represent ±SE of the mean values of replicates. Statistical significance levels indicated by case letters: a–c.

pattern associated molecular pattern (PAMP)-triggered immunity (Boller and Felix, 2009) and their negative regulation suggests that *Trichoderma* colonization is recognized as a non-pathogen by the host. Moreover, the putative genes involved in downstream functions like activating stress-related signaling, ROS generation, hypersensitive response and secondary metabolite production were also predominantly downregulated indicating that the host might be negatively regulating stress-related genes to promote *Trichoderma* colonization in the host.

Further, a downregulation of several of the peroxidases and laccases which play a vital role in plant defense response against pathogen attack, indicated that *Trichoderma* is sensed as a non-alarming entity by the host. Peroxidase (POX) not only helps in ROS scavenging but also aids to deter the spread of a pathogen through the formation of polymerized phenolic barriers around the sites of infection by pathogens (Siddaiah et al., 2017) resulting in cell wall reinforcement thereby triggering the synthesis of anti-nutritive, antibiotic, and cytotoxic compounds causing enhanced resistance against pathogens (Smit and Dubery, 1997).

Similar to peroxidases, laccases are key enzymes involved in lignification. A 20–40% reduction in lignin content has been observed in the knockout mutants of two laccase genes (*LAC4* and *LAC17*) in Arabidopsis (Berthet et al., 2011). Moreover, the triple mutant of *LAC4*, *LAC11*, and *LAC17* completely lost lignin deposition in roots (Zhao et al., 2013). Thus it is understandable that downregulation of lignin forming peroxidases and laccase allows colonization of *Trichoderma* inside the roots of DCS-107. In general, plants appear to balance generation of ROS leading to activation of peroxidases as the first line of defence and reducing cell wall reinforcements after perceiving *Trichoderma* as no obvious threat in order to allow the symbiotic relationship to be established between them.

The jacalin-like mannose-binding lectin domain containing proteins which are reported to bind to the T-antigen and act as an agglutinin in higher organisms, were found to interact with endogenous carbohydrates especially in disease signaling pathway (Naithani et al., 2021). However, in response to *Trichoderma*, the putative lectin domain gene was observed to be down regulated in agreement that *Trichoderma* is recognized as a non-pathogen. Likewise, Serine carboxypeptidases like proteins (SCPLs) which were upregulated against *Magnaporthe grisea* infection in rice (Liu et al., 2008) were found to be downregulated in response to *Trichoderma*.

Conversely, a reduced number of the putative methyl transferases related to the family of *O*-methyltransferases (OMTs) with a putative role in secondary metabolites including phenylpropanoids, flavonoids, and alkaloids were observed. In addition, the genes involved in secondary metabolite biosynthesis, cell wall modifications, disease signaling and transduction were also downregulated confirming that *Trichoderma* is regarded by the host plant as a non-harmful agent.

Likewise downregulation of the putative transcription factors which include *BIM1*, myb family transcription factor *PHL8*, transcription factor *bHLH90*, GATA transcription factor4 indicated the repression of brassinosteroid signaling in response to *Trichoderma*. The putative *BIM1*, a bHLH protein is involved in brassinosteroid signaling and is reported to control Arabidopsis embryonic patterning via interaction with DORNROSCHEN (DRN) and DORNROSCHEN-LIKE (DRNL) transcription factors (Chandler et al., 2009; Jiang et al., 2015). The multimeric transcription factor complex formed by the trio genes suggested not only a role of brassinosteroids in embryonic development but also as a possible point of hormonal crosstalk with auxin in embryonic patterning, since DRN is involved in auxin signaling as well.

Similar to *BIM1*, the downregulation of other members of *bHLH* transcription factors, *bHLH90* and *bHLH74* confirmed the repression of brassinosteroid signaling which functions in photomorphogenesis, light signal transduction and secondary metabolism in response to stress (Guo et al., 2021). Likewise, downregulation of a myb family transcription factor *PHL8*, indicated that *Trichoderma* colonization is perceived as beneficial to the host, since *MYB* family of transcription factors are involved in controlling various cellular responses to biotic and abiotic stresses (Ambawat et al., 2013). Whereas GATA transcription factor4 which is known to be involved in light-dependent gene regulation and nitrate assimilation was observed to be downregulated in agreement with studies revealing that repression of the transcription factor *bHLH74* by a miR396a promoted root growth in Arabidopsis seedlings (Bao et al., 2014).

4.2. Putative genes upregulated in castor in response to Trichoderma

A predominant number of serine threonine-protein kinase members were upregulated suggesting their role in plant growth and development, besides aiding in recognition of plant invaders comprising of both pathogenic as well as non-pathogenic organisms. The upregulated serine/threonine-protein kinase *WNK4* might be essential to act as a molecular switch that can alter the balance between NaCl reabsorption and K^+ secretion to maintain integrated homeostasis of the host cells (Kahle et al., 2005). Further, WINK4 gene has been reported as a key player in regulating plant growth and development in maize (Patil and Senthil-Kumar, 2020).

Likewise, upregulation of a putative inositol-tetrakisphosphate 1-kinase 3 gene, which plays a fundamental role in phosphate signaling to connect cell wall and membrane sensors with ion homeostasis and transport-mediated processes has previously been demonstrated in *Arabidopsis thaliana* to catalyse the synthesis of phytate (inositol hexakisphosphate; $InsP_6$) synthesis and is indispensable for maintaining P_i homeostasis (Stevenson-Paulik et al., 2005). Recent studies have demonstrated that Arabidopsis inositol 1,3,4-trisphosphate 5/6 kinase 2 is required for the permeability of seed coat and seed coat development (Tang et al., 2013). The elevated gene expression levels of a putative proline-rich receptor-like protein kinase *PERK8* observed in the present study might be required for the floral organ development as demonstrated Chen and associates (2020) by a proline-rich extension-like receptor protein kinase (*PERK*) in *Brassica rapa* and its association with the pollen development. Likewise, an increased mRNA levels of a putative 2-oxoglutarate-dependent dioxygenase which aids in enhanced phytohormone formation such as ethylene, gibberellins, anthocyanidins and pigments that are catalysed by the enzymes containing 2OG dioxygenase domains were also observed in Arabidopsis with its importance in not only plant growth, development and metabolism but also in adaptive responses to low oxygen conditions (Iacopino and Licausi, 2020).

Besides plant growth, the receptor-like protein kinases with a role in symbiotic association were also upregulated which include cysteine-rich receptor-like protein kinase 10 (*CRK*), and LysM domain receptor-like kinase 3 suggesting the recognition of *Trichoderma* by the host as a endosymbiont. The findings are in accordance with the study on the biological roles of *CRKs* in various tissues of the plants belonging to the genus, *Phaseolus* during diverse biological processes including *Phaseolus*-mycorrhiza/rhizobia symbiosis (Quezada et al., 2019). Another potential candidate with a unique role in both the arbuscular mycorrhizal (AM) and the rhizobium-legume (RL) symbioses in response to signal molecules was detected in the present study similar to the reported the LysM receptor-like kinases (LysM-RLKs), known as *NFP/NFR5*, *LYK3/NFR1*, and *LYR3/LYS12* which were detected for root endosymbiosis in *Medicago truncatula* and *Lotus japonicus* (Gough et al., 2018; Buendia et al., 2018).

4.2.1. Putative genes upregulated with a role in cellular metabolism and detoxification

Glutathione S-transferases are one of the most important detoxifying enzymes that play a major role in stress tolerance in plants and systemic infection by rice black streaked dwarf virus (RBSDV) in rice showed an induction of GST 23 gene (Xu et al., 2013; Hasanuzzaman et al., 2017). In agreement, an upregulation of GST which helps to combat oxidative stress caused due to interaction with *Trichoderma* was observed for limiting ROS triggered by Pathogen triggered immunity (PTI).

The mRNA transcripts of Glycerol-3-phosphate dehydrogenase NAD (+) 2 gene with a putative role in glycolysis and homeostasis, a probable glutathione peroxidase 2 gene to function in cellular metabolism and energy production, Glutathione S-transferase L3 with a role in cellular metabolism and detoxification of a variety of xenobiotic compounds and few peroxidases which include L-ascorbate peroxidase 6, Peroxidase 5, Cationic peroxidase 1 were upregulated as a natural response against an invading organism to minimise cell damage caused due to ROS accumulation. Further, the findings from the present study were in agreement with the previous report on *Trichodema* inoculation in tomato (Chen et al., 2019). Chen et al. (2019) reported a significant increase in the glutathione (*GSH*) content, the activity of glutathione S-transferase (GST) and the transcript levels of *GSH*, *GST1*, *GST2* and *GST3* along with the activity of peroxidase and polyphenol peroxidase that are involved in the xenobiotic conversion. In addition, expression of several detoxification genes such as Cytochrome P450 suggests that *Trichoderma asperellum* stimulates plant detoxification potential in all three phases (conversion, conjugation and sequestration) of xenobiotc metabolism in the roots of castor.

Both plants and microbes encode for phosphatases to mineralize organic phosphate (P) compounds. However, purple acid phosphatases (PAPs) an important class of plant APases that are secreted by plants into the rhizosphere to utilize organic phosphorus (Po) for plant growth and development were found to be upregulated in castor roots in response to *Trichoderma*. The upregulation of YTH domain-containing protein ECT4 gene in our study with a putative role in leaf organ formation has been demonstrated to be associated with developmental timing and morphogenesis in Arabidopsis (Arribas-Hernández et al., 2018). Likewise, growth regulating factor (GRF1)-interacting factor1 which was upregulated in the study have been presented as positive regulators of cell proliferation and are involved in the regulation of stem and leaf development (Zhang et al., 2018), whereas *WALLS ARE THIN1* (*WAT1*), a plant-specific protein which was also upregulated controls secondary cell wall thickness of wood fibres and facilitates auxin export required for auxin homoeostasis as demonstrated from isolated Arabidopsis vacuoles into yeast and Xenopus oocytes (Ranocha et al., 2013). A putative polygalacturonase upregulated might be involved in promoting plant growth and floral organ patterning to produce higher proportions of flowers (Xiao et al., 2014).

Ubiquitination and subsequent proteasomal degradation of target

proteins are essential for molecular processing and housecleaning to maintain homeostasis of plant cells. Several proteins which include, RING-H2 finger protein ATL11, Receptor homology region, transmembrane domain- and RING domain-containing protein 1, RING-H2 finger protein ATL66, Nudix hydrolase 2 gene, ferrous ascorbate-dependent oxidoreductase family, F-box protein FBW2, protein of the SKP1 family, SNF1-related protein kinase regulatory subunit gamma-1-like, SKP1-like protein 21 and UDP-glycosyltransferase with a role in regulating mechanisms involving proteasomal degradation, cellular detoxification and homeostasis in the host (Hacquard et al., 2022; Guzmán, 2012; Ge and Xia, 2008; Zhao et al., 2003).

4.2.2. Upregulated genes with a role in defense responses and signaling

While majority of the genes involved in ROS and hypersensitive responses were downregulated, it is interesting to note that a few of the defense response genes were upregulated in *Trichoderma*-treated castor plants along with the two putative resistance genes (*RPV1* and *RPS2*) indicating that a basal level of response was activated at 48 hpi to an incoming foreign organism. The upregulation of F-box/kelch-repeat protein, known as KFB1 is a member of a group of Kelch repeat F-box proteins that negatively regulate phenylpropanoid biosynthesis by targeting the phenypropanoid biosynthesis enzyme, phenylalanine ammonia-lyase suggesting its role in the downregulation of SA-mediated responses. Our research findings are in agreement with previous report indicating that upregulation or downregulation of KFB1 reciprocally affects the phenylpropanoid pathway (Zhang et al., 2013). Also, Thaumatin-like proteins are classified into the PR-5 protein family which is a characteristic of the SA pathway (Anisimova et al., 2021). Downregulation of such Thaumatin-like proteins also indicate a possible downregulation of SA-mediated protein response in *Trichoderma* treated roots of DCS-107.

Likewise, elevated expression of putative gene transcripts of cold-regulated 413 plasma membrane protein 2, a positive regulator of ABA responses (Hu et al., 2021), TPL-binding domain as a repressor of auxin signaling (Navarrete et al., 2022) and a plant-specific Zinc finger protein ZAT5 responsive to multiple plant hormones (Fan et al., 2021) suggested interplay of different phytohormones in *Trichoderma*-mediated defense signaling in castor. Further, a SNF1-related protein kinase regulatory subunit gamma-1-like gene, a member of SnRK2 which is reported as a global positive regulator of ABA signaling was upregulated. In addition, a hike in the Serine carboxypeptidase-like 18 gene transcripts, a candidate with promoter elements responsive to both abscisic acid (ABA) and methylated jasmonic acid (MeJA) confirmed that *Trichoderma* induced both ABA and JA mediated responses in castor. Our findings are in agreement with the studies of Moura and associates (2001) which identified the type I SCP gene in tomato (*Lycopersicon esculentum* Mill.) as one of the "late wound-inducible genes" based on its induced expression by wounding, systemin and methyl jasmonate (MeJA). Likewise, a recent studies on functional analysis of *cis*-acting elements of promoter sequences of *TaSCPL* genes in wheat (*Triticum aestivum* L.) confirmed that those sequences are enriched in drought-, ABA- and MeJA-responsive elements (Xu et al., 2021). *WRK71*, belonging to a large family of transcription factors was seen upregulated. *WRK71* protein that is usually upregulated by several signaling molecules like salicylic acid, methyl jasmonate or on wounding and pathogen invasion has shown an enhanced resistance in rice in response to *Xanthomonas oryzae* pv. *oryzae* (Liu et al., 2007).

4.2.3. Trichoderma-induced molecular remodeling, chaperones and transcription factors

S-adenosylmethionine (SAM) is a dominant metabolic intermediate and ubiquitous cofactor and SAM-dependent methyltransferases (MTases) are responsible for methylation affecting several pathways involving macromolecules like lipids, proteins and nucleic acids in addition to the biosynthesis of small-molecule metabolites (Struck et al., 2012; Bennett et al., 2017; Luo et al., 2019). Our study also revealed several methy transferases including the highly upregulated S-adenosylmethionine-dependent methyltransferase with putative role in methylation processes of key regulatory genes involved in plant growth and development.

A few molecular chaperone genes like hsc70-interacting protein, peptidyl-prolyl cis-trans isomerase CYP37 and Peptidyl-prolyl cis-trans isomerase CYP38, chloroplast were upregulated suggesting that heat shock proteins (hsp) which include Hsc70-interacting protein are essential to aid in folding of newly synthesized polypeptide chains and translocation of proteins across membranes (Berka et al., 2022).

Of the several upregulated transcription factors with a putative role in plant growth and development, the putative Transcription Factor, *E2FB* predominantly expressed followed by Lipid remodeling regulator1 (*LRL1*). *E2FB* is reported as a key target for auxin to determine whether cells should proliferate or exit the cell cycle, enlarge, and endoreduplicate their DNA (Magyar et al., 2005) and also in coordinating cell proliferation with seed maturation (Leviczky et al., 2019). The transcription factor, lipid remodeling regulator1 (*LRL1*) is shown to be differently involved in the phosphorus-depletion response in *Chlamydomonas reinhardtii* (Hidayati et al., 2019). A putative BPI/LBP family protein At1g04970 transcript accumulation indicated the possibility of a lipopolysaccharide (LPS)-based elicitation by *Trichoderma* which in turn upregulated phosphatidylinositol-glycan biosynthesis to generate the lipid anchor protein, glycophosphatidylinositol (GPI) suggesting that *Trichoderma* treatment not only induced lipid biosynthesis but also lipid based signaling in castor.

The other transcription factors, Agamous-like MADS-box protein AGL30 and MADS-box protein AGL29 play a crucial role in pollen maturation and flower development (Roy Choudhury et al., 2012; Alvarez-Buylla et al., 2019). The other transcription factors that were upregulated include *bHLH68*, *KAN2* and *PIF3* which are required for photo morphogenesis, light signal transduction, lateral organ polarity and to promote and optimize growth under different photoperiodic and phytohormonal conditions while the *WRKY* transcription factors; *WRKY71*, *WRKY40* and *WRKY55* were found to be marginally upregulated in response to *Trichoderma*. Our findings are in accordance with the previous studies (Alfano et al., 2007; Shoresh et al., 2010; Morán-Diez et al., 2012) which showed alteration of stress and defense response components in response to *Trichoderma*, though the level of the change remains quantitatively marginal. Therefore, the preliminary response of the plant to *Trichoderma* invasion involves the activation of several physical and biochemical responses to ensure persistent endophytic relation with the host.

5. Conclusions

The study revealed that *Trichoderma* association with castor resulted in vast transcriptomic reprogramming of the plant genome which lead to the alteration of genes associated with stress and defense in castor. Together, the pattern of altered gene expression observed in castor roots due to *Trichoderma* colonization suggests a complex system of communication involving genetic cross talk between various molecular and biological processes. As explained in the graphical abstract, *Trichoderma* interaction leads to a complex reprograming of stress response genes. Downregulation of peroxidases, laccase, PR proteins, methyltransferase and endoglucanase along with WIN2, enables the development of an efficient mutualistic relationship between castor and *Trichoderma* that also protects castor from oxidative damage. At the same time, early colonization causes upregulation of genes promoting jasmonic acid (JA)- mediated ISR responses in *Trichoderma*-treated castor. Thus, a strong endophytic association between the host, castor and the BCA, *Trichoderma,* is not only mutually beneficial to both the interacting members, but also aids in priming the host to elicit faster and enhanced immune response to subsequent pathogen attack. Along with genes involved in elevated ISR response, low molecular weight secondary metabolites with antimicrobial properties were also upregulated in

response to *Trichoderma* which could be exploited to confer resistance to pests and pathogens in castor.

Author contributions

DAP: Performed experiments, data analysis and manuscript preparation. RM: Conceptualized, planned, supervised, obtained funding and revised the manuscript.

Declaration of competing interest

The authors declare that they have no known competing financial interests or personal relationships that could have appeared to influence the work reported in this paper.

Data availability

Data will be made available on request.

Acknowledgements

The funding from the Indian Council of Agricultural Research (ICAR)-NFBSFARA (F. No. NFBSFARA/BS-3007/2012-13 provided to RM is acknowledged. The authors acknowledge Indian Institute of Oilseeds Research (IIOR), Hyderabad for providing castor genotype and *Trichoderma* fungal strain; Nucleome Informatics Ltd., Hyderabad, India for transcriptome sequencing services, Mr. Harish for helping in data submission; Facilities at the University of Hyderabad (UoH) including IOE, DBT-BUILDER, DST-FIST, UGC-SAP, PURSE, DBT CREBB and Plant Culture Facility are acknowledged. Also, the financial support as fellowship (UGC-SRE) to Doris A Pradhan (DAP) is acknowledged.

Appendix A. Supplementary data

Supplementary data to this article can be found online at https://doi.org/10.1016/j.rhisph.2023.100745.

References

Alfano, G., Ivey, M.L., Cakir, C., Bos, J.I., Miller, S.A., Madden, L.V., Kamoun, S., Hoitink, H.A., 2007. Systemic modulation of gene expression in tomato by *Trichoderma hamatum* 382. Phytopathology 97, 429–437.

Alvarez-Buylla, E.R., García-Ponce, B., Sánchez, M.-P., Espinosa-Soto, C., García-Gómez, M.L., Piñeyro-Nelson, A., Garay-Arroyo, A., 2019. MADS-box genes underground becoming mainstream: plant root developmental mechanisms. New Phytol. 223, 1143–1158.

Ambawat, S., Sharma, P., Yadav, N.R., Yadav, R.C., 2013. MYB transcription factor genes as regulators for plant responses: an overview. Physiol. Mol. Biol. Plants 19, 307–321.

Anisimova, O.K., Shchennikova, A.V., Kochieva, E.Z., Filyushin, M.A., 2021. Pathogenesis-related genes of PR1, PR2, PR4, and PR5 families are involved in the response to *Fusarium* infection in garlic (*Allium sativum* L.). Int. J. Mol. Sci. 22, 6688.

Arribas-Hernández, L., Bressendorff, S., Hansen, M.H., Poulsen, C., Erdmann, S., Brodersen, P., 2018. An m6A-YTH module controls developmental timing and morphogenesis in Arabidopsis. Plant Cell 30, 952–967.

Bao, M., Bian, H., Zha, Y., Li, F., Sun, Y., Bai, B., Chen, Z., Wang, J., Zhu, M., Han, N., 2014. miR396a- Mediated basic helix-loop-helix transcription factor bHLH74 repression acts as a regulator for root growth in Arabidopsis seedlings. Plant Cell Physiol. 55, 1343–1353.

Bennett, M.R., Shepherd, S.A., Cronin, V.A., Micklefield, J., 2017. Recent advances in methyltransferase biocatalysis. Curr. Opin. Chem. Biol. 37, 97–106.

Benítez, T., Rincón, A.M., Limón, M.C., Codón, A.C., 2004. Biocontrol mechanisms of *Trichoderma* strains. Int. Microbiol. 7, 249–260.

Berka, M., Kopecká, R., Berková, V., Brzobohatý, B., Černý, M., 2022. Regulation of heat shock proteins 70 and their role in plant immunity. J. Exp. Bot. 1894–1909.

Berthet, S., Demont-Caulet, N., Pollet, B., Bidzinski, P., Cézard, L., Le Bris, P., Borrega, N., Hervé, J., Eddy, Blondet, E., Balzergue, S., Lapierre, C., Jouanin, L., 2011. Disruption of LACCASE4 and 17 results in tissue-specific alterations to lignification of *Arabidopsis thaliana* stems. Plant Cell 23, 1124–1137.

Bolger, A.M., Lohse, M., Usadel, B., 2014. Trimmomatic: a flexible trimmer for illumina sequence data. Bioinformatics 30, 2114–2120.

Boller, T., Felix, G., 2009. A renaissance of elicitors: perception of microbe-associated molecular patterns and danger signals by pattern-recognition receptors. Annu. Rev. Plant Biol. 60, 379–406.

Buendia, L., Girardin, A., Wang, T., Cottret, L., Lefebvre, B., 2018. LysM receptor-like kinase and LysM receptor-like protein families: an update on phylogeny and functional characterization. Front. Plant Sci. 9, 1531.

Chandler, J.W., Cole, M., Flier, A., Werr, W., 2009. BIM1, a bHLH protein involved in brassinosteroid signalling, controls Arabidopsis embryonic patterning via interaction with DORNROSCHEN and DORNROSCHEN-LIKE. Plant Mol. Biol. 69, 57–68.

Chen, S., Yan, Y., Wang, Y., Wu, M., Mao, Q., Chen, Y., Ahammed, G.J., 2019. *Trichoderma asperellum* reduces phoxim residue in roots by promoting plant detoxification potential in *Solanum lycopersicum* L. Environ. Pollut. 259, 113893.

Chen, G., Wang, J., Wang, H., Wang, C., Tang, X., Li, J., Zhang, L., Song, J., Hou, J., Yuan, L., 2020. Genome-wide analysis of proline-rich extension-like receptor protein kinase (PERK) in *Brassica rapa* and its association with the pollen development. BMC Genom. 21, 401.

Fan, Y., Zhang, Y., Rui, C., Nan, X., Zhang, H., Wang, J., Malik, W.A., Han, M., Zhao, L., Lu, X., Chen, X., Chen, C., 2021. Zinc finger transcription factor ZAT family genes confer multi-tolerances in *Gossypium hirsutum* L. J Cotton Res 4, 24.

Ge, X., Xia, Y., 2008. The role of AtNUDT7, a Nudix hydrolase, in the plant defense response. Plant Signal. Behav. 3, 119–120.

Gough, C., Cottret, L., Lefebvre, B., Bono, J.-J., 2018. Evolutionary history of plant LysM receptor proteins related to root endosymbiosis. Front. Plant Sci. 9, 923.

Guo, J., Sun, B., He, H., Zhang, Y., Tian, H., Wang, B., 2021. Current understanding of bHLH transcription factors in plant abiotic stress tolerance. Int. J. Mol. Sci. 22, 4921.

Guzmán, P., 2012. The prolific ATL family of RING-H2 ubiquitin ligases. Plant Signal. Behav. 7, 1014–1021.

Hacquard, T., Clavel, M., Baldrich, P., Lechner, E., Pérez-Salamó, I., Schepetilnikov, M., Derrien, B., Dubois, M., Hammann, P., Kuhn, L., Brun, D., Bouteiller, N., Baumberger, N., Vaucheret, H., Meyers, B.C., Genschik, P., 2022. The Arabidopsis F-box protein FBW2 targets AGO1 for degradation to prevent spurious loading of illegitimate small RNA. Cell Rep. 39, 110671.

Hasanuzzaman, M., Nahar, K., Anee, T.I., Fujita, M., 2017. Glutathione in plants: biosynthesis and physiological role in environmental stress tolerance. Physiol. Mol. Biol. Plants 23, 249–268.

Hidayati, N.A., Yamada-Oshima, Y., Iwai, M., Yamano, T., Kajikawa, M., Sakurai, N., 2019. Lipid remodeling regulator 1 (*LRL1*) is differently involved in the phosphorus-depletion response from PSR1 in *Chlamydomonas reinhardtii*. Plant J. 100, 610–626.

Hu, X., Liu, J., Liu, E., Qiao, K., Gong, S., Wang, J., Zhang, J., 2021. Arabidopsis cold-regulated plasma membrane protein Cor413pm1 is a regulator of ABA response. Biochem. Biophys. Res. Commun. 561, 88–92.

Iacopino, S., Licausi, F., 2020. The contribution of plant dioxygenases to hypoxia signaling. Front. Plant Sci. 11, 1008.

Jiang, J., Zhang, C., Wang, X., 2015. A recently evolved isoform of the transcription factor BES1 promotes brassinosteroid signaling and development in *Arabidopsis thaliana*. Plant Cell 27, 361–374.

Kahle, K.T., Wilson, F.H., Lifton, R.P., 2005. Regulation of diverse ion transport pathways by WNK4 kinase: a novel molecular switch. Trends Endocrinol. Metabol. 16, 98–103.

Kashyap, P.L., Rai, P., Srivastava, A.K., Kumar, S., 2017. *Trichoderma* for climate resilient agriculture. World J. Microbiol. Biotechnol. 33, 155.

Kashyap, P.L., Solanki, M.K., Kushwaha, P., Kumar, S., Srivastava, A.K., 2020. Biocontrol potential of salt-tolerant *Trichoderma* and hypocrea isolates for the management of tomato root rot under saline environment. J. Soil Sci. Plant Nutr. 20, 160–176.

Leviczky, T., Molnár, E., Papdi, C., Őszi, E., Horváth, G.V., Vizler, C., Nagy, V., Pauk, J., Bögre, L., Magyar, Z., 2019. E2FA and E2FB transcription factors coordinate cell proliferation with seed maturation. Development 146, 179333.

Li, R.X., Cai, F., Pang, G., Shen, Q.R., Li, R., Chen, W., 2015. Solubilisation of phosphate and micronutrients by *Trichoderma harzianum* and its relationship with the promotion of tomato plant growth. PLoS One 10, e0130081.

Liu, Q., Meng, X., Li, T., Raza, W., Liu, D., Shen, Q., 2020. The growth promotion of peppers (*Capsicum annuum* L.) by *Trichoderma guizhouense* NJAU4742-based biological organic fertilizer: possible role of increasing nutrient availabilities. Microorganisms 8, 1296.

Liu, H., Wang, X., Zhang, H., Yang, Y., Ge, X., Song, F., 2008. A rice serine carboxypeptidase-like gene OsBISCPL1 is involved in regulation of defense responses against biotic and oxidative stress. Gene 420, 57–65.

Liu, X., Bai, X., Wang, X., Chu, C., 2007. OsWRKY71, a rice transcription factor, is involved in rice defense response. J. Plant Physiol. 164, 969–979.

Livak, K.J., Schmittgen, T.D., 2001. Analysis of relative gene expression data using real-time quantitative PCR and the 2-ΔΔCT method. Methods 25, 402–408.

Luo, H., Hansen, A.S.L., Yang, L., Schneider, K., Kristensen, M., Christensen, U., 2019. Coupling S-adenosylmethionine-dependent methylation to growth: design and uses. PLoS Biol. 17, e2007050.

Magyar, Z., De Veylde, r L., Atanassova, A., Bakó, L., Inzé, D., Bögre, L., 2005. The role of the Arabidopsis *E2FB* transcription factor in regulating auxin-dependent cell division. Plant Cell 17, 2527–2541.

Martínez-Medina, A., Fernández, I., Sánchez-Guzmán, M.J., Jung, S.C., Pascual, J.A., Pozo, M.J., 2013. Deciphering the hormonal signalling network behind the systemic resistance induced by *Trichoderma harzianum* in tomato. Front. Plant Sci. 4, 206.

Mathys, J., De Cremer, K., Timmermans, P., Van Kerckhove, S., Lievens, B., Vanhaecke, M., Cammue, B.P., De Coninck, B., 2012. Genome-wide characterization of ISR induced in *Arabidopsis thaliana* by *Trichoderma hamatum* T382 against *Botrytis cinerea* infection. Front. Plant Sci. 3, 108.

Morán-Diez, E., Rubio, B., Domínguez, S., Hermosa, R., Monte, E., Nicolás, C., 2012. Transcriptomic response of *Arabidopsis thaliana* after 24 h incubation with the biocontrol fungus *Trichoderma harzianum*. J. Plant Physiol. 169, 614–620.

Moura, D.S., Bergey, D.R., Ryan, C.A., 2001. Characterization and localization of a wound-inducible type I serine-carboxypeptidase from leaves of tomato plants (*Lycopersicon esculentum* mill.). Planta 212, 222–230.
Naithani, S., Komath, S.S., Nonomura, A., Govindjee, G., 2021. Plant lectins and their many roles: carbohydrate-binding and beyond. J. Plant Physiol. 266, 153531.
Navarrete, F., Gallei, M., Kornienko, A.E., Saado, I., Khan, M., Chia, K.S., Darino, M.A., Bindics, J., Djamei, A., 2022. TOPLESS promotes plant immunity by repressing auxin signaling and is targeted by the fungal effector Naked1. Plant Commun. 3, 100269.
Nishad, R., Ahmed, T., Rahman, V.J., Kareem, A., 2020. Modulation of plant defense system in response to microbial interactions. Front. Microbiol. 3, 1298.
Patil, M., Senthil-Kumar, M., 2020. Role of plant kinases in combined stress. In: Protein Kinases and Stress Signaling in Plants: Functional Genomic Perspective. John Wiley & Sons, Ltd., pp. 445–458
Qualhato, T.F., Lopes, F.A., Steindorff, A.S., Brandão, R.S., Jesuino, R.S., Ulhoa, C.J., 2013. Mycoparasitism studies of *Trichoderma* species against three phytopathogenic fungi: evaluation of antagonism and hydrolytic enzyme production. Biotechnol. Lett. 35, 1461–1468.
Quezada, E.H., García, G.X., Arthikala, M.K., Melappa, G., Lara, M., Nanjareddy, K., 2019. Cysteine-rich receptor-like kinase gene family identification in the Phaseolus genome and comparative analysis of their expression profiles specific to mycorrhizal and rhizobial symbiosis. Genes 10, 59.
Rajani, P., Rajasekaran, C., Vasanthakumari, M.M., Olsson, S.B., Ravikanth, G., Shaanker, R.U., 2021. Inhibition of plant pathogenic fungi by endophytic *Trichoderma* spp. through mycoparasitism and volatile organic compounds. Microbiol. Res. 242, 126595.
Ranocha, P., Dima, O., Nagy, R., Felten, J., Corratgé-Faillie, C., Novák, O., Morreel, K., Lacombe, B., Martinez, Y., Pfrunder, S., Jin, X., Renou, J.P., Thibaud, J.B., Ljung, K., Fischer, U., Martinoia, E., Boerjan, W., Goffner, D., 2013. Arabidopsis *WAT1* is a vacuolar auxin transport facilitator required for auxin homoeostasis. Nat. Commun. 4, 2625.
Robinson, M.D., McCarthy, D.J., Smyth, G.K., 2010. edgeR: a bioconductor package for differential expression analysis of digital gene expression data. Bioinformatics 26, 139–140.
Roy Choudhury, S., Roy, S., Nag, A., Singh, S.K., Sengupta, D.N., 2012. Characterization of an AGAMOUS-like MADS box protein, a probable constituent of flowering and fruit ripening regulatory system in banana. PLoS One 7, e44361.
Saber, W.I.A., Ghoneem, K.M., Rashad, Y.M., Al-Askar, A.A., 2017. *Trichoderma harzianum WKY1*: an indole acetic acid producer for growth improvement and anthracnose disease control in sorghum. Biocontrol Sci. Technol. 27, 654–676.
Shoresh, M., Harman, G.E., Mastouri, F., 2010. Induced systemic resistance and plant responses to fungal biocontrol agents. Annu. Rev. Phytopathol. 48, 21–43.
Siddaiah, C.N., Satyanarayana, N.R., Mudili, V., Gupta, V.K., Gurunathan, S., Rangappa, S., Huntrike, S.S., Srivastava, R.K., 2017. Elicitation of resistance and associated defense responses in *Trichoderma hamatum* induced protection against pearl millet downy mildew pathogen. Sci. Rep. 7, 43991.
Singh, V., Upadhyay, R.S., Sarma, B.K., Singh, H.B., 2016. *Trichoderma asperellum* spore dose depended modulation of plant growth in vegetable crops. Microbiol. Res. 93, 74–86.
Smit, F., Dubery, I.A., 1997. Cell wall reinforcement in cotton hypocotyls in response to a *Verticillium dahliae* elicitor. Phytochemistry 44, 811–815.
Stevenson-Paulik, J., Bastidas, R.J., Chiou, S.T., Frye, R.A., York, J.D., 2005. Generation of phytate-free seeds in Arabidopsis through disruption of inositol polyphosphate kinases. Proc. Natl. Acad. Sci. U. S. A. 102, 12612–12617.
Struck, A.W., Thompson, M.L., Wong, L.S., Micklefield, J., 2012. S-adenosyl-methionine-dependent methyltransferases: highly versatile enzymes in biocatalysis, biosynthesis and other biotechnological applications. Chembiochem 13, 2642–2655.
Tang, Y., Tan, S., Xue, H., 2013. Arabidopsis inositol 1,3,4-trisphosphate 5/6 kinase 2 is required for seed coat development. Acta Biochim. Biophys. Sin. 45, 549–560.
Tucci, M., Ruocco, M., De Masi, L., De Palma, M., Lorito, M., 2011. The beneficial effect of *Trichoderma* spp. on tomato is modulated by the plant genotype. Mol. Plant Pathol. 12, 341–354.
Xiao, C., Somerville, C., Anderson, C.T., 2014. POLYGALACTURONASE INVOLVED IN EXPANSION1 functions in cell elongation and flower development in Arabidopsis. Plant Cell 26, 1018–1035.
Xie, C., Mao, X., Huang, J., Ding, Y., Wu, J., Dong, S., Kong, L., Gao, G., Li, C.Y., Wei, L., 2011. KOBAS 2.0: a web server for annotation and identification of enriched pathways and diseases. Nucleic Acids Res. 39, W316–W322.
Xu, Q., Ni, H., Chen, Q., Sun, F., Zhou, T., Lan, Y., Zhou, Y., 2013. Comparative proteomic analysis reveals the cross-talk between the responses induced by H_2O_2 and by long-term rice black-streaked dwarf virus infection in rice. PLoS One 8, e81640.
Xu, X., Zhang, L., Zhao, W., Fu, L., Han, Y., Wang, K., Yan, L., Li, Y., Zhang, X.-H., Min, D.-H., 2021. Genome-wide analysis of the serine carboxypeptidase-like protein family in *Triticum aestivum* reveals *TaSCPL184-6D* is involved in abiotic stress response. BMC Genom. 22, 350.
Zhang, X., Gou, M., Liu, C.J., 2013. Arabidopsis Kelch repeat F-box proteins regulate phenylpropanoid biosynthesis via controlling the turnover of phenylalanine ammonia-lyase. Plant Cell 25, 4994–5010.
Zhang, D., Sun, W., Singh, R., Zheng, Y., Cao, Z., Li, M., Lunde, C., Hake, S., Zhang, Z., 2018. GRF-Interacting factor1 regulates shoot architecture and meristem determinacy in maize. Plant Cell 30, 360–374.
Zhao, D., Ni, W., Feng, B., Han, T., Petrasek, M.G., Ma, H., 2003. Members of the Arabidopsis-SKP1-like gene family exhibit a variety of expression patterns and may play diverse roles in Arabidopsis. Plant Physiol. 133, 203–217.
Zhao, Q., Nakashima, J., Chen, F., Yin, Y., Fu, C., Yun, J., Shao, H., Wang, X., Wan, g Z.Y., Dixon, R.A., 2013. Laccase is necessary and nonredundant with peroxidase for lignin polymerization during vascular development in Arabidopsis. Plant Cell 25, 3976–3987.

Deciphering molecular mechanism of induction of biotic stress tolerance by Trichoderma spp. in castor (Ricinus communis L.)

by Doris Pradhan

Librarian
Indira Gandhi Memorial Library
UNIVERSITY OF HYDERABAD
Central University P.O.
HYDERABAD-500 046.

Submission date: 23-Jan-2024 03:02PM (UTC+0530)
Submission ID: 2276593169
File name: Thesis-Plagarisim_check.pdf (13.55M)
Word count: 34758
Character count: 192340

Deciphering molecular mechanism of induction of biotic stress tolerance by Trichoderma spp. in castor (Ricinus communis L.)

ORIGINALITY REPORT

71%	12%	69%	8%
SIMILARITY INDEX	INTERNET SOURCES	PUBLICATIONS	STUDENT PAPERS

PRIMARY SOURCES

1	Doris A Pradhan, Ragiba Makandar. "Delineating host responses induced by Trichoderma in castor through comparative transcriptome analysis", Rhizosphere, 2023 Publication	30%
2	Doris A. Pradhan, Prathyusha Bagagoni, Ragiba Makandar. "Assessing rhizosphere Trichoderma asperellum strains for root colonizing and antagonistic competencies against Fusarium wilt through molecular and biochemical responses in castor", Biological Control, 2023 Publication	20%
3	Doris A Pradhan, Prathyusha Bagagoni, Saharika Slathia, R. Durga Prasad, Ragiba Makandar. "Characterization of Trichoderma strains for novel species-specific markers by multiplex PCR and antagonistic property against Alternaria ricini in castor (Ricinus	16%

The total of 66% similarity shown related to the student own papers. The actual similarity by deducting 66% out of the total 71% similarity is 5% only.

14/02/2024

RAGIBA MAKANDAR
Professor
Department of Plant Sciences
School of Life Sciences
University of Hyderabad
Hyderabad 500 046 India

	communis L.)", Biocatalysis and Agricultural Biotechnology, 2023 Publication	
4	Submitted to University of Hyderabad, Hyderabad Student Paper	3%
5	"Advances in Trichoderma Biology for Agricultural Applications", Springer Science and Business Media LLC, 2022 Publication	<1%
6	www.paduco.ps Internet Source	<1%
7	www2.mdpi.com Internet Source	<1%
8	www.ncbi.nlm.nih.gov Internet Source	<1%
9	discovery.researcher.life Internet Source	<1%
10	www.science.gov Internet Source	<1%
11	dokumen.pub Internet Source	<1%
12	Fungal Biology, 2016. Publication	<1%

13	K. Kumar, K. Xi, T. K. Turkington, A. Tekauz, J. H. Helm, J. P. Tewari. "Evaluation of a detached leaf assay to measure fusarium head blight resistance components in barley", Canadian Journal of Plant Pathology, 2011 Publication	<1 %
14	vdoc.pub Internet Source	<1 %
15	Huzefa A. Raja, Andrew N. Miller, Cedric J. Pearce, Nicholas H. Oberlies. "Fungal Identification Using Molecular Tools: A Primer for the Natural Products Research Community", Journal of Natural Products, 2017 Publication	<1 %
16	Sheetal M Bhosle, Ragiba Makandar. " Comparative transcriptome of compatible and incompatible interaction of and garden pea reveals putative defense and pathogenicity factors ", FEMS Microbiology Ecology, 2021 Publication	<1 %
17	v3r.esp.org Internet Source	<1 %
18	www.ijcmas.com Internet Source	<1 %
	www.sciencegate.app	

19	Internet Source	<1 %
20	Submitted to Universiti Brunei Darussalam Student Paper	<1 %
21	Vos, Christine MF, Kaat De Cremer, Bruno PA Cammue, and Barbara De Coninck. "The toolbox of Trichoderma spp. in biocontrol of Botrytis cinerea disease : Trichoderma biocontrol of Botrytis cinerea disease", Molecular Plant Pathology, 2014. Publication	<1 %
22	"Trichoderma", Springer Science and Business Media LLC, 2020 Publication	<1 %
23	prr.hec.gov.pk Internet Source	<1 %
24	ir.nbu.ac.in Internet Source	<1 %
25	"Fungal Biotechnology and Bioengineering", Springer Science and Business Media LLC, 2020 Publication	<1 %
26	www.researchgate.net Internet Source	<1 %
27	Lee, Dong Hyeon, Sun Keun Lee, Sang Yong Lee, and Jong Kyu Lee. "Development of SCAR	<1 %

	Markers for the Identification of Phytophthora katsurae Causing Chestnut Ink Disease in Korea", Mycobiology, 2013. Publication	
28	Submitted to Nottingham Trent University Student Paper	<1 %
29	ueaeprints.uea.ac.uk Internet Source	<1 %
30	www.chemijournal.com Internet Source	<1 %
31	bio-protocol.org Internet Source	<1 %

Exclude quotes	On	Exclude matches	< 14 words
Exclude bibliography	On		